UNIVERSITY OF SOUTHAMPTON

Fractionated Radioimmunotherapy of Non-Hodgkin's Lymphoma

Michael Christopher Bayne

Doctor of Medicine

Faculty of Medicine, Health and Life Sciences

School of Medicine

Cancer Sciences Division

May 2005

UNIVERSITY OF SOUTHAMPTON

ABSTRACT

FACULTY OF MEDICINE, HEALTH AND LIFE SCIENCES

SCHOOL OF MEDICINE

CANCER SCIENCES DIVISION

Doctor of Medicine

FRACTIONATED RADIOIMMUNOTHERAPY OF NON HODGKIN'S LYMPHOMA

By Michael Christopher Bayne

Despite highly promising results with radioimmunotherapy (RIT) in 'low grade' NHL there remains uncertainty as to the optimal treatment approach. Currently the majority of patients are treated with a single non-myeloablative dose of murine radiolabelled anti-CD20 monoclonal antibody (mAb). The use of murine mAbs, with the potential for the development of human anti-mouse antibody responses, may prevent more than one administration. Impressive durable responses from clinical studies using higher myeloablative dose RIT followed by peripheral blood stem cell transplant (PBSCT) suggest that there may be a radiation dose response for RIT. With the development of rituximab, a chimeric mAb, multiple or fractionated treatments are possible. This may enable higher cumulative doses of RIT to be delivered without the need for PBSCT and may offer the potential for improving the biodistribution of the radioactive antibody. Here the fractionation of RIT has been investigated both in murine models and in the context of a clinical trial. Using a dose escalation protocol the clinical trial tests the safety and efficacy of fractionated RIT in relapsed CD20 positive NHL using 2 fractions of ^{131}I-rituximab given with an 8-week interval. The feasibility of producing clinical grade ^{131}I-rituximab and delivering the treatment has been demonstrated with high response rates and acceptable toxicity seen in the first 3 dose cohorts. Pharmacokinetic analysis has involved measurement of the clearance of the radioimmunoconjugate as well as the development of an assay to measure serum rituximab concentrations. Wide inter-patient variability in pharmacokinetics and a strong association between the availability of CD20 antigen and clearance of both the radioimmunoconjugate and the unlabelled mAb has been seen. The results support individualisation of the dose and scheduling of RIT. The anti-rituximab idiotype mAb developed in order to assay serum rituximab concentrations by enzyme linked immunosorbent assay has also provided a tool for studying the binding of rituximab to CD20.

TABLE OF CONTENTS

Acknowledgements

Abbreviations

FSC	forward scatter
Abs	absorbance
ADCC	antibody dependent cellular cytotoxicity
AML	acute myeloid leukaemia
ASCO	American Society of Oncology
ASH	American Society of Haematology
CALGB	Cancer and Leukaemia Group B
CDC	complement dependent cytotoxicity
CDR	complementarity determining regions
CFA	Complete Freund's Adjuvant
CHOP	cyclophosphamide adriamycin vincristine prednisalone
CR	complete response
CTL	cytotoxic T lymphocyte
CVP	cyclophosphamide vincristine and prednisalone
DEAE	diethylaminoethyl
DLBC	diffuse Large B cell lymphoma
DMEM	Dulbecco's modified essential media
EBRT	external beam radiotherapy
ELISA	enzyme-linked immunsorbant assay
EORTC	European Organization for Research and Treatment of Cancer
FDA	Food and Drug Agency
Gy	gray
HAMA	human anti-murine antibodies
HPLC	high performance liquid chromatography
HDR	high dose rate
HRP	horse radish peroxidase
IFA	Incomplete Freund's Adjuvant
ITLC	instant thin layer chromatography
^{131}I	iodine-131
K_A	affinity constants

LAL	limulus amebocyte lysate
LDR	low dose rate
LE	labelling efficiency
mAb	monoclonal antibodies
MALT	extranodal marginal zone lymphoma
MARA	mouse anti-rat mAb
MBq	Mega Bequerel
MDS	myelodysplastic syndrome
MHC	major histocompatibility complex
MIRD	medical internal radiation dose
MTD	maximum tolerated dose
NHL	non Hodgkin's Lymphoma
o-PD	o-PhenylDiamine free base
OR	overall response
PBSCT	peripheral blood stem cell transplant
PEG	polyethylene glycol
QA	quality assurance
RIT	radioimmunotherapy
SCID	severe combined immunodeficient
SEER	survival, epidemiology, and end results
SPE	serum protein electrophoresis
SPECT	single photon emission computed tomography
SPR	surface plasmon resonance
SWOG	South West Oncology Group
TBI	total body irradiation
3D	three-dimensional
WHO	World Health Organization
^{90}Y	yttrium-90

Chapter 1

INTRODUCTION

1.   INTRODUCTION

It is over 30 years since the development of mAb technology [1] and nearly 100 years since the concept of antibody targeted therapy for cancer was proposed by Paul Ehrlich. After years of promise but little clinical success we are now finally seeing antibody-targeted therapy for cancer entering the mainstream of anti-cancer therapeutics. Since Rituximab became the first antibody to be licensed by the US Food and Drug Agency (FDA) for the treatment of cancer 6 years ago there has been an explosion of interest in this field with over 80 monoclonal antibodies (mAb) now being actively developed in clinical trials [2]. Many of these mAb are cytotoxic in their own right, however single agent response rates are generally disappointing. The conjugation of radioisotopes to mAb as part of radioimmunotherapy (RIT) however enables the additional delivery of targeted radiotherapy and thus offers the possibility of enhancing the therapeutic potency of mAb.

With the recent FDA approval of two radioimmunoconjugates, Yttrium-90 (^{90}Y) labelled ibritumomab tiuxetan (Zevalin^{TM}) and Iodine-131 (^{131}I) labelled tositumomab (Bexxar^{TM}), the potential of this conceptually appealing approach, is now rapidly being realised. Having demonstrated the efficacy of RIT in the treatment of relapsed low-grade NHL the challenge now is to determine the optimum approach and schedule to enable integration of this new treatment modality with established chemotherapy and radiotherapy regimens. It is hoped that as we dissect out the components that determine successful RIT and gain greater understanding of the mechanism at play we may be able to improve upon the current clinical results with lymphoma and apply RIT to a broader spectrum of malignancies.

The aim of the work described in this thesis was to enhance our understanding of some of the components of successful RIT. It focuses on the impact of scheduling on the pharmacokinetics and biodistribution of a radioimmunoconjugate and investigates the feasibility and toxicity of the fractionation of RIT in the context of a phase I/II clinical trial. The current state of therapeutics for NHL will initially be described illustrating the need for novel agents and strategies before describing the various components of current RIT schedules and exploring potential avenues for improvement. One of these avenues is fractionation. The rationale for the fractionation of RIT will be explained and illustrated by a review of the available clinical and experimental literature before describing the pre-clinical and clinical experimental work carried out in this study.

1.1 NON HODGKIN'S LYMPHOMA

1.1.1 Epidemiology

NHL is a term used to represent a diverse group of lymphoid malignancies. NHL may affect all age groups, and although it is principally a disease of older adults with the peak incidence occurring in individuals over 60 years. Because of the relatively young average age of the lymphoma population, it has been ranked fourth in terms of economic impact among cancers in the United States [3]. It is the 5th and 6th most common malignancy in males and females respectively in the Western World with approximately 8000 new cases seen per year in the UK. For reasons that remain unclear, for the past 25 years, the incidence of NHL has been rising at a rate faster than that of any other malignancy (see figure 1.1). Data from the Survival, Epidemiology, and End Results (SEER) project indicate a 2 fold rise in incidence (8/100,000 to 16/100,000) between 1973 and 1995 [4]. Observational studies have demonstrated an association between NHL and some infectious agents and immunodeficiency states as well as exposure to radiation and chemical toxins; however, in most individuals the cause is not known.

Figure 1. 1. NHL SEER incidence by age 1973-1975 vs. 1994-1996.
Adapted from [5]
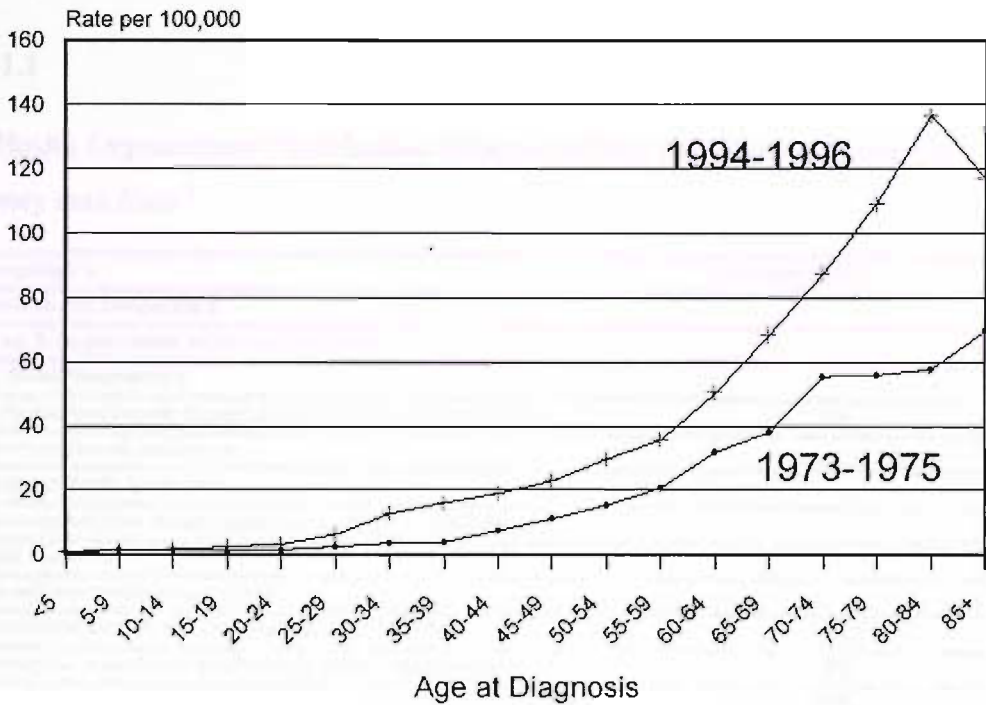
1.1.2 Classification

The NHL are a heterogeneous group of diseases with a broad clinical spectrum ranging from very indolent conditions with a long natural history, such as grade 1 follicular lymphoma, to very aggressive but highly curable conditions such as Burkitt's Lymphoma. Over recent decades there have been a series of different pathological classifications often with conflict between clinical utility and histopathological and biological accuracy. With advances in immunophenotyping and cytogenetics it became apparent that many distinct definable diseases were being classified together and a new classification was required to take into account all the available clinical and pathological information. The new classification termed the Revised European-American Lymphoma classification [6] incorporates these new insights and has been largely adopted by the World Health Organization (WHO) classification illustrated in table 1.1 [7]. Within this new classification the concept of grouping lymphoid malignancies according to their

13

presumed normal counterparts is retained but the division into high, intermediate and low-grade categories has been discarded.

Table 1.1

Word Health Organization Classification Scheme for Non-Hodgkin's Lymphoma. Frequency data from [8].

B-cell Neoplasm's	Frequency (%)
Precursor B-cell Neoplasm's	
Precursor B-lymphoblastic leukemia/lymphoma	
Mature B-cell Neoplasm's	
B-cell chronic lymphocytic leukemia/small lymphocytic lymphoma	7%
B-cell prolymphocytic leukaemia	
Lymphoplasmacytic lymphoma	
Splenic marginal zone B-cell lymphoma (± villous lymphocytes)	
Hairy cell leukaemia	
Plasma cell myeloma/plasmacytoma	
Extranodal marginal zone B-cell lymphoma of MALT type	8%
Nodal marginal zone B-cell lymphoma (± monocytoid B cells)	2%
Follicular lymphoma	22%
Mantle-cell lymphoma	6%
Diffuse large B-cell lymphoma	31%
Mediastinal large B-cell lymphoma	
Primary effusion lymphoma	
Burkitt's lymphoma	
T-cell and NK-cell Neoplasms	
Precursor T-cell Neoplasms	
Precursor T-lymphoblastic lymphoma/leukemia	2%
Mature T-cell Neoplasms	
T-cell prolymphocytic leukaemia	
T-cell granular lymphocytic leukaemia	
Aggressive NK-cell leukaemia	
Adult T-cell lymphoma/leukemia (HTLV-1 +)	
Extranodal NK/T-cell lymphoma, nasal type	
Enteropathy-type T-cell lymphoma	
Hepatosplenic gamma-delta T-cell lymphoma	
Subcutaneous panniculitis-like T-cell lymphoma	
Mycosis fungoides/Sezary syndrome	
Anaplastic large-cell lymphoma, T/null cell, primary cutaneous type	
Anaplastic large-cell lymphoma, T/null cell, primary systemic type	2%
Peripheral T-cell lymphoma, not otherwise characterized	
Angioimmunoblastic T-cell lymphoma	

HTLV-1, human T-cell leukemia virus 1; MALT, mucosa-associated lymphoid tissue; NK, natural killer

1.1.3 The Natural History of Indolent NHL

Although the new WHO classification no longer uses the terms, the concept of high and low grade disease remains useful in clinical management. High grade or aggressive lymphomas are generally characterised as being composed of large cells with a high proliferation rate. Patients usually present with advanced disease, which progresses rapidly but can be cured by intensive chemotherapy in a significant proportion of cases.

Low grade or indolent lymphomas in contrast are generally characterised as tumours of small lymphocytes, which have a low proliferation rate, and a high proportion of resting cells. Over 80% of patients present with bone marrow involvement and the clinical pattern is of initial sensitivity to chemotherapy and radiotherapy but almost inevitable relapse with progressive resistance to new lines of therapy and a tendency to transform into a more aggressive large cell lymphoma. The median survival is 7-10 years and during the course of the disease most patients will receive multiple sequential courses of chemotherapy with progressively lower response rates and shorter times to progression with each successive treatment episode [9]. For the purposes of this thesis 'Indolent Lymphoma' will include those subtypes listed in Table 1.2.

Table 1.2. Indolent B cell Lymphomas.
Adapted from [10]

Indolent B cell Lymphomas
Follicular Lymphoma, grade 1-2, grade 3 Small Lymphocytic Lymphoma/Leukaemia Lymphoplasmacytic Lymphoma Extranodal Marginal Zone Lymphoma (MALT) Nodal Marginal Zone Lymphoma Splenic Marginal Zone Lymphoma

1.1.4 Current Therapy For Indolent NHL

The common indolent lymphomas (follicular lymphoma and small lymphocytic lymphoma) rarely present with localised disease, but for the 10-20% that do, external beam radiotherapy (EBRT) has for many years been the treatment modality of choice, offering local treatment that obtains long term control in the majority. Whether this treatment is curative remains contentious due to the occurrence of late relapses and the limited number of studies that have followed patients for greater than 10 years. In spite of this, for patients with stage 1 follicular lymphoma treated with involved field radiotherapy, a progression free survival of greater than 50% at 15 years can be expected and patients who remain disease free at 10 years very rarely relapse [11] [12]. This curative potential of radiotherapy for localised disease is in contrast to treatment outcomes reported for the majority of patients who present with advanced disease. In this group earlier and more aggressive approaches with chemotherapy and/or radiotherapy do not appear to prolong disease free survival [13]. As a result the focus has been on minimising the toxicity of treatment and identifying treatments that prolong the disease and therefore treatment and symptom free interval. Initially a watch and wait strategy is often employed with treatment commenced only in those with significant symptoms or evidence of organ dysfunction.

The generally adopted approach after 'watchful waiting' for many patients in the UK is to offer a single alkylating agent such as chlorambucil, although increasing numbers of lymphoma clinicians are using combination chemotherapy such as the combination of cyclophosphamide vincristine and prednisalone (CVP) with or without rituximab. A number of recently published studies support the addition of rituximab to chemotherapy in this setting reporting increased response rates and prolonged time to relapse[14] [15]. If successful the initial treatment may be repeated with subsequent relapse or followed by regimens containing anthracyclines or purine analogues. Once again the addition of rituximab to conventional chemotherapy at relapse increases frequency and durability of response[16]. More aggressive chemotherapy regimens such as high dose chemotherapy followed by autologous stem cell transplantation have promised prolonged disease free

survival however there is so far no evidence that this intensive therapy alters the overall survival. Allogeneic stem cell transplantation results in high rates of complete remission and there is a suggestion that this brings about a plateau in the survival curve however this is at the expense of what many would consider unacceptable treatment related toxicity [17]. As a result these aggressive chemotherapy regimens are not considered a viable option for the majority of patients with indolent NHL.

Interestingly, despite the disseminated nature of advanced indolent lymphoma, radiation has been successfully employed not only for the management of locally recurrent tumour masses but also to treat widespread disease in the form of total body irradiation (TBI). Delivering doses of only 2 Gray (Gy) x 2 to sites of nodal relapse, a response rate of 92% has been recorded with a complete response rate of 61% and median time to local progression of 25 months [18] making this a very attractive low toxicity regimen for symptom control. In addition, low dose TBI delivering a total dose of just 1.5 Gy in 10 fractions has been shown to be equivalent to combination chemotherapy in the treatment of relapsed disease [19] and has been incorporated into a Phase III European Organisation for Research and Treatment of Cancer (EORTC) trial [20]. The clinical results from this approach illustrate the remarkable sensitivity of lymphoma to even very low doses of radiation and emphasise the potential of radiation if it can be effectively delivered to all sites of disease.

It is perhaps surprising that despite the sensitivity of most lymphomas to initial therapy and significant advances in chemotherapy, radiotherapy, and supportive care patients with advanced "low grade" lymphomas remain incurable. Furthermore survival for these conditions has not altered since the early 1960's [21]. Conventional treatment involves repeated courses of chemotherapy often over several years resulting in substantial morbidity and impact on healthcare economics. There is therefore an urgent need to identify alternative treatment strategies and improve these unsatisfactory results.

With the arrival of effective therapies derived from monoclonal antibody technology a host of new treatment options are emerging. It is to be hoped that as well as offering

treatments with low toxicity and lacking cross resistance with current chemotherapy these antibody based treatments will bring about the long over due improvements in survival from this disease.

1.2 MONOCLONAL ANTIBODY THERAPY FOR NHL

1.2.1 The History Of Antibody Therapy

A major problem with both chemotherapy and radiotherapy as cancer treatments is the relative lack of specificity for tumour cells. This often results in a narrow therapeutic window and substantial toxicity if doses sufficient to offer the prospect of cure are administered. Almost a century ago Paul Ehrlich introduced the "magic bullet" concept of targeting therapeutic agents to specific tissues in order to reduce systemic toxicity and 50 years ago it was observed that antibodies could selectively target tumour cells in patients.

It was not until the development of mAb technology by Kohler and Milstein in the 1970's that the prospect of targeted therapy became a reality [1]. Early studies with unconjugated rodent antibodies were largely fruitless. MAb clearly delivered a high degree of specificity, which led to a remarkable expansion in the number of such reagents available for biological research and diagnostics. However for most cancer patients mAb showed only transient or partial response within the clinic, with little evidence of long term benefit [22]. The exception to this was in the use of anti-idiotype mAb for the treatment of NHL [23,24]. Customised patient specific mAbs were derived from mice immunised with the patient's tumour. Response rates of over 60% were seen, however the logistical difficulties in creating the customised mAb and the propensity of the tumours to develop idiotype negative clones or clones with changes in their idiotype has limited the application of this therapy. These studies however provided substantial data to aid the subsequent identification of the optimum targets for antibodies, as well as indicating the significant problem of the development of human anti-murine antibodies

18

(HAMA). A HAMA response rarely causes clinically significant adverse reactions although 'flu-like' symptoms and mild to moderate anaphylactic reactions may be seen. More importantly a HAMA reaction may seriously alter the mAb pharmacokinetics through the formation of immune complexes that are rapidly cleared by the reticuloendothelial system preventing adequate targeting of the tumour.

These observations have stimulated the development of engineered mAb that have a mouse variable region but human constant region. Such engineered mAb have the advantage of lower antigenicity and an improved ability to recruit human immune effectors. It is since the arrival of these engineered mAbs that mAbs have finally begun to make an impact in the clinic. Before describing the current status of clinical immunotherapy for NHL the components of antibody therapy and our current understanding of their mechanisms of action is described.

1.2.2 The Target

NHL provides an attractive model in which to develop antibody therapy not only because of the vascularity of these tumours enabling relatively easy access of the antibody to most tumour cells but also because of the plethora of potential target antigens expressed on the surface of lymphoma cells. The ideal target would be an antigen that is present only on tumour cells but that, in contrast to the idiotype, is not unique for each patient avoiding the problems of manufacturing patient customised antibodies described above (1.2.1). In practice tumour specific antigens rarely exist and tumour-associated antigens, that is antigens that are expressed both on tumour cells and some normal tissues, are used instead. As the majority of lymphomas are of B cell origin the pan-B cell antigens have been extensively evaluated as targets for immunotherapy (Figure 1.2).

Figure 1.2 Antigen targets on B cells.
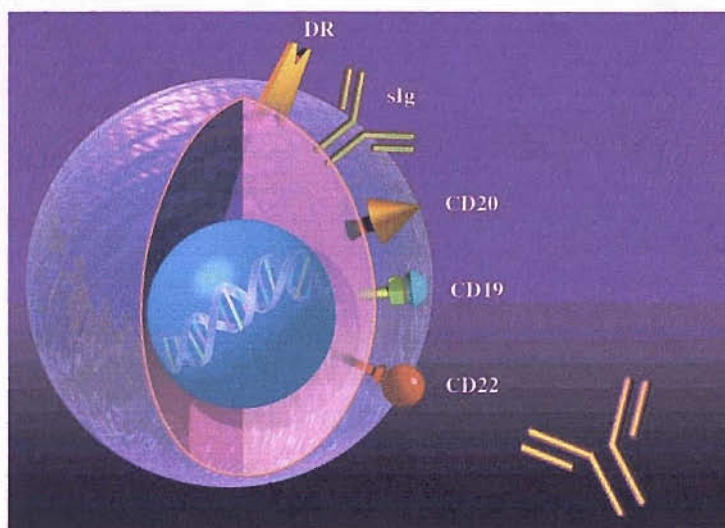
Fortuitously several of these pan-B cell antigens, including the CD20, CD37, CD19, CD22 and MHC class II antigens which, are highly expressed on the majority of B cell lymphomas are not expressed on stem cells or plasma cells, so that after treatment the B cell pool can be replenished. The transient treatment related loss of mature B cells results in little clinical toxicity due to the long half-life of plasma cells and circulating immunoglobulins, which maintain adequate humoral immunity until the B cell population recovers. In addition to being preferentially expressed on tumour cells, for successful antibody therapy, the target antigen must be expressed on the cell surface at sufficient density and remain on the surface for long enough to recruit immune effectors without being internalised or shed. The success of antibodies targeting the CD20 antigen seems to arise not only from the ability of the antibodies to bind and recruit immune effectors but also because binding the antigen results in pro-apoptotic signals hence an antigen that is critical for target cell survival or provides an important intracellular signal

is also included in the list of characteristics required for an ideal target antigen listed in table 1.3. [25].

Table 1.3. The characteristics of an ideal target antigen. Adapted from [25]

The characteristics of an ideal target antigen
Tumour cell specific
Highly expressed on tumour cells
No tendency to mutation
Not secreted or shed
Not rapidly modulated on antibody binding
Critical for target cell survival
Not expressed on critical or non renewable host cells

1.2.3 The Antibody

As indicated earlier, on binding a cell surface antigen, unconjugated mAb may bring about anti-tumour effects through recruitment of the host immune system or through direct signalling. The relative contribution of these components to successful immunotherapy remains contentious but each will now be described in turn and is illustrated in figure 1.3.

Figure 1.3. Potential mechanism of antibody induced tumour cell death.
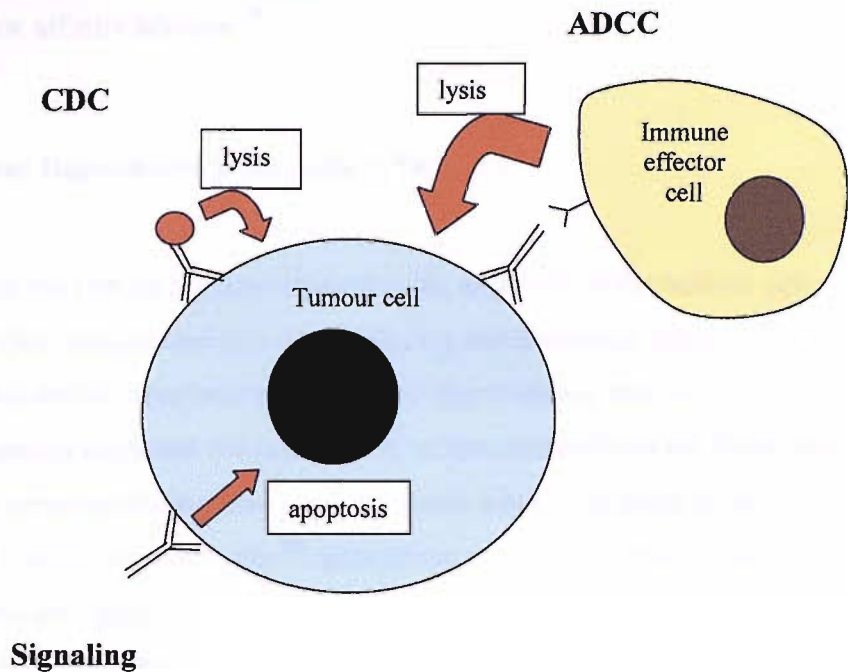
1.2.3.1 Antibody Dependent Cellular Cytotoxicity (ADCC)

Immune effector cells such as the macrophages and natural killer cells possess membrane receptors for the Fc region of the antibody molecule. When antibody is specifically bound to the target tumour cells these Fc receptor bearing cells can bind to the antibody where they subsequently cause tumour cell lysis. The importance of this mechanism for antibody efficacy was supported by early in vitro and animal studies in which a close correlation was found between the ability of an antibody to induce ADCC in vitro and its in vivo efficacy [26] [27].

The importance of ADCC is also indicated by some recent work with FcR deficient mice in which the full therapeutic effect of rituximab was only seen in mice expressing the

stimulatory, gamma chain associated FcR [28]. This work has been further supported by the observation that patients expressing the high affinity variant of the FcR gamma IIIa receptor (158V allotype) have a greater likelihood of response following rituximab than those carrying the low affinity allotype [29].

1.2.3.2 Complement Dependent Cytotoxicity (CDC)

In addition to binding the FcR of immune effector cells, antibody on the tumour cell surface may activate the complement cascade producing the membrane attack complex and aiding the recruitment of other immune effectors. The evidence that this plays an important part in antibody mediated tumour cell kill in vivo comes from the observation that complement is consumed during rituximab treatment where it appears to be associated with much of the acute toxicity [30]. In addition pre-clinical studies have demonstrated that in a xenograft model in SCID mice the effect of rituximab may be abrogated by the addition of cobra venom factor a substance that blocks complement activity [31]. This remains however an area of some controversy due to the observation that the therapeutic activity of rituximab does not appear to correlate with the expression levels of the complement defence molecules CD55 and CD59 [32].

1.2.3.3 Signalling

Initially all the anti-tumour effect of mAb was thought to occur through the recruitment of the immune effectors described above. Over recent years however it has become apparent that many of the mAb used in successful immunotherapy are directly cytotoxic and that by cross-linking or blocking membrane receptors mAb may generate transmembrane signals that alter tumour cell growth or trigger apoptosis [33] [34]. This is important because it suggests that the combination of antibodies with chemotherapy or radiotherapy may offer the possibility of additive or even synergistic therapeutic activity. Indeed there is growing preclinical and clinical data to support this combined approach both with chemotherapy and radiotherapy [35-38].

1.2.3.4 Activation Of The Host Immune Response

One of the interesting observations from successful mAb therapy for NHL has been the delayed time to maximal response. This delayed response has been seen both following rituximab and following treatment with RIT using ^{131}I tositumomab and ^{90}Y ibritumonab tiuxetan. A potential explanation for this type of delayed response is the possibility that the antibody therapy may contribute to the induction of a host immune response against the tumour. This might occur through the induction of potentially protective cytotoxic T cell responses. It is well established that dendritic cells may ingest cell debris and present tumour associated antigens on MHC class 1 molecules, a mechanism called 'cross presentation'. An in vitro study supports the possibility that such cross presentation may be promoted by antibody therapy with rituximab in the Daudi cell model [39]. The possibility that radiation combined with antibody therapy may enhance this effect is illustrated by recently published work from our laboratory [40]. The conclusions from this work are that the radiation may induce an initial kill of lymphoma cells, probably by apoptosis, which releases tumour antigens and slows the progression of the malignancy to allow generation of a curative cytotoxic T lymphocyte (CTL) response promoted by the immunoregulatory anti-CD40 mAb. With anti-CD40, which is known to trigger the activation of antigen presenting cells enabling them to present tumour antigens to cytotoxic T cells, an explanation for the induction of the cytotoxic T cell response is apparent, however for other antibodies, like rituximab, the picture is far less clear.

An alternative mechanism for production of a host anti-tumour immune response has been suggested based on the idiotype network theory [41]. According to this theory a therapeutic antibody may induce the production of antibodies by the host that recognise the idiotype of the administered antibody and eventually an anti-anti-idiotypic response may be produced in the patient. It is proposed that these anti-anti-idiotype antibodies may recognise the tumour cell antigen resulting in anti-tumour activity that may persist long after the administered therapeutic antibody has been cleared. The production of such anti-anti-idiotype antibodies with anti-tumour activity has recently been described in a

single patient following treatment for NHL with the anti-MHC class II mAb Lym-1 affording at least some credibility to this theory [42].

Whether the delayed responses and prolonged remissions seen with antibody therapy can be accounted for by these mechanisms remains to be determined. However evidence is emerging that in some cases antibody therapy induces active immunity. Defining the underlying host immunological mechanisms and identifying strategies to exploit these is an important under-explored area for future research.

1.2.3.5 Antibody Engineering

Having produced a mAb with the appropriate specificity to effectively target tumour, it is now possible to engineer the antibodies in an attempt to optimise recruitment of the immune effectors, minimise immunogenicity, prolong circulating half-life and improve tumour penetration. By altering the antibody subclass, the ability to recruit the immune system may be enhanced, with IgG2a reported as the most efficient for ADCC whilst IgG3 is most effective at mediating CDC. This recruitment of immune effectors can be further enhanced by chimerising or humanising the antibody to provide mAb with human Fc regions (see figure 1.4). This also has the benefit of reducing the exposure to murine protein limiting the problems of HAMA responses described above (1.2.1), and enabling repeated administration. One of the substantial limitations of antibody therapy is the large size of the antibody molecule inhibiting penetration into tumour masses. Attempts to overcome this have been made by producing fragments of antibody that retain the specificity inducing variable region but due to their much smaller size have demonstrated substantially improved biodistribution [43][44]. Because these fragments lack the Fc domain necessary for recruiting immune effectors they have been developed principally as vehicles for the delivery of radioactive isotopes for imaging or conjugated with toxins for therapy.

Figure 1.4. Diagrammatic representation of antibody constructs adapted from Farah et al. Chimeric mAbs have Human Fc domains but murine Fv domains. In humanised antibodies all the protein except the complementarity determining regions (CDR) are human [45]
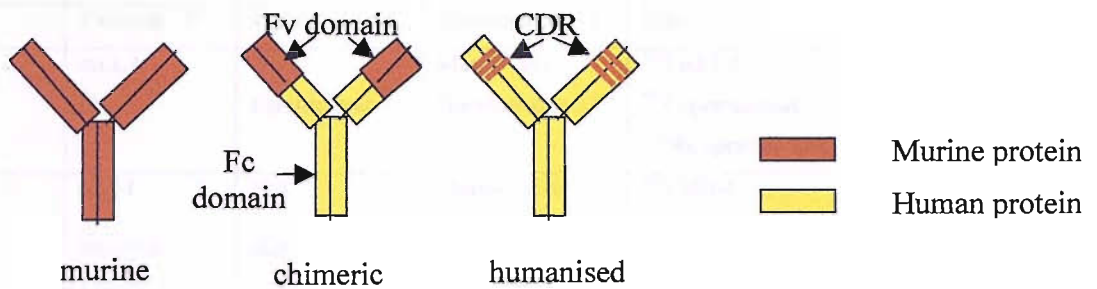
1.2.4 Unconjugated Antibody Therapy For NHL

In the last decade mAb therapy has finally started to make a significant impact on the clinical management of NHL. Rituximab and alemtuzumab are now well-established approved therapies in the treatment of lympho-proliferative disorders. Many other mAbs have entered clinical trials. Some of the mAb that are in use or have been recently tested are listed in table 1.4.

Table 1.4. List of the targets used in therapy of B cell NHL with the relevant mAb and radioimmunoconjugate. * indicates FDA approval

Antigen target	Unconjugated mAb	Generic name	Construct form	Radioimunoconjugate	Reference
CD20	2B8	Ibritumomab	Murine IgG1	^{90}Y ibritumomab tiuxetan*	46
	C2B8	Rituximab*	Chimeric IgG1	^{131}I Rituximab	47
	B1	Tositumomab	Murine IgG2a	^{131}I tositumomab*	48
CD52	Campath-1H	Alemtuzumab*	Humanised IgG1	N/A	27
CD22	mLL2		Murine IgG1	^{131}I mLL2	49
	hLL2	Epratuzumab	Humanised IgG1	^{90}Y epratuzumab/ ^{186}Re epratuzumab	50
CD37	MB-1	N/A	Murine IgG1	^{131}I MB-1	51
HLA-DR	Hu1D10	N/A	Humanised IgG1		52
	Lym-1	N/A	Murine IGg2a	^{131}I / ^{67}Cu / ^{90}Y Lym-1	53

1.2.4.1 CD20 As A Target For Immunotherapy

Antibodies that target the CD20 antigen have dominated the field of immunotherapy for NHL. CD20 is a non-glycosylated cell surface 33-37 kDa phosphoprotein with a structure comprising of 4 transmembrane regions [54]. It is expressed exclusively on B-cell precursors and mature B cells but lost following differentiation into plasma cells. Greater than 95% of B cell lymphomas express the CD20 antigen which, following the identification of surface immunoglobulin, was the first cell differentiation antigen of human B cells to be identified. The physiological role of CD20 remains to be elucidated and no natural ligand has yet been identified. There is however an increasing body of evidence concerning the nature of rituximab binding to the CD20 antigen. On binding unlike many cell surface antigens there is no modulation and therefore no resulting internalisation of the antibody [55]. The stability of the CD20 surface antigen offers a clear advantage in terms of induction of ADCC and CDC, as while the antigen and antibody complex remain on the surface of the cell the Fc component of the mAb remains available for interaction with complement and immune effector cells. For RIT using ^{131}I

this lack of internalisation is also an important feature of the target antigen as iodinated radioimmunoconjugates are rapidly dehalogenated upon internalisation resulting in the excretion of ^{131}I molecules from the cell and therefore from the target. In addition to the induction of ADCC or CDC that can be attributed to the Fc component of the binding mAb, ligation and cross linking of the CD20 antigen has been shown to initiate intracellular cell signalling pathways that can precipitate cell cycle arrest and apoptosis. The nature of these intracellular signals, the factors that are necessary in an anti-CD20 mAb to maximise apoptosis on binding and the clinical relevance of antibody induced apoptosis remains an area of active research. There is some evidence that CD20 functions as a calcium channel subunit and perhaps regulates cell cycle progression through maintaining calcium levels [56]. More recent work indicates that CD20 ligation can lead directly to apoptosis using the same intracellular pathway as apoptosis triggered by the B cell receptor [57] and there is evidence supporting both caspase dependent and caspase independent modes of cell death.

1.2.4.2 Rituximab

Since gaining FDA approval in 1997 rituximab has been administered to well over 100,000 people and is now included in chemotherapy treatment schedules for many patients with B cell NHL. Rituximab is a chimeric mouse/human antibody bearing the human IgG1 and kappa constant regions, with murine variable regions specific for the CD20 antigen. Pre-clinical studies have shown it to be effective in both the induction of ADCC and CDC. In addition rituximab brings about cross-linking on the cell surface that can initiate downstream signalling that leads to apoptosis. Rituximab is just one of several anti-CD20 mAbs currently being investigated. It appears that anti-CD20 mAb can be broadly classified into 2 groups based on pre-clinical studies. The first group are those that redistribute CD20 into membrane bound rafts like rituximab, which are particularly effective at inducing CDC, and the second group are those that do not distribute CD20 into membrane bound rafts like B1 which appears to be particularly effective at inducing apoptosis. The possible clinical relevance of these differences has as yet not been fully

defined. However, it is interesting to note that B1 may in addition to delivering targeted radiation, also directly induce apoptosis.

1.2.4.3   Rituximab Clinical Trials

Initial phase 1 dose escalation trials performed by Maloney and colleagues [58] demonstrated the safety of a dose of $375mg/m^2$ given weekly for 4 weeks. This dose was therefore used in the pivotal phase II trial, which led to FDA approval. This trial included 166 patients with relapsed indolent B cell NHL there was an overall response (OR) rate of 48% (6% complete response (CR)). The mean duration of response was 13.2 months with some patients remaining in remission as long as 3.5 years [59]. Clinical responses have been seen in all CD20 expressing indolent NHL though more impressive responses are seen with follicular than with small lymphocytic lymphoma. Subsequent studies have demonstrated efficacy in bulky disease [60] and high response rates when used as initial therapy [61]. Response rates for more aggressive NHL histologies are lower than for follicular lymphoma, however when used in combination with CHOP chemotherapy for diffuse large B cell lymphoma in patients over 60 a 10% increase in overall survival was seen [37]. The addition of rituximab to CHOP is the first new intervention to have a significant impact on the outcome for DLBCL for over a quarter if a century.

1.2.4.4   Rituximab Scheduling And Pharmacokinetics

Therapeutic monoclonal antibodies do not follow the conventional paradigm that increasing the dose results in greater anti-tumour effect and greater toxicity, with the optimum dose being the highest dose achievable with acceptable toxicity. The clinical development of rituximab followed the usual pattern of sequential phase I and II clinical trials. The initial phase I ($10\text{-}500mg/m^2$) single administration dose escalation trial, in which clinical activity but no dose limiting toxicity was seen [62], was followed by a phase 1 multiple dose escalation trial (125, 250 and $375mg/m^2$ weekly for 4 weeks) which also revealed no dose limiting toxicity [58]. The response rate was 33% at all 3-dose levels. This

highest dose level (at that time limited by availability and cost) was taken forward into the pivotal phase II trial following which it has become established as the standard dose for the administration of single agent rituximab [43]. From pharmacokinetic studies within these early trials, it was established that the maximum concentration and serum half-life of rituximab increased between the first and fourth infusions for most patients. In the pharmacokinetic study of the patients in the pivotal phase II clinical trial of rituximab the $T_{1/2}$ after the first dose was 76.3 hrs increasing to 205.8 hrs after the fourth infusion. This increase is thought to be secondary to the clearance of circulating B cells from the peripheral blood and saturation of CD20 binding sites [63]. Wide inter-patient variability was noted and at all time points the median serum levels of rituximab were higher in responders than non-responders. An inverse correlation with tumour bulk and histological subtype was also found. Patients with small lymphocytic lymphoma had significantly lower serum rituximab levels. The accumulation of antibody in the serum with sequential doses suggests that rituximab is saturating antigenic sites with this multi-dose regimen and the resulting long serum half-life leads to prolonged exposure of tumour to antibody.

In a study by Berinstein et al rituximab was still detectable in many patients 6 months after administration of the antibody[63]. This would not be expected if the rituximab level continued to decline from the reported peak of 450μg/ml with a half-life of about 200 hours as is seen immediately after the 4th infusion. It is suggested therefore that this persistence of rituximab in the serum may be the result of the 'on/off' phenomenon, with rituximab being released from coated but not lysed tumour or B cells that act as a reservoir maintaining the serum rituximab concentration at unexpectedly high levels. The association of high serum antibody concentration with response and lower tumour bulk may simply indicate that the serum rituximab level is a surrogate measure of low tumour bulk, which is in itself a favourable prognostic factor. An alternative explanation might be that higher concentrations of rituximab may be mediating more effective tumour regression suggesting that higher doses may be necessary to induce the optimum response in patients with bulky disease.

In a study of extended rituximab therapy in which patients were given 8 weekly doses of 375mg/m^2 the post infusion serum rituximab levels reached a plateau after the 6th infusion. Again a correlation between peak serum level and response was seen but the question of whether achieving higher serum levels in patients with bulky disease would enhance response has not been answered [64].

The prolonged serum half-life of rituximab and a possible association with clinical response has led many investigators to consider whether maintenance rituximab might offer clinical benefit. Three studies have approached this question in different ways. Hainsworth and colleagues administered rituximab (4 weekly doses) every 6 months as maintenance to patients who had stable disease or an objective response 6 weeks after an initial course of rituximab [61]. Ghielmini et al administered a single additional rituximab dose (375mg/m^2) at 2 monthly intervals in a randomised trial to patients who had SD or a response to an initial 4-week course of rituximab[65]. Gordan et al have attempted to reduce the frequency and expense of maintenance therapy by measuring serum rituximab levels monthly after the initial 4 weekly infusions and then administering a further single dose only when serum levels drop below 25µg/ml [66]. In this randomised study there was no significant improvement in the OR rate or CR rate, however, the median duration of response was doubled in the maintenance treatment arm. The high response rates and prolonged progression free survival in all three studies, although impressive, do not however provide definitive proof of benefit from this approach as parallel studies have indicated similar benefit from re-treatment with rituximab at the time of relapse. In the absence of rituximab or any other treatment providing a curative option, re-treatment at relapse with rituximab may be a more appropriate treatment.

Repeated treatment of B cell lymphoma with conventional chemotherapy often results in drug resistance and generally the response rate and the time to relapse reduces with each sequential line of treatment. This is in marked contrast to the position with rituximab. In a series published by Coiffier et al, 93% of patients that had previously demonstrated a response to rituximab, responded again when retreated with rituximab (+/- chemotherapy) at relapse [67]. Interestingly in this group the time to relapse was longer

following the second treatment than after the first correlating with observations by Davis et al in a similar study [68].

These studies highlight limitations in our understanding both of the mechanisms of resistance to rituximab and the mechanisms underlying the therapeutic effect of rituximab. The current standard schedule was driven as much by drug availability and economics as efficacy and further careful studies are warranted to derive the optimum dose and schedule. In practice it is becoming increasingly likely that rituximab will be delivered predominantly in conjunction with chemotherapy or as a radioimmunoconjugate. Such combination approaches are likely to have a substantial impact on the pharmacokinetics of rituximab. These pharmacokinetic effects will need to be taken into account when analysing the efficacy of these combinations and designing new schedules.

1.3   RADIOIMMUNOTHERAPY

Rituximab has been greeted with enthusiasm by the clinical community and has been rapidly accepted into treatment protocols world-wide. This is largely due to its excellent safety profile with minimal toxicity and its clinical efficacy and ease of addition to chemotherapy. Despite this relative success, half of patients with relapsed indolent lymphoma either fail to respond or have minor responses to rituximab. The median time to progression for those that responded is only around 13 months [43]. To enhance the therapeutic potency of antibodies, they have been conjugated to radioisotopes, enabling targeting of radiotherapy specifically to tumour sites. A range of antibodies, isotopes and schedules have been studied both in the laboratory and in the clinic. The challenge now is to identify the optimum radioimmunoconjugate and optimise the scheduling of radioimmunotherapy.

1.3.1 Theoretical Advantages of RIT

The sensitivity of lymphoma to radiotherapy, the lack of cross resistance with chemotherapy and the observation that radiotherapy is used with curative intent in localised follicular lymphoma make targeting of radiotherapy in advanced disease an attractive concept [69]. The ability of radioimmunoconjugates to emit beta particles that are cytotoxic over many cell diameters are additional advantages that overcome, to some extent, problems with tumour penetration, the presence of antigen negative tumour variants and immune function rendered defective by the disease or previous treatment [70].

1.3.2 The Delivery Vehicle

The availability of antibodies that can target antigens present on the surface of tumour cells has been reviewed above. Until recently in RIT, the antibody has been considered simply as a vehicle for delivering radiation. Research has concentrated on improving the ability of the antibody to deliver radiation preferentially to tumour with the objective being to produce a durable, localised dose distribution in the target site with rapid elimination of the radioisotope from normal tissue [71]. More recently it has become apparent that the intrinsic anti-tumour activity of the antibody also plays an important role in the efficacy of RIT [35 38]. Despite this, enhancing the delivery of radiation to the target by optimising scheduling and selection of antibody constructs remains a primary goal in RIT research.

There are a number of factors that influence the ability of an antibody to penetrate into tumours and deliver tumour selective radiation. They can be divided into antibody factors and tumour factors.

Antibody factors   1. Binding specificity

2. Antibody binding avidity

3. Molecular weight of the antibody

4. Circulating half life of the antibody

5. Antibody dose/schedule

Tumour factors   1. Antigen density

2. Binding site barrier

3. Blood perfusion of the tumour

4. Permeability of tumour vessels

5. Interstitial/ intratumoural pressure

1.3.2.1 Antibody Factors

As described above there are a large number of potential targets expressed on the surface of B-NHL cells (1.2.2). A wide range of antibodies that target these antigens have been developed and are outlined in table 1.4. Each of these was initially selected for its affinity and avidity to a B cell specific target and several have been subsequently engineered to reduce immunogenicity and enhance recruitment of immune effectors and a number have been conjugated with radioisotopes. An antibody is specific if it recognises an epitope on the antigen, affinity describes the strength of this interaction and avidity, also referred to as the functional affinity, takes into account the valence of this interaction. Therapeutic antibodies are forced towards the centre of a tumour mass by a concentration gradient between the circulating antibody and the tumour. The greater the initial dose of mAb, the steeper the concentration gradient, but also in the case of RIT the greater the exposure of normal tissues to radiation. The magnitude of this gradient changes with time. As antibody is cleared from the circulation the gradient will decrease until eventually the gradient will reverse favouring antibody leaving the tumour. Antibodies with a high avidity will remain bound in the tumour despite this reversed concentration gradient. The higher the initial dose and the longer the concentration gradient favouring diffusion of antibody into the tumour is maintained the greater the dose delivered to the tumour will

be. The aim with RIT is not simply to maximise the tumour dose, but also to maximise the ratio of the dose to tumour versus that to normal tissue. An antibody that percolates rapidly into a tumour down the concentration gradient where it binds with high avidity while all remaining radioimmunoconjugate is rapidly excreted will optimise this ratio.

The molecular weight of a protein restricts its mobility within a tissue. One of the principle difficulties with RIT is achieving sufficient penetration of the relatively high molecular weight immunoglobulin molecules into tumour nodules. This can be overcome to some extent by using smaller antibody fragments such as the F(ab)2, Fab or scFv constructs illustrated in figure 1.4 [72].

Figure 1.5. MAb constructs for improved tumour penetration.

F(ab)2   Fab   scFv
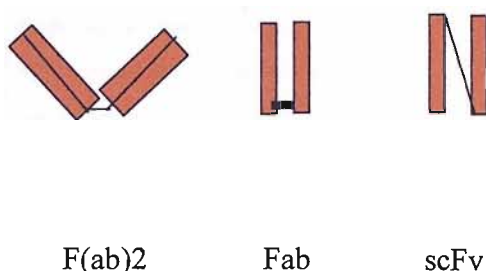
These smaller molecules not only penetrate tumour tissue with greater efficiency than intact mAb [44][73] but also have a shorter serum half life indicating the potential for more rapid clearance of radioimmunoconjugate from normal tissue and thereby enhancing the tumour to normal tissue radiation dose ratio. Unfortunately these constructs also have lower avidities and shorter tumour retention times. Overall mAb fragments despite improved tumour penetration have resulted in appreciably lower percent injected doses per gram of tumour than intact mAb [74] and due to their rapid renal excretion result in unacceptably high renal radiation doses. Currently these disadvantages have out-weighed the penetration advantages and intact molecules for most investigators have been preferred for clinical RIT studies [70].

Table 1.5 The properties of available antibody constructs.

mAb form	Advantage	Disadvantage
Intact mAb - murine	High antigen specificity	Immunogenic – HAMA Poor diffusion/ penetration of tumour
Intact mAb –human/chimeric	High antigen specificity Antibody effector functions (ADCC/CDC) Reduced immunogenicity	Poor diffusion/ penetration of tumour Reduced affinity Slow clearance from blood
$F(ab)_2$ Fab	Rapid clearance from blood Improved diffusion/penetration into tumour. Improved tumour/normal tissue ratio Reduced immunogenicity	Reduced affinity Lower percentage dose delivered to tumour
Fv fragments	Rapid clearance from blood Reduced immunogenicity High tumour to normal tissue ratio Excellent diffusion/penetration of tumour	High renal dose Low percentage of injected dose delivered to tumour

The circulating half-life of a radioimmunoconjugate will influence both the delivery of radiation to the target tumour and the dose to normal tissues. To achieve optimal results, radiolabelled antibodies must have a circulating half-life long enough to permit adequate percolation into tumour nodules, but short enough to prevent protracted irradiation of normal organs by radioactivity circulating in the bloodstream. Blood clearance of mAb constructs depends not only on their size, relative to the renal threshold and charge but also on their immunogenicity and Fc and Fv receptor binding [72 75]. Radiolabelled murine mAbs such as ^{131}I tositumomab and ^{90}Y ibritumomab tiuxetan have effective blood half-lives of 54 and 28 hours respectively. This time scale correlates well with the reported time taken for maximal penetration of murine antibodies into tumour sites. Press et al using tumour biopsies and quantative gamma camera imaging have demonstrated that maximal penetration occurs approximately 24-48 hours after murine antibody infusion [76]. These studies were performed in murine models with subcutaneous lymphoma and whilst the results from these models may be respresentative of the time taken for penetration of

radioimmunoconjugate of advanced tumour nodules from lymphoma or from solid tumours, it is less likely that results from this type of model system will be respresentative of targeting of lymphoma in the bone marrow or lymph nodes found in the clinical situation. In patients with preserved nodal architecture maximal tumour as well as BM penetration is likely to occur far more rapidly. Logically the optimum blood effective half-life should be such that most of the radioactivity is emitted around the time of maximal tumour uptake. A longer half-life would result in excess normal tissue exposure to non-targeted circulating immunoconjugate and shorter would result in much of the radiation being emitted before the conjugate has reached the tumour.

With the advent of chimeric and humanised antibodies, constructs of lower immunogenicity with substantially longer half-lives are now available. The benefit this confers in terms of improved tumour penetration and enhanced ability to recruit host immune effectors versus the potential for increased toxicity due to the prolonged circulation of radioimmunoconjugates has not been fully investigated. Initially due to concerns that this increased half-life would substantially increase toxicity there was reluctance to use chimeric or humanised mAb in RIT. This explains why despite the arrival and success of rituximab the only commercially available radioimmunoconjugates are derived from murine mAb. More recently studies have been undertaken with chimeric radioimmunoconjugates and to date this excess toxicity has not been manifest [77] [78]. When discussing the pharmacokinetics of radioimmunoconjugates it is important to remember that the pharmacokinetics of therapeutic radioimmunoconjugates for NHL may also vary substantially between patients depending on tumour burden, antigen density, presence of circulating antigen and the spleen size. This is most dramatically illustrated by the dosimetry studies performed prior to the administration of ^{131}I tositumomab which indicate a greater than 3-fold variation in the whole body effective half-life between patients. This variabilty results in a need for individualised patient dosimetry for the safe and effective delivery of this agent, the details of which are discussed below (1.4.1).

Surprisingly the assumption that, the higher the avidity of a mAb for its tumour antigen the better it would be for RIT, suggested above appears to be incorrect. Antibodies with high avidities will bind irreversibly to the most accessible antigen in peripheral locations or in the perivascular space and only when all these sites are saturated will it penetrate to more inaccessible deeper parts of the tumour [79]. Antibodies with lower avidity on the other hand will diffuse more rapidly down the concentration gradient into the centre of the tumour as has been illustrated by a series of experiments in which quantitative images of the temporal and spatial heterogeneity of a series of antibodies in tumour were acquired using radioluminography. The specific antibodies delivered a high dose to the viable peripheral cells of the tumour while non-specific antibodies accumulated and became trapped in the necrotic centre of the tumour. This effect of antibody avidity on tumour penetration called the 'binding site barrier' principally effects large tumour masses and its importance in RIT is described in section 1.3.2.2.

1.3.2.2   Tumour Factors

The binding site barrier referred to above seems not only to effect large solid tumour masses but also appears to be important when there is a significant amount of tumour antigen on accessible normal tissues such as the spleen. In this situation the spleen acts as an antigen 'sink' trapping much of the administered radioimmunoconjugate and diminishing the dose to the target tumour sites. Early biodosimetry studies identified this negative impact of splenomegaly on the targeting of RIT to tumour and revealed that this could be overcome by administering a 'pre-dose' of unlabelled antibody. Buchsbaum et al, using the Raji lymphoma xenograft model in athymic nude mice, were the first to investigate the concept of the pre-dose. These workers demonstrated that administration of unlabelled antibody (B1) resulted in a 44% increase in tumour uptake when an ^{131}I labelled dose of B1 was administered 2 hours later. There was a corresponding reduction in the uptake in the spleen while the blood activity was significantly greater. The benefit from pre-dosing was greater than administering the additional unlabelled simultaneously and the benefit increased as the dose of unlabelled antibody was increased from 36 to 96

then 996µg although there was a plateau at the highest pre-dose level [80]. This benefit has also been seen in other preclinical models [81]. It has been hypothesised that the benefit from the pre-dose results from saturation of competing antibody binding sites on B cells in the blood and spleen in addition to non-specific FcR binding. The pre-dose has the effect of ensuring that the radiolabeled antibody remains available for binding to the target tumour cells. It also has the effect of substantially increasing the serum half-life of the radioimmunoconjugate which as discussed above may improved penetration of tumour nodules. [82 83].

The pre-dose was investigated in the clinical setting by Kaminski and colleagues during the first ^{131}I tositumomab clinical studies. They confirmed that administration of a pre-dose consistently prolonged both blood and whole body clearance of radioimmunoconjugate and that in a patient with splenomegaly administration of the pre-dose dramatically improved tumour targeting [48]. This observation was confirmed in the phase I dose escalation trial that followed and in studies of ^{90}Y ibritumomab tiuxetan [84] [85]. The practice of administering an unlabelled predose is now well established in clinical practice although the optimum dose, timing and the mechanisms underlying, the benefit remain incompletely understood. There is little doubt that a pre-dose improves the biodistribution of radiolablelled antibodies to tumour in patients with splenomegaly and in those with high numbers of circulating tumour cells, however it may not be necessary for all patients.

For bulky tumour masses in addition to the binding site barrier there is the slow and inefficient diffusion and convection of antibodies to the centre of large tumour masses to contend with. In solid tumours it is well established that intra-tumoural pressure increases with tumour size further opposing the percolation of antibody to the centre of tumour. In haematological malignancy the importance of this factor is less clear however even in lymphoma, which generally arises from vascular nodal structures, as tumours become advanced the normal nodal architecture is lost and diffusion of antibody to the centre of the lymphoma tumour mass may become a limiting factor.

Figure 1.6. Physical barriers to delivery of radioimmunoconjugate to tumour cells.
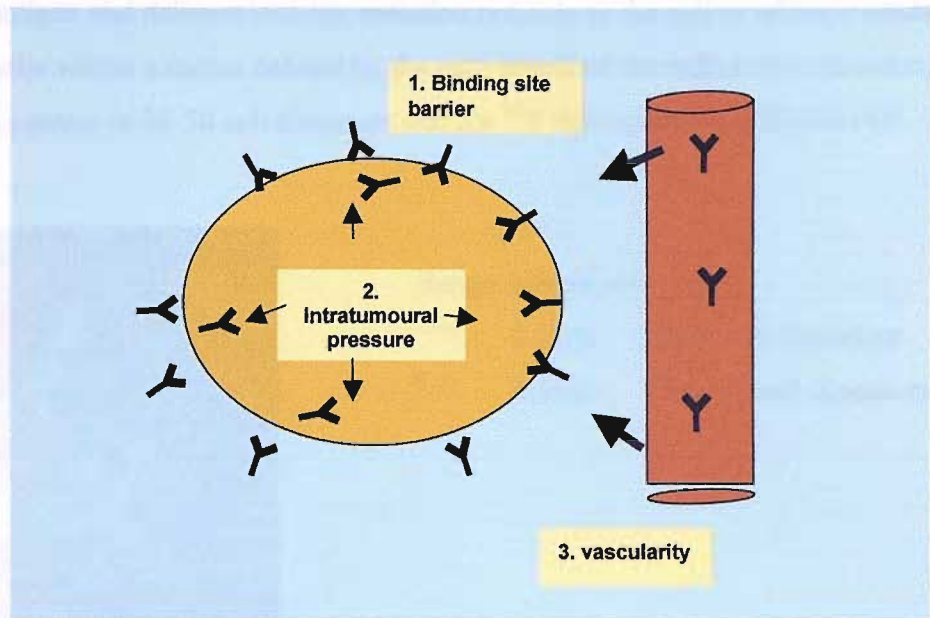
All the factors described above and illustrated in figure 1.6 combine to ensure that even in optimum conditions with the best antibody construct and delivery schedule antibody will be unable to reach a significant proportion of tumour cells. It is this fact that makes the addition of a radioisotope to mAb so attractive. In RIT every cell does not need to be targeted for successful therapy as, with a path length measured in millimetres, beta emitters will deliver cytotoxic doses of radiation not only to the targeted cell but many surrounding cells through the so called 'cross fire effect' as illustrated in figure 1.7.

Figure 1.7 The cross-fire effect. MAb conjugated to a radioisotope binds to tumour associated antigen and delivers ionising radiation not only to the cell to which it binds but also to cells within a radius defined by the path length of the radioactive emission. For ^{131}I this equates to 30-50 cell diameters and for ^{90}Y this equates to 200-300 cell diameters.
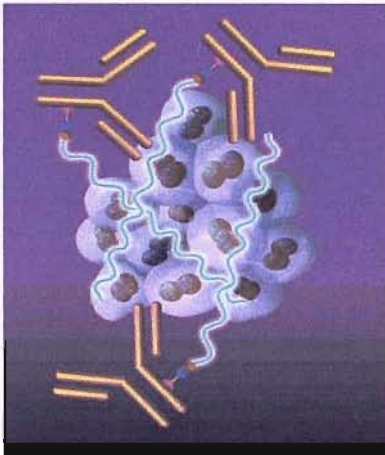
Range of beta particle

^{131}I	0.8mm	30-50 cell diameters
^{90}Y	5.3mm	200-300 cell diameters

1.3.3   The Isotope

Radioactive isotopes may emit a variety of ionising particles capable of killing eukaryotic cells. Choosing an isotope with the optimum emission characteristics is integral to successful RIT. A wide range of isotopes have now been tested both in the preclinical and clinical setting. The factors thought to be important in choosing a radionuclide for RIT are

1. Type of emission, alpha, gamma or beta and the range and energy of ionising radiation emitted.
2. Radionuclide chemical labelling properties and stability.
3. Radionuclide conjugate physical and biological half-life.
4. Size and distribution of targeted tumour deposits.

Analysis of these factors has identified the properties required of the ideal radionuclide. This will have a half-life of 1.5 to 3 times the time taken for optimum tumour to normal tissue conjugate distribution to be achieved. It will have a non-penetrating emission of high energy such that it is cytotoxic to both the targeted cell and those around. The optimum range of this cytotoxicity will depend on the size of the tumours being treated. For bulky tumours a range of as much as a 1cm may be optimum whilst for small tumour nodules a range of 1-2 mm will be preferable to avoid excessive deposition of radiation outside the tumour target. An additional gamma emission is preferable to enable imaging of targeting and dosimetry calculations. This should be of low energy (100-200 KeV) for optimum resolution and a minor component of the total radiation emission in order to avoid excessive normal tissue irradiation and the problems with radiation exposure to medical personnel and the general public. The radionuclide should produce conjugates that are stable in vivo with simple chemistry to facilitate local conjugation as well as being relatively inexpensive and readily available.

No single radionuclide has all these properties but several have now been extensively studied both in the preclinical and clinical setting. [131]I has the advantage of a proven safety profile and familiarity with a long history of successful use in the management of thyroid cancer [86]. It is readily available, inexpensive, easily conjugated and emits both beta particles with a path length of 1mm and penetrating gamma emissions. The gamma emissions enable imaging but due to the high energy of these emissions at 0.37 MeV the resolution of the images is poor. As these gamma emissions make up over 80% of the total emission they result in a significant non-specific normal tissue dose and lead to radioprotection issues such that non myeloablative doses administered in the UK require a 5-6 day hospital admission. [131]I immunoconjugates have relatively poor in vivo stability with rapid dehalogenation on internalization however provided the thyroid gland has been adequately saturated with potassium iodate before hand the free iodine will be rapidly excreted through the kidneys minimizing further exposure of normal tissues to untargeted radiation.

^{90}Y offers a number of theoretical advantages over ^{131}I. It is a pure beta emitter delivering higher energy radiation (2.3MeV v 0.6MeV) at a longer path length (5mm v 1mm). This enhances the "crossfire effect" and may be advantageous in treating larger, poorly vascularised tumour nodules or tumours with heterogeneous antigen expression [87]. This longer path length will however increase the normal tissue dose when targeting microscopic disease for which the shorter path length of ^{131}I may be preferable. The absence of penetrating gamma emissions enables delivery as an outpatient and minimizes radiation exposure to staff and public. Conjugation, though requiring more complex chelation chemistry, results in a stable product that if internalized, will be retained within the cell so called 'residualising'. The disadvantages of ^{90}Y are its greater expense, the need to use a surrogate isotope Indium-111 (^{111}In) to obtain images for dosimetry and its propensity to accumulate in bone with the resulting potential for increasing the non-targeted radiation dose to the bone marrow. The half-life of ^{90}Y is 64 hours while that of ^{131}I is 192 hours making handling for both relatively straight forward and ensuring that the radioisotopes have not decayed excessively before the conjugate reaches its target.

Rhenium-186 and Copper-67 have physical and chemical properties that make them attractive alternatives as indicated in table 1.6 however their availability is limited and they will not therefore be discussed further [53].

Astatine-211 is an alpha emitter producing a particle of very high energy but with a very short path length. The high Linear Energy Transfer radiation of alpha emitters may be lethal to cells with a single hit however the very short path length means that the isotope must be internalised to be effective and has no cross fire effect. This makes them suitable only for easily accessible tumours such as leukaemic cells in blood or bone marrow. In addition the half-life of 7 hours is likely to severely limit availability for the foreseeable future despite promising preclinical and clinical results [88] [89].

From this discussion it is apparent that no one radionuclide is optimal for every clinical situation. The physical properties of ^{90}Y may be better for bulky disease while ^{131}I may be better for smaller tumour nodules and Astatine-211 may have a place in the treatment

of minimal residual disease and leukaemias where treatment is aimed at individual cells. Currently the logistics of combining multiple radionuclides in a single treatment are sufficiently challenging that this type of approach has not been adopted, however such an approach could theoretically improve the delivery of radiation to the target tumour cells and may find a place in the therapeutic strategies in the future.

Table 1.6 Properties of available radionuclides. X_{90} is the range within which 90% of the energy of a beta particle is deposited. Adapted from [90]

Radioisotope	Half-life	Emission		Pathlength X_{90} (beta emission)	Optimal tumour diameter for cure
Iodine-131	8.1 days	Beta	0.6 MeV	0.8mm	3.4mm
		Gamma (81%)	0.37 MV		
Yttrium-90	2.5 days	Beta	2.3 MeV	5.3mm	34mm
		Gamma	nil		
Rhenium-186	3.7 days	Beta	1.1 MeV	1.8mm	9mm
		Gamma (9%)	0.14 MV		
Copper-67	2.5 days	Beta	0.4-0.6 MeV	0.6mm	2mm
		Gamma	0.185 MV		
Astatine-211	7 hours	Alpha	5.9 MeV	0.08mm	Single cells
		Electron capture 7.45 MeV			

1.3.4 Dose Rate and RIT

Radiation whether in the form of X-rays, gamma rays, beta particles or alpha particles is conventionally considered to kill cells by inflicting irreversible damage on DNA, thereby preventing cells from replicating and carrying out other vital cell functions. It is well established that as the dose of radiation delivered increases the number breaks in DNA increases and greater tumour cell killing is seen. With sparsely ionising radiation as delivered by gamma rays and beta particles, single strand breaks in DNA are predominantly produced which are potentially reversible provided they are repaired

before another event occurs nearby resulting in a double strand break. This ability to repair single strand breaks has an important impact on the efficacy of RIT, which delivers radiation at a low exponentially declining dose rate. Low dose rate (LDR) radiation in delivering a dose over a time course that is >600 x longer than that required for the administration of the same dose of conventional or high dose rate (HDR) EBRT allows substantial time for repair of these single strand breaks. As might be expected, for some tumour types, such as melanoma, a dose of LDR radiation will be substantially less effective than the equivalent dose of HDR radiation [91] [92]. Interestingly for lymphoma LDR appears to confer an advantage over HDR. This may be because lymphoma cells have less potential for DNA damage repair, reducing the effect of lowering the dose rate, furthermore some cells including lymphoma cells may become arrested at the G2/M interface of the cell cycle when exposed to low dose rate radiation. These cells trapped in this radiosensitive phase of the cell cycle are more susceptible to the lethal effects of radiation causing a phenomenon known as the inverse dose rate effect [70]. The impact of these dose rate effects in vivo remains unproven however the success of RIT in the treatment of lymphoma when delivering remarkably small doses of radiation supports the theory that a LDR is advantageous in the treatment of lymphoma.

1.4 RIT DOSIMETRY

Determining the dose delivered both to tumour and critical normal tissues such as the bone marrow represents a major challenge in the context of RIT and complicates attempts to optimise the dosimetry of RIT through dose escalation or alterations in scheduling.

1.4.1 Bone Marrow Dosimetry

As with any anti-neoplastic therapy there is a constant effort to maximise the cytotoxic effect of the treatment on the tumour whilst minimising the adverse effect on normal tissues. Despite the targeting ability of mAb, with RIT, normal tissues will absorb the majority of the administered radiation dose. A significant proportion of the dose will be absorbed by the bone marrow and it is this radiosensitive organ that limits the radiation dose that can be safely administered. Measuring the dose absorbed by the bone marrow is far from straight forward and it has proved difficult in studies to identify a clear correlation between, the estimated bone marrow dose and the resulting bone marrow toxicity. Indeed it has also proved extremely difficult to demonstrate a correlation between tumour dose received and the tumour responses. It seem likely that for both these situations it is not that there is not a dose response but that it is difficult to measure due to substantial inter-patient variation and confounding factors such as underlying bone marrow reserve, tumour radiosensitivity and cytotoxic effects of the unlabelled antibody obscuring the dose-effect relationship.

During RIT the bone marrow is exposed to beta radiation from radioimmunoconjugates circulating in the blood, which is direct communication with the red bone marrow space. Furthermore many of the antibodies used to treat NHL will preferentially accumulate in the bone marrow as they bind not only to tumour cells that frequently reside in the bone marrow but also to normal B cells expressing the tumour associated antigens used for

this targeted therapy. Bone marrow toxicity is manifest as thrombocytopenia and leukopenia/neutropenia. Non dividing maturing cells within the bone marrow are relatively radioresistant and it is known that mature platelets, granulocytes and red cells will tolerate higher radiation doses. Stem cells and progenitor cells are, on the other hand, very radiosensitive with a D_0 of 0.6 to 1.2 Gy [93]. Our current understanding suggests that it is damage to these progenitor cells that results in thrombocytopenia and neutropenia 4-6 weeks after administration of a radioimmunoconjugate.

A range of methods has evolved for measuring the dose to the bone marrow. These include a method based on the measurement of the blood clearance of radioactivity. This assumes that the concentration of radioactivity in the marrow is always approximately 0.36 x that in the blood [94]. Such a method is inadequate for conjugates that target elements of the marrow, as used in treatment of haemopoetic malignancies such as NHL, or when there is significant involvement of the bone marrow by the targeted tumour. In these situations estimates of bone marrow dose have been obtained using imaging methods, obtaining planar imaging data from selected regions of marrow such as the lumbar vertebrae or sacrum. A frequent problem with such methods is the presence of tumour overlying the sacral and lumbar spine areas. Although such techniques in skilled hands have provided evidence of a correlation between the calculated marrow dose and haematological toxicity [95] there is a large potential for error and the results have not been replicated when used in a multi-institutional setting [96]. A further technique for estimating the radiation dose to bone marrow has been exploited by Wong et al [97]. This involves measuring the increase in frequency of stable chromosomal translocations in peripheral blood lymphocytes following a dose of RIT. Using this technique the strongest correlation to date has been observed between radiation dose and bone marrow toxicity. However, this technique, even with advances in the automated counting of stable chromosomal translocations remains slow and laborious and is likely to remain as a research tool for the foreseeable future.

The complexities associated with the clinical application of complicated imaging protocols and the subsequent calculations for bone marrow dosimetry have stimulated the

development of a surrogate dose estimate to indicate the relative magnitude of bone marrow radiation dose [98]. This is the calculated total body absorbed radiation dose, first used in the dose escalation phase I study of ^{131}I tositumomab. In this study population, which had less than 25% bone marrow involvement by tumour the total body dose was found to be a robust predictor of haemopoetic toxicity and a total body dose of 75cGy was established as the Maximum Tolerated Dose (MTD). The total body dose is calculated by delivering a dosimetric dose of 185 Mega Bequerel (MBq) of radioimmunoconjugate followed by quantitative gamma camera images at three time points over the course of the next week. The corrected whole body counts at the three time points are used to model an exponential clearance rate for the radiolabeled antibody. From this the residence time of the conjugate can be calculated. This is the time taken for the activity to fall to $1/e$ (about 37%) of its initial value. This residence time can then be used to calculate the size of therapeutic dose in MBq that it is necessary to administer to give the desired total body exposure (see Chapter 2 section 2.9.1).

The importance of using the individualised patient dosimetry described above for the administration of ^{131}I tositumomab is clearly demonstrated by an analysis in which the MBq/kg dose calculated to deliver a total body dose of 75cGy varied over a greater than 3-fold range. If the prescription had been based on weight alone more than half of patients would have received >10% more or less than the target dose [99]. Such wide pharmacokinetic variation has not been seen with the use of the residualising radiometal isotopes such as ^{90}Y where there is very little renal excretion of the isotope. Probably as a result of this difference no comparable correlation between whole body absorbed dose and myelotoxicity has been seen with ^{90}Y ibritumomab tiuxetan. In an analysis of 4 clinical trials with this agent, including a total of 179 patients, no correlation was seen between haematological toxicity, estimates of red marrow radiation absorbed dose, total body radiation absorbed dose, blood effective half-life or blood AUC. At non-myeloablative doses administration based on body weight alone resulted in only transient and reversible haematological toxicity and appeared to be safe in patients with adequate bone marrow reserve and less than 25% bone marrow involvement[100]. For ^{90}Y ibritumomab tiuxetan therefore in contrast to ^{131}I tositumomab the variation in bone

marrow reserve outweighs any pharmacokinetic variability simplifying administration and enabling delivery without a prior dosimetric study.

1.4.2 Tumour Dosimetry

Radiation dosimetry is routinely performed prior to clinical EBRT. Direct measurement of absorbed dose is difficult due to the invasive nature of even the smallest dosimeters, however dose estimations can be accurately calculated based upon known dosimetry and computerised tomography software algorithms. For RIT such estimates are made more complex by the low exponentially decreasing dose rate of the radiation, heterogeneity in the distribution of radiation within the tumour, the combination of gamma and beta emissions and in the case of radiosensitive NHL changes in the volume of the tumours over a timescale comparable to the effective half-life of the radioimmunoconjugate. In pre-clinical studies directly measuring the activity within a given piece of tissue after dissection from the study animal and quantifying the dose as activity in MBq/gram can overcome these problems. In clinical studies estimates of dose have until recently been based on information from planar gamma camera views. Even with reasonably accurate volumes determined by CT, the use of conjugate view scintigraphy provides information with a high standard error due to overlap between blood vessels, tumour and normal organs [101]. Using newer single photon emission computed tomography (SPECT) approaches with CT to SPECT data transformation and appropriate corrections for attenuation and scatter more accurate quantitation may be achieved and with such technology a relationship between tumour response and tumour radiation dose from RIT using ^{131}I tositumomab has been reported.[102]. Other investigators however, using this same technology on a similar group of patients, have failed to duplicate this finding [103]. The complexity of calculating the estimated dose to tumour is emphasized in a recent study by Siantar et al in which an attempt was made to take into account the effect of nodal regression during delivery of RIT in the form of ^{131}I Lym-1. A dose correction of up to a factor of 5 had to be applied when nodal regression was taken into account and for 50 % of the nodes studied a correction factor of greater than or equal to 2 was required [104]. When factors of this magnitude are being applied to calculations requiring

multiple steps each of which incorporates a significant potential error the practical value of the final tumour dose estimate makes its overall validity questionable.

1.5 CLINICAL EXPERIENCE WITH RIT FOR NHL

Following the development of robust techniques that enable the safe delivery of non-myeloablative doses of RIT for NHL, a wide range of clinical studies have been performed attempting to determine the efficacy of the available radioimmunoconjugates and identify the optimum clinical setting for their use. It is 15 years since the first use of RIT in the treatment of lymphoma and several thousand patients have now been treated using this modality. Mature follow-up data now indicates that extremely durable remissions are achievable even in heavily pre-treated patients. The two reagents that have been most extensively investigated are ^{131}I tositumomab (Bexaar^{TM}) and ^{90}Y ibritumomab tiuxetan (Zevalin^{TM}).

1.5.1 ^{131}I Tositumomab

Tositumomab was interestingly the first mAb discovered against a B-cell antigen and thus was designated as B1, named before the antigen was re-designated as CD20 with the advent of the first cluster designation workshops. Kaminski and colleagues at the University of Michigan have pioneered the non-myeloablative approach with this radiolabeled murine mAb. Since 1990 over 800 patients with "low grade" and transformed NHL have been treated with ^{131}I tositumomab within clinical trials. Long term follow up data was presented at ASH 2002 on 250 of these patients indicating a response rate of 56% with 30% of patients achieving a CR. Most impressive was that 70% of the patients who achieved a CR are alive and remain in CR at up to 7.8 years with a median follow up of almost 4 years [105]. An analysis of prognostic factors has confirmed that this remarkable durability of response cannot be accounted for by patient selection in the reported trials [106]. Of the patients that achieved CR 89% had stage III/IV disease, 32% had no response to their last therapy, 45% had >4 prior therapies, 69% had

a modified IPI greater than or equal to 2, 50% had bulky disease and 43% had bone marrow involvement.

Impressive response rates have also been seen in patients that were refractory to rituximab. Horning and colleagues have treated 40 patients with low grade NHL, 72% of which had received four or more previous lines of therapy and 60 % of whom had failed to respond to rituximab. An overall response rate of 68% with a CR rate of 30% was noted and a median duration of response of 14.7 months reported. Again the durability of the responses is impressive with 9 of the 12 complete responders remaining in CR at the last analysis, with follow-up ranging from 12-26 months [107]. More recently an analysis of 230 patients treated with ^{131}I tositumomab was made. Independently assessed durable CR's were noted with a similar frequency in patients with rituximab-refractory disease (28%) and rituximab naïve, but chemotherapy refractory disease (23%). With a median follow-up of 4.6 years, 75% of the patients with a durable CR continue in complete remission [108].

Recent data with ^{131}I tositumomab have confirmed that this form of RIT is more than targeted radiation. In a study comparing unlabeled tositumomab versus ^{131}I tositumomab an improvement in responses rates was seen with the conjugation of ^{131}I but significant responses were also seen with the unlabelled mAb alone confirming the in vitro activity of tositumomab previously discussed. In this study of the 78 patients treated an overall response of 55% with ^{131}I tositumomab (Bexxar) versus 19% (p=0.002) with tositumomab alone was reported. The CR rate was 33% versus 8% (p=0.002) and the median duration of OR not reached versus 28.1 months. Of the patients who had a CR after ^{131}I tositumomab, 71% (10/14) remained in CR for 29.8+ to 71.1+ months. Two patients who achieved a CR following unlabelled tositumomab have ongoing responses at 48.1+ to 56.9+ months [109].

Highly promising results have also been seen in the frontline treatment of previously untreated low-grade lymphomas using ^{131}I tositumomab. Kaminski et al have reposted results for 76 patients with a median follow-up of 5.1 years. An encouraging overall

response rate of 95% was seen with 74% achieving CR and a median progression free survival of 6.1 years [110].

The long-term adverse effects with ^{131}I tositumomab appear to include, a clinically significant rate of hypothyroidism of 12% at 4 years [105]. This can however be easily managed with thyroid hormone replacement. Of greater clinical significance treatment related myelodysplastic syndrome (MDS) and acute myeloid leukaemia (AML) are potential concerns following exposure of the bone marrow to radiation during RIT. The most recent update of an analysis addressing this question for 1071 patients treated with ^{131}I tositumomab who had received a median of three different prior chemotherapy regimens is however reassuring and shows that the incidence of MDS/AML is consistent with that expected from chemotherapy and radiotherapy alone in this patient group at 1.6% per year. Of the 25 cases of MDS/AML analyzed, 10 were found to have MDS in their pre-^{131}I tositumomab bone marrow biopsy specimens [111].

1.5.2 [90]Y Ibritumomab Tiuxetan

[90]Y-ibritumomab tiuxetan was the first radioimmunoconjugate to be granted FDA approval. One of the studies included in the submission to the FDA was a randomised controlled trial whereby ^{90}Y-ibritumomab tiuxetan was compared with rituximab in relapsed or refractory low-grade B-cell NHL [46]. Seventy-three patients received two doses of rituximab $250mg/m^2$ a week apart as pre-dosing followed by a single dose of ^{90}Y-ibritumomab tiuxetan 0.4mCi/kg. Seventy patients in the control arm received rituximab $375mg/m^2$ weekly for 4 weeks. The overall response rate was 80% for the labelled antibody group versus 56% for the rituximab alone group (P=0.002). Complete responses were 30% and 16% in the ^{90}Y-ibritumomab tiuxetan and rituximab groups respectively. This data was recently updated at ASCO 2003 and although the study was not powered to demonstrate differences in time to event variables the maturing results indicate that for the patients with follicular lymphoma the median duration of response was 16.7 months versus 11.2 months in the rituximab alone arm [112]. These highly promising results demonstrated for the first time that RIT can lead to superior overall and

complete response rates to those seen with "naked" mAb. Both regimens were well tolerated but as expected there was more myelosuppression in the RIT group. An analysis of all patients treated in ^{90}Y ibritumomab tiuxetan trials (n = 261) indicates that 28% will experience grade 4 neutropenia and 8% will experience grade 4 thrombocytopenia [113]. [90]Y ibritumomab tiuxetan like ^{131}I tositumomab also appears able to deliver durable remissions and for those patients that achieve a CR, a median duration of response approaching 2 years and ongoing responses of more than 4 years have been reported [112].

Clinical responses have also been observed for ^{90}Y ibritumomab tiuxetan in transformed follicular and relapsed de novo diffuse large B cell lymphoma (DLBC). A phase I/II study reported a response rate of 58% with a 33% CR rate in a group of patients that had relapsed following 2 previous chemotherapy regimens that included CHOP [114]. A confirmatory phase II trial of 104 patients over the age of 60 with relapsed DLBC was reported at ASH in 2004 reporting an ORR of 44%. The results were stratified according to prior exposure to rituximab and even for the group previously exposed to rituximab there was a response rate of 19%[110].

Another radioimmunoconjugate, which has been investigated, targets the HLA-DR variant antigen using the Lym-1 mAb. This is an IgG2 murine antibody generated after immunisation of mice with Burkitt's lymphoma. The first published clinical RIT studies in B cell lymphoma and CLL were reported by DeNardo and colleagues using this antibody in 1988 [115]. Although this agent has not been developed commercially to the same extent as the anti-CD20 radioimmunoconjugates, an extensive series of pre-clinical and clinical studies labeling the antibody with a variety of isotopes and delivering the conjugate according to a range of doses and schedules has proved valuable in advancing our understanding of this field [53 87 116 117].

Epratuzumab, a humanized mAb directed against the CD22 antigen, is also in advanced stages of clinical development. CD22 is expressed on a large proportion of B cell lymphomas and is rapidly internalized on binding. The initial studies using epratuzumab

conjugated to ^{131}I, but given the known internalization, further work has been performed with epratuzumab conjugated to ^{90}Y and the results suggest increased efficacy of this approach. A recent dose escalation trial reports 9 of 20 assessable patients showing objective responses with 2 complete responses [118].

1.5.3 RIT and Chemotherapy

Despite these promising results it seems unlikely that RIT used alone will be a curative approach for most lymphomas. The future for RIT is therefore likely to involve integration into chemotherapy schedules. Recently published data with ^{131}I tositumomab suggests that this type of approach offers great promise for the future. There are currently a number of important clinical trials recruiting or awaiting publication that will substantially help in determining the optimal approach to take. One of these is a multi-centre European study randomising to treatment with or without ^{90}Y ibritumomab tiuxetan after CVP chemotherapy in "low grade" follicular lymphoma. Meanwhile the South West Oncology Group (SWOG) have studied the feasibility and tolerability in a phase II trial of CHOP chemotherapy followed by ^{131}I tositumomab for previously untreated follicular lymphoma [119]. The response rates were high at 95% with acceptable haematological toxicity occurring predominantly in the CHOP phase of the protocol. This group and the CALGB are currently conducting a prospective randomised trial (S0016) comparing CHOP plus rituximab or CHOP plus ^{131}I tositumomab in patients with newly diagnosed follicular lymphoma. Based on the success of combining rituximab with CHOP chemotherapy in the elderly the combination of ^{90}Y ibritumomab tiuxetan with CHOP chemotherapy is being investigated for the treatment of diffuse large B cell lymphoma in a UK based investigator led phase I/II study.

1.5.4 Myeloablative RIT

All the studies described above have delivered RIT at non-myeloablative doses. It is however possible to deliver 3 fold higher doses of RIT if reconstitution of the bone marrow is subsequently provided by infusion of stored peripheral blood stem cells. Press and colleagues in Seattle, have pioneered this myeloablative approach and have arguably achieved the best results thus far reported in clinical RIT, albeit in a highly selected group of patients. They first performed a dose escalation study using a dosimetric study to determine the radiopharmaceutical dose that would deliver no more than the defined maximum radiation doses to normal organs, excluding marrow, in each patient. Cardiopulmonary toxicity was experienced at the highest organ doses of 27 and 31 Gy and 27 Gy has subsequently been used as the MTD [120]. In this high dose study, a clear correlation was observed between administered radiation dose, calculated radiation dose, and toxicity to heart, lung and kidneys. This contrasts with the experience at non-myeloablative doses of RIT where the dose response in the bone marrow is largely obscured by inter-patient variability in bone marrow reserve and targeting of RIT to the bone marrow space. In a group of multiply relapsed patients with low grade lymphoma, a durable CR rate of 73% was reported [121] and outcomes have been shown to be superior to conventional high dose chemotherapy and stem cell transplantation in a non randomized cohort analysis [122]. Following this success the same group have reported a CR rate of 91% and a progression free survival of 61% at 3 years in poor prognosis mantle cell lymphoma using high dose RIT with Cyclophosphamide and Etoposide chemotherapy followed by autologous stem cell transplant [123]. Currently however there are very few centres in the world that have the necessary facilities to attempt such an approach resulting in potential sick highly radioactive patients making the more widespread establishment of this approach unlikely at the current time.

1.6 DOSE RESPONSE FOR RIT

The excellent results in selected patients with myeloablative doses of RIT supports the notion that in NHL escalating the dose of RIT to deliver a greater dose of radiation to the tumour may improve the response. This would be in keeping with the experience for most tumour types whereby escalation of the dose of EBRT has been shown to improve responses. The picture is however much less clear in the management of NHL where, as described above, remarkable responses can be seen at very low doses of EBRT with 1.5Gy of fractionated TBI producing respectable response rates [20] and 2Gy x 2 IFRT also producing useful durable responses [18]. There are few trials that have looked systematically at the dose response relationship for EBRT in NHL and it is hard to draw firm conclusions from the available data. Until recently up to 40 Gy in 20 fractions was the widely practised standard supported by a retrospective analysis of 644 patients with stage I/II indolent NHL in which an in field control rate of 78% was found in patients treated doses of <25Gy vs 91% in patients treated with >25Gy [124]. Conflicting with this however a review of the EORTC radiotherapy data[125] has reported no improvement in control for follicular lymphoma above 25 Gy. For aggressive NHL the evidence is also limited but again the ceiling of the dose response effect seems to lie between 30 and 40Gy [126]. The optimal EBRT dose for treatment of localised NHL is remains under investigation. Increasingly 30Gy in 15 fractions is being utilised for aggressive NHL and it represents the experimental arm of the currently recruiting NCRI radiation dose study where the control arm is 40 Gy. For indolent NHL this same radiation dose study randomises patients between 24Gy and 40 Gy.

Determining whether a radiation dose response exists for RIT remains a challenge for a number of reasons. RIT differs from EBRT in terms of dose-rate, heterogeneity of dose distribution and the complexity of calculating the absorbed dose to a given tumour described above. Preclinical studies in a number of different models appear to support the presence of a tumour dose response. Beaumier working on small cell lung cancer xenografts treated with the specific mAb, NR-Lu-10 labelled with rhenium-186

demonstrated that response correlated with estimated absorbed tumour dose (though not injected dose)[127]. DeNardo et al working with breast cancer tumours (HBT 3477) in mice demonstrated that higher doses of ^{90}Y-DOTA peptide-ChL6 produced longer periods of regression with a dose response that reached significance. Other groups working with models in which the conditions are carefully controlled and the tumours remain within a narrow size range have also demonstrated a correlation between both injected dose and estimated tumour absorbed dose and response [128].

Despite these pre-clinical results in solid tumours, early clinical trials of RIT showed either an absent or weak relationship between radionuclide dose and response. Even using the current state of the art technology for defining tumour volume and dose, as described in section 1.4.2 clinical studies have failed to consistently identify a tumour dose response. This failure to identify a tumour dose response is likely be due to a combination of factors. These include, the heterogeneity of the populations studied, most of whom have had multiply relapsed advanced indolent NHL, the difficulty in accurately estimating the radiation dose to tumour because of dose heterogeneity, the effect of nodal regression during the course of the RIT and the inherent limitations in the imaging upon which the dose calculations are based. Probably the most important factor however is the intrinsic tumour cytotoxic activity of the targeting antibody. In many cases this plays a significant part in the clinical response to RIT and may obscure any radiation dose response, as this component of RIT is not measurable using a gamma camera.

In spite of these observations there is some evidence that supports a radiation dose response for RIT. In the selected patients who have received myeloablative doses of RIT remarkably high and durable response rates have been seen [129]. In addition, in the initial studies of ^{131}I tositumomab from the University of Michigan there was a longer disease free survival for the patients that received > 50cGy versus < 50cGy total body dose [130]. More direct evidence comes from a study of previously untreated low-grade NHL in which the dose to individual tumour nodules was carefully calculated and correlated with response to ^{131}I tositumomab. The mean radiation dose to tumours that achieved CR was 720 cGy compared to 369 cGy for tumours that only achieved PR. This difference just

failed to reach statistical significance. When, however, the reduction in tumour size was measured and correlated with the SPECT- corrected tumour dose a positive and significant correlation between dose and the percentage reduction in tumour volume was seen [102].

Given this evidence that increasing the tumour dose in RIT may enhance the response, investigating strategies that enable delivery of a greater tumour dose without increased toxicity should be important. Strategies for improving the selective delivery of radiotherapy to the targeted tumour by, optimising the selection of antibody construct and radionuclide as well as improving the radiation dose distribution by using a 'pre-dose' of cold antibody have been discussed above. Delivering the dose in multiple fractions is an approach that has been shown to be highly successful both in the delivery of EBRT and chemotherapy and therefore warrants investigation as an approach for escalating the dose of RIT.

1.7 FRACTIONATION OF RIT

1.7.1 Rationale

The benefit of fractionation for external beam radiotherapy (EBRT) is well established. The basis for the advantage is that fractionation enhances the differential effect of radiation on tumour and normal tissue, enabling increased anti-tumour efficacy with relative normal tissue sparing. Radiobiological mechanisms that account for this effect include: repair, reoxygenation and redistribution[131]. In contrast to the multiple short bursts of radiation that characterise fractionated EBRT and classically result in tumour cell death through necrosis, RIT delivers continuous and continuously decreasing low dose rate radiation that in NHL appears to kill cells primarily through apoptosis [132]. Because of this difference the fractionation of a dose of RIT is likely to have a different radiobiological effect from that afforded by EBRT however there are a number of reasons for expecting that fractionation may offer a therapeutic advantage.

One mechanism through which fractionation may offer an advantage in RIT for lymphoma is by enabling improved penetration of tumour with subsequent fractions thereby overcoming some of the microscopic non-uniformity of dose. In practice however there may be a range of other factors that come into play. These may include an ability to deliver a greater total dose for a given normal tissue toxicity and additional opportunities to exploit the interaction between radiation, the signalling antibody and the immune system.

As discussed above antibody distribution within a solid tumour is heterogeneous. It is influenced by the variation in vascular density and blood flow within a tumour as well as by elevation of the interstitial pressure and the presence of antigen acting as a binding site barrier inhibiting the inward diffusion of antibody from the periphery towards the centre of a tumour. Despite the use of radionuclides with emissions that traverse many cell diameters, non-uniform radiation dose to different regions of the tumour continues to be a problem for RIT. Griffith et al performed quantitative autoradiography of ^{131}I-Lym-1 mAb in Raji B-cell lymphoma xenografts to obtain a correlation of film density with dose determined by sectioned microthermoluminescent dosimeters implanted in the tumours. The measured absorbed dose heterogeneity varied by up to 400% [133]. Roberson and Buchsbaum investigated the tumour uptake of ^{131}I labelled 17-1A mAb in subcutaneous LS174T colon cancer xenografts as a function of time after injection. Three-dimensional (3D) activity distributions were determined from serial section autoradiographs and used to construct a mathematical description of spatial and temporal changes in dose rate distributions. The characteristic pattern was of a high tumour surface dose at early time points after injection with slow diffusion of activity towards the centre of the tumour. The average 3-D dose rate distributions clearly illustrated the heterogeneity in dose rate throughout the tumour as a function of time [134].

Provided the pattern of radionuclide distribution changes from fraction to fraction, it might be expected that fractionation of a dose of RIT may achieve a more uniform distribution of the radiation dose throughout the tumour. This could result from a

response to the first fraction with a reduction in tumour size leading to a reduction in interstitial pressure and redistribution of blood flow, enabling subsequent fractions to access regions initially poorly perfused by the radioimmunoconjugate.

In addition to reducing the heterogeneity of dose distribution through fractionation, it might be anticipated that by allowing time for recovery of the bone marrow between doses of RIT a greater total tumour dose may delivered. For fractionation to offer a therapeutic advantage the recovery of bone marrow stem cells must be more rapid than the recovery of tumour cells. As bone marrow stem cells are considered to be acutely reacting tissues, with little propensity for repair of sublethal or potentially lethal DNA damage between closely timed fractions, it would, at first inspection, appear that there may be little advantage for close fractionation of RIT on bone marrow toxicity grounds using conventional radiobiology principles. [135]. Despite this theoretical consideration it is clear from both pre-clinical and clinical studies that dividing a dose of RIT will reduce bone marrow toxicity and allow tumour dose escalation. This tolerance to escalation in radiation dose may be explained by the complexity of the bone marrow as an organ that is made up not only of haematopoietic precursors but also stromal cells. These stromal cells may be characterised as late responding tissues with an ability to repair sublethal radiation damage. If this is the case, fractionation would be expected to spare the stromal cells which are needed to support the proliferation of surviving bone marrow stem cells.

A final theoretical mechanism through which fractionation of a dose of RIT may offer an advantage is proposed by Meyn et al [136]. Low dose rate radiation appears to induce cell death predominantly through apoptosis. Lymphoma cells have a particular propensity to undergo apoptosis and this may account to some extent for the success of RIT in lymphoma. Meyn demonstrated that low doses of radiation induced substantial apoptosis in lymphoma cell lines but that the dose response levelled off at doses greater than 7.5Gy. He suggested that this is because only a subset of cells in the tumour have the propensity for radiation induced apoptosis at any discrete time. He demonstrated in his model that multiple smaller fractions of radiation produced a higher total of apoptotic cells than a single larger dose, suggesting that an apoptotic subpopulation emerged

between doses in the fractionated protocols. The hypothesis is therefore that fractionation of RIT can capitalise on this effect for therapeutic advantage.

1.7.2 Preclinical RIT Evidence

Jeffrey Schlom and colleagues first demonstrated an advantage from fractionated RIT in a human colon carcinoma xenograft model, showing that an otherwise lethal dose when fractionated could be delivered safely and resulted in reduced or eliminated tumour growth in 90% of mice [137]. In contrast to a single 600 µCi dose of ^{131}I-B72.3 IgG, after which 60% of mice died of toxic effects, two 300 µCi doses of the same antibody reduced or eliminated tumour growth in 90% of mice and only 10% died of toxic effects. Furthermore, dose fractionation permitted escalation to three weekly doses giving a total of 900 µCi. This resulted in even more extensive tumour reduction and minimal toxic effects. Buchsbaum et al also demonstrated a therapeutic advantage from fractionation when using shorter fraction intervals delivering 3 doses within a week again in human colon cancer xenografts [138]. Further studies using the same model have demonstrated that a higher concentration of the labelled antibody ^{125}I-CC49 is maintained in the periphery of the tumour following two treatments with a 3-day interval than following a single administration of the same total dose. Using serial section autoradiographs Buchsbaum et al and Roberson et al compared the three dimensional dosimetry of LS174T human colon carcinoma xenographs in athymic mice for a single dose, three fractions and a continuous infusion. The fractionated dose produced superior results with reduced radiation dose rate heterogeneity [139 140].

1.7.3 Clinical RIT Evidence

Clinical studies of fractionated RIT are limited in number. This is largely due to that fact that most of the mAb developed for use in RIT have thus far been murine in origin. As a result multiple administrations frequently result in HAMA production, limiting administration to a single dose. Despite this, the DeNardo's have produced some promising results with fractionation using ^{131}I Lym-1 [141]. In the heavily pre-treated patients selected for his study the development of a HAMA response was relatively rare probably due to the underlying relative immunosuppression in this patient group. Thirty patients with indolent NHL or CLL who had progressed despite standard treatment entered the study. All 5 CLL patients had extensive bone marrow involvement and 12 of the 25 NHL patients had substantial infiltration of the bone marrow that would have normally precluded safe RIT. They were treated with ^{131}I labelled Lym-1, a murine mAb that targets the HLA-DR antigen on B cells. Patients were treated with 30 or 60 mCi at intervals of 2-6 weeks. 11 patients completed the intended 300 mCi. Treatment was interrupted by haematological toxicity in 3 patients and HAMA in 3 patients. An objective response rate of 57% was reported which is impressive for a group usually considered untreatable with RIT approaches because of concerns regarding the targeting of this treatment to heavy tumour infiltrates within the bone marrow that may subsequently result in unacceptable myelosuppression. Following the success of this strategy a dose escalation trial was performed to define the MTD of the first 2 of a maximum of 4 doses of ^{131}I Lym-1 given 4 weeks apart [142]. ^{131}I dose was escalated from 40 to 100mCi/m^2 and the non-myeloablative MTD was found to be 100mCi/m^2 for the first 2 doses in patients with no more than 25% bone marrow involvement. All 3 patients at this dose level achieved a CR and 2 of the 3 tolerated the study maximum of 4 treatment doses. In these patients, despite total radionuclide doses corresponding to the MTD for single dose RIT, no incidences of significant bleeding or neutropenic sepsis were reported.

Another study of fractionated RIT reported on 12 patients with metastatic colon cancer treated with ^{131}I chimeric B72.3 [143]. The degree of bone marrow suppression was significantly less for a total dose of 36mCi/m^2 when fractionated into 2 or 3 weekly fractions than seen with the same amount given as a single dose. This confirms the observation that significant dose escalation may be possible without exceeding bone marrow tolerance through fractionation.

Only one study to date has been reported with multiple dosing of radiolabelled anti-CD20 antibodies. This is a phase I study of sequential dosing with ^{90}Y ibritumomab tiuxetan [144]. The doses were given 6 months apart so this can not conventionally be considered fractionation, however the study does demonstrate that following a dose of RIT at the MTD a further dose of radioimmunoconjugate may be safely delivered after a period of bone marrow recovery. In this study the MTD for the second dose was 0.2mCi/kg meaning that a total of 0.6mCi/kg can be given according to this schedule as compared to the single dose MTD of 0.4mCi/kg.

These pre-clinical and clinical studies indicate that fractionation can enable delivery of a greater total dose of RIT without increasing normal tissue toxicity and support the possibility that such an approach will improve the anti-tumour effect. Many issues remain to be addressed if fractionated RIT is to be optimised. These include 1) the number of doses, 2) the dose per fraction, 3) the interval between doses, and 4) the choice of radioimmunoconjugate for a given fractionation schedule.

Two principal approaches to the choice of the fractionation interval can be taken. One option is to take an approach analogous to that used with chemotherapy of giving the MTD, allowing time for bone marrow recovery then repeating the dose. The alternative is to give multiple sub MTD fractions with a relatively short inter-fraction interval, an approach more akin to that used in EBRT, and identify the MTD for the given fractionated dose. There is concern with such an approach, in the context of the delayed nadir seen with RIT, that by delivering further fractions of RIT when the bone marrow is just beginning to recover from the preceding dose and stem cells are proliferating, more

profound bone marrow damage may be sustained. Little progress has been made thus far in determining which of these approaches is preferable because of the large number of potential dose and fractionation schedules to be tested. Attempts to answer this question have therefore turned to mathematical modelling. Shen et al have developed a model for murine bone marrow and tumour that allows prediction of the nadir and duration of thrombocytopenia for various RIT doses and fractionation schemes. This remains to be validated in preclinical studies but indicates that there is a clear theoretical advantage to splitting a dose into 2 fractions but no additional advantage is seen when increasing from 4 to 7 fractions. The output from this model will of course vary depending on the pharmacokinetics of the radioimmunoconjugate used but it may be a tool that enables accelerated identification of the optimum fractionation schedules for subsequent testing in clinical trials [145].

1.8   CONCLUSIONS

In the last 10 years RIT has emerged as a valuable treatment modality in relapsed or refractory indolent NHL. High response rates and remarkably durable remissions have been achieved even in some patients that have exhausted all conventional forms of treatment. Evidence is emerging to support a tumour dose response for RIT and with the advent of chimeric and humanised mAbs fractionation of the RIT dose has become feasible, offering the potential not only for dose escalation but also for improved microscopic tumour dose distribution.

The mechanisms that underlie the success of RIT remain incompletely understood and with the availability of increasing numbers of antibodies and radioisotopes selecting the optimum radioimmunoconjugate is complex and requires pre-clinical and clinical testing. For the radionuclide the choice needs to take into account the emission spectrum, path length, half-life, method of metabolism or excretion and required radiation protection measures. For the mAb the specificity, avidity, size and immunogenicity must be considered as well as the intrinsic anti-tumour efficacy of the antibody both through

recruitment of immune effectors but also and possibly more importantly through direct signalling.

Optimising the scheduling of RIT demands an improved understanding of the pharmacokinetics of mAbs and radioimmunoconjugates and how this varies not only between radioimmunoconjugates and schedules but also between patients.

In order to further investigate the potential of fractionated radioimmunotherapy further pre-clinical and clinical studies are required to address some of the many factors that may influence radioimmunoconjugates. Some of these experiments form the basis of this work described in this thesis.

1.9   AIMS

The focus of this study was to investigate the potential of fractionated RIT in NHL. The aims were:

1. To establish an animal model of fractionated RIT.

2. To set up a phase I/II clinical trial to investigate the pharmacokinetics, feasibility, toxicity and efficacy of fractionated RIT for relapsed or refractory indolent NHL using ^{131}I rituximab.

3. To derive an anti-rituximab idiotype mAb with which to develop an assay for the measurement of serum rituximab concentrations and to use this in the pharmacokinetic analysis of the above clinical trial.

Chapter 2

Materials and Methods

2 MATERIALS AND METHODS

2.1 CELL QUANTITATION

Cell concentrations were determined using a Coulter Industrial D Cell counter (Coulter Electronics, Bedfordshire).

2.2 CULTURE MATERIALS

All cell-lines were cultured in RPMI 1640 medium (Gibco) or Dulbecco's Modified Essential media (DMEM) both supplemented with 100IU/ml penicillin (Glaxo), 100 µg/ml streptomycin (Evans), 50 IU/ml amphotericin B (Fungizone; Squibb and Sons), 2 mM L-glutamine (Gibco), 1 mM pyruvate (Gibco) and 10 % Myoclone Plus Foetal Calf Serum (FCS; Gibco)

2.3 CELL-LINES

2.3.1 Human Lymphoma Cell Lines

The Burkitt's lymphoma cell lines EHRB, Daudi and Raji, the T cell lymphoma cell line Jurkatt, and the myeloma cell line NS-1 were maintained in culture medium described above at 37°C in a 5 % CO_2 humidified incubator. Medium was replenished every 2-3 days. Cells were maintained in log phase of growth for at least 24 hours prior to experiments.

2.3.2 Murine Lymphoma Cell Lines

BCL_1 is a B-cell leukaemia that arose spontaneously in a 2-year old BALB/c mouse and is transplanted into syngeneic recipients by injection of spleen lymphocytes from leukaemic animals[146]

.

A31 is a B cell leukaemia that arose in 1971 in a female CBA/H mouse that had been injected with ^{90}Strontium intra-peritoneally 19 months previously[147]. Experiments described within this thesis were initiated with cells isolated within the first 6 passages after recovery of the cells from cryopreservation. Both tumours develop primarily in the spleen, with a terminal leukemic overspill.

2.4 ANIMALS

BALB/c, CBA, SCID mice and Louvain rats were supplied by Harlan UK Limited (Blackthorn, UK) and bred and maintained in local animal facilities under Home Office regulations. All animals were sacrificed when in the terminal phase of disease or if they exhibited signs of significant distress by exposure to gradually increasing concentrations of CO_2 then cervical dislocation. For the SCID mice with the human lymphoma xenografts the terminal phase was defined as the onset of hind leg paralysis.

2.5 ANTIBODIES

The antibodies used in this thesis are recorded in table 2.1 and 2.2

Table 2.1 Anti-Mouse mAb.

Antibody Clone	Specificity	Isotype	Affinity (Ka M^{-1})	Source/Ref
TI2-3	MHC Class II	Rat IgG1	5.3×10^8	Tenovus
MB2-A4	Rituximab Id	Rat IgG2a	6×10^{10}	Tenovus
MB2-H2	Rituximab Id	Rat IgG2a	1.4×10^{10}	Tenovus
MB2-G3	Rituximab Id	Rat IgG1	1.08×10^{10}	Tenovus

Table 2.2 Anti-Human mAb

Antibody Clone	Specificity	Isotype	Affinity K_A (M^{-1})	Source/Ref
Rituximab(C2B8)	CD20	Chimeric IgG1	$1.25\text{-}2 \times 10^8$	IDEC, San Francisco, CA
Ibritumomab (2B8)	CD20	Murine IgG1		IDEC, San Francisco, CA
B1	CD20	Murine IgG2a	$1.7\text{-}3.3 \times 10^8$	Coulter, Miami, FL
AT80	CD20	Rat IgG1		Tenovus
1F5	CD20	Rat IgG2a	$1\text{-}3.3 \times 10^7$	ECACC Hybridoma
F3.3	MHC class II		1×10^8	Tenovus
AT13/5	CD38	Rat IgG1		Tenovus
OKT3	CD3			
SB2-H2	Human Fc			Tenovus

2.5.1 Antibody Dialysis

Dialysis of samples was performed using Slide-A-Lyzer Dialysis Cassettes (Pierce, Rockford, USA). Samples were dialysed 1:1000 in at least three changes for a time of at least 2 hours per change.

2.5.2 Fluorescein Conjugation Of Antibodies

Antibodies were fluorescein labeled by the method of Holborow and Johnson [148]. 4.5ml of normal saline (0.15 M NaCl, pH 7.4) was added to 50 mg of antibody in the presence of 1mg of the FITC isomer I (BDH) dissolved in 0.5 M carbonate buffer pH 9.5 and incubated for 45 min at 25 °C. Unconjugated FITC was then removed by passage of the reaction mixture through a G-25 Fine (Pharmacia) column, equilibrated with 0.0175M phosphate buffer, pH 6.3, followed by passage through a Diethylaminoethyl (DEAE)-cellulose column.

The majority of the FITC-conjugated antibody was eluted with 0.25 M NaCl in 0.0175 M phosphate as determined by measuring conjugate: protein ratios during elution (calculated as absorbance (Abs) at 495nm and 280nm respectively). Material with a ratio of 0.4-1.0 was pooled for use with final antibody concentration calculated as:
Antibody Concentration (mg/ml) = Abs (280nm) - (0.26 x Abs (495nm)) / 1.35

2.6   ANALYSIS OF ANTIBODY CELL BINDING

2.6.1   Cell-Surface Binding - Radiolabeled Mab.

The binding of radiolabeled antibodies to cells was determined using a method described by Elliot et al.[149]. Briefly, antibodies were radiolabeled with ^{125}I using Iodogen beads as described below. The radiolabeled antibodies were then serially diluted before incubating

70

with $0.5-1.25 \times 10^6$ cells, in a final volume of 1ml, in complete medium for 2 hours at 37 °C. Endocytosis of bound antibody was prevented by the inclusion of NaN_3 (15 mM) and 2-deoxyglucose (50 mM). Following incubation, cells with bound antibody were rapidly separated from unbound antibody by centrifugation through a 1.1:1 (v/v) mixture of dibutylphthalate: dioctyl phthalate oils. This latter step allows separation of bound antibody from free without disturbing the binding equilibrium, facilitating calculation of antibody affinity. The cell pellets with bound radiolabeled antibodies were counted on a gamma counter (LKB Wallace).

2.6.2   Cell-Surface Binding -Immunofluorescence

Cells at 1×10^6/ml were incubated at 4 °C for 30 minutes with the fluorescein conjugated (direct) or unlabeled (indirect) antibody of choice (50 µg/ml final concentration). Cells were then washed once (direct) or twice (indirect) in PBS-BSA-azide (PBS, 1% Bovine Serum Albumin fraction V (BSA; Wilfred Smith Ltd, Middlesex), 20 mM NaN_3) and resuspended at approximately 1×10^6/ml. For indirect immunofluorescence, cells were further incubated for 30 minutes at 4 °C with an FITC-conjugated secondary antibody directed to the first antibody and washed once in PBS-BSA-azide before resuspension to 1×10^6/ml and subsequent analysis.

Analysis was performed on a FACScan flow cytometer (Becton Dickinson, Mountain View, CA, USA). Routinely, 10,000 events were collected per sample for analysis. Cell debris was excluded by adjustment of the forward scatter (FSC) threshold parameter. FITC was excited at 488 nm with emission intensity being recorded in the 515-545 nm wavelength region. Samples were analysed using LYSIS II software (Becton Dickinson). Fluorescence intensities were assessed in comparison to negative control samples and expressed as histograms of fluorescence intensity versus cell number.

2.7 MAB RADIOIODINATION

2.7.1 Iodination

For animal studies ^{125}I and ^{131}I were supplied as sodium iodide in dilute sodium hydroxide solution at pH 10 and free from reducing agent (Amersham International, plc, UK). For clinical study ^{131}I was supplied by MDS Nordion Belgium. Purified antibodies in PBS were iodinated using IODO-beads (Pierce Chemicals Co, Rockford, IL) according to the manufacturers' instructions. For the clinical trial the method was optimized as detailed in chapter 4 (4.3.1.1). The final trial protocol required the addition of 6 IODO-beads to 5mg rituximab (0.5 mls) (Roche Pharmaceuticals) and the required activity of ^{131}I supplied as Na iodide in dilute NaOH buffer at pH10 (27-100 µl) (Nordion MDS) in a sterile reaction vial. The mixture was gently agitated continuously on a mechanical rotator for 15 minutes. The reaction mixture was then separated from the beads by pipette terminating the reaction before dilution into a volume of 30 mls with N Saline and subsequent analysis as below for quality assurance. All handling of the reaction mixture occurs in an isolator (Envair CDE 2GR) maintained to good manufacturing practice.

2.7.2 Labelling Efficiency

Labelling efficiency was determined as the amount of radioactive iodine incorporated into the recovered product as compared to the amount added to the reaction mixture. This varied between 90 and 99% as determined both by instant thin layer chromatography (ITLC) and high performance liquid chromatography (HPLC).

2.7.2.1 Instant Thin Layer Chromatography (ITLC)

A 1 µl sample of reaction mixture was placed 1cm from the end of a strip of chromatography paper (Gelman Sciences Ann Arbor, MI.) cut to be 1cm wide by 10 cm

long. The strip was then placed vertically in 80% methanol of 0.5 cm depth. After 2 minutes the strip was removed and cut in half ensuring that the methanol has migrated well over half way up the strip. The activity in the two halves was then counted in the gamma counter. The iodinated antibody remains confined to the lower half while free antibody migrates with the methanol.

Labelling efficiency = (counts in lower half/ total counts) x100

During development of the labelling protocol for the clinical trial ITLC was performed as described above. During the clinical trial for consistency and convenience Tec control strips for monoclonal antibodies (Bright Technologies, Sheffield) were developed with 0.9% saline according to the manufacturers instructions. Radiolabeled protein remained at the origin while unbound ^{131}I moved with the solvent front.

2.7.2.2   High Performance Liquid Chromatography (HPLC)

HPLC analysis was performed during development of the trial labelling protocol then on all samples prior to patient administration. The HPLC analysis (ProStar Analytical system, Varian) was performed on a 300 x 7.5 mm Biosep SEC S 4000 column (Phenomenex). Columns were equilibrated with 0.1 M phosphate buffer pH 6.75. Flow rate 1 ml/min. Radioactivity was continuously monitored using a NaI detector (Lab Logic, Sheffield). Simultaneously the protein was analysed by UV absorption at 254 nm wavelength.

2.7.3   Immunoreactivity

The immunoreactivity of radio-iodinated mAb was determined using a rapid assay modification of the method described by Elliot et al. [149]. Briefly, Daudi cells in log phase growth were prepared in complete medium at a concentration of 5×10^7/ ml. Serial dilutions were then performed before incubation with the radio-iodinated mAb prepared

at a concentration of approx 2 µg/ml in PBS. 50micl of antibody was added to 500 µl of the cell suspension to give a final volume of 550 µl. The mixture was incubated on rotating wheel to ensure adequate mixing for 1 hour at room temperature. Following incubation, 200 µl of the cell suspension was transferred into a gamma counter tube. A further 200 µl of the cell suspension was centrifuged through a 1.1:1 (v/v) mixture of dibutyl phthalate: dioctyl phthalate oils separating the bound antibody from free antibody without disturbing the binding equilibrium. The resulting cell pellet and 200 µl of suspended cells were counted on a gamma counter (LKB Wallace). The immunoreactivity was estimated by determining the plateau of a graph plotting:

counts in cell pellet / counts in suspension   *against*   *cell concentration.*

It is assumed that this plateau equates to percentage of mAb binding in conditions of infinite antigen excess. Within the clinical trial the immunoreactivity assay was performed on all samples prior to patient administration. To minimise radiation exposure for samples with high specific activity additional dilution was performed and correspondingly fewer cells were required.

2.7.4   Limulus Amebocyte Lysate (LAL) Assay

The rituximab and ^{131}I were supplied sterile and of clinical grade. The IODO-beads were supplied sterile but not licensed for clinical use. The reaction was performed in a registered nuclear medicine pharmacy in a sterile isolator (Envair CDE 2GR). All batches of IODO-beads were tested prior to patient administration using the LAL assay to exclude microbiological contamination. The LAL assay is used to detect endotoxins associated with Gram negative bacteria. The gel clot method was used which is based on the fact that LAL clots in the presence of endotoxin. Reagents for the assay were provided by Cambrex Bioproducts and used according to the manufacturers instructions.

2.8 ^{131}I RITUXIMAB PHARMACOKINETICS AND DOSIMETRY

2.8.1 Whole Body ^{131}I Rituximab Clearance And Whole Body Absorbed Dose Calculation

Whole body radioimmunoconjugate clearance and the administered activity required to deliver a given whole body absorbed dose was determined according to the method described by Wahl et al and detailed below [98].

With any radioimmunoconjugate, a small percentage of the isotope is unconjugated or released from the antibody. Therefore, to prevent free iodine being taken up by the thyroid a daily administration of potassium iodate was commenced 3 days before administration of the radioimmunoconjugate and continued for a total of 35 days. On the day of administration of the dosimetric dose, following premedication with paracetamol and chlorpheniramine, 100 mg/m^2 unlabelled rituximab was administered as a pre-dose followed 2-3 hours later by a 20-minute infusion of 185 MBq ^{131}I rituximab diluted in 30 mls normal saline. Serial whole body gamma camera counts were then obtained immediately, on day 4 and day 6 corrected for background counts and used to determine the clearance rate of the radioimmunoconjugate. An example of the serial gamma camera images is shown in figure 4.6. A source of known activity called 'the standard' was also imaged as a quality control step. Assuming the activity recorded at the time of the first scan was 100%, the percentage of the injected activity remaining at each time point was calculated from quantitative analysis of the gamma camera images. This was plotted on a logarithmic scale and a best-fit line drawn (figure 4.7). The effective half-life is the time taken for the activity to fall to 50% and the residence time is the time taken for the activity to fall to 1/e (about 37%) or 1.443 x the effective half-life. The residence time is the average time that the administered activity spends in the body and is represented graphically in figure 4.8. Because ^{131}I rituximab does not distribute into fatty tissues, the patients maximum effective mass is used to calculate the required therapeutic dose. The effective mass is derived from a table based upon height, weight and gender. Which ever is greater the maximum effective mass or the patients true weight is used to calculate the

required dose in MBq that must be administered to achieve the desired whole body absorbed does in cGy. The equation for this calculation is:

$$\text{Therapeutic dose} = \frac{\text{Activity hours}}{\text{Residence time}} \quad x \quad \frac{\text{desired TBD (cGy)}}{75 \text{ cGy}}$$

The activity hours parameter is obtained from a table derived from the Medical Internal Radiation Dose (MIRD) system [150] utilising height and weight and assuming that the patient is ellipsoid and that the radiation is distributed uniformly through the patient after injection [151].

2.8.2 Determination of Blood Radioimmunoconjugate Clearance

In selected patients blood samples were drawn from the contra-lateral arm of the injection site at serial time points after administration of the radioimmunoconjugate. The activity of the whole blood was measured in a calibrated well counter with corrections made for background activity and decay.

2.8.3 Imaging Of Targeting

Following each dosimetric dose of RIT in addition to the 3 gamma camera images taken for quantitating the whole body clearance of the radioimmunoconjugates additional images were obtained using longer acquisition times to improve the resolution and enable visualisation of targeting of sites of tumour by the radioimmunoconjugate.

2.9 FRACTIONATED RIT CLINICAL TRIAL

2.9.1 Trial Protocol

See appendix 1.

2.9.2 Toxicity Recording

2.9.2.1 Haematological toxicity

According to the trial protocol (appendix 1) following RIT a weekly full blood count was performed until 8 weeks after the second RIT dose or recovery of the platelet count to greater than 100 whichever was longer. The trial protocol dictates that haematological toxicity was graded according to National Cancer Institute of Canada Common Toxicity Criteria and the dose level increased, provided, grade 2 toxicity had not been seen in more than 2 patients 6 weeks after the second RIT infusion. Dose limiting toxicity was defined as any of the following adverse events occurring during the first cycle of RIT.

1. Nadir neutrophil count
   - Absolute neutrophil count (ANC): $< 0.5 \times 10^9 / L$ for > 7 days or
     $$< 0.1 \times 10^9 / L \text{ for } > 3 \text{ days}$$
2. Febrile neutropenia defined as :
   - ANC $< 0.5 \times 10^9/L$ and
   - fever either as three elevations of oral temperature above > 38 °C in a 24-hour period, measured every 8 hours,
   - or a single oral temperature > 38.5 °C, provided that single episode of fever is not clearly related to other events (e.g. blood transfusion)
3. Thrombocytopenia
   - $< 25 \times 10^9 / L$ or thrombocytopenia with bleeding, or requiring platelet transfusion

2.9.2.2 Non Haematological Toxicity

According to the trial protocol biochemistry was also performed weekly with analysis of renal function, liver function and bone profile. In view of the potential for ^{131}I uptake by the thyroid gland TSH was assayed 3 monthly during the first 2 years of follow up and annually thereafter. No other major organ toxicity was anticipated in this study however investigations were to be guided by regular clinical assessment and recorded according to NCIC defined criteria.

2.10 ENZYME-LINKED IMMUN0SORBANT ASSAY (ELISA)

ELISA assays were routinely performed to detect a number of different proteins, but mainly for the determination of serum rituximab concentrations in patient samples. Primary antibody or coating molecule was diluted in coating buffer (15 mM Na_2CO_3, 28.5 mM $NaHCO_3$, pH 9.6) and added 100 µl / well to 96 well plates (Maxisorb, Nunc) either for 1 hour at 37 °C or overnight at 4 °C. Unbound antibody was removed by flicking the plates. The non-specific binding sites on the plates were blocked by the addition of blocking solution (1% (w/v) BSA in PBS) for 1 hour at 37 °C. The plate was then washed three times with wash solution (PBS + 0.05 % polyethylene sorbitan (tween-20 Sigma) using ELISA washer and the next reagent (usually the diluted serum sample), added in a final volume of 100 µl / well, with all dilutions being made in blocking solution. Following incubation for 90 minutes at 37 °C, the plate was washed x 5 in wash solution. A horse radish peroxidase (HRP)-conjugated antibody, specific for the previous reagent, was then diluted to its working concentration in blocking buffer and added (100 µl / well) for a final 90 minutes. Following washing (x5), HRP substrate (20mg o-PhenylDiamine free base (o-PD), 100 ml phospho-buffered citrate pH 5.0 + 20 µl (60 % w/v) H_2O_2) was added and incubated in the dark at 37 °C. The reaction was terminated by the addition of 50 µl/well 5 M H_2SO_4 and the subsequent colour change quantified by measurement of absorbance at 495nm on an automatic fluorimeter (Dynatec 400, Dynatec). Colour change was proportional to protein concentration and

unknowns were determined using standard calibration curves of known concentration, on the day of each ELISA.

2.11 ANTI-RITUXIMAB IDIOTYPE ANTIBODY PRODUCTION

2.11.1 Production of Polyclonal Anti-Rituximab Idiotype Antibody

2.11.1.1 Production of Rituximab F(ab)$_2$ Fragments

Rituximab at 10 mg/ml was dialysed into 0.1 M Na acetate pH 7.5 at 4 °C and then the pH lowered to 4.2 using 2 M Na Acetate pH 3.7. Pepsin (Sigma) was dissolved in 0.07 M Na acetate containing 0.05 M NaCl, pH 4 to give a concentration of 10 mg/ml. With both reactants at 37 °C the pepsin was added to the immunoglobulin at a 3% ratio to give the final digest mixture. A sample was removed immediately to obtain an HPLC profile and the mixture then returned to 37 °C. A 10µl sample was then taken every hour and run on the HPLC when the F(ab)$_2$ peak was no longer increasing the reaction was stopped by raising the pH to 8 by the addition of 2 M TE8. The F(ab)$_2$ was isolated from the mixture by size exclusion chromatography using 2 x ACA44 columns equilibrated in 0.2 M TE.

2.11.1.2 Immunizations

Lou Rats were immunised initially by intra-dermal injection of 100µg of purified Rituximab F(ab)$_2$ protein emulsified in Complete Freund's Adjuvant (CFA). Rats were subsequently challenged 21 days later with secondary boosts of 100 µg Rituximab F(ab)^2 protein emulsified with Incomplete Freund's Adjuvant (IFA) presented by intra-peritoneal injection. Two to three weeks later, mice were given a further 100 µg of protein in PBS by intraperitoneal injection. 6 days later blood was harvested by cardiac puncture and pooled from all rats.

2.11.1.3 Polyclonal purification from serum

The pooled serum was passed through a Protein G (Pharmacia Biotech) column in 0.03 M Tris buffer containing 0.01 M EDTA pH 6.5 to which all immunoglobulins bind. Unbound protein was then washed away by the addition of two column volumes of buffer, and the bound protein eluted with buffer containing 0.5 M NaCl/ 0.5 M Tris and 0.01 M EDTA, pH 8.7. Eluted protein was then blended with an equal volume of this buffer and passed onto a column coated with human IgG (10 ml Sepharose H4B and normal Hu IgG), equilibrated in 0.5 M Tris buffer containing 0.01 M EDTA, pH 8.7 in order to extract all rat anti-human immunoglobulin. The remaining unbound rat anti-mouse immunoglobulin was then run through a column coated with rituximab (5ml Sepharose H4B + 20mg rituximab). Unbound protein was then washed by the addition of two column volumes of buffer and bound Ig (rat anti rituximab idiotype) was subsequently eluted. This was then run through a size separation column to remove rituximab/antirituximab immune complexes.

Despite these purification steps when used to coat the ELISA plate a high background resulted almost certainly due to residual rituximab anti-rituximab immune complexes. The remaining sample was therefore run through a column coated with Sheep anti Hu Ig to extract any rituximab complexes. The Sheep anti Human Ig was first absorbed against rat and bovine Ig to remove any cross reactivity that may extract the rat anti-rituximab idiotype antibody (2 ml sepH4B + sheep anti Hu IgG absorbed against Bovine IgG and Rat IgG).

2.11.2 Production of Hybridoma Secreting Rat Anti-Rituximab Idiotype mAb

2.11.2.1 Immunizations

Performed as described above in section 2.12.1.2 except that three days after the final boost the spleen was harvested for fusion. In addition a blood sample was taken from the animal, the serum of which was used to provide a positive control in subsequent screening.

2.11.2.2 Hybridoma Fusion

Hybridoma fusions were performed based upon the methods of Kohler and Milstein[1], with minor modifications. Immunised rat spleen cells were fused with NS-1 myeloma cells. Log-phase, semi-confluent, myeloma cells (5×10^7/spleen) were washed several times by centrifugation (1500 rpm, 5 min) and resuspension with serum free DMEM to remove all FCS. Ultimately, cells were resuspended into a final 15 ml volume of serum free media. These cells were then incubated at 37 °C until fusion with the splenocytes.

The spleen from the immunised animal was removed, cut up and made into single cell suspension in serum free DMEM by passage through a 70 μm cell strainer (Beckton Dickinson). The suspension was then transferred into a plastic universal and the larger fragments allowed to settle. The supernatant was withdrawn and washed several times in serum free DMEM as above, before resuspension into 10 ml of serum-free DMEM. Spleen cells were then counted and added to myeloma cells at a ratio of 2:1. The resulting mixture was then centrifuged as before and all of the supernatant removed. Over 1 minute, 0.5 ml of 48% (w/v) polyethylene glycol (PEG) in DMEM was slowly added. Maintaining the temperature at 37 °C using a water bath, the cell pellet was gently broken and the cells continually agitated during the addition of 25 ml of serum-free DMEM over 5 min. Cells were then gently sedimented by centrifugation at 800 rpm for 5 min, before gently resuspending the pellet in 100 ml of HAT media (100 μM Hypoxanthine, 400 nM Aminopterin, 16 μM Thymidine in 15 % complete DMEM) in a glass bottle. The bottle was then incubated for one hour at 37 °C to help the clumps disperse before before distributing the medium across the wells of ten 96 well plates (Nunc). Cells were then incubated (37 °C, humidified CO_2 incubator) before demi-feeding (remove 100 μl medium and replace with 100 μl fresh HAT medium) 4 and then again, 7 days later.

2.11.2.3 Screening of Fusions

Screening was routinely carried out on day 10. ELISA was initially used to screen fusions. For the basic method see Section 2.11. Briefly, rituximab and AT13/5 (chimeric anti CD38) were coated onto parallel ELISA plates. Subsequently, the hybridoma supernatant was added to both sets of plates and a secondary anti-rat IgG HRP conjugate was used to detect the presence of bound antibody. Cross-analysis of Rituximab coated and AT13/5 coated plates revealed potential anti-rituximab idiotype specific antibodies.

2.11.2.4 Production of feeder layer

To stimulate the growth of selected positive clones a feeder layer was required to provide the necessary growth factors. To produce the feeder layer a 4-6 week old BALB/c mouse was culled and the thymus removed under sterile conditions into a universal containing 15% FCS/DMEM. A single cell suspension was then produced by teasing the spleen through a cell strainer (Beckton Dickinson) and then suspending the cells in 50 mls of 15% FCS/DMEM.

2.11.2.5 Cloning

Positive wells were semi-cloned by taking the contents of a positive well diluting into 1ml of 15%FCS-HT/DMEM then dispensing drop wise into column 1 of a 96 well plate that had been prepared with 200 µl/well of culture medium with thymocytes to produce the feeder layer (2.12.2.4). 200 µl of medium was then transferred from column one to column 2 of the 96 well plate and this repeated until column 6 from which 200µl was then placed back in column one thereby double diluting the positive cells across half a plate. The semi-cloned plates were re-screened as above (2.12.2.3) after 7 days. Positive wells with single colonies were selected and cloned in the same way as described above but the cells double diluted across a whole plate before culture. Sceening for positive wells was performed again on day 7-10. The cloning process was repeated for each potential clone until a single colony had

been re-cloned twice and no wells with cells that were negative for secretion could be identified.

2.11.2.6 Purification Of Rat Anti-Rituximab Idiotype Mab

Hybridomas that screened positive on ELISA for the secretion rat anti-rituximab idiotype were expanded in culture with progressive weaning to minimum possible concentration of fetal calf serum, usually 5 %. The resulting culture supernatant was analyzed for the presence of a monoclonal protein band by Serum Protein Electrophoresis (SPE) (2.12.2.7). A volume of 500 mls was collected, centrifuged (1500 rpm for 5 mins) and filtered before passing through a Protein G column (Pharmacia Biotech) as described in section 2.12.1.3 resulting in the production of a series of pure anti-rituximab idiotype antibodies. In some cases the protein G column was insufficient to purify the monoclonal antibody with significant amounts of normal IgG remaining. In these cases the eluted protein was concentrated and passed onto a DEAE cellulose column in 50 mM TE8 (50 mM Tris-HCL-0.01 M EDTA pH8) then eluted at a series of increasing NaCl concentrations 0.025 M - 0.2 M. The eluted products were tested for the presence of the monoclonal band by SPE.

2.11.2.7 Serum Protein Electrophoresis

Performed using Paragon Serum Protein Electrophoresis System Kit (P/N 655900) (Beckman Coulter) according to manufacturer's instructions.

2.11.3 Characterization of Rat anti Rituximab Idiotype mAb

2.11.3.1 BIAcore Analysis

The purified anti Rituximab idiotype antibodies were analysed using a BIAcore^{TM} 2000 biosensor. This system utilizes the measurement of changes in Surface Plasmon Resonance (SPR) to enable the real-time detection and monitoring of biomolecular binding events. In

BIAcore systems, the incident p-polarized light is focused into a wedge-shaped beam providing simultaneously a continuous interval of light wave vectors kx. This range covers the working range for the plasmon wave vector ksp during biomolecular interaction analysis. An increased sample concentration in the surface coating of the sensor chip causes a corresponding increase in refractive index which alters the angle of incidence required to create the SPR phenomenon (the SPR angle). This SPR angle is monitored as a change in the detector position for the reflected intensity dip (from I to II). By monitoring the SPR-angle as a function of time the kinetic events in the surface are displayed in a sensorgram.

Figure 2.1 Diagrammatic representation of BIAcore.
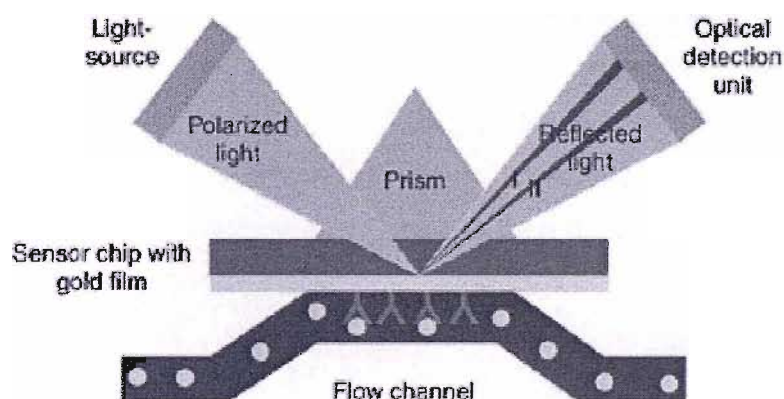
All experiments were performed at 25 °C in HBS buffer (150 mM NaCl, 10 mM Hepes, pH 7.4 and 0.005 % (v/v) surfactant P20 (Biacore AB, Uppsala, Sweden)). Proteins were covalently bound to the carboxylated dextran matrix by amine coupling using amine coupling kit (Biacore AB). 3 μg Rituximab was diluted in 10 mM sodium acetate buffer, pH 4.5 and bound to the chip at a flow rate of 5 μl / minute for 6 minutes. Ethanolamine HCl was then added for 6 minutes to block all the uncoupled ester groups. The surface was then rinsed with 0.1 M glycine HCl buffer (pH 2.5) for 3 minutes to remove any non-specifically bound proteins. Anti-Id mAb were then injected at 4-5 μl / minute for 5-7.5 minutes. The association and dissociation rate constants for each interaction were determined using the BIAevaluation software 2.1 (Pharmacia-Biosensor). Between

injections the surface on the chip was regenerated to remove non-covalently bound proteins by injection of 5 μl 10 mM HCl.

2.11.3.2 Detemination of mAb isotype

MAb isotype was determined using a Rat Monoclonal Antibody Isotyping Testing Kit (Serotec) according to manufacturers instructions.

Chapter 3

Pre-Clinical Investigation of Fractionated RIT

3 PRE-CLINICAL INVESTIGATION OF FRACTIONATED RIT

3.1 INTRODUCTION

Despite the recent clinical success of RIT in the treatment of NHL many questions remain unanaswered. These include the optimum antibody, isotope and RIT schedule aswell as whether multiple fractions may increase efficacy. Answering these questions in the context of clinical trials is laborious, time consuming and often simply not acheivable. Due to the clinical heterogeneity of NHL, compounded by the requirement to initiate experimental protocols in patients that have already relapsed following conventional therapy, gaining a clear answer to a single question can be challenging. In view of the wide range of scheduling options it is therefore appealing to utilise the controlled conditions of animal models to gain an increased insight into the mechanisms of RIT and to test novel schedules that may then be used as a basis for subsequent clinical trials.

Useful syngeneic animal models of RIT in B cell lymphoma have already been established in our laboratory and tested with a panel of B cell specific antibodies [35]. The syngeneic models have the advantage of being able to analyse the efficacy of RIT schedules in the context of an intact host immune system with normal tissue cross-reactivity. These models have been used to effectively evaluate the importance of antibody effector mechanisms such as ADCC, CDC and signal transduction in the clearance of tumour in RIT [34 35 152]. In this chapter the potential for using these models to study the fractionation of RIT was explored.

At the time of starting this work there was no anti-murine CD20 mAb available equivalent to the anti-human CD20 mAbs (rituximab and tositumomab) that could be used in the syngeneic mouse models. In order to mimic the effects of anti-CD20 mAbs in the murine model we therefore planned to adopt the approach of using multiple mAbs simultaneously, combining a mAb chosen for it ability to deliver targeted radiation with a second mAb chosen for its ability to produce signal transduction and recruit immune effectors [38]. Very recently, following the completion of this work, after 20 years of trying, Tedder's group have published their findings with a panel of anti-murine CD20 mAbs [153]. These anti-mouse CD20 mAb are however not currently available to the wider scientific community.

An alternative strategy, that enables use of the same reagents that are used in the clinic, is to use human xenografts in mice that have been genetically modified to induce immunodeficiency thereby preventing immunological rejection of the implanted human tumours. The most popular model uses mice that express the phenotype of Severe Combined Immunodeficiency (SCID). These mice, which lack T cells and B cells but not macrophages, NK cells or complement, enable the study of human tumours and their response to treatment in vivo.

The use of SCID mice is not without its problems. SCID mice by definition will lack a complete immune system and will therefore have a limited ability to demonstrate mAb immune effector mechanisms. This is further compounded by the fact that the human Fc on the therapeutic antibody may not completely cross-react with murine Fc receptors. In addition SCID mice xenograft models, lack expression of the human target antigen on normal tissues and this is likely to significantly impact on the biodistribution and toxicity of the antibody. Finally SCID mice are extremely sensitive to radiation [154]. Cells from SCID mice are approximately 2-3 fold more sensitive to ionisng radiation than cells from immunologically competent mice. This is reflected by the low MTD reported in published studies of RIT in SCID mice resulting in a narrow therapeutic window for effective therapy [155] [156]. In spite of these caveats and the low MTD, useful therapy has

been seen in SCID mice xenograft models so they remain a useful tool in which to study the potential of fractionation schedules for RIT[156].

The work described in this chapter explores the utility of both the syngeneic and human xenograft pre-clinical models for the study of fractionated RIT.

3.2 ANTIBODY CHARACTERISATION

A series of experiments were performed at the outset of this pre-clinical study to characterise the binding properties of antibodies subsequently to be used within the mouse models.

3.2.1 Materials and Methods

The antibodies used and their sources are listed in chapter 2 (table 2.1 and 2.2). All antibodies were obtained from stocks held within Tenovus or directly from the manufacturer. Prior to characterisation experiments mAbs were dialysed (2.5.1) into PBS and purity was confirmed by Serum Protein Electrophoresis (2.11.2.7). In these studies the anti-T cell mAb OKT3 was used as a negative control. For analysis of binding, antibodies were radiolabelled with ^{125}I (2.7). Labelling efficiency was determined by ITLC (2.7.2.1) and considered acceptable if greater than 95%. The immunoreactivity of the antibodies was determined (2.7.3) and the cell surface binding assessed (2.6). By knowing the number of counts per mg of antibody, the molecular weight of the antibody and the number of molecules (Avagadros number) per mole (M) of antibody as well as the number of cells per millilitre it was possible to calculate the number of molecules per cell at each mAb concentration using the equation below.

No. of molecules per mg of mAb   =   (conc. of mAb/ MW of mAb) x Avagadros No.

No. of molecules per cell   =   (No. of counts per tube x no. molecules per count)
                                        No. of cells per tube

Using this calculation the data was plotted as a series of saturation binding curves and then analysed by the method of Scatchard [157]. The gradient of the curves generated by this method equate to the equilibrium binding constant Ka [158].

To confirm the relative levels of antibody binding obtained from these experiments parallel studies were performed by analysing the binding of flouresceinated mAbs (2.5.2) to tumour cells on a flow cytometer (2.6.2).

3.2.2 Results - Binding properties of mAbs

A panel of mAbs targeting the human anti-CD20 antigen and the human MHC class II antigen (F3.3) were characterised according to the method described above. The intention was to subsequently use the anti-CD20 mAbs, with their combined ability to target radiation, signal apoptosis and recruit immune effectors, in the human lymphoma xenograft SCID mouse model. A comparison could then be made with the efficacy of RIT delivered by the anti-MHC class II mAb (F3.3) that would serve as a mAb carrier for targeted radiation and has been demonstrated to have no or little therapeutic effect when delivered unlabelled,

Figure 3.1 illustrates representative saturation binding curves for the Daudi human B cell lymphoma cell line following incubation with the panel of radiolabelled mAbs. As anticipated F3.3, the anti-MHC class II mAb, demonstrates the greatest binding reaching saturation at 4×10^5 molecules per cell indicating the potential utility of this mAb for delivering targeted radiation. The anti-CD20 mAbs despite each binding to the same target saturate at different levels. Rituximab is shown to bind approximately twice as many molecules on each cell as B1. IF5 demonstrates a weaker binding affinity producing a flatter curve but at higher mAb concentrations binds at similar levels to rituximab. These results are in keeping with those previously published for the anti-CD20 mAb from our laboratory[159].

From the saturation binding curves Scatchard plots were derived, as illustrated in Figure 3.2, and the affinity constants (K_A) for each antibody derived from the gradient of the plots. The affinity constants (K_A) for a representative experiment are recorded in the graph legend. These results correlate well with previous results from our laboratory.

Figure 3.1. Binding curves for B1 (tositumomab), ritux (rituximab), IF5, F3.3 and OKT3 (control) when incubated with Daudi cells. A low level of non-specific binding to the control anti-CD3 mAb OKT3 is seen. The level of binding of the remaining mAb is discussed in the text.
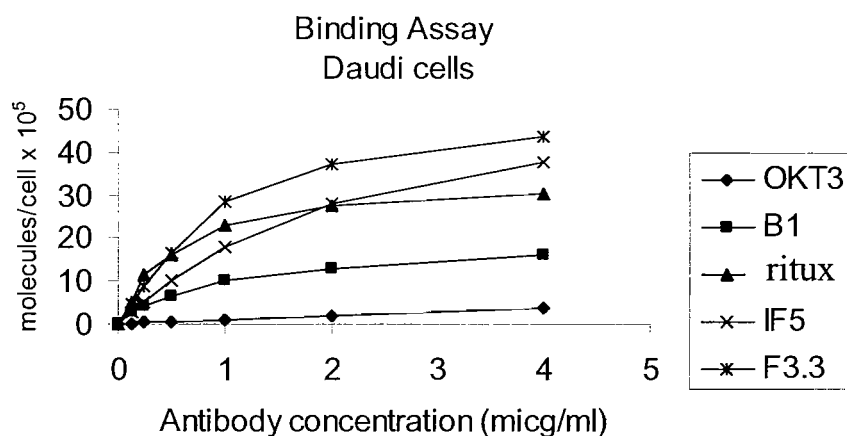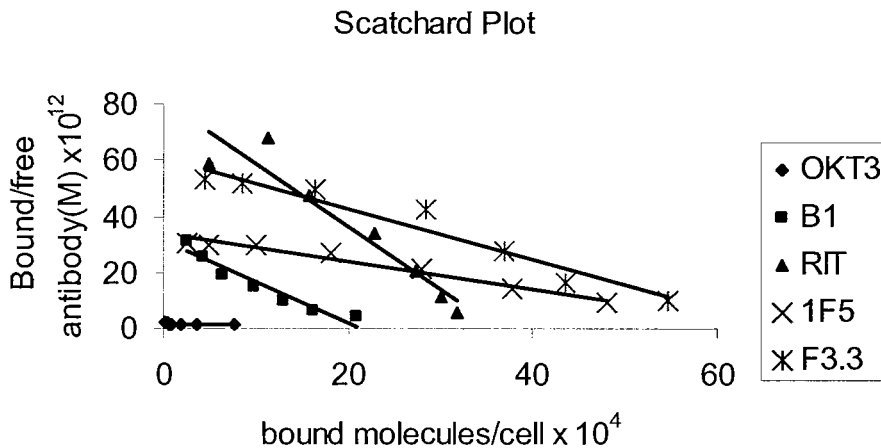

Binding Assay
Daudi cells

Legend:
- OKT3
- B1
- ritux
- IF5
- F3.3

x-axis: Antibody concentration (micg/ml)
y-axis: molecules/cell x 10^5

Figure 3.2. From the binding curves scatchard plots have been derived. The binding affinity of an antibody is equal to the gradient of the scatchard plot. The binding affinity of each mAb is indicated below.

Scatchard Plot

mAb	Equation of line	Binding affinity
OKT3	y = -0.0557x + 1.7241	K_a =0.0.56 x 10^8
B1	y = -1.4575x +31.009	K_a =1.46 x 10^8
RIT	y = -2.2428x + 81.394	K_a =2.24 x 10^8
1F5	y = -0.4925x + 33.603	K_a =0.493 x 10^8
F3.3	y = -0.913x + 60.983	K_a =0.913x 10^8

The relative binding levels of B1, Rituximab and F3.3, after incubation with both Raji and Daudi human lymphoma cell lines were also measured by flow cytometry. The results correlate well with those obtained with radiolabeled antibodies described above and are illustrated in Figure 3.3 lending additional support to the findings.

The mAb TI-23 was selected for use in studies using the syngeneic mouse B-cell NHL model. The binding properties of TI-23, a rat anti-mouse anti-MHC class II mAb have been previously described and reveal a high surface expression and binding of the MHC class II antigen with no significant modulation on binding. In addition it has been demonstrated that this antibody when delivered unlabelled, despite eliciting effective ADCC in vitro has no significant therapeutic effect in vivo [35]. These characteristics make this mAb an excellent vehicle for delivering targeted radiotherapy in our syngeneic mouse model, with no apparent inherent immunotherapeutic effects unlabelled.

Figure 3.3. Fluorescence intensity as measured by flow cytometry for (A) Daudi cells and (B) Raji cells incubated with B1, rituximab and F3.3 before incubation with FITC labelled anti human IgG mAb indicating that the relative binding levels correlate with those seen in the assays of iodinated mAb binding.

mean fluorescence intensity
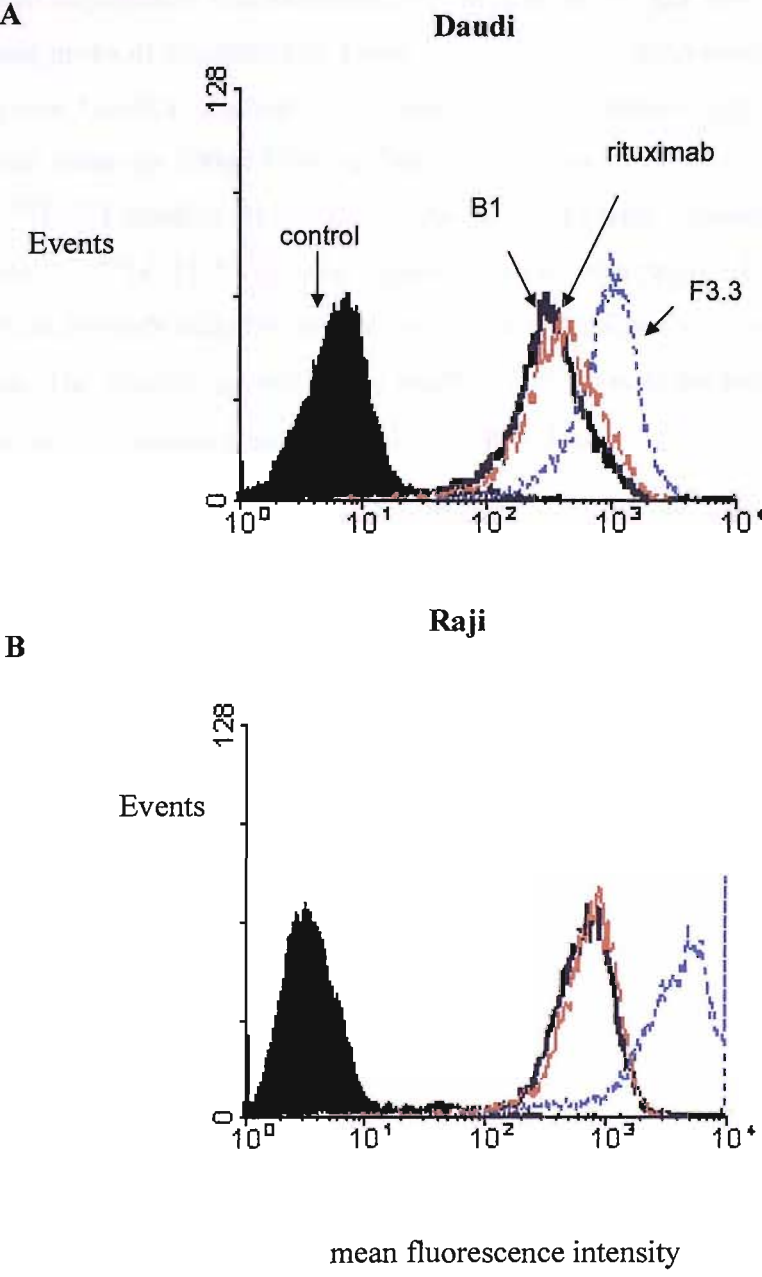
3.3 SYNGENEIC MOUSE MODEL OF FRACTIONATED RIT

3.3.1 Materials and Methods

Groups of 5, CBA mice and BALB/c mice (as described in 2.4) were inoculated by tail vein injection with 1×10^6 A31 and 1×10^5 BCL_1 tumour cells respectively (2.3.2) based on previous published experience. Radiolabeled mAb was given by tail vein injections according to the treatment protocol illustrated in Table 3.1. Prior to administration of radiolabeled mAb mice were given Lugol's solution (5ml Lugol's stock / 400ml H_2O; Lugols stock: 10g KI, 5g elemental iodine in 100ml H_2O) in their drinking water for 3 days to minimise thyroid uptake of the ^{131}I. ^{131}I labelled TI-23 was prepared (2.7.1) with a labelling efficiency of > 95% as measured by ITLC (2.7.2.1). The required activity was prepared for each group of mice and unlabelled antibody added to ensure equal total mAb doses in all mice and an injected volume of 200μl. The specific activity of the labelled TI-23 was in the range 40-60MBq/mg. The total protein dose per animal was 300μg for each RIT dose.

Table 3.1. Schedule of fractionated RIT experiment. Tumour inoculated on D0. RIT administered D7, 14 and 21 with dose in MBq.

Time	D0	D7	D14	D21	Total dose (MBq)
Control	BCL_1 /A31				0
Single fraction	BCL_1 /A31	4.625			4.625
	BCL_1 /A31	9.25			9.25
	BCL_1 /A31	18.5			18.5
Two fraction	BCL_1 /A31	9.25	9.25		18.5
	BCL_1 /A31	9.25		9.25	18.5
	BCL_1 /A31	6.17		6.17	12.25

Analysis for the induction of a mouse anti-rat mAb (MARA) in mice receiving repeated doses of RIT was performed by ELISA. Samples of blood from mice both in this study and additional studies being performed in parallel in our laboratory were obtained by

cardiac puncture at the time of culling. The serum was separated and stored at -20°C until analysis. An ELISA was performed according to the technique described in section 2.10. Briefly, the ELISA plate was coated with the therapeutic antibody (TI2-3), then non-specific antigen binding sites blocked by the addition of 1% BSA/PBS. Following this serial dilutions of the mouse serum were added and the presence of mouse anti-rat antibodies detected by incubation with polyclonal HRP labelled anti-mouse Fc antibodies and exposure to substrate.

3.3.2 Results

This set of experiments was designed to act as a pilot for future RIT fractionation experiments. The aim was to demonstrate the feasibility of fractionated RIT in two models and to identify the optimum dose and inter-fraction interval for future experiments. Three significant observations were obtained from this series of experiments. Firstly in these models a clear dose response for RIT was demonstrated (Fig 3.4). Secondly fractionating the dose does not appear to significantly alter the efficacy of the therapy at the doses and time intervals studied (Fig. 3.5). Thirdly, there was substantial acute unexpected toxicity with the fractionated regimen, which prevented further experimentation with fractionation using these models.

The therapeutic benefit observed and apparent dose response to a single fraction of ^{131}I labelled TI2-3 was encouraging and suggested that this might represent a useful model for the study of fractionation and the potential therapeutic advantage of dose escalation through fractionation. However when the second dose of RIT was delivered to mice an immediate adverse response was documented with almost all of the mice becoming acutely unwell, with increased respiratory rate, reduced activity and spiky fur. With a one-week interval between RIT doses, all the mice recovered completely within 12 hours and eventually succumbed to tumour progression. With a two-week interval between RIT doses, 6 of the 20 mice became sufficiently distressed to justify being culled or died within 2 hours of receiving RIT. The mice that survived again went on to ultimately succumb to progressive tumour. The survival curves shown in figure 3.5 indicate

equivalence between a single dose and 2 fractionated doses. Mice culled or dying from the procedure are excluded from the analysis.

Figure 3.4. Survival curves **A)** Balb-c mice inoculated with bcl_1 and **B)** CBA mice inoculated with A31 tumour cells on day 0 then treated with ^{131}I-TI-23 with activity ranging from 0 to 18.5MBq/mouse on day 7. A clear dose response is seen.

A

RIT Dose Response
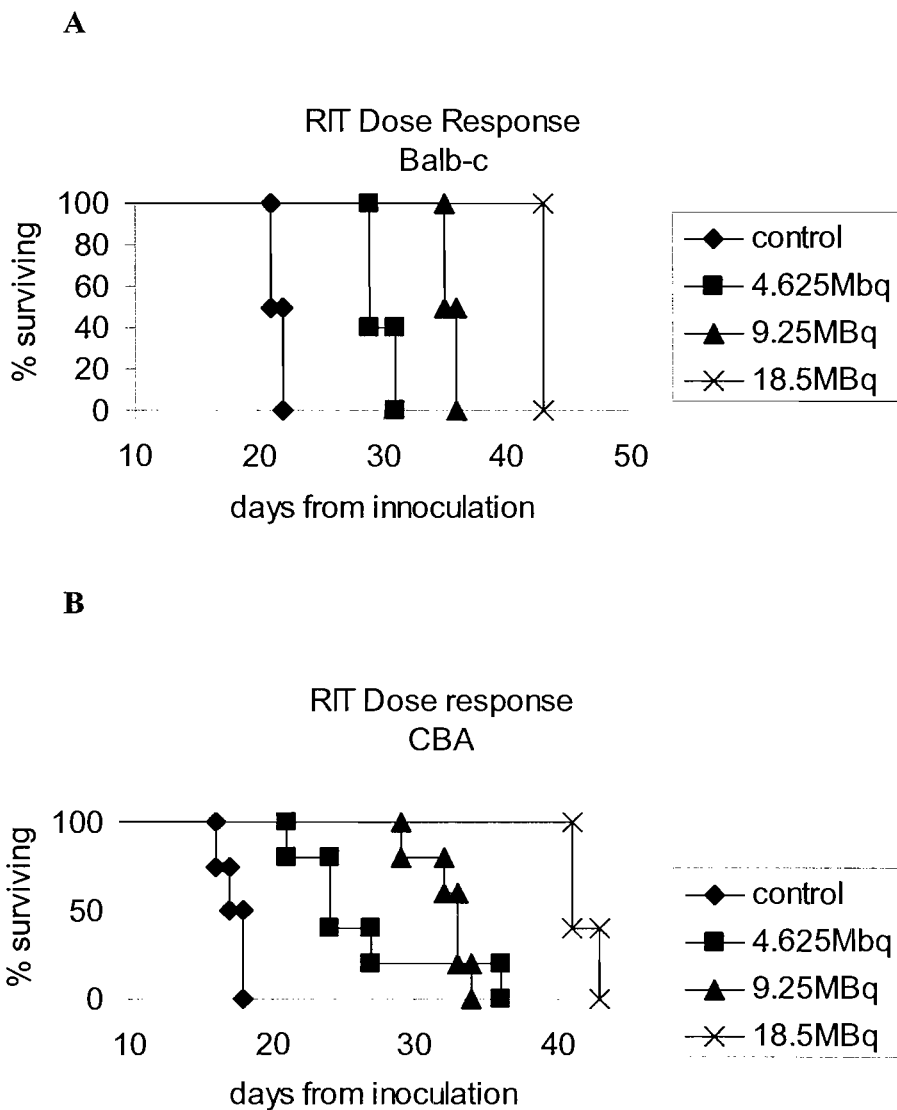Balb-c

B

RIT Dose response
CBA

95

Figure 3.5. Survival curves of **A)** Balb-c mice inoculated with bcl_1 tumour cells and **B)** CBA mice inoculated with A31 tumours cells on day 0 then treated with a single dose of 18.5MBq ^{131}I TI2-3 or the same total dose divides into two 9.25MBq fractions 1 or 2 weeks apart. No significant difference between survival from the single dose or the fractionated dose is seen.

A

Fractionated RIT
BALB-c

B

Fractionated RIT
CBA
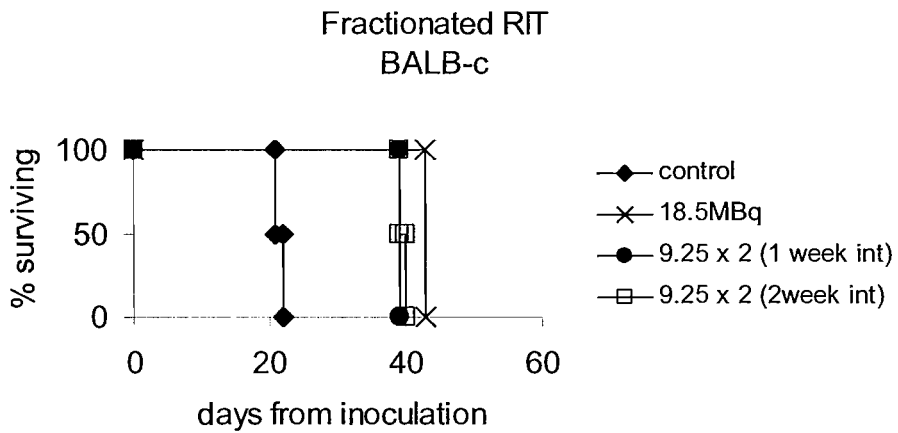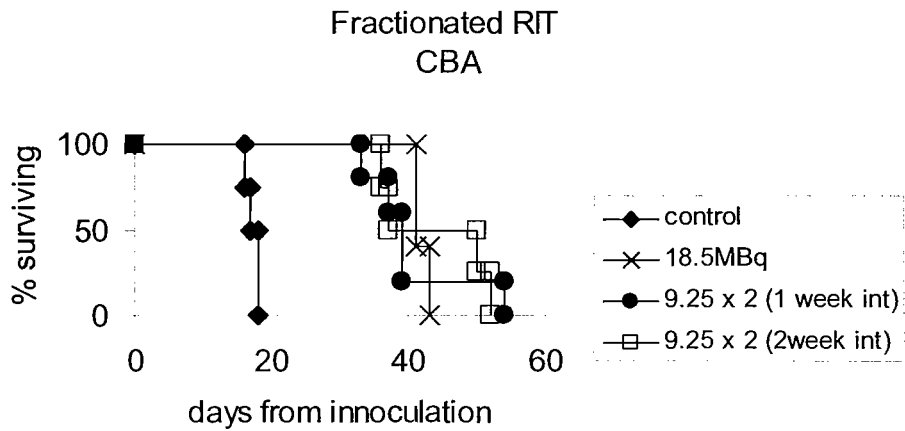
The increase in severity of the adverse effect with increased time interval between fractions was suggestive of an antibody mediated anaphylactic response. This hypothesis was subsequently confirmed by analysing the serum of surviving mice for the presence of a MARA response. An ELISA that effectively detected the presence of a control rat anti-mouse IgG was developed as illustrated in figure 3.6. This standard curve illustrates that the assay can detect MARA to a concentration of 10ng/ml. Using this assay the relative quantities of MARA present in the serum of surviving mice was determined as indicated in figure 3.7. It demonstrates that after a single dose of TI2-3 a significant MARA response occurs. In mice that survived 2 doses a greater MARA titre is seen when the doses were delivered 2 weeks apart than if delivered 1 week apart. This data correlates with experience from vaccination in mice where it is observed that a 2-3 week time interval between antigen doses is optimum for promoting an antibody response and strongly suggests that a MARA response was responsible for the adverse events seen.

Figure 3.6. Standard curve generated from an ELISA to detect the presence of MARA. Using the control mouse anti-rat mAb M359-F10 the assay is shown to be sensitive to a concentration of <10ng.

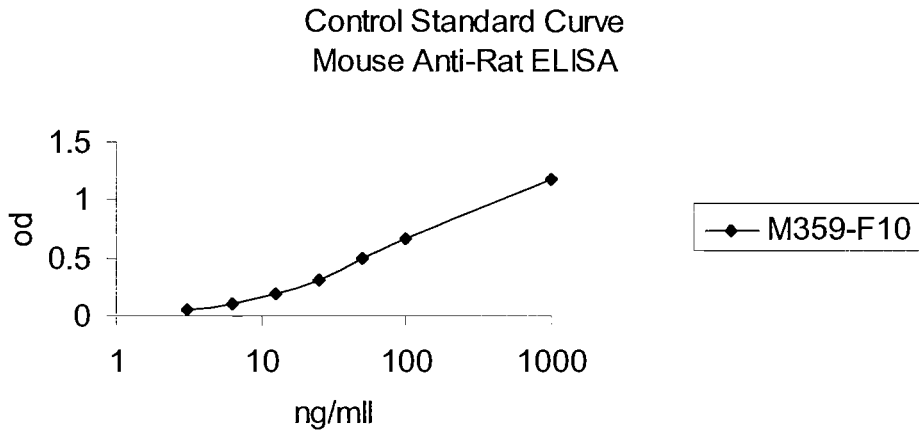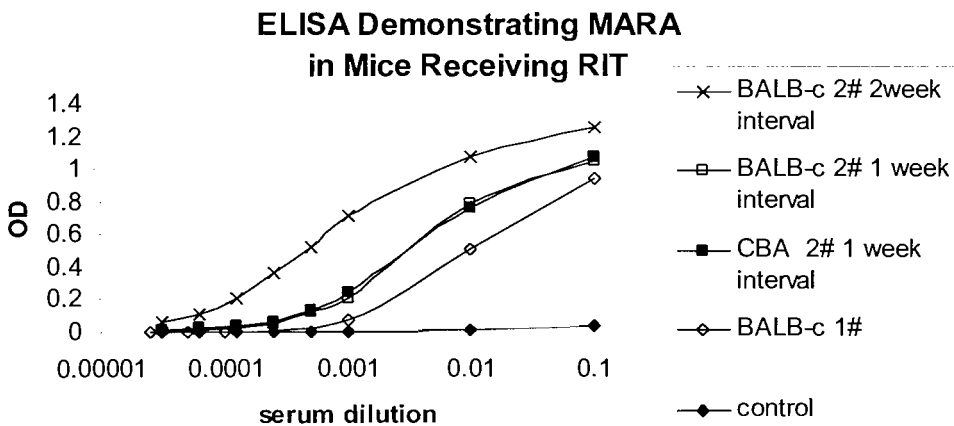**Control Standard Curve**
Mouse Anti-Rat ELISA

Figure 3.7. Applying serial dilutions of mouse serum to the MARA ELISA, the relative concentration of MARA in CBA or BALB-c mice treated with single dose or fractionated ^{131}I TI2-3 is shown. 2 fractions given 2 weeks apart produces the highest MARA titre.

ELISA Demonstrating MARA
in Mice Receiving RIT

3.4 HUMAN XENOGRAFT SCID MOUSE MODEL OF RIT

In order to test RIT schedules using anti-CD20 antibodies and increase our understanding of the mechanisms that may be important in RIT using rituximab, with its well established single agent activity, the potential for using a SCID mouse model with human B cell lymphoma xenografts was explored.

3.4.1 Methods

Groups of 5, 6-8 week old SCID mice (as described 2.4) were inoculated with freshly prepared Raji or Daudi tumour cells respectively (2.3.1). The tumour cells were given via the tail vein and according to previous experience 5×10^6 cells were given per mouse. In the first set of experiments unlabelled antibody mAb was given by tail vein injections according to the treatment protocol illustrated in Table 3.2. Mice were culled at the onset of hind leg paralysis according to established practice with this well published model [155].

Table 3.2 Schedule for dose finding experiment using unlabelled mAbs in the SCID model.

Group		D0	D7
1A	5 SCID mice	5×10^6 Daudi cells	Control- no mAb
2A	5 SCID mice	5×10^6 Daudi cells	F3.3 100 µg
3A	5 SCID mice	5×10^6 Daudi cells	Rituximab 10 µg
4A	5 SCID mice	5×10^6 Daudi cells	Rituximab 50 µg
5A	5 SCID mice	5×10^6 Daudi cells	B1 10 µg
6A	5 SCID mice	5×10^6 Daudi cells	B1 50 µg
1B	5 SCID mice	5×10^6 Raji cells	Control- no mAb
2B	5 SCID mice	5×10^6 Raji cells	F3.3 100 µg
3B	5 SCID mice	5×10^6 Raji cells	Rituximab 10 µ g
4B	5 SCID mice	5×10^6 Raji cells	Rituximab 50 µ g
5B	5 SCID mice	5×10^6 Raji cells	B1 10 µg
6B	5 SCID mice	5×10^6 Raji cells	B1 50 µ g

In the second set of experiments the model was set up in the same way and groups of animals received unlabelled anti-CD20 mAb alone or ^{90}Y labelled ibritumomab tiuxetan (^{90}Y-Zevalin) at a range of doses. The therapeutic antibodies were given on day 13 post tumour inoculation due to the limited availability of the ^{90}Y-Zevalin at this time. Group sizes were restricted to 3 mice for the administration of ^{90}Y-Zevalin due to limited availability of SCID mice and concern regarding the potential toxicity of RIT in SCID mice. All groups received the same 10µg total dose of mAb. The treatment schedule is illustrated in table 3.3.

**Table 3.3** Schedule for pilot experiment using unlabelled anti-CD20 mAb and ^{90}Y Zevalin in the SCID model.

| Group		D0	D13
1a	4 SCID mice	5×10^6 Daudi cells	Control- no mAb
2a	4 SCID mice	5×10^6 Daudi cells	Rituximab 10 µg
3a	4 SCID mice	5×10^6 Daudi cells	B1 10µ g
4a	3 SCID mice	5×10^6 Daudi cells	5MBq Y^{90} Zevalin
5a	3 SCID mice	5×10^6 Daudi cells	3MBq Y^{90} Zevalin
6a	3 SCID mice	5×10^6 Daudi cells	1MBq Y^{90} Zevalin
1b	5 SCID mice	5×10^6 Raji cells	Control- no mAb
2b	3 SCID mice	5×10^6 Raji cells	Rituximab 10 µg
3b	3 SCID mice	5×10^6 Raji cells	B1 10µg
4b	3 SCID mice	5×10^6 Raji cells	5MBq Y^{90} Zevalin
5b	3 SCID mice	5×10^6 Raji cells	3MBq Y^{90} Zevalin
6b	3 SCID mice	5×10^6 Raji cells	1MBq Y^{90} Zevalin

3.4.2 Results

The first set of experiments with the SCID xenograft model was designed to identify the optimum dose of unlabelled mAb for use in subsequent RIT experiments. All previous SCID immunotherapy studies in our laboratory have used doses of 50-100µg per animal. At these doses unlabelled anti-CD20 antibodies result in significantly improved tumour protection making it difficult to identify the added benefit of RIT. By reducing the dose of unlabelled mAb to 10µg as illustrated in Fig 3.8a and 3.8b the therapeutic effect of rituximab was attenuated to 5-10 days over control in the Daudi model and 2-5 days over control in the more aggressive Raji model. In both tumor models B1 proved the more effective antibody and by reducing the dose some attenuation of this effect was seen.

Figure 3.8. Survival curves of SCID mice inoculated with **A)** Daudi tumour cells and **B)** Raji tumour cells on day 0 then treated with a range of concentrations of rituximab (Ritux), B1 and F3.3 on day 7.

A.
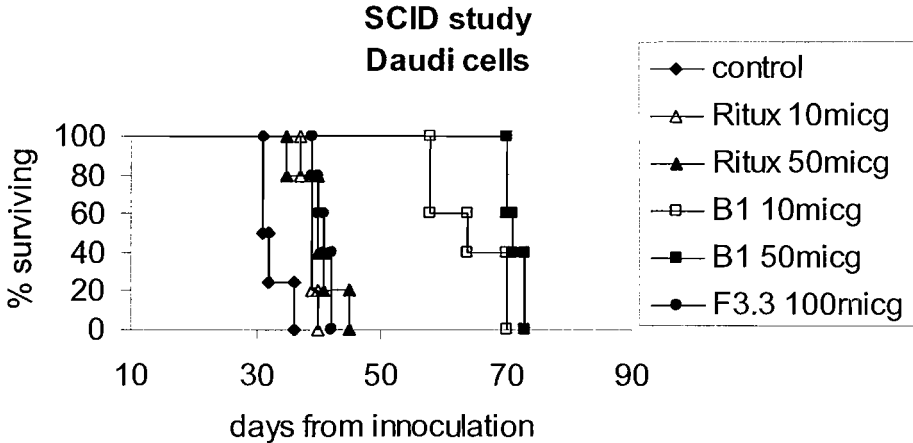
B.
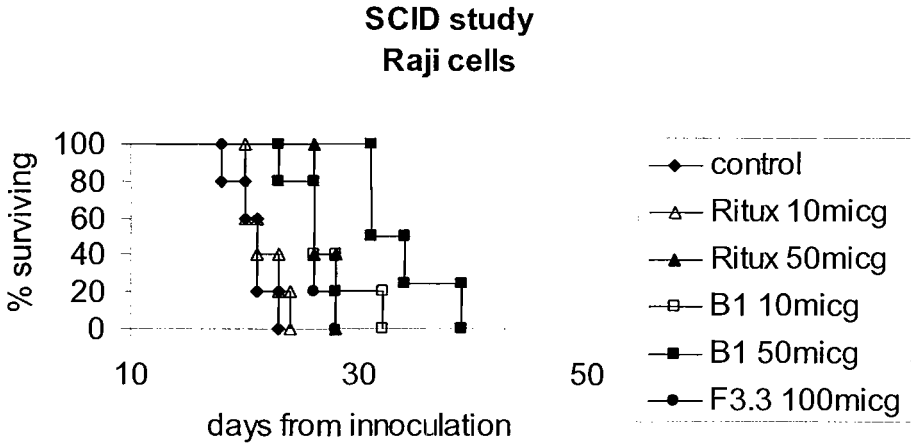
The anti-MHC class II mAb, F3.3 given at a higher dose of 100 µg showed minimal therapeutic activity in both models increasing the survival by 5-7 days over control at this dose. These results confirmed that this mAb may be a potentially useful tool for delivering targeted radiotherapy without the confounding effect of a vehicle mAb that signals apoptosis or recruits immune effectors.

RIT in this model was investigated using ^{90}Y Zevalin. A series of experiments was set up to determine the MTD of ^{90}Y Zevalin in SCID mice and investigate whether a dose response exists and to compare the efficacy of RIT to unlabelled mAb. The results of these experiments are illustrated in Figures 3.9 and 3.10 using both the Raji and Daudi SCID mouse models.

From both these experiments the most important observation is that, as anticipated, even relatively low doses of RIT may cause significant toxicity with 3 MBq proving to be the MTD. Greater radiation doses induced acute toxicity and death. As a result of these experiments we can conclude that the therapeutic window is very narrow. Because of the unexpected delay in treatment with the therapeutic antibody given on day 13, unlabelled B1 and rituximab had very little effect in the aggressive Raji tumour model. With 1 MBq of ^{90}Y Zevalin there was also no significant prolongation of survival however in the narrow window before dose limiting toxicity was seen 3 MBq achieved a significant therapeutic benefit. With the less aggressive Daudi tumour model the findings are the same except that unlabelled antibody and the 1 MBq dose of ^{90}Y Zevalin achieved some therapeutic benefit in this setting.

Figure 3.9. Survival curve of SCID mice inoculated with **A)** Daudi tumour cells and **B)** Raji tumour cells on day 0 then treated with ^{90}Y Zevalin with an activity ranging from 1-5 MBq/mouse. All the 5MBq dose level mice died of acute toxicity within 7 days of treatment. Significant prolongation of survival was seen at the 3 MBq dose level.

A.

^{90}**Y-Zevalin Dose Response**
Daudi

B.

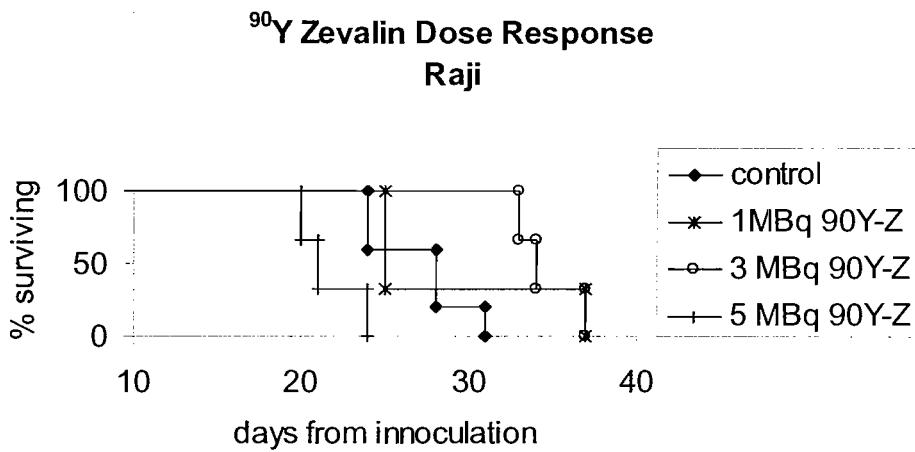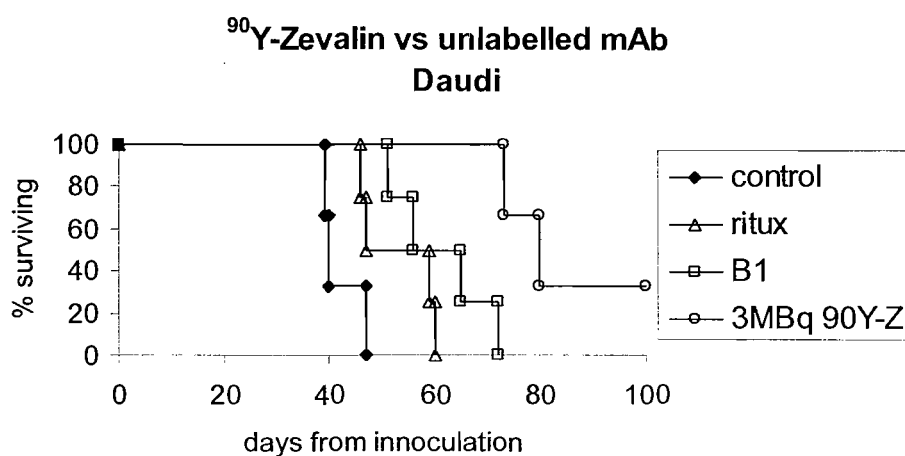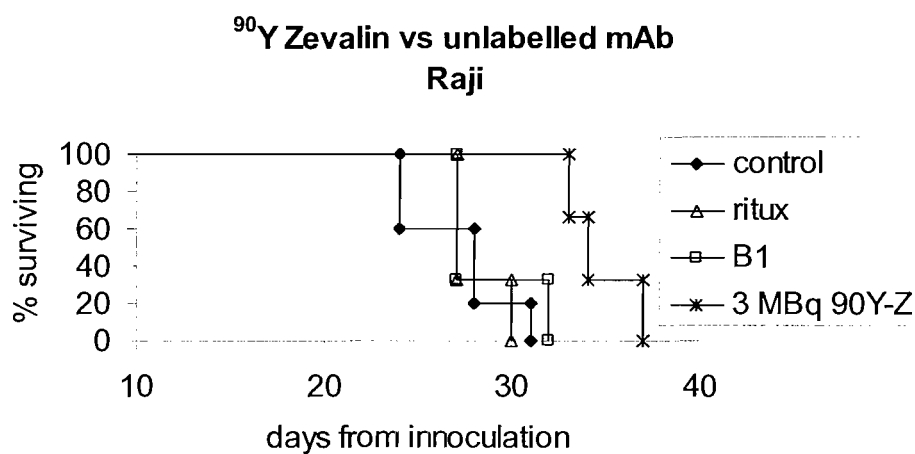^{90}**Y Zevalin Dose Response**
Raji
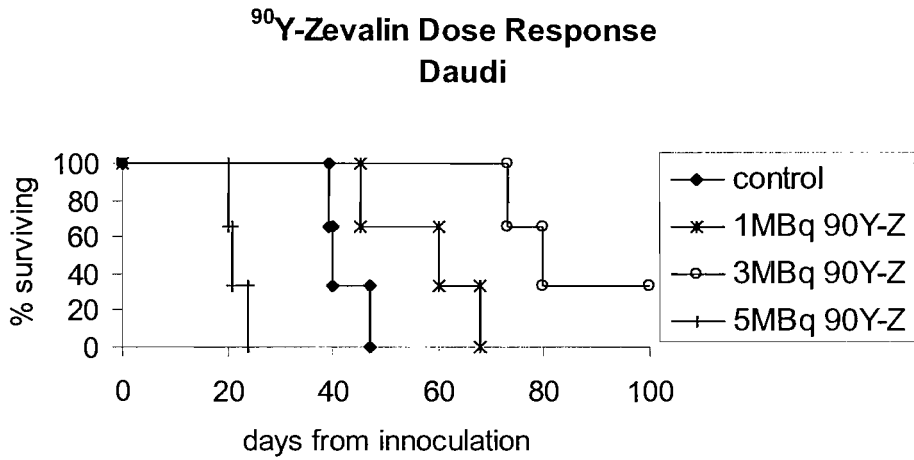
Figure 3.10. Survival curves of SCID mice inoculated with **A)** Daudi tumour cells and **B)** Raji tumour cells on day 0 then treated with unlabelled rituximab (ritux), B1 or 3 MBq of ^{90}Y Zevalin. 3 MBq ^{90}Y Zevalin produces survival superior to unlabelled mAb in both models.

A.

B.

3.5 DISCUSSION

In this chapter some important observations regarding RIT using murine B cell NHL models have been made.

1. In both the syngeneic and the SCID models a dose response for RIT has been demonstrated.

2. RIT with radiolabelled anti-CD20 mAb is superior to unlabelled anti-CD20 mAb therapy.

3. In the SCID model unlabelled B1 is superior to unlabelled rituximab.

4. In the syngeneic models, 2 dose fractionated RIT appears to have similar efficacy to a single larger fraction.

5. Multiple doses of radiolabelled rat mAb are not possible due the generation of a MARA response preventing further administration of rat mAb.

The identification of a clear dose response to both ^{131}I TI2-3 and ^{90}Y ibritutumomab tiuxetan is an important observation. As previously described (1.6) the issue of whether a dose response exists for RIT remains controversial. In clinical studies multiple confounding factors may account for the frequent lack of an apparent dose response. In both these preclinical models evidence for a dose response lends support to the hypothesis that one of the potential benefits of fractionating a dose of RIT may be through a resulting ability to escalate the total dose of RIT.

At the time of experimentation it was not possible to deliver therapeutic doses of ^{131}I labelled antibodies to SCID mice because the required sterile isolators were not present in the designated 'hot room'. During the course of a clinical trial with ^{90}Y Zevalin, an opportunity arose to use this radioimmunoconjuagate. ^{90}Y is a pure beta emitter and in the absence of penetrating gamma emissions it was possible to safely carry out the RIT experiments in the facility dedicated to SCID mice. Using this model the demonstration that ^{90}Y Zevalin may achieve survival superior to both rituximab and B1 in the SCID mouse models is of interest and supports the findings from a recent clinical phase 3 trial comparing treatment with rituximab to ^{90}Y Zevalin. In this randomised clinical study the

response rate in those patients receiving RIT was superior to the response rate for those receiving rituximab. There was no statistically significant survival advantage with RIT reported this study however the study was not powered to demonstrate differences in time to progression or survival and a trend towards prolonged survival with RIT is certainly seen[46].

The observation that B1 is superior to rituximab in the SCID mouse model concurs with observations made previously in our laboratory. Using this model Cragg et al have demonstrated that the therapeutic effect of rituximab is derived largely from its ability to recruit complement and can be abrogated by the use of cobra venom factor, an inhibitor of complement factors [31]. B1 on the other hand derives its therapeutic effect principally from signal transduction bringing about apoptosis. It seems likely that such profound differences in the mechanism through which these unlabelled mAbs bring about therapy may be important when they are used as the vehicle for RIT. Certainly Illidge et al have previously demonstrated that signal transduction may be an important component of RIT in the syngeneic murine models [35]. This question has not been further explored in this thesis however a comparison of the efficacy of RIT using a mAb that signals apoptosis like B1, with RIT using a mAb like rituximab that is less good at signalling would be potentially of great clinical interest. Of the two commercially available radioimmunoconjugates for the treatment of NHL Bexxar uses the B1 whilst Zevalin uses the murine precursor of rituximab, ibritumomab.

The absence of a clear benefit from fractionation in the limited study of fractionation performed in the syngeneic mouse models needs to be considered in context. Firstly, no attempt was made to measure haematological toxicity in this study. Previously using this model 9.25MBq of ^{131}I labelled TI2-3 has been shown to induce significantly less myelotoxicity than 18.5MBq [152]. Since some recovery of the bone marrow may have occurred between RIT fractions it is therefore likely that the fractionation may have substantially reduced the haematological toxicity. This suggestion is supported by the original studies of fractionated RIT by Schlom et al in which escalation of the dose in the fractionation arm of the study was achieved without increased toxicity [137]. Secondly, in

the fractionation study therapy was delivered on day 7. At this point there was no palpable tumour in the spleen and tumour deposits are likely to have been sub-millimetre in size. In this situation the benefit from the fractionation of RIT to overcome radiation dose inhomogeneity will be minimised particularly in the context of a haematological tumour that arises in the well vascularised spleen. Thirdly, the final factor that may account for a failure to demonstrate the superiority of fractionation and the main limitation of the model used in this pre-clinical study is the clear evidence of induction of MARA. It is likely that the presence of MARA will have had a substantial negative impact on the biodistribution of the second dose of RIT with antibody complexes forming and resulting in rapid clearance of the immunoconjugate from the circulation, dehalogenation and excretion of the ^{131}I.

In the treatment of lymphoma the frequency of induction of HAMA responses has been relatively low largely because the population treated is significantly immunosuppressed as a result of the disease and prior chemotherapy treatment. The observation of a significant MARA response in our syngeneic mouse model although precluding the further use of this model for the investigation of fractionation may make it a useful model in which to investigate techniques for ameliorating anti-antibody responses.

The very narrow therapeutic window for treating SCID mice with ^{90}Y based RIT is likely to prevent further study of this particular set up. It is possible however that by using alternative isotopes with emissions of a shorter path length the therapeutic window in this model may be increased. For ^{90}Y the 5.3mm path length of the beta particle emissions means that the mouse is far from ideal for testing as the size of the animal results in a significant proportion of the dose being delivered outside the target tumour in normal tissues. The use of shorter pathlength isotopes was employed successfully by Ochakovskaya et al using Indium-111 and Gallium-67 [156]. These agents exert their therapeutic effect through the production of low energy Auger electrons, which require internalisation for effective cytotoxicity and so cannot be used to model RIT with the clinically available anti-CD20 mAbs. A further strategy for increasing the therapeutic window could be to study the human B cell lymphoma xenografts in the nude mouse

model. These mice are significantly more tolerant of the adverse effects of radiation. Using a nude mouse model with subcutaneous human lymphoma xenografts an MTD of greater than 5MBq of ^{90}Y 1F5 has previously been demonstrated [160].

In conclusion these pilot experiments have demonstrated both the potential and the limitations of studying RIT in animal models and will be used as a basis for future studies within our laboratory.

Chapter 4

Clinical Investigation of Fractionated Radioimmunotherapy

4 CLINICAL INVESTIGATION OF FRACTIONATED RIT

4.1 INTRODUCTION

Although some of the principles governing the scheduling of RIT can be approached with animal models such approaches ultimately require testing within the context of a clinical trial. Clinical trials are particularly important when studying antibody-based treatments where the interaction between the host immune system, the tumour and the antibody are so critical both to the pharmacokinetics and the efficacy of the trial drug. The primary aim of this thesis was therefore to set up a clinical trial of fractionated RIT for relapsed low grade NHL. The reasons for wishing to study fractionated RIT are described in section 1.7 and summarised below.

Evidence from high dose RIT with peripheral blood stem cell transplant (PBSCT) suggests a benefit from escalating the dose of RIT. Delivering high single doses of RIT is technically challenging due to the need to handle high doses of radioisotope and to manage highly radioactive patients. Pre-clinical studies suggest that fractionation of the dose of RIT may enable the safe delivery of a higher total dose without the need for PBSCT. Fractionation of the RIT dose may have the additional advantage of improving the biodistribution of the radioimmunoconjugate as sequential fractions gain access to different parts of the tumour as the tumour responds to the initial treatment.

The clinical trial design evolved over a period of months, as the feasibility of the scheduling and the most important questions that we felt needed answering became

clearer. In this chapter the rationale behind the trial protocol is described along with the development of the antibody labelling and quality assurance procedures. The available results on the pharmacokinetic, dosimetry, toxicity and efficacy aspects of the study are then described.

4.2   CLINICAL TRIAL PROTOCOL

4.2.1   Rationale

The final trial protocol was for a phase I/II dose escalation study of fractionated RIT using ^{131}I labelled rituximab delivered in two fractions separated by eight weeks for patients with relapsed or refractory indolent NHL. The characteristics of both ^{131}I and rituximab have been extensively described in sections 1.3.3 and 1.2.4.1. The reasons for choosing this combination of radionuclide and vehicle are listed below.

The radionuclide - ^{131}I .

1. Straightforward chemistry with well established methods for conjugating ^{131}I to protein that can be performed locally.
2. Successfully used in current RIT protocols (Bexxar)
3. Penetrating gamma emission facilitating individualised dosimetry.
4. Relatively short path length of beta emission with 90% of energy delivered within 1mm radius.
5. Easily available and relatively inexpensive.

The short path length is anticipated to be an advantage for a dose fractionation study in which, due to response to the first fraction of RIT, by the time of administration of the second fraction the volume of remaining tumour nodules will often be small. In this situation a radionuclide such as ^{90}Y with an emission of greater path length would deliver a substantial proportion of its radiation outside the tumour nodule thereby potentially increasing normal tissue toxicity for a given tumour dose.

The mAb – rituximab

1. Well-established clinical single agent activity in indolent NHL.
2. A chimeric antibody minimising the risk of development of a HAMA response and so enabling its repeated administration as part of a fractionation protocol.
3. Shown to be effective both in recruiting immune effectors and signalling apoptosis offering the potential for a synergistic interaction between the mAb and radiation.
4. Easily available with substantial local experience in its administration

An interval of 8 weeks between the therapy doses of radioimmunoconjugate was chosen because of the well established pattern of myelosuppression seen in studies of single agent ^{131}I tositumomab and ^{90}Y ibritumomab tiuxetan. The dose limiting toxicities when single dose RIT is given are thrombocytopenia and neutropenia occurring with a nadir at 4-6 weeks and usually recovered by 8 weeks. By leaving a substantial interval between doses there is also more scope for the tumour to respond and shrink following the first dose enabling the second dose to access previously inaccessible parts of the tumour. We therefore elected to deliver the fractions in a manner analogous to the delivery of repeated cycles of chemotherapy given at intervals that allow substantial recovery of the bone marrow between doses. The study was limited to 2 fractions, as a practical and manageable approach, in order to first demonstrate the feasibility and efficacy of fractionation before moving onto a study with a greater fraction number.

An induction course of rituximab given weekly for 4 weeks at a dose of 375 mg/m^2 prior to the administration of RIT was included in the protocol in the knowledge that many patients are excluded from RIT protocols because of excessive bone marrow infiltration at the outset. This induction rituximab was intended to clear the bone marrow of tumour cells increasing the proportion of patients eligible to receive RIT within the trial. For those patients with significant bone marrow involvement at the outset, in order to confirm the efficacy of this induction course in clearing the bone marrow, a repeat bone marrow trephine was obtained following the induction course of rituximab prior to

112

commencing RIT. This enabled confirmation, before commencing RIT, that the bone marrow involvement by lymphoma had fallen below the threshold of 25%, considered necessary to avoid unpredictable excessive myelotoxicity. In addition to this induction course of rituximab a pre-dose of unlabelled rituximab (100 mg/m^2) was given immediately prior to the ^{131}I labelled rituximab. This was given with the intention of improving the biodistribution of the RIT as has been discussed in section 1.3.2.2.

Within the trial protocol 7-14 days prior to each therapy dose of RIT a dosimetry study was performed. This enabled individualised dosimetry and analysis of the pharmacokinetics of the radioimmunoconjugate. It also provided an opportunity for imaging the targeting of radioimmunoconjugate to the tumour. Analysis of the pharmacokinetics from the first cohort of patients revealed a clearance of ^{131}I rituximab that was substantially longer than that previously reported [161]. In order to determine whether this important finding could be explained by an effect of the RIT scheduling on the clearance of ^{131}I rituximab it was decided to add an additional dosimetric study to the protocol. This was performed without any pre-dose prior to the induction rituximab in order to replicate the conditions under which Scheidhauer et al had previously examined the pharmacokinetics of ^{131}I rituximab.

Finally, the protocol dictates a dose escalation structure to the study with strict assessment for toxicity and rules for stopping the trial when the MTD has been identified. Table 4.1 is a diagrammatic representation of the trial schedule, table 4.2 indicates the dose escalation schedule and table 4.3 indicates the timing of events for each cycle of fractionated RIT. The full trial protocol is included in appendix 1.

Table 4.1 Fractionated RIT trial protocol schedule summary indicating timing of administration of rituximab and dosimetric and therapeutic doses of ^{131}I rituximab.

Schedule Summary

Week	-2	-1	0	1	2	3	4	5	6	7	8	9	10	11	12	13	14	15	16	17

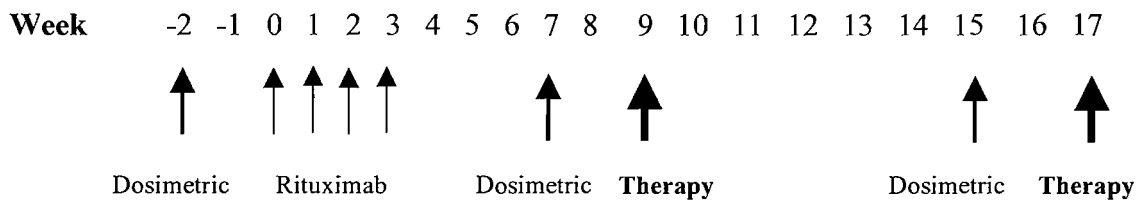| Dosimetric	Rituximab	Dosimetric	**Therapy**	Dosimetric	**Therapy**

Table 4.2 Fractionated RIT trial dose escalation schedule. Further cohorts containing a minimum of three patients will be recruited with a dose increment of 15 cGy/fraction until dose-limiting toxicity is seen. In practice the dosimetric doses contributed approximately 6.5 cGy on each occasion to the total delivered dose increasing the delivered dose by 10-15 cGy at each dose level (see Table 4.5)

Dose cohort	**Fraction 1**	**Fraction 2**	**Total**
1	15 cGy	15 cGy	30 cGy
2	30 cGy	30 cGy	60 cGy
3	45 cGy	45 cGy	90 cGy
4	60 cGy	60 cGy	120 cGy

Table 4.3 Fractionated RIT trial schedule for administration of each fraction of RIT.

Day	Time	Intervention
D-3		Commence potassium iodate tablets continued for 5 weeks
D0	0930	Pre-med 1g paracetamol po + 10mg chlorpheniramine iv.
	1030	Commence rituximab infusion 100mg/m^2 iv.
	1430	Dosimetric dose of 5mg of 185 MBq ^{131}I rituximab
	1500	Ist gamma camera scan
D4		2nd gamma camera scan
D6		3rd gamma camera scan
D14	0930	Pre-med 1g paracetamol po + 10mg chlorpheniramine iv.
	1030	Commence rituximab infusion 100mg/m^2 iv.
	1430	Therapy dose ^{131}I rituximab iv
		Discharge from hospital dependent on activity 0-4 days

4.3 ^{131}I LABELLING OF RITUXIMAB

The aims of radiolabelling are to obtain a sterile clinical grade product in which the ^{131}I and rituximab are stably conjugated retaining the binding ability and function of the rituximab with as little free ^{131}I present as possible. Using the IODO-bead^{TM} method standard manufacturers protocols were modified over the course of several months of experimentation in order to consistently produce ^{131}I labelled rituximab of clinical grade for the study.

4.3.1   Materials and Methods

The IODO-bead™ method was chosen as it provides a reproducible, technically simple means for radio-iodination of mAbs without damaging the integrity of the mAb structure. IODO-beads™ are non-porous polystyrene beads coated with the iodination reagent N-chloro-benzenesulphonamide. This oxidises the iodine enabling incorporation into the mAb (2.7.1). The IODO-beads™ were initially used according to the manufacturers instructions. Modifications of this method were introduced following preliminary labelling studies in which the reaction volume, the total mAb dose, the number of beads, the reaction time and the mixing schedule were varied. The optimum conditions for labelling were identified as determined by the labelling efficiency (LE) of the reaction product. LE is defined as the amount of radionuclide that is bound to the mAb as a fraction of the total radionuclide present in the reaction mixture. ITLC (2.7.2.1) was used as a convenient and rapid method for determining LE in these initial experiments. Samples for patient administration were also analysed by HPLC (2.7.2.2), which allows the LE to be confirmed and provides additional information regarding the presence of any complexes, fragments or other impurities. Obtaining a radioimmunoconjugate with stable retention of the radionuclide and minimal free radionuclide is critical to the success of RIT. In the past the Chloramine-T method was favoured for iodination. This method results in a labelling efficiency of 50-70% and therefore to obtain a product that could be delivered to a patient a further step of purification to remove the free iodine was required to complete the labelling process. To avoid the additional radiation exposure to staff that would result from this additional step, every effort was made to achieve a LE of greater than 95% through optimisation of the IODO-bead protocol. The final protocol is detailed in chapter 2 (2.7.1). To complete the quality assurance (QA) of the ^{131}I conjugated mAb, prior to patient administration, an assay was performed to determine the immunoreactivity of the labelled mAb (2.7.3) and exclusion of microbial contamination was confirmed by LAL testing (2.7.4).

4.3.2   Results

4.3.2.1   Labelling Efficiency

First labelling attempts using 35 mg (3.5 mls) rituximab incubated with 10 IODO beads and 185MBq ^{131}I produced an LE of only 75%. Washing the beads in phosphate buffer as suggested by the manufacturer did not improve the result however the LE improved to 90% when 10mg (1ml) of rituximab was incubated with 5 IODO beads. Reducing the amount of mAb further, despite resulting in less mAb available for labelling, by decreasing the volume of the reaction mixture, dramatically improved the LE to greater than 95%. A time course experiment was then performed with samples withdrawn from the reaction mixture at one minute intervals to identify the optimum incubation time for the reaction. The optimum LE occurs with an incubation time of 10-14 minutes (figure 4.1). There is a significant fall in the LE if the incubation is prolonged. This may be because with prolonged exposure the oxidizing bead begins to degrade the protein.

Prior to commencing the clinical study an experiment was performed to confirm that with this labelling protocol, using just 5mg of rituximab, it would be possible to obtain a product with sufficient activity for the treatment of patients in the highest planned dose cohort. No significant difference in LE was found when labelling with activity over the range 80 to 3100 MBq.

An analysis of the stability of the radioimmunoconjugate was also performed with reassessment of LE at a series of time points over the course of 7 days at room temperature. Figure 4.2 illustrates the stability of the iodinated rituximab under these conditions with a less than 10% fall in LE over 7 days and no evidence of significant radiolysis even with the highest ^{131}I specific activity required for the clinical trial.

During the course of the clinical study a labelling efficiency of >90% for biodistribution work and at least 95% for a larger therapeutic dose was required before the radioimmunoconjugate was administered to patients. This was achieved on all but two

occasions when for unexplained reasons the labelling failed. In these situations the RIT was delayed for one week and the labelling then successfully repeated.

The LE was consistently found to be the same when measured by HPLC and ITLC. Figure 4.3 shows a series of HPLC traces using the gamma detector, illustrating first in figure 4.3a the position of free ^{131}I on the trace then, in figure 4.3b the profile obtained when the reaction mixture is analysed. The smooth narrow profile of the first peak on this trace represents the radioimmunoconjugate and indicates that there is no significant complex formation. The double peak that follows represents unconjugated ^{131}I. By integrating the area beneath the two peaks a measure of LE can be obtained. The unusual shape of the free iodine peak is believed to be due to the formation of iodine dimers in the presence of the IODO-beads^{TM}. Finally in figure 4.3c there is a trace demonstrating the ability of passage through a PD10 sephadex-containing column (Pharmacia Biotech) to enable separation of the radioimmunoconjugate from the free ^{131}I. Although resulting in a purer product, as the passage through a PD10 column resulted in an unacceptable increase in the finger dose to the operator and the small amounts of free ^{131}I were not thought to be clinically relevant, this additional purification step was not incorporated into the routine clinical trial protocol.

Figure 4.1. Variation in LE with reaction mixture incubation time. Aliquots of the reaction mixture were removed from the reaction vial at 1 minute intervals and analysed by ITLC to identify the optimum incubation time for the labelling reaction.
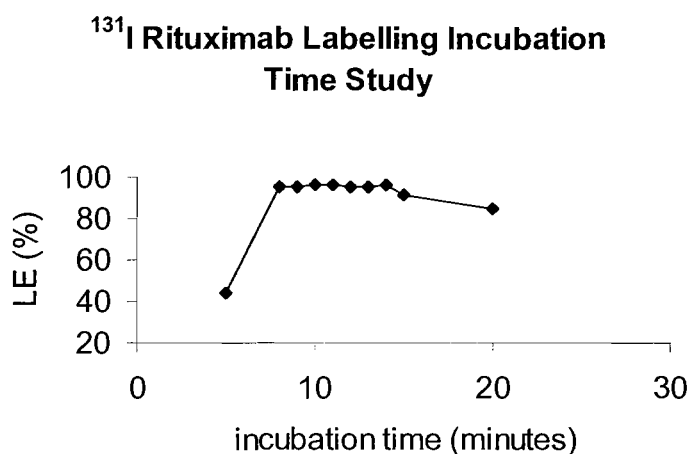

^{131}I Rituximab Labelling Incubation Time Study

Figure 4.2. Stability of ^{131}I rituximab illustrated by change in LE over the course of 7 days both with low and high ^{131}I specific activity. No significant difference is seen in the initial LE or the rate of fall between in LE with increasing ^{131}I activity. The fall in LE of <10% over 7 days indicates a stable product with minimal radiolysis.
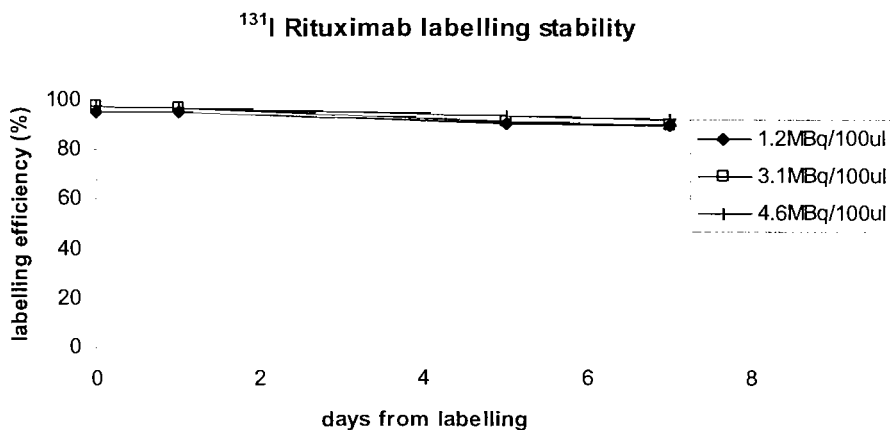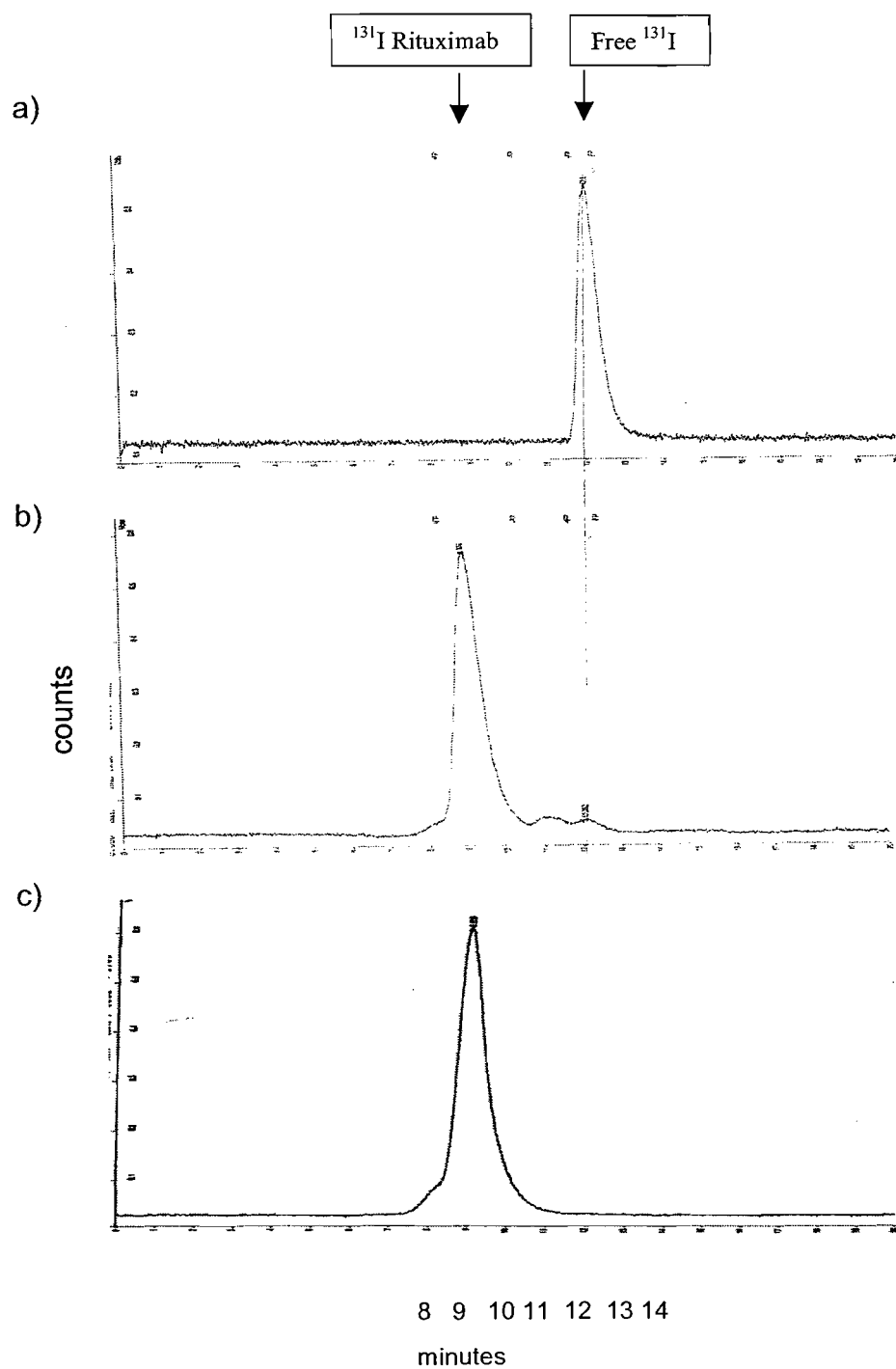

^{131}I Rituximab labelling stability

— 1.2MBq/100ul
— 3.1MBq/100ul
— 4.6MBq/100ul

Figure 4.3. HPLC trace using gamma counter of **a)** free ^{131}I, **b)** [131]I labelled rituximab, **c)** [131]I labelled rituximab after purification on PD10 column.

4.3.2.2 Immunoreactivity

To confirm that the act of radiolabelling was not adversely affecting the binding ability of rituximab, a series of immunoreactivity studies were performed. Immunoreactivity for the purposes of this study was defined as the percentage of radioimmunoconjugate bound to antigen in conditions of near infinite antigen excess as described in section 2.7.3. To confirm the validity of the assay a control assay was performed first using Jurkat cells, a T cell lymphoma cell line with no expression of the CD20 antigen, and then using Daudi cells pre-incubated with saturating concentrations of unlabelled rituximab to block all available binding sites. In both situations, as illustrated in figure 4.4, very little non-specific binding was seen. The immunoreactivity was also assessed after labelling with higher doses of ^{131}I in the range 80-3200 MBq to confirm, as shown in figure 4.5, that at the higher activities there was no adverse effect on the rituximab binding ability.

Figure 4.4. Immunoreactivity assay. Specific binding of ^{131}I rituximab to CD20+ Daudi cells is shown compared to minimal non-specific binding of ^{131}I rituximab to Jurkat cells (T cell line) that have no CD20 expression, or to Daudi cells pre incubated with saturating doses of rituximab to block all available rituximab binding sites.
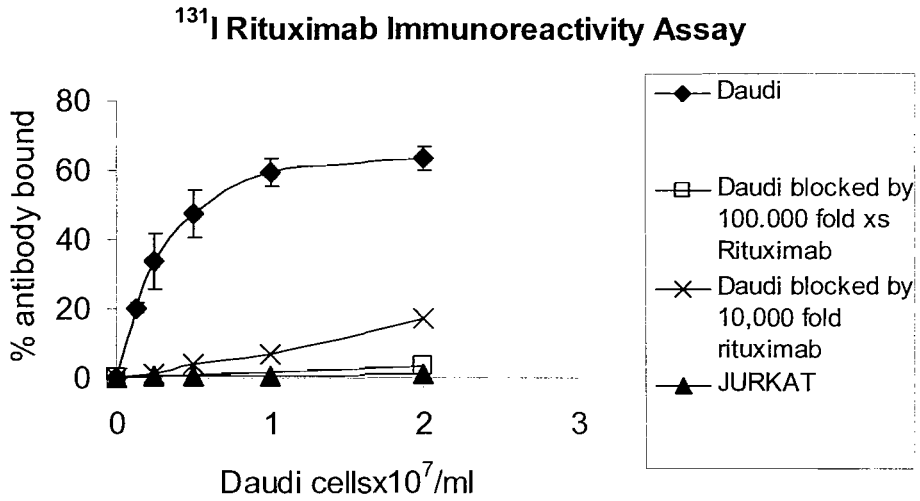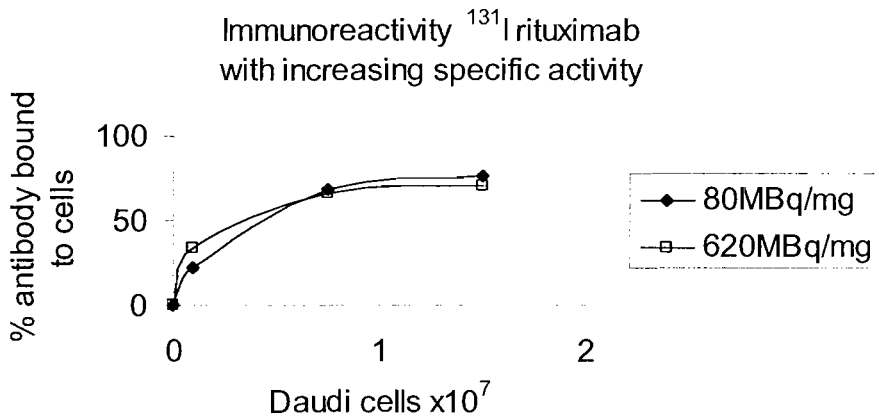

Figure 4.5 Assay indicating stable ^{131}I rituximab immunoreactivity over a wide range of specific activities.

4.4 ^{131}I RITUXIMAB DOSIMETRY AND PHARMACOKINETICS

The importance of individualised patient dosimetry for ^{131}I tositumomab has been previously discussed (1.4). The variability in the effective half-life seen with ^{131}I tositumomab is likely to be similar for all iodinated anti-CD20 mAbs. Therefore, in consultation with nuclear medicine colleagues, we decided to use a method of individualised patient dosimetry for our study similar to that, which has become well established in the delivery of ^{131}I tositumomab. As previously described (1.4) this is based upon the observation that the whole body absorbed dose appears to be a reasonable predictor of bone marrow toxicity and so can been used as a surrogate for bone marrow dose in the dosimetry of iodinated radioimmunoconjugates.

4.4.1   Materials and Methods

Whole body radioimmunoconjugate clearance and the administered activity required to deliver a given whole body absorbed dose was determined according to the method described by Wahl et al. This method is detailed in chapter 2 (2.8.1). Briefly, administration of a small (dosimetric) dose of ^{131}I rituximab is followed over the course of 7 days by 3 quantitative whole body gamma camera scans. Based on the decline in whole body activity recorded on these gamma camera scans it is possible to calculate the effective half-life and residence time of the radioimmunoconjugate within the patient and from this calculate the required administered activity of ^{131}I rituximab to deliver a given whole body absorbed dose. An example of the serial gamma camera images is shown in figure 4.6. The effective half-life is the time taken for the activity to fall to 50% (figure 4.7) and the residence time is the time taken for the activity to fall to $1/e$ (about 37%) or 1.443 x the effective half-life. The residence time is the average time that the administered activity spends in the body and is represented graphically in figure 4.8. Making the assumption that the patient approximates to an ellipsoid and that the radiation is distributed uniformly through the patient after injection, using the MIRD system, the ^{131}I activity required to deliver a given whole body absorbed dose can be calculated [150].

Figure 4.6 Quantitative gamma camera images showing the activity of the standard used as a reference for quality assurance (A), the distribution of activity minutes after injection (B), then 4 days (C) and 6 days later (D). The D0 image shows most of the activity confined to the blood pool. By D4 and D6 activity can be seen localising at sites of lymphoma in the pelvis and axillae (arrows).
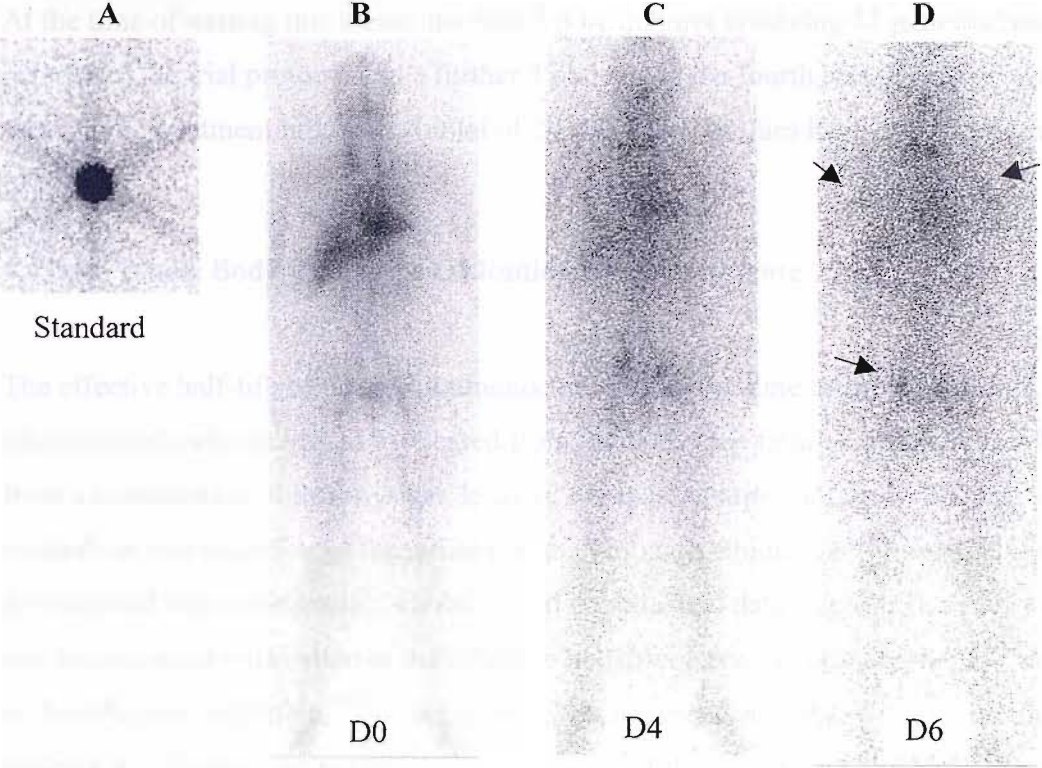
In selected patients blood clearance of ^{131}I rituximab was determined by taking sequential blood samples as described in chapter 2 (2.8.2). In all patients gamma camera imaging was performed as described in chapter 2 (2.8.3) in order to visualise sites of targeting of the radioimmunoconjugate to tumour.

4.4.2 Results

At the time of writing this thesis, the first 3 dose cohorts involving 12 patients have completed the trial protocol and a further 3 patients in the fourth cohort are part way through the treatment protocol. A total of 29 dosimetric studies have been performed.

4.4.2.1 Whole Body Clearance Of Radioimmunoconjugate

The effective half-life of the radioimmunoconjugate is the time taken for half the administered radioactivity to be cleared from the body (see figure 4.7) and is derived from a combination of the physical decay of the radioisotope and, the biological catabolism and excretion of the radioimmunoconjugate. Studies of ^{131}I tositumomab have documented wide inter-patient variation and unpublished data suggests that bulky disease and splenomegaly may shorten the effective half-life. Here we have studied the variation in the effective half-life of ^{131}I rituximab between patients and also within individual patients at different time points during the course of their treatment and therefore with different degrees of tumour load. Table 4.4 shows the effective half-life from each dosimetric study with the prescribed and administered dose and activity for each therapeutic administration.

Figure 4.7. The concept of effective half-life ($T_{1/2}$Eff). This is the time taken for the activity in the body to fall to half the injected activity.
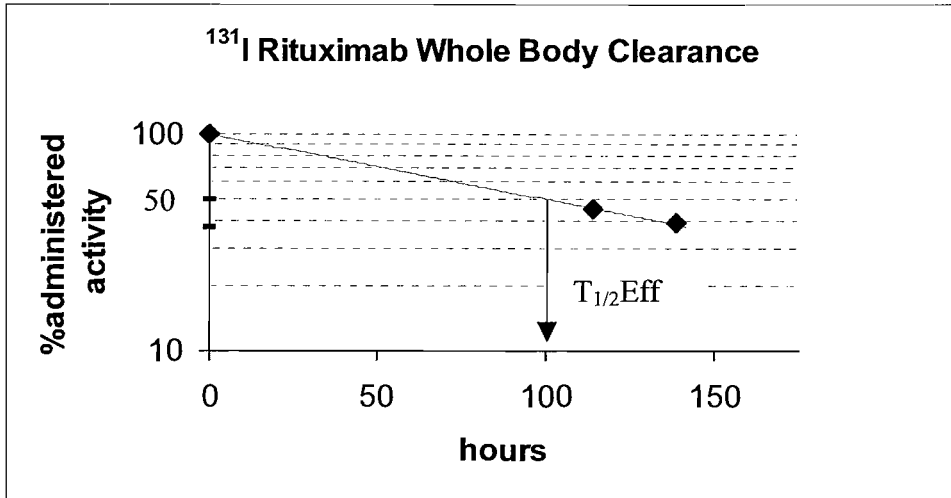

Figure 4.8. The concept of residence time. The area under the activity time curve Ah(t) is equal to that of the rectangle giving the residence time (th) which is the average time the administered activity stays in the body.
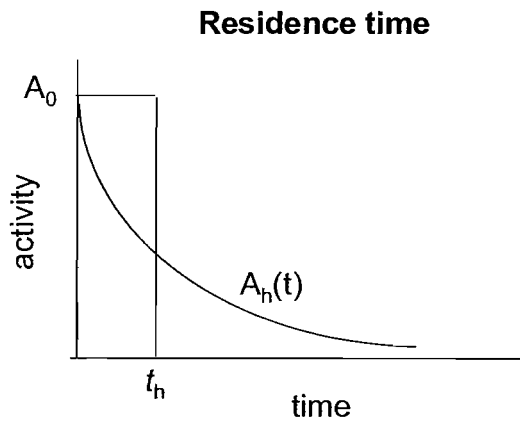

126

Table 4.4 The effective half-life with prescribed and delivered radiation dose in fractionated RIT trial patients.

Patient	Effective half- life (hours)	Prescribed whole body dose (cGy)	Prescribed activity (MBq)	Actual administered activity (MBq)	Actual whole body dose (cGy)
Fraction 1					
JB	119.5	15	335	337	15
NM	100.4	15	336	322	14.4
RJ	99	15	469	401	12.8
JH	80.6	15	527	498	14.2
HJ	100.4	30	693	653	28.3
TP	90.0	30	875	857	29.4
RH	93.6	30	874	839	31.3
CH	106.7	30	682	739	32.5
RD	103.3	45	1128	1151	45.9
MF	113.6	45	1240	1196	43.4
SY	81.7	45	1300	1324	45.8
IB	66.7	45	2106	2092	44.7
Fraction 2					
JB	123.8	15	327	335	15.4
NM	101.9	15	331	308	14
RJ	103.5	15	449	491	16.4
JH	115.5	15	368	354	14.5
HJ	96.3	30	723	769	31.9
TP	111.8	30	728	712	29.3
RH	93.6	30	864	864	28.5
CH	115.6	30	629	629	30
RD	105	45	1119	1094	44
MF	119.2	45	1204	1226	45.8
SY	100.6	45	1055	1013	43.2
IB	93.3	45	1480	1280	38.9

Due to the long effective half-life and the use of repeated dosimetric studies it became apparent that the dosimetric studies were contributing significantly to the total administered dose. The dose from each administration and the total cumulative dose are recorded in table 4.5.

Table 4.5 The dose for each in administration and the total cumulative whole body radiation dose for each patient tabulated in cGy.

Initials	Dosimetric Pre-induction	Dosimetric 1	Dosimetric 2	Therapy 1	Therapy 2	Total Dosimetric	Total Therapy	Total Dose (cGy)
JB		5.6	10.7	15	15.4	16.3	30.4	**46.7**
NM		7.1	7.6	14.4	14.0	14.7	28.4	**43.1**
RJ		2.8	6.4	12.8	16.4	9.2	29.2	**38.4**
JH		5.0	7.3	14.2	14.5	12.3	28.7	**41.0**
HJ		7.8	7.3	28.3	31.9	15.1	60.2	**75.3**
TP		6.3	7.5	29.4	29.3	13.8	58.7	**72.5**
RH		4.9	6.4	31.3	28.5	11.3	59.8	**71.1**
CH		7.7	9.3	32.5	30.0	17.0	62.5	**79.5**
RD	2.9	7.8	5.9	45.9	44.0	16.6	89.9	**106.5**
MF	2.9	6.4	6.7	43.4	45.8	16.0	89.2	**105.2**
SY	3.2	6.2	7.6	45.8	43.2	17.0	89.0	**106.0**
IB	2.5	3.8	5.7	44.7	38.9	12.0	83.6	**95.6**

As anticipated a wide range in the effective half-life was seen. The mean effective half-life for ^{131}I rituximab was 101.7 hours (range 66.7 -123.8). This is substantially longer than the half-life seen with the murine radioimmunoconjugate ^{131}I tositumomab which is

59.3 hours (range 24.6-88.6)[130]. This difference in half-life is perhaps to be expected as the chimeric mAb has a human Fc and thus substantially longer biological half-life than the murine counterparts. Most interesting however is the variability within the same patient during the course of the protocol. Figure 4.9 illustrates the average clearance rate prior to the first fraction, prior to the second fraction and in a cohort of four patients in whom we have performed a dosimetric study at the outset of the protocol prior to any induction rituximab and without a pre-dose. In table 4.6 the effective half-life and residence time of ^{131}I rituximab is documented prior to each administration and in figure 4.10 the sequential effective half-lives are recorded graphically for each individual patient.

Table 4.6 The effective half-life and residence time of ^{131}I rituximab.

patient	Pre- rituximab dosimetric		1st dosimetric		2nd dosimetric	
	residence time (hours)	effective half-life(hours)	residence time (hours)	effective half-life (hours)	residence time (hours)	effective half-life (hours)
JB			172.4	119.5	178.6	123.8
NM			144.9	100.4	147.1	101.9
RJ			149.3	99.0	149.3	103.5
JH			116.3	80.6	166.7	115.5
HJ			144.9	100.4	138.9	96.3
TP			129.9	90.0	161.3	111.8
RD	55.6	38.6	149.4	103.3	151.5	105.0
RH			135.1	93.6	135.1	93.6
CH			153.9	106.7	166.7	115.6
MF	71.4	49.5	163.9	113.6	172.4	119.2
SY	58.8	40.8	117.6	81.7	144.9	100.6
IB	59.5	41.3	96.0	66.7	134.4	93.3
median		45.2		99.7		104.3
mean		42.6		96.6		106.7

These figures suggest that the very prolonged mean effective half-life of ^{131}I rituximab seen in this study is not simply the result of using a chimeric mAb but also results from the scheduling of the RIT with the initial 4 weeks of unlabelled induction rituximab having a substantial impact on the kinetics of ^{131}I rituximab in subsequent doses.

Figure 4.9. The mean clearance of ^{131}I rituximab is shown prior to the first fraction (Dose 1), second fraction (Dose 2) and in the patients who received ^{131}I rituximab with no pre-dose or induction rituximab (pre rituximab). Exposure to induction rituximab and the pre-dose dramatically prolongs the clearance of ^{131}I rituximab.
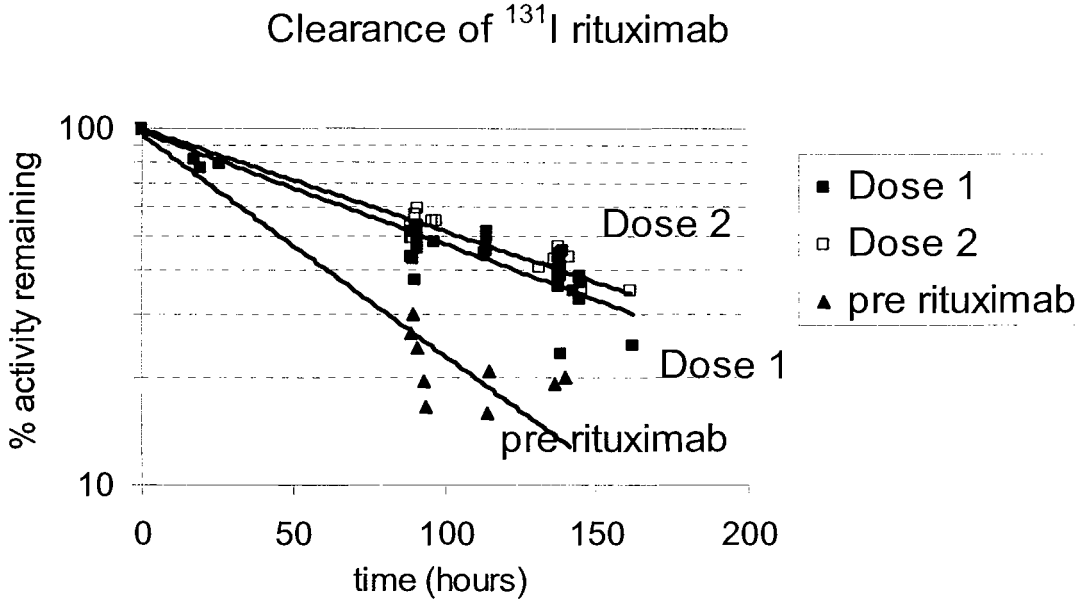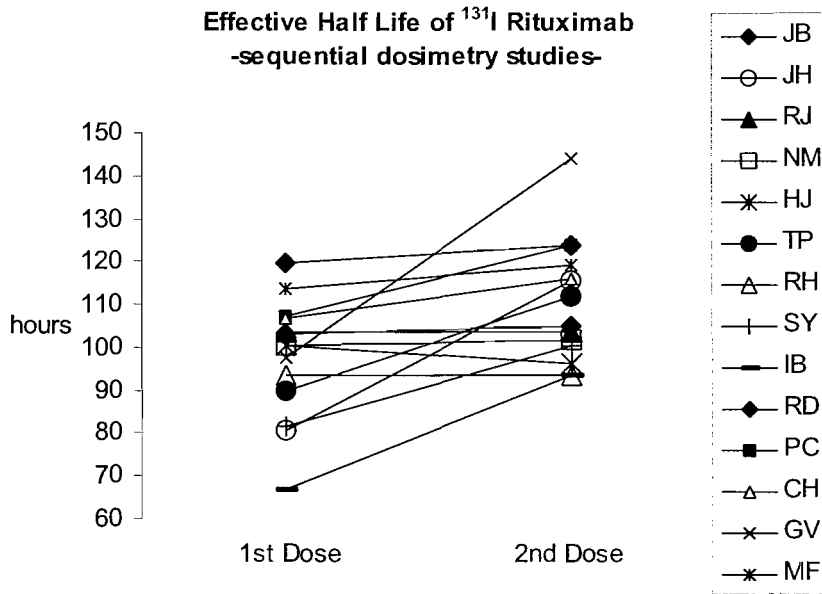

Clearance of ^{131}I rituximab

Figure 4.10. A The effective half-life of ^{131}I rituximab is shown for each patient prior to the first and second fraction of demonstrating substantial inter-patient variability and a trend towards a longer effective half-life with the second fraction. **B** In 4 patients the effective half-life is shown before any rituximab is delivered as well as prior to each fraction of ^{131}I rituximab. The induction rituximab and pre-dose dramatically prolong the clearance of ^{131}I rituximab.

A

Effective Half Life of ^{131}I Rituximab
-sequential dosimetry studies-

Legend A: JB, JH, RJ, NM, HJ, TP, RH, SY, IB, RD, PC, CH, GV, MF

hours (y-axis: 60 to 150)
x-axis: 1st Dose, 2nd Dose

B

Effective Half Life of ^{131}I Rituximab
-sequential dosimetry studies-

Legend B: SY, IB, RD, GV, MF

hours (y-axis: 30 to 150)
x-axis: Pre-, 1st Dose, 2nd Dose
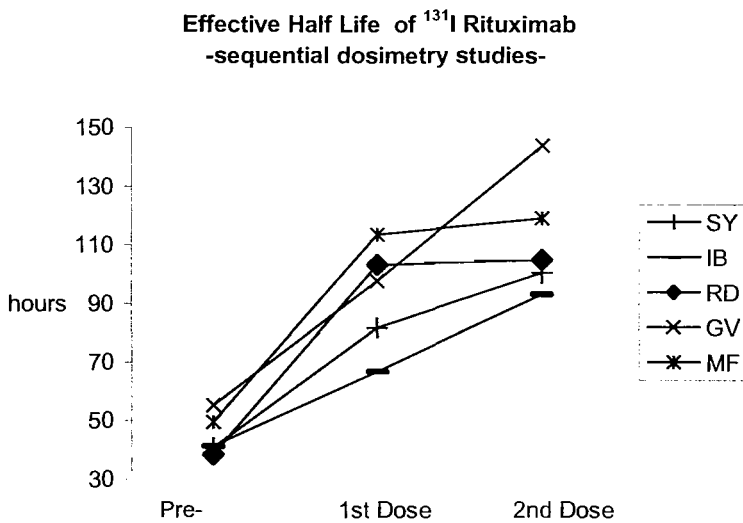
The induction rituximab results in a dramatic prolongation of the effective half-life of the radioimmunoconjugate. This increase in the half-life is probably due to the clearing CD20 positive B cells from the circulation, spleen and bone marrow and a reduction in the volume of disease. In addition for some patients the effective half-life has increased with the second fraction as compared to the first. This observation was most marked in patient JH who had extensive bone marrow involvement at the outset and who had a dramatic clinical response to the RIT between the first and second fractions as illustrated in figure 4.11. These results support the conclusion that tumour load appears to be one of the most significant factors to impact on the rate at which the radioimmunoconjugate is cleared from the patient.

Figure 4.11. Patient JH had a dramatic clinical response between the first and second fraction of RIT. **A)** shows resolution of scalp infiltration, facial oedema and neck lymphadenopathy correlating with reduction in uptake from scalp and pre auricular nodes as well as a reduction in the width of mediastinum (arrows). **B)** CT scans before and after completion of the RIT protocol illustrate resolution of the splenomegally (s) and para-aortic lymphadenopathy (white arrow). **C)** The response between the 2 fractions of RIT correlates with a marked increase in the effective half-life of the radioimmunoconjugate in this patient.
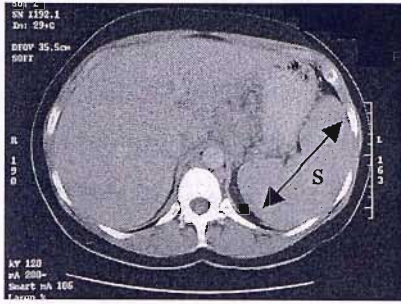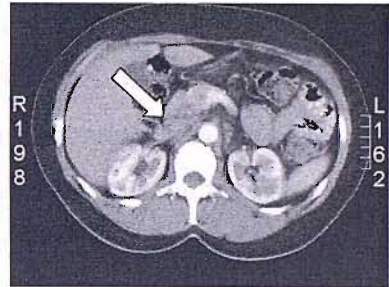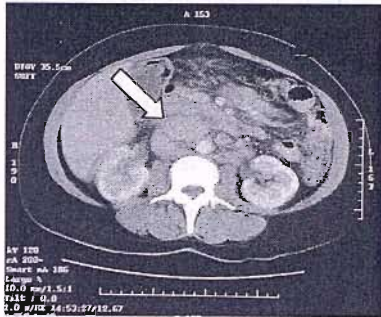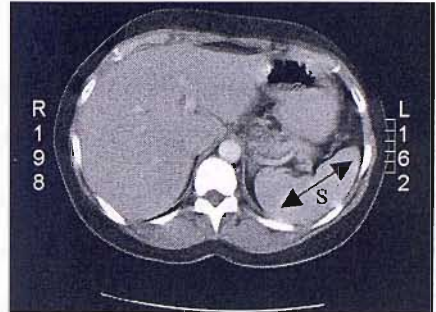
A) JH Pre #1 RIT   JH Pre #2 RIT
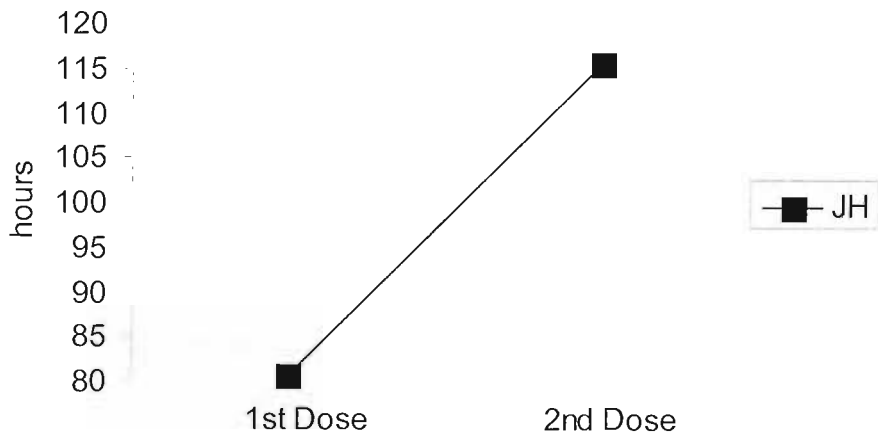
B) Pre RIT   Post RIT

C)

Effective Half Life of Sequential Doses of ^{131}I Rituximab

4.4.2.2 Blood Clearance Of Radioimmunoconjugates

To increase our understanding of the pharmacokinetics of the radioimmunoconjugate and in particular the impact of induction rituximab and the pre-dose on the biodistribution of the ^{131}I rituximab in selected patients the blood clearance of the radioimmunoconjugate was determined. The rapid initial clearance is consistent with redistribution of the radioimmunoconjugate from the blood compartment into the extra-vascular space, while the subsequent slower clearance correlates with the whole body effective half-life reflecting physical radioactive decay combined with catabolism and excretion of the radioimmunoconjugate. Interestingly the initial rate of blood clearance following the dosimetric dose given without prior exposure to rituximab was substantially more rapid than with a dosimetric dose performed after induction rituximab and the pre-dose prior to the fist dose of ^{131}I rituximab. Figure 4.12 demonstrates the clearance both with and without pre-dose and induction rituximab over the first 150 hours. Figure 4.13 shows the clearance over the first 4 hours demonstrating that it is this very early clearance rate that predominantly accounts for the difference seen with and without prior rituximab. These observations support the conclusion that the initial clearance of ^{131}I rituximab from the circulation and from the body as a whole is likely to be dependent on the quantity of accessible CD20 antigen available for binding. The amount of available CD20 antigen will be reduced after the induction rituximab as this will result in a fall in the number of CD20 expressing B cell in the blood, bone marrow and spleen as well as potentially bringing about a reduction in the number of accessible CD20 positive tumour cells. The pre-dose may similarly effect the rate of blood clearance of ^{131}I rituximab by binding accessible CD20 antigen in the blood, bone marrow and spleen and thereby blocking the binding of circulating ^{131}I rituximab.

Figure 4.12. Blood clearance of ^{131}I rituximab. A clear difference is seen between the rate of clearance when there has been no prior exposure to rituximab (pre), when compared to the rate of clearance with the first fraction of RIT given after both induction rituximab and a pre-dose (#1).

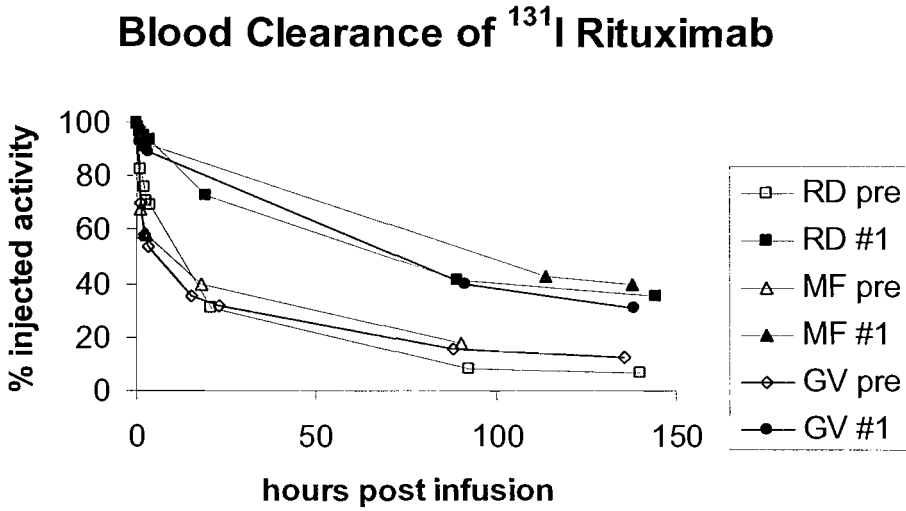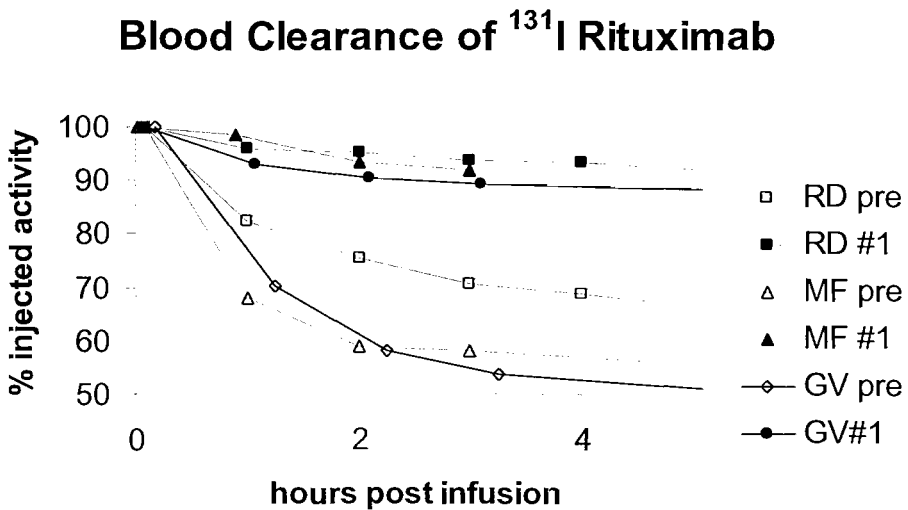## Blood Clearance of ^{131}I Rituximab

Figure 4.13. Blood clearance of ^{131}I rituximab. The difference in rate of clearance of ^{131}I rituximab when previously exposed to rituximab (#1) when compared to no previous exposure to rituximab (pre) occurs predominantly within the first 2 hours after administration.

## Blood Clearance of ^{131}I Rituximab

135

4.4.2.3 Gamma Camera Imaging Of Tumour Targeting

The relatively high energy of the gamma emission limits the resolution of the images that can be obtained using a gamma camera with ^{131}I labelled mAb. With prolonged acquisition times in this study it was however possible to demonstrate effective targeting of the radioimmunoconjugate to sites of tumour in the majority of patients. Examples of such targeting are illustrated in figures 4.14 - 4.16. It is interesting to note that by the time of the second dosimetric dose prior to the second fraction of RIT, the targeting seen with the first fraction is no longer detectable. This is likely to correlate with a response to therapy in all patients such that by the time of the second dose there was a substantial reduction in the volume (or resolution) of all clinically palpable lymphadenopathy. This suggests that the failure to see tumour with gamma camera images may be because sites of persisting tumour are too small to be resolved with ^{131}I imaging rather than a failure of the radioimmunoconjugate to target tumour. Figure 4.16 demonstrates targeting of ^{131}I rituximab to tumour in a patient that has had no pre-dose or induction illustrating that although in some patients the pre-dose may be necessary to optimise targeting in many patients, good targeting may be seen without a pre-dose. By contrast Figure 4.17 demonstrates failure of the radioimmunoconjugate to target sites of tumour in a patient with widespread nodal disease, mild splenomegaly and bone marrow involvement. In this case in the absence of a pre-dose all the activity has been concentrated in the spleen at the expense of tumour sites elsewhere in the body. These two examples illustrate that at least for some patients, especially those with a heavy tumour burden or splenomegaly a pre-dose of unlabelled antibody is necessary to improve the biodistribution of the RIT.

Figure 4.14 A) Gamma camera images of patient TP taken prior to the first fraction of RIT indicating targeting of ^{131}I rituximab to the axillae and pelvis correlating with sites of pathologically enlarged lymph nodes demonstrated on the pre treatment CT. **B)** Gamma camera images of patient TP prior to second fraction of RIT showing absence of previously seen targeting correlating with clinical response and resolution of all palpable lymph nodes. The CT images confirm the clinical response but are taken 8 weeks after completion of the second fraction of RIT.

A)   **TP Pre #1 RIT**
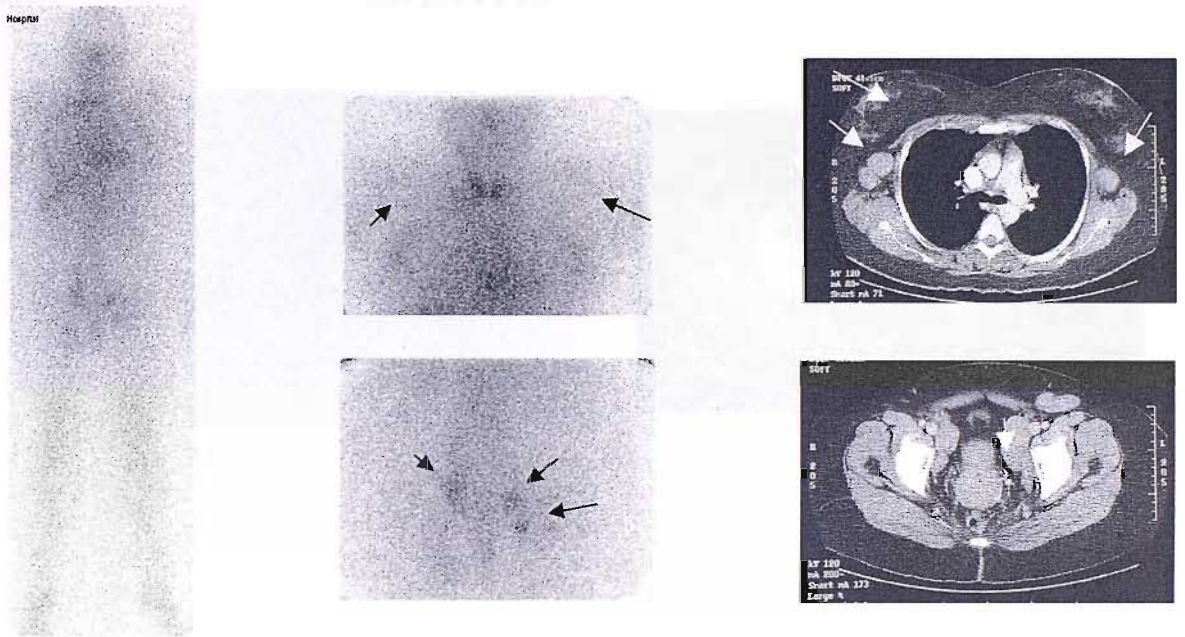
B)   **TP Pre #2 RIT**
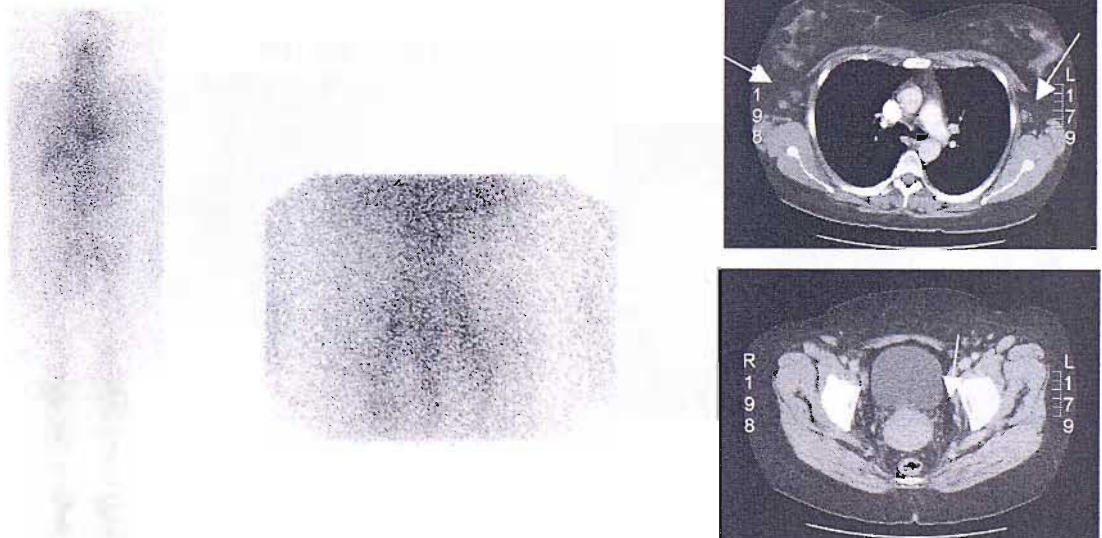
Figure 4.15 A) Gamma camera images of patient RH taken prior to the first fraction of RIT indicating targeting of ^{131}I rituximab to the pelvis (arrows) correlating with the site of bulky pathologically enlarged lymph nodes demonstrated on the pre treatment CT. **B)** Gamma camera images of patient RH prior to second fraction of RIT showing some reduction in intensity of uptake in the pelvis. This appears to correlate with clinical response and partial resolution of the palpable right iliac fossa mass confirmed on CT scan performed at week 25.

A)   **RH pre #1 RIT**
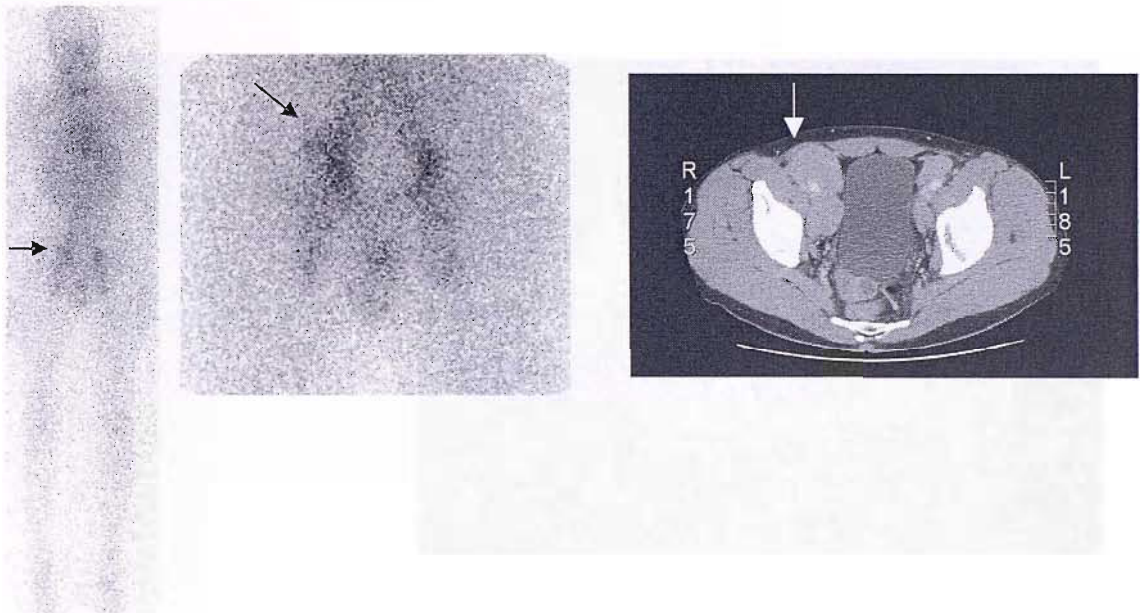
B)   **RH pre #2 RIT**
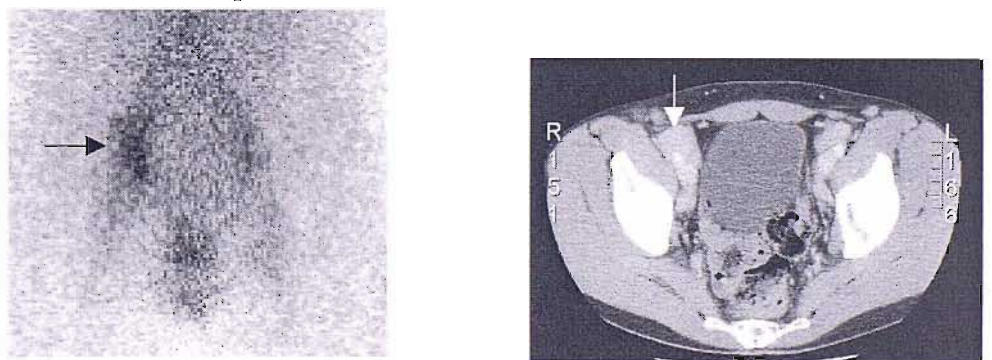
Figure 4.16. A) Gamma camera image taken on day 4 post dosimetric dose administered to patient RD without prior induction rituximab or pre-dose. Activity localised to the left neck (arrow) correlates with a 5 cm mass of lymphoma demonstrated on the CT (arrow). B) Gamma camera image taken 4 days after 1st dose of RIT having completed induction rituximab and been given pre-dose. The activity in the left neck is no longer present correlating with almost complete clinical resolution of the mass.

A.   **RD Pre RIT (no induction or pre-dose)**
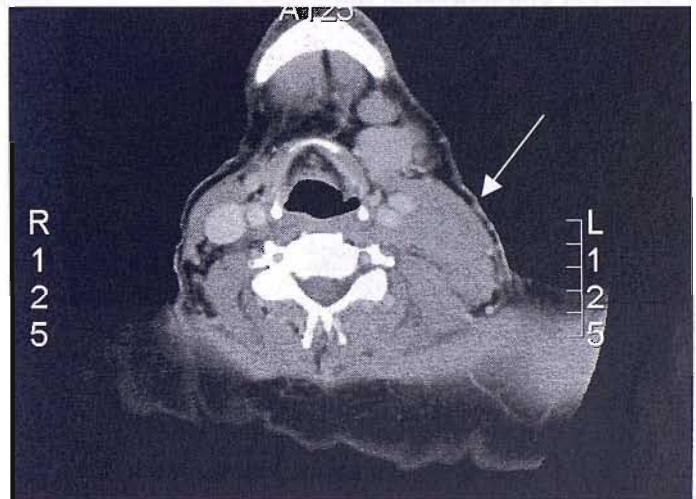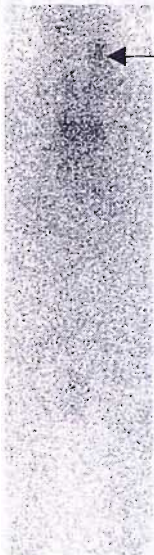
B.   **Following Induction and pre-dose**

Figure 4.17 Gamma camera image taken on day 4 post dosimetric dose administered to patient SY without prior induction rituximab or pre-dose (A). Despite extensive nodal involvement documented on CT almost all the activity is concentrated in the mildly enlarged spleen. Following a course of induction rituximab and the predose the day 4 image in the same patient shows loss of the activity in the spleen with evidence of targeting of ^{131}I rituximab to axillary, abdominal and pelvic lymph nodes (arrows).

A. Pre RIT (no induction or pre-dose)   B. Following induction and pre-dose
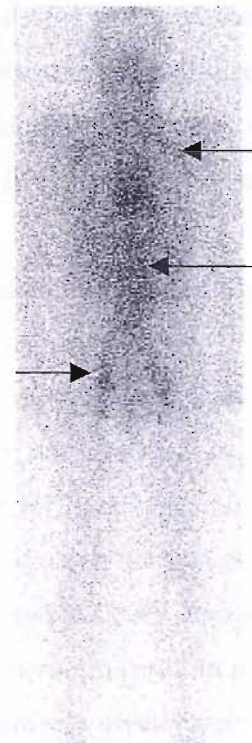
4.1   TOXICITY

One of the primary outcome measures of a phase I/II clinical trial is to document toxicity. The extensive experience with RIT for lymphoma has given a clear picture of the toxicity to be anticipated following the delivery of single non-myeloablative doses of murine anti-CD20 RIT. The non-haematological toxicity is manifested by acute reactions to the administration of the unlabelled mAb. This reaction is thought to result from the recruitment and activation of complement by the infused antibody binding to CD20 bearing B cells. This type of reaction is usually minimised by pre-medication with paracetamol and an anti-histamine. When necessary the reaction can usually be easily managed by slowing or stopping the infusion and administering further paracetamol, antihistamine and, if the reaction is more severe, hydrocortisone and nebulised salbutamol. These acute reactions rarely prevent completion of the delivery of mAb and are rarely life threatening especially if established supportive care protocols are utilised.

The dose limiting toxicity for non-myeloablative RIT is haematological. Following a single dose of murine anti-CD20 RIT this is manifest as neutropenia and thrombocytopenia occurring with a nadir at 6-8 weeks. The myelosuppressive kinetics are thought to be secondary to an effect of the radiation on bone marrow stem cells. Although there is substantial clinical experience with RIT for lymphoma using murine radioimmunoconjugates there is relatively little published data on the toxicity of chimeric or humanised radioimmunoconjugates and their development has been delayed by concerns that the longer circulating half-life of these agents might result in prolonged exposure of the bone marrow to radiation and thus unacceptable myelotoxicity. Due to this concern and the limited data on the effect of a second dose of RIT on the bone marrow shortly after recovery from a previous dose, the dose escalation within this study protocol started from a relatively low dose, substantially lower than the established safe dose for the murine anti-CD20 radioimmunoconjugate, ^{131}I tositumomab. Based on the previous pre-clinical and clinical studies of fractionated RIT discussed in section 1.7 it is anticipated that the severity of haematological toxicity will be reduced by the fractionation of the RIT. By using this fractionated schedule, escalation of the cumulative

whole body dose to greater than that achievable with a single administration, may be possible.

4.4.3   Toxicity Results

4.4.3.1   Haematological

No dose limiting toxicity was seen with the first dose cohort (figure 4.18) and only minor reductions in neutrophils and platelets have so far been seen in the second dose cohort as documented in figure 4.20. Neutropenia occurred in one patient in the first dose cohort (figure 4.19). The timing of this appeared incompatible with radiation toxicity as it occurred earlier than would have been expected and recovery was seen when radiation toxicity is usually manifest. Similarly in one patient in the second dose cohort (patient HJ) neutropenia was seen, once again there is substantial doubt as to whether this neutropenia can entirely be ascribed to radiation toxicity due to its timing and the absence of concurrent thrombocytopenia (figure 4.21). In an attempt to explain this idiosyncratic neutropenia blood samples were sent for analysis to exclude the development of anti-neutrophil antibodies in patient JB (Jeff Lucas, National Blood Service, Bristol), but no such antibodies were found. Alternative explanations for these episodes of neutropenia will be discussed below (4.6). From the data available to date no dose limiting haematological toxicity has been seen in dose cohort 3 (figure 4.22).

Figure 4.18. Haematological toxicity Dose Cohort 1. **(A)** Weekly platelet count demonstrates no significant fall following RIT. **(B)** Weekly neutrophil count demonstrates a significant fall in just one patient (see below). The timing of administration of rituximab(+) and ^{131}I rituximab (*) is indicated on each graph.

A)

Dose Cohort 1
Platelets

B)

Dose Cohort 1
Neutrophils
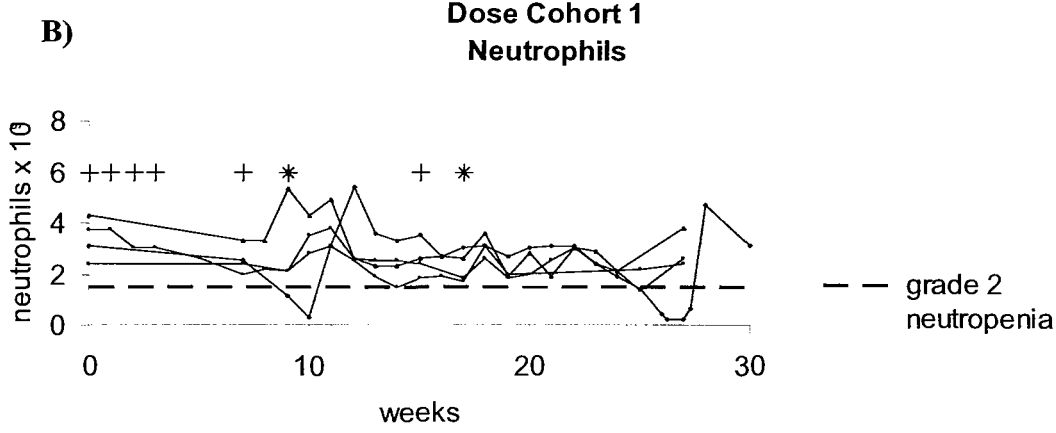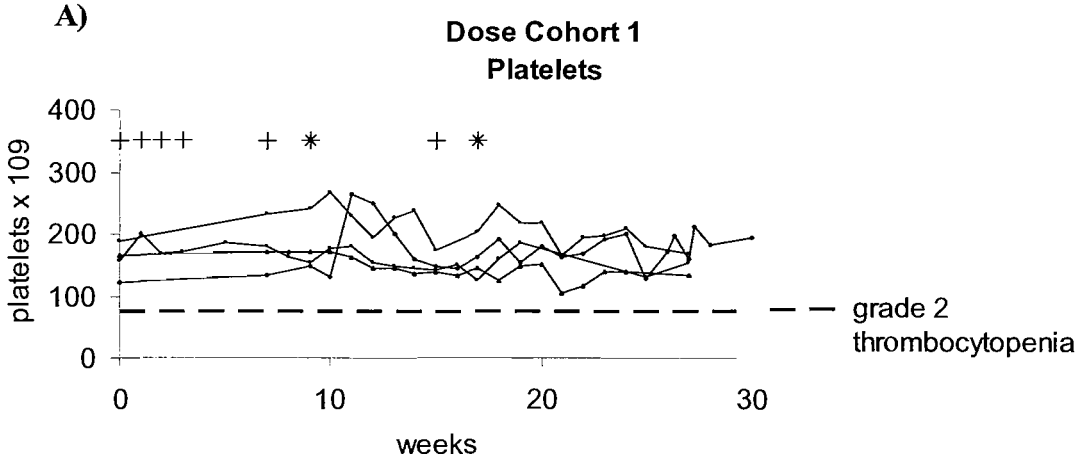
Figure 4.19. The weekly neutrophil count for patient JB from dose cohort 1 identified 2 episodes of profound neutropenia occurring with timing incompatible with radiation toxicity and therefore ascribed to an idiosyncratic response to rituximab.
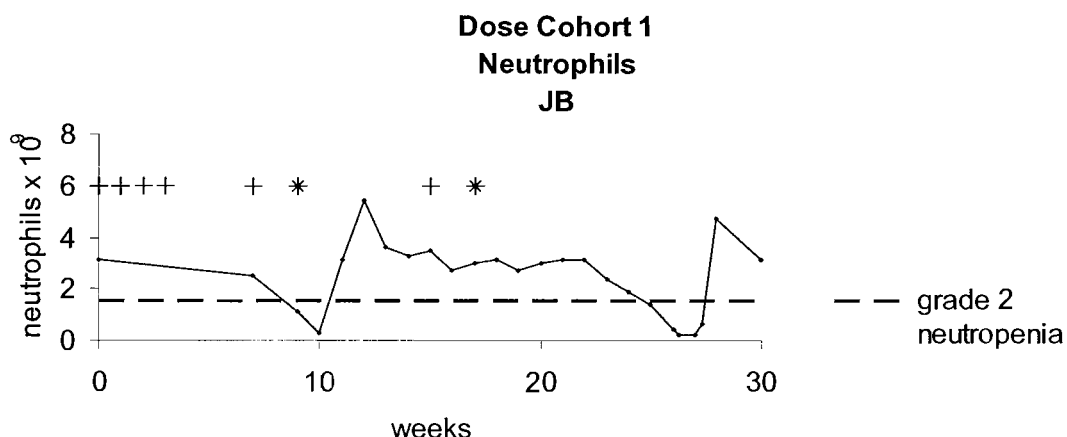
Figure 4.20. Haematological toxicity dose cohort 2. Weekly platelet **(A)** and neutrophil **(B)** counts are illustrated demonstrating minor asymptomatic myelosuppression without reaching the threshold defined in the protocol to indicate MTD.

B)

Dose Cohort 2
Neutrophils
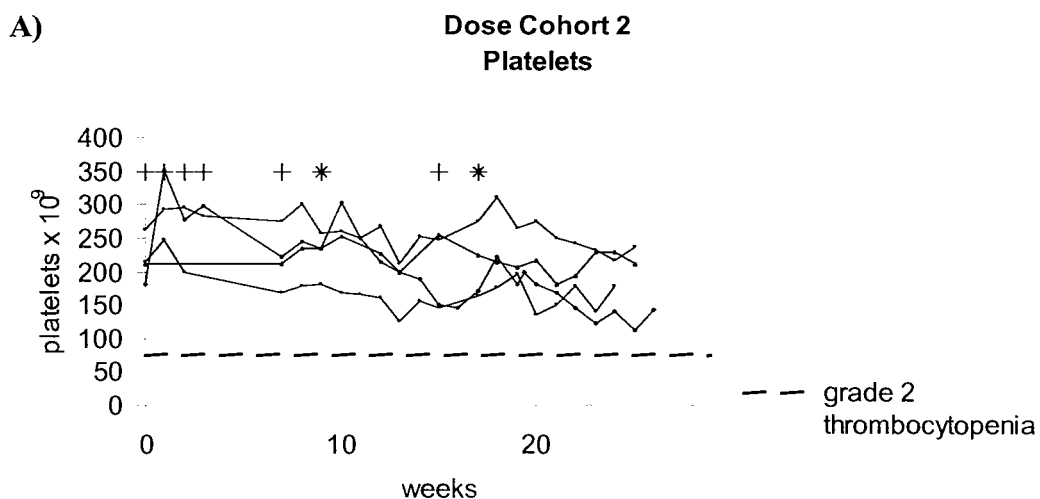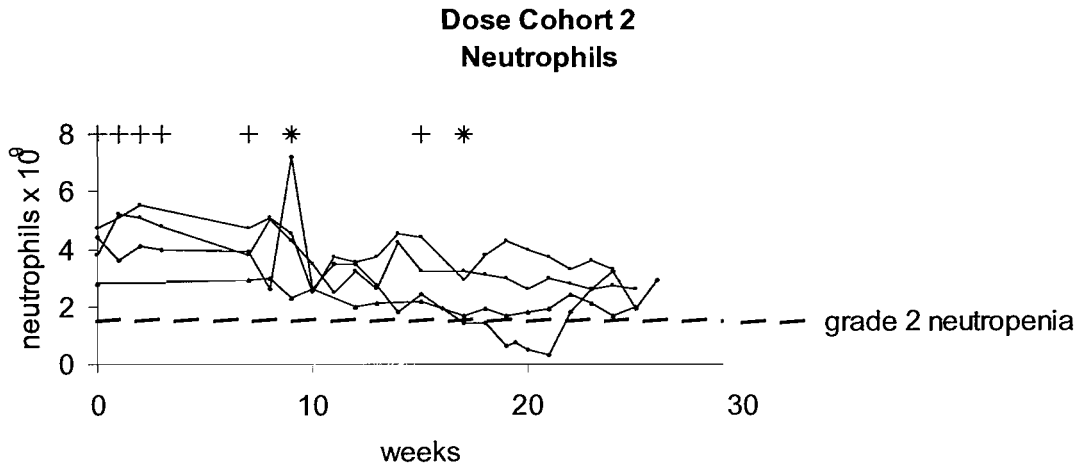
Figure 4.21 The weeky neutrophil count for patient HJ dose cohort 2 identified significant neutropenia occuring 2-3 weeks after the second therapy dose. This is earlier than normally anticipated following RIT and was not accompanied by significant thrombocytopenia.

Dose Cohort 2
Neutrophils
HJ
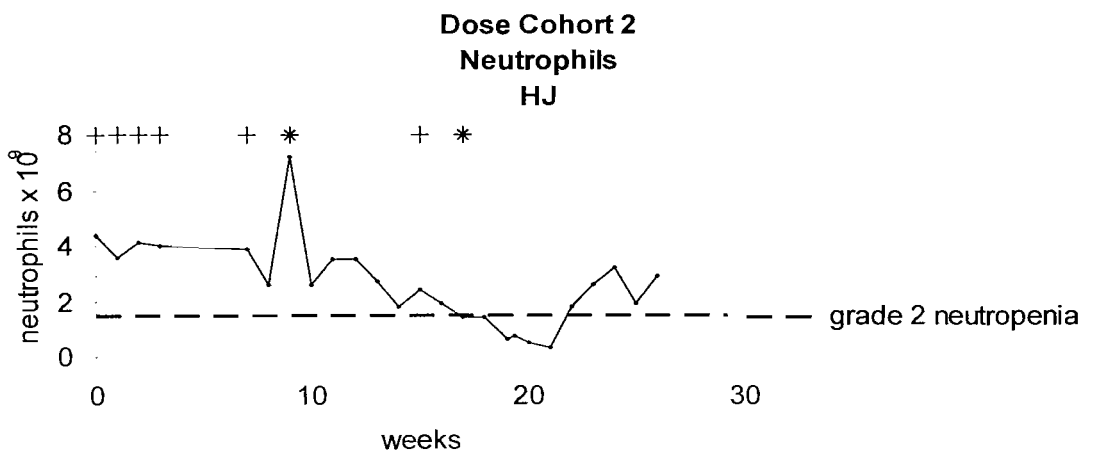
Figure 4.22. Haematological toxicity dose cohort 3. Weekly platelet **(A)** and neutrophil **(B)** counts are illustrated demonstrating minor asymptomatic myelosuppression without reaching the threshold defined in the protocol to indicate MTD.

Dose Cohort 3
Platelets

Dose Cohort 3
Neutrophils
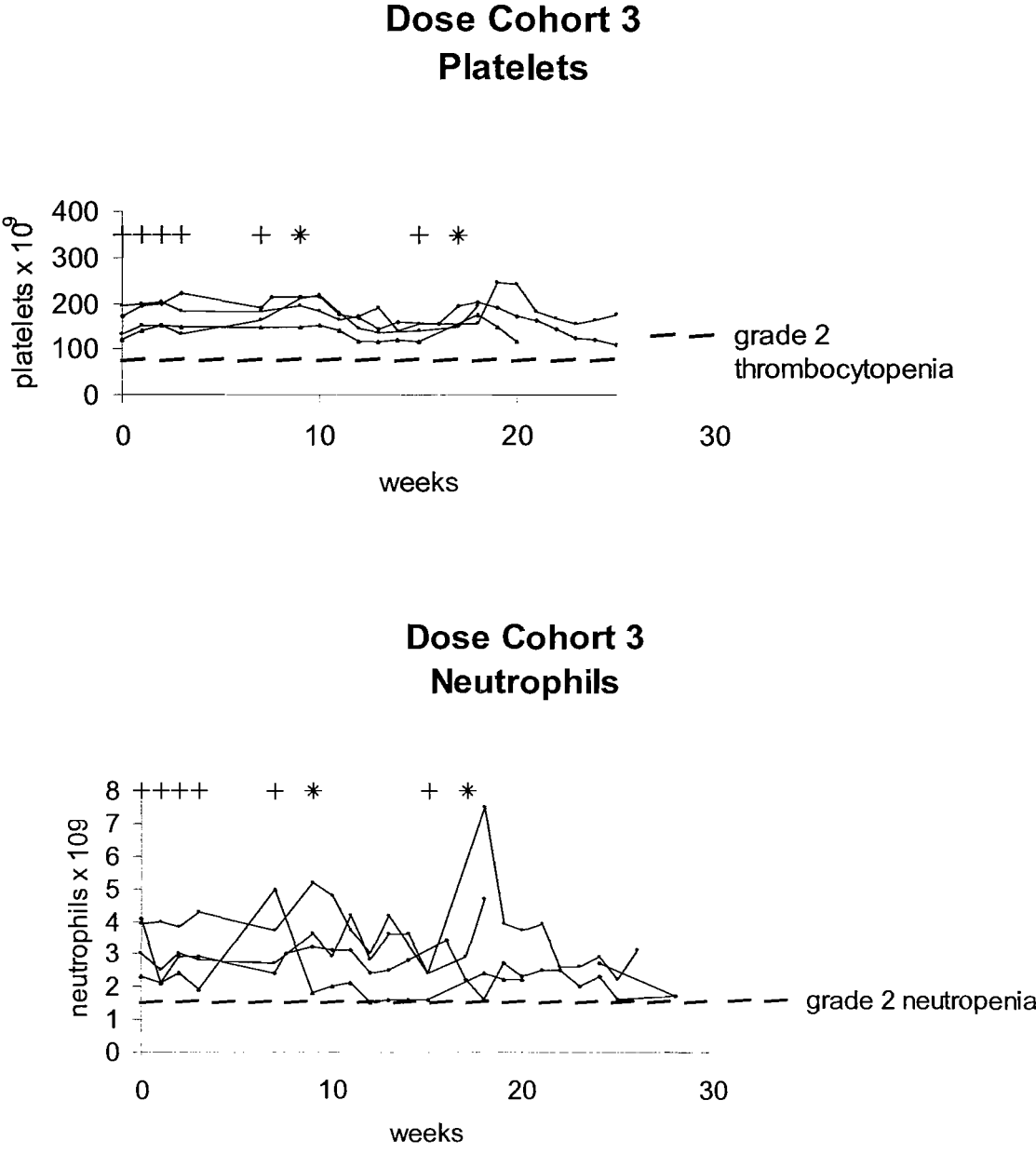
4.4.3.2 Non Haematological Toxicity Results

The only non-haematological toxicity seen to date has taken the form of acute infusion reactions. These have comprised fever, rash, wheeze, facial oedema and transient diarrhoea. All such reactions have responded to slowing or transiently suspending the infusion combined with the administration of hydrocortisone, additional chlorpheniramine, paracetamol and in one case nebulised salbutamol. No other significant non haematological toxicity has been reported (> grade 2 NCIC). All biochemistry parameters have remained within normal limitsand thus far there has been no elevation of TSH. As anticipated immunoglobulins declined during the course of the therapy but no adverse infectious complications have been reported.

4.5   ASSESSMENT OF RESPONSE TO RIT

4.5.1   Materials and Methods

Following completion of the study protocol patients are being followed up with regular clinical assessment, cross-sectional imaging using computerised tomography (CT) and for those with bone marrow involvement a follow up bone marrow. Determination of the status of the patient as PR, CR, SD or PD is according to the guidelines of The International Workshop to Standardize response Criteria for NHL [162]. The schedule for timing of follow up investigations is documented in Appendix 3.

4.5.2   Results

Preliminary follow up data is available for all the patients in the first 3 dose cohorts. All 12 patients demonstrated a response at the first assessment 8 weeks after completion of the protocol.

Cohort 1   1mixed response(MR), 2PR,1 CR.

Cohort 2   3PR, 1CR.

Cohort 3   3PR, 1CR.

Table 4.7 documents the responses seen in the first 2 dose cohorts with patient characteristics at time of trial entry. Importantly in all except one of the patients in the first 2 dose cohorts the duration of response has exceeded that seen with their preceeding chemotherapy regimen. Follow up data on the third dose cohort is too short to give a meaningful indication of the duration of response. Figure 4.23 shows CT scans illustrative of one of the responses. Even at the low doses administered in the first dose cohort it is possible to achieve durable responses with the first two patients remaining in remission 18 months after completion of the treatment protocol.

Table 4.7 Response correlated with patient characteristics at the time of trial entry

		Dose cohort 1				Dose Cohort 2			
Patient		JB	NM	RJ	JH	HJ	TP	RH	CH
PS		1	1	0	1	0	0	0	1
Stage		4A	2A	3A	4A	4A	3A	4A	4A
No. of previous courses of chemo		3	1	3	3	2	2	4	2
Duration + quality of response to prior chemo		13mo PR	5mo CR	2mo PR	3mo PR	7mo PR	4mo PR	3mo PR	- NR
LDH		874	392	369	431	416	NA	343	478
BM %		15	0	0	50	5	0	20	5
Time of assesment									
Week 6	BM	-	-	-	20%	-	-	-	
Week 25	CT BM	PR 0%	CR -	SD -	PR <5%	CR 0%	PR -	PR 0%	PR 0%
Week 52	CT	Good PR	CR	SD	PD	PD	PD	PD	PD
Week 78	CT	CR	CR	PD					
Duration of response		>18mo	>18mo	12mo	9mo	9mo	6mo	3mo	5mo

Figure 4.23. Sequential CT scans of patient JB taken at **A)** entry to trial, **B)** 6 months and **C)** 1 year indicating a good partial response with improvement in the quality of the response between 6 months and 1 year as shown by reduction in the size of retroperitoneal lymph nodes (arrow)

A) JB   Pre RIT
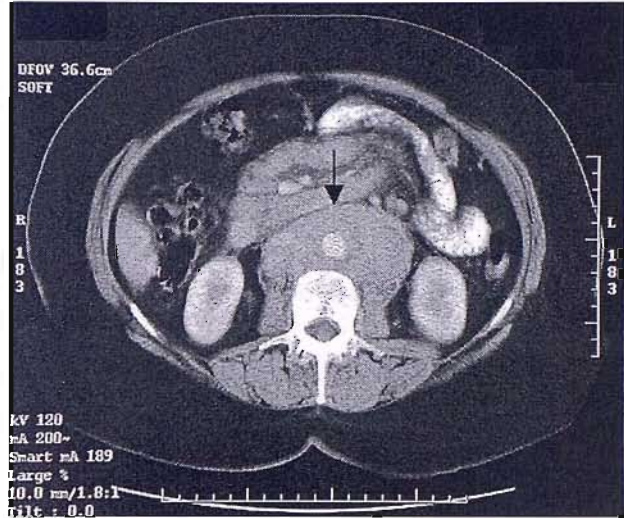
B) JB 8 weeks post RIT
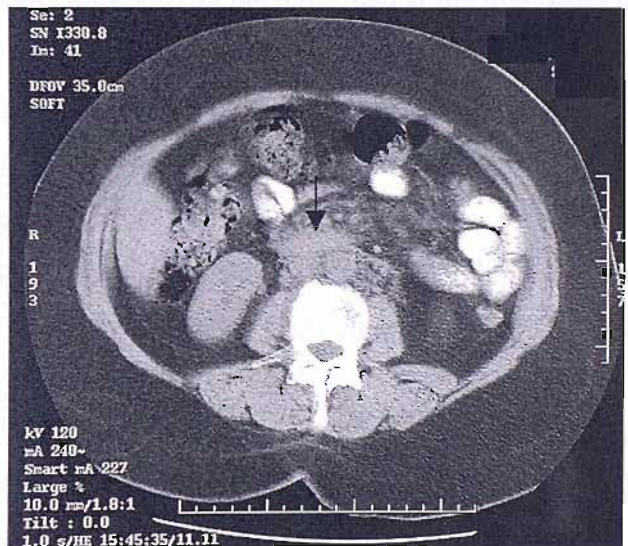
C) JB 8 months post RIT
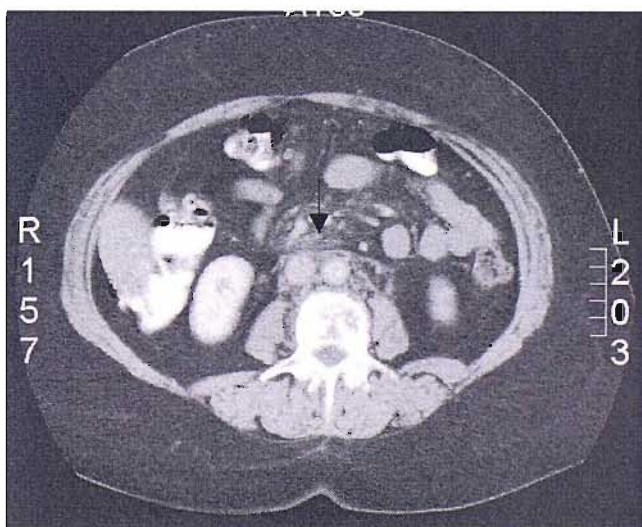
4.6   DISCUSSION AND CONCLUSIONS

The initial results from this clinical study have produced a number of interesting findings.

1. A simple and reliable method of producing clinical grade ^{131}I labelled rituximab has been established.

2. Delivery of fractionated ^{131}I rituximab to patients with relapsed or refractory indolent NHL is feasible with promising durable response rates.

3. The maximum tolerated dose has not been reached at the third dose level, which is more than 30% above that tolerated for a single infusion.

4. The effective half-life of the chimeric anti-CD20 radioimmunoconjugate is longer than that previously seen with murine anti-CD20 radioimmunoconjugates.

5. The scheduling of the radioimmunoconjugate appears to have a dramatic impact on both the blood and the whole body clearance of radioimmunoconjugate.

6. Minimal haematological toxicity has been seen with isolated reversible neutropenia that did not correlate with the timing or dose of radiation and was probably related to an idiosyncratic effect of rituximab.

Using the trial protocol described above by December 2004 a total of 14 patients had received fractionated ^{131}I rituximab. The toxicity and impact of the treatment on quality of life compares extremely favourably with the chemotherapy regimens to which they would have otherwise been subjected.

The response data to date are encouraging though must be interpreted with caution as this is a non randomised phase I/II study of a highly selected group of patients. It is notable that even at this early stage in the assessment of response there is evidence of ongoing improved quality of response (PR to CR) between 6 months and 1 year concurring with the observation discussed in section 1.2.3.4 that the time to maximum response with RIT may be substantially delayed and suggesting the possibility that the treatment activates some form of host immune response.

Optimisation of the iodogen bead method of labelling rituximab with ^{131}I has enabled reliable production of clinical grade radioimmunoconjugate without excessive exposure of staff to radiation. Delivery of the radioimmunoconjugate has proven straightforward with no acute reactions over and above those conventionally anticipated with the delivery of unlabelled rituximab. Dose limiting haematological toxicity has not yet been seen at the third dose level. However 2 cases of neutropenia have been reported that have occurred in the absence of significant thrombocytopenia. This and the timing of the neutropenia makes radiation toxicity as a cause unlikely. A review of the literature suggests that an idiosyncratic reaction to rituximab is the most likely cause of this neutropenia though the mechanism remains unexplained.

Since the start of the study new data has been reported indicating a significant incidence of delayed neutropenia in patients receiving unlabelled rituximab. Chaiwatanatorn et al report an incidence of grade 4 delayed onset neutropenia of 13% (95% confidence interval 7-27%) per course of treatment with rituximab [163]. Previous studies have reported a substantially lower incidence of such neutropenia ranging between 0.6% and 5.4% however this may in part be due to the lower frequency of monitoring of the blood count in these studies [43 68 164 165]. Recent unpublished data from Ghielmini et al of the Swiss SAKK group indicates an incidence of delayed neutropenia of 15% when rituximab is given in the context of a maintenance study with frequent monitoring of haematological parameters. The mechanism of such idiosyncratic neutropenia remains obscure. The evolution of a population of large granular natural killer lymphocytes previously proposed as a cause in 2 patients [166] has not been supported by subsequent

observations and certainly no such population was seen in patient JB who had a bone marrow aspirate and trephine during her second unexplained episode of neutropenia. It seems likely that the delayed neutropenia is a consequence of the disordered immunological status following rituximab administration and perhaps an aberrant process of B cell reconstitution resulting in the production of auto-antibodies or other factors that influence the neutrophil count. As the neutropenia recorded in patient JB is unlikely to be due to the radiation dose the results were excluded from the analysis of toxicity for the purposes of indicating the MTD.

Perhaps most dramatic findings so far in this study are derived from pharmacokinetic analysis of the radioimmunoconjugate. The chimeric radioimmunoconjugate has been demonstrated to have an effective half-life after administration that is nearly twice as long as that of its murine counterpart. This prolongation of the effective half-life is to be expected secondary to the human Fc portion of the chimeric antibody however the scale of the difference is surprising and is substantially longer than the only previously published pharmacokinetic data on ^{131}I rituximab provided by Scheidhauer et al in which a mean effective half-life of 88 hours is reported as compared to the mean effective half-life in our study of 102 hours [161]. Despite this prolonged half-life and the resulting prolonged exposure of bone marrow to circulating radioimmunoconjugate, at the doses studied, to date this does not appear to have resulted in unacceptable haematological toxicity. More detailed analysis of our pharmacokinetic data reveals the explanation for the discrepancy between the effective half-life in our study and that published by Scheidhauer. Sequential analysis of both the blood clearance of radioimmunoconjugate and the whole body effective half-life in individual patients at a series of points within the treatment protocol reveals the substantial impact of the scheduling of the radioimmunoconjugate on the blood and whole body clearance. Induction rituximab and the pre-dose is seen to result in substantial prolongation of the effective half-life of the subsequently infused radioimmunoconjugate. With sequential doses of radioimmunoconjugate the effective half-life has tended to become longer correlating with response and reduction in the tumour load. These findings suggest that the clearance of radioimmunoconjugate both from the blood and the whole body is in part dependent

on the quantity of available CD20 antigen for binding. In the pharmacokinetic study by Scheidhauer no pre-dose or induction rituximab was given. Rapid binding to and subsequent clearance of radioimmunoconjugate on normal CD20+ B cells in the blood, bone marrow and spleen will therefore have significantly shortened the measured half-life of the ^{131}I rituximab.

Why binding of ^{131}I rituximab to either normal B cells or CD20+ lymphoma cells should result in such rapid clearance of the ^{131}I is not immediately clear. It is well established that the CD20 antigen does not modulate on being bound by an antibody and that the antibody remains on the cell surface [55]. This is important for RIT, as iodinated mAb are relatively unstable in vivo. On internalisation iodinated radioimmunoconjugates are rapidly catabolised, producing iodo-tyrosine, which rapidly diffuses from the cell and is renally excreted resulting in loss of targeting and increased exposure of normal tissues to radiation. Despite the in-vitro observation that anti-CD20 antibodies do not internalise on binding, it is likely that the in vivo situation is more complex. If an antibody binds to a cell triggering ADCC it is likely that the antibody will be phagocytosed along with the cell by macrophages resulting in catabolism of the radioimmunoconjugate. Likewise if a radioimmunoconjugate precipitates CDC or cell death through apoptosis or necrosis it is likely that the debris will by mopped up by macrophages, once again resulting in catabolism of the radioimmunoconjugate and the rapid excretion of the [131]I. Even if mAb binds to a cell upon which it has no immediate effect there is evidence that the mAb will be gradually internalised probably because of bulk turnover of cell surface constituents [167]. The typical half-life for such turnover is reported to be about 2 days, which is well within the timescale relevant to RIT. It seems clear therefore that once ^{131}I rituximab has bound to the CD20 antigen it will be relatively rapidly catabolised and the ^{131}I excreted. This would explain the relatively short effective half-life seen when the radioimmunoconjugate is delivered without induction or a pre-dose of unlabelled rituximab. In this situation much of the ^{131}I rituximab will bind circulating B cells and accessible B cells in the spleen or bone marrow before being quite rapidly catabolised and excreted. By clearing this accessible antigen from the blood and bone marrow, as well as reducing the tumour load, the induction rituximab and pre-dose ensure that at the

time of administration there is much less easily accessible CD20 antigen. The images from patient SY (figure 4.17) illustrate the dramatic negative impact excess binding to antigen within the spleen can have on tumour targeting and how this can be overcome by delivering induction rituximab and the pre-dose. The benefit of the induction rituximab or pre-dose maybe mediated not only by reducing the quantity of non-tumour specific antigen and therefore increasing the probability of radiolabelled mAb binding tumour but also through the resulting substantially prolonged blood and effective half-life that results. This prolonged half-life may improve the ability of the radioimmunoconjugate to penetrate tumour nodules by increasing the time during which the mAb can percolate down the concentration gradient to the centre of the tumour. On the other hand this prolonged circulation of radioimmunoconjugate may expose the bone marrow and other normal tissues to more untargeted radiation and may therefore increase the haematological toxicity of the therapy. Which of these factors is the most important may vary from patient to patient, although from this study in the first 3 dose cohorts this does not appear to be the haematological toxicity. The observation of such a dramatic prolongation of radioimmunoconjugate effective half-life through the use of an induction course of rituximab and the variation with tumour load is of great interest and suggests that there may be a need for individualising the scheduling of RIT. Patients with bulky disease as illustrated in figure 4.17 being more likely to benefit from induction therapy with the resulting long effective half-life, while patients with relatively low volume disease (figure 4.16) may be better treated without induction rituximab thereby minimising exposure of normal tissue to non targeted radiation.

Additional results are awaited from the trial that may add greater weight to these initial pharmacokinetic and biodistribution observations as well as confirming the apparently high efficacy of the schedule and identifying the MTD.

Chapter 5

Serum Rituximab Concentration Analysis

5   SERUM RITUXIMAB CONCENTRATION ANALYSIS

5.1   INTRODUCTION

Despite the administration of rituximab to many thousands of patients with integration into the treatment of various B cell Lymphomas we still have a relatively poor understanding of how rituximab mediates its therapeutic effects. In addition, for a drug that is so widely used the available pharmacokinetic data is limited and the optimum dose and schedule have not yet been defined. The current approved single agent dosing of 375 mg/m^2 weekly for 4 weeks was based more on availability at the time of initial testing rather than efficacy or toxicity. There is now evidence emerging that outcomes for some patients may be improved by escalation of the dose or delivery of maintenance rituximab. With the increasing use of rituximab in conjunction with both chemotherapy and radioisotopes a whole range of new treatment schedules and doses are entering clinical practice that have been derived empirically with little or no basis on the pharmacokinetics or mechanism of action of the antibody (1.2.4.4). This situation has arisen at least in part due to a lack of well-characterised highly specific reagents to detect rituximab in vivo. The few pharmacokinetic studies that have been completed have used an assay based on a limited supply of polyclonal goat anti-rituximab antibody [63 168]. To answer the many dosing and scheduling questions that persist in the clinical application of rituximab, a more widely available assay is needed. During the clinical trial of fractionated RIT described in chapter 4, rituximab is administered intermittently over a period of 4 months. Pharmacokinetic analysis of the variation in serum rituximab levels during this schedule was planned to provide greater insight into the factors influencing serum rituximab levels and how best to deliver the pre-dose in RIT. As there were no commercially available reagents we elected to derive our own assay for the measurement

of serum rituximab concentration and in doing so developed a highly specific mAb directed to the idiotype region of rituximab. This has proven useful both in the measurement of serum rituximab concentrations and also in gaining an insight into the mechanism of binding of rituximab to antigen on the tumour cell surface.

5.2 PRODUCTION OF ANTI-RITUXIMAB IDIOTYPE ANTIBODIES

In order to develop a sensitive and specific assay for measuring serum rituximab concentration it was necessary first to derive an antibody specific for rituximab. Both polyclonal and then monoclonal anti-rituximab idiotype antibodies were produced as described below.

5.2.1 Materials and Methods

The method is described in Chapter 2.11. Briefly, the $F(ab)_2$ fragment of rituximab was derived by pepsin digestion (2.11.1.1). Rats were then immunized with the rituximab $F(ab)_2$ (2.11.1.2). Using the $F(ab)_2$ fragment rather than whole rituximab was intended to increase the yield of antibodies specific to the rituximab idiotype rather than to the non-specific highly immunogenic Fc portion of the antibody. Initially the serum from 4 immunised rats was pooled and polyclonal rat anti-rituximab antibodies purified from this. Production of the polyclonal anti-rituximab antibody was confounded by difficulties in the purification step (2.11.1.3.). Four steps were required, a protein G column to extract the immunoglobulin from the rat serum, a rituximab coated column to extract the anti-idiotype antibodies from the immunoglobulins and then a size separation column in an attempt to exclude rituximab antibody complexes from the product followed by a further anti-human IgG coated column to remove persisting rituximab from within the product. Subsequently an additional rat was vaccinated according to the same protocol but on this occasion the spleen was harvested 3 days after the final immunisation. Splenocytes were fused with cells from a myeloma cell line (NS-1) and the resulting hybridomas cultured (2.11.2.2). The hybridoma cells secreting a rituximab specific mAb,

were selected through sequential screening by ELISA (2.11.2.3) using a standard ELISA protocol (2.10) and cloning procedure as described (2.11.2.5). Rituximab specific hybridoma clones were cultured and expanded. The supernatant from the growing clones was collected, concentrated and the contained mAb purified (2.11.2.6). The purity of the monoclonal anti-rituximab idiotype antibodies produced was confirmed by serum protein electrophoresis (2.11.2.7). The purified mAbs were then characterised using the BIAcore system. A sensorgram for each mAb was generated as it passed over a rituximab coated BIAcore chip enabling determination of the 'on' and 'off' rates and using the BIA evaluation software comparison of the binding affinities of the mAbs (2.11.3). Finally the isotype class of the anti-rituximab idiotype mAbs obtained were determined (2.11.3.2).

5.2.2 Results

Despite the multiple purification steps in the production of the polyclonal mAb a relatively high background was seen when the product was analysed by ELISA suggesting persistent contamination by rituximab. In addition because of the multiple purification steps required only a very limited amount of product was obtained from the 4 rats immunised. Despite these limitations the principle of using rat immunisation with rituximab $F(ab)_2$ to produce anti-rituximab idiotype antibodies was validated as demonstrated by the ELISA illustrated in figure 5.1. Although there is a high background limiting the range of over which an assay using this antibody could measure serum rituximab levels, the specificity of the polyclonal antibody for rituximab as compared to the two control chimeric antibodies (chAT80, chAT13/5) and normal serum is clearly demonstrated. No significant binding to chAT13/5 is seen. This is an anti-CD38 mAb of the same isotype as rituximab indicating that the specificity of the polyclonal antibody is to the idiotype containing Fv portion of rituximab. Minor binding of chAT80 is seen which is to be expected, as there is significant homology between the variable region of rituximab and chAT80 another anti-CD20 mAb. In view of the difficulties encountered in the purification steps required to produce this polyclonal antibody, rather than pursue production of useful quantities of polyclonal anti-rituximab idiotype antibody using more

rats or by vaccination of a larger mammal, production of a monoclonal anti-rituximab idiotype antibody was undertaken.

Figure 5.1. Ability of purified polyclonal rituximab anti-idiotype antibody to detect rituximab by ELISA. The affinity purified polyclonal anti-rituximab idiotype antibody was coated to the surface of ELISA plates before blocking non-specific binding sites and adding various dilutions of either pure serum or serum spiked with 100 μg/ml of rituximab, chAT13/5(anti-CD38) or chAT80(anti-CD20). The amount of human Fc captured to the plate was then detected using anti-human Fc coupled to HRP.

Polyclonal anti-rituximab idiotype antibody
Analysis of specificity
background 1.272
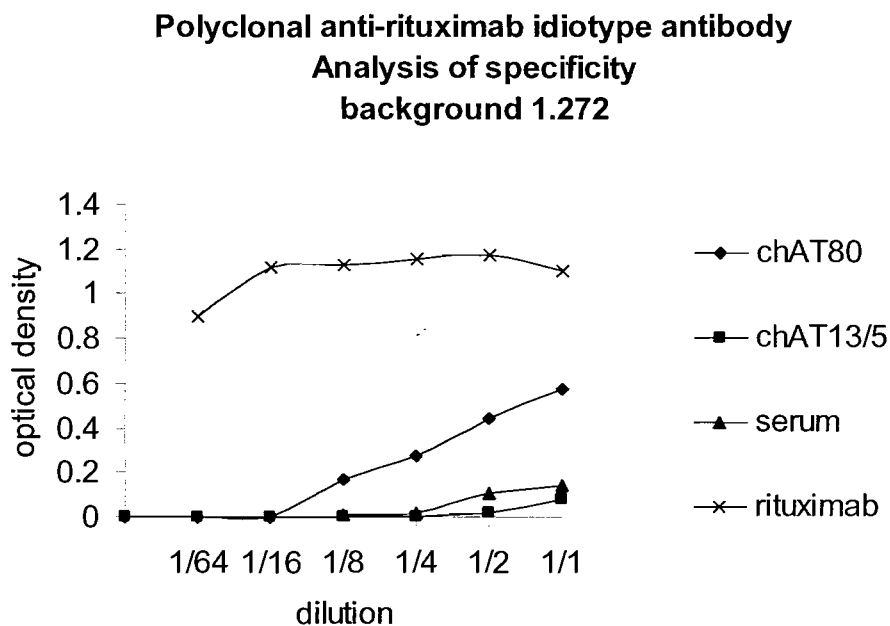
A total of 7 hybridoma clones were derived, using the fusion protocol described in section 2.11.2.2. Figure 5.2 demonstrates the results from a series of ELISAs performed using the supernatant from each of the cultured hybridomas and demonstrates the high sensitivity of the mAbs, enabling detection of rituximab at nanogram (ng) concentrations. Importantly, these mAb did not bind to normal IgG in serum or other chimeric mAbs either directed to CD20 (chAT80) or CD38 (chAT13/5) indicating their specificity for the rituximab idiotype.

Four of the hybridomas grew well in culture enabling expansion and collection of substantial quantities of supernatant from which the mAbs were purified. Figure 5.3 illustrates, using serum protein electrophoresis (SPE), the proteins present in the concentrated hybridoma supernatant before and after eluting the supernatent from a protein G column. For hybridoma MB2-H2 a monoclonal band is easily seen with little of the contaminating non-specific immunoglobulin originating from the fetal calf serum used to feed the hybridoma. For MB2-A4 and MB2-G3 the monoclonal band is less clearly seen obscured by contaminating protein in the beta globulin region. For MB2 E9 no monoclonal band is seen suggesting that this hybridoma clone is secreting poorly and producing very little mAb. The mAbs were further purified using DEAE ion exchange chromatography as illustrated in figure 5.4. After elution using an NaCl gradient the eluted fractions were analysed by SPE and the cleanest monoclonal band used for further characterisation. For MB2 H2 it can be seen that there was no need for the DEAE ion exchange chromatography purification step (figure 5.5). The three purified mAbs MB2-A4, MB2-G3, MB2-H2 were then characterised as described below.

Figure 5.2. The supernatent from each hybridoma was assayed by ELISA to determine the sensitivity and specificity for the rituximab idiotype. The ELISA plate was coated with rabbit anti rat IgG, blocked with hybridoma supernatent, incubated with chimeric mAb and detected with anti-Human Ig–HRP. 7 hybridomas were found to produce mAb demonstrating comparable sensitivity to the previously purified polyclonal antibody enabling detection of rituximab at concentrations of less than 10ng/ml and achieving greater specificity with little or no positivity with chAT80 or chAT13/5.

MB2 polyclonal — Ritux / AT80 / AT13/5

MB2 H2

MB2 G3

MB2 H6

optical density

MB2 E9

MB2 E12

MB2 F9

MB2 A4

mAb concentration (ng/ml)
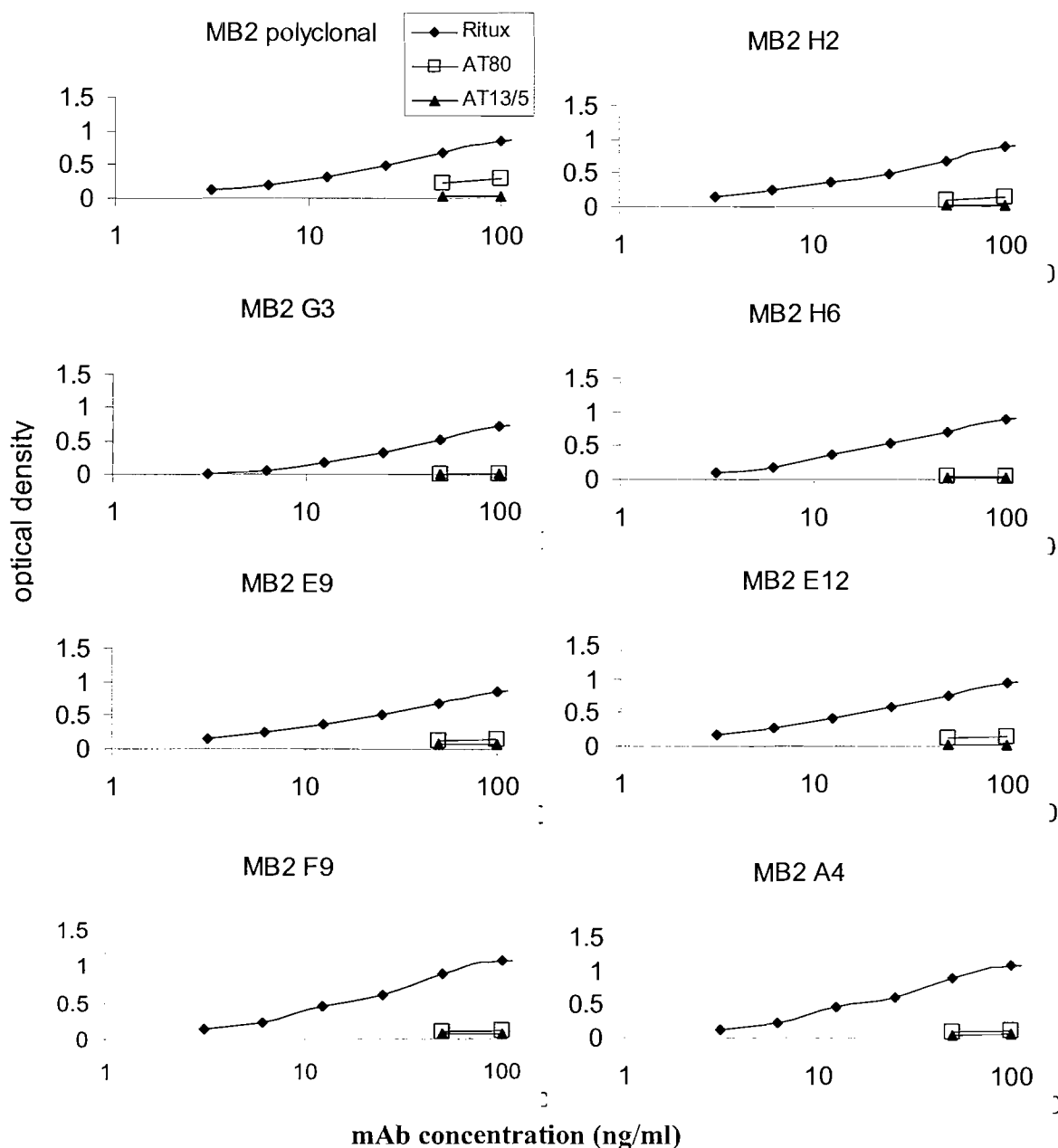
Figure 5.3. SPE gel of hybridoma supernatent from 4 MB2 clones (A4, E9, H2,G3) before and after run down protein G column. A4 monoclonal band present in beta globulin region therefore partially obscured by contaminating protein (white arrow). E9 no monoclonal band seen. H2 monoclonal band easily visualised (black arrow). G3 monoclonal band present again almost in beta region therefore partially obscured (black arrow).
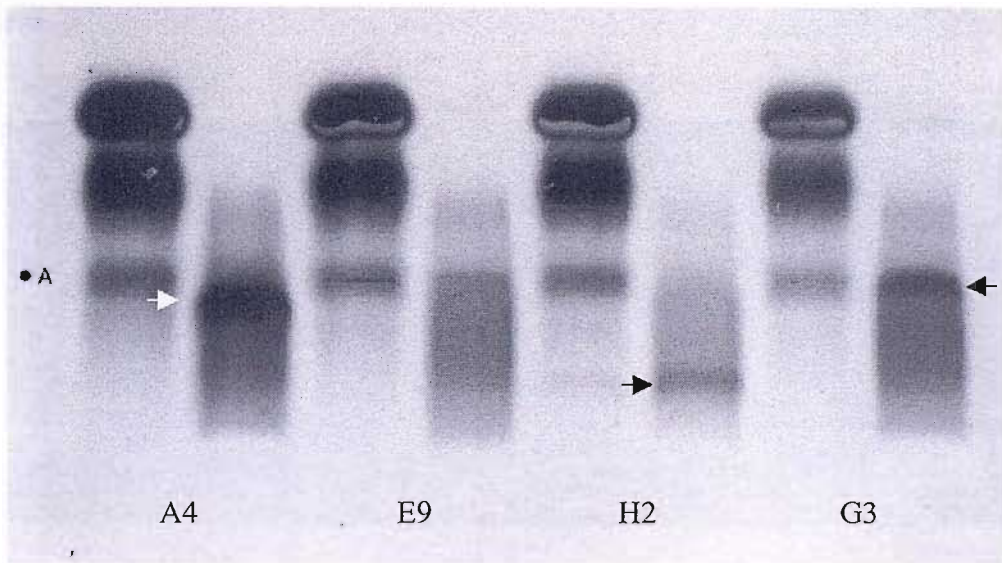
Figure 5.4. Following purification on protein G column supernatents dialysed with 20mM TE80 run down a DEAE column and eluted with 20mM TE80 and a gradient of NaCl concentrations. Eluted material checked on SPE gel for presence of monoclonal band as shown here for MB2 A4. **(A)** concentrated peak post protein G. **(B)** eluted from DEAE with 20mM DEAE. **(C)** eluted from DEAE with 20mM TE8 +0.025M NaCl **(D)** + 0.5M NaCl **(E)** +0.1M NaCl **(F)** +0.2M NaCl **(G)** +0.5M NaCl. **(H)** +1M NaCl. Fraction D (black arrow) taken as pure fraction with no visible remaining contaminating protein.
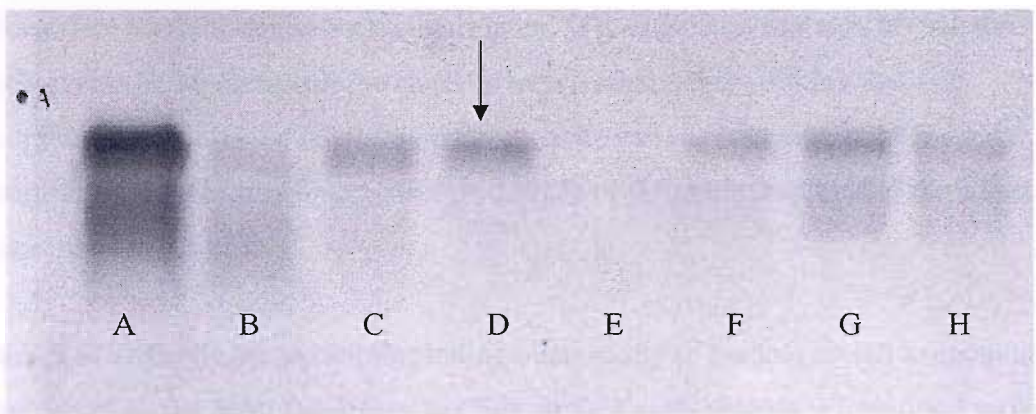
Figure 5.5. SPE gels of (A) MB2H2 supernatent concentrated post protein G column then (B) eluted from DEAE column with 50mM TE8. In this case there was no need for a NaCl concentration gradient to separate the monoclonal band from normal immunoglobulins.
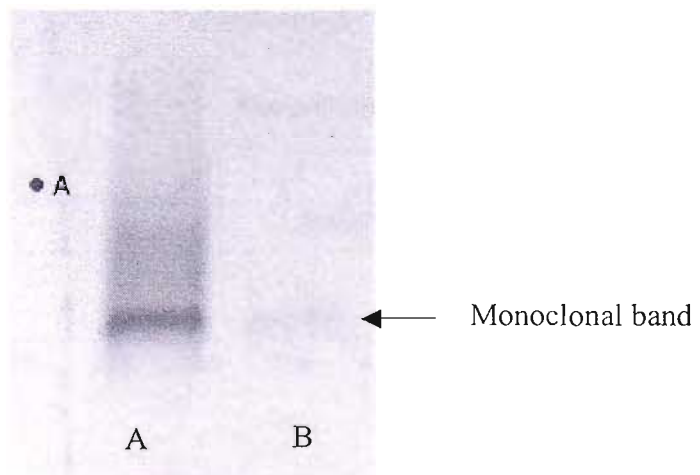
5.3 CHARACTERISATION OF ANTI-RITUXIMAB IDIOTYPE MABS.

The three purified anti-rituximab idiotype mAbs were analysed using the BIAcore system. This system utilises the measurement of changes in Surface Plasmon Resonance (SPR) to enable the real-time detection and monitoring of biomolecular binding events. By coating a sensor chip that has a gold film surface with rituximab then passing a known concentration of the test mAb over the chip surface a sensorgram can be generated. The sensorgram reflects changes in the concentration of mAb in the surface coating of the chip. The concentration of mAb at the chip surface dictates the surface refractive index and therefore the SPR angle. By monitoring the SPR-angle as a function of time the kinetic events in the surface of the chip can be recorded. Figure 5.6 is a stylised sensorgram illustrating the relationship between the various components of the sensorgram and molecular binding events. Details of the method applied to the BIAcore are described in 2.11.3.1.

Figure 5.6. Stylised sensorgram illustrating relationship of binding events to components of the curve. As the mAb flows over the chip surface mAb binding is quantified by an increase in the resonance signal measured in response units. This reaches a plateau when the binding sites are saturated. When mAb is no longer flowing over the chip the rate of dissociation is measured again by a decline in the resonance signal.
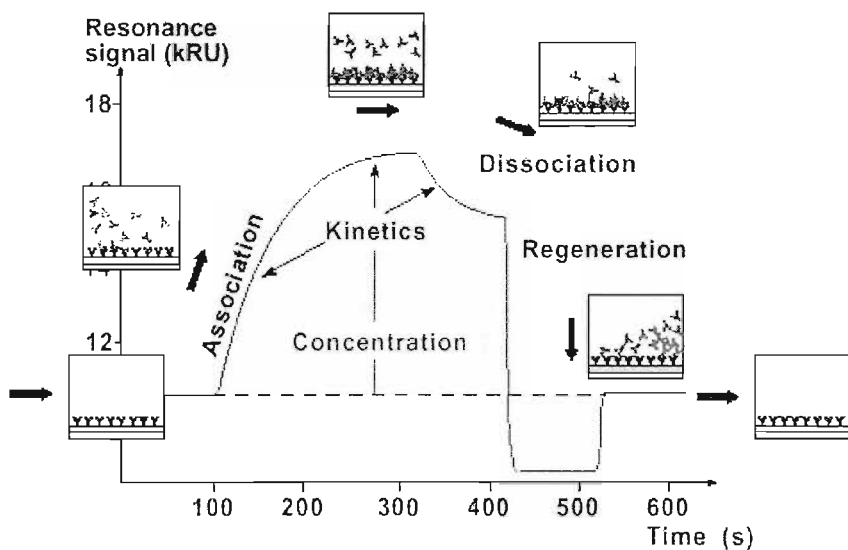
This system enabled the determination of the affinity constants for each antibody as well as whether all the produced antibodies bind the same or overlapping epitopes. Figure 5.7 illustrates the rapid binding of the MB2 A4 mAb to rituximab and the very slow subsequent dissociation. Analysis using the BIA evaluation software to mathematically model the association and dissociation curves enabled determination of the association and dissociation constants from which the affinity constant was derived as shown in figures 5.7 and 5.8. The sensorgrams for each mAb are illustrated superimposed in figure 5.8 indicating that all three mAbs were of high affinity with MB2-A4 being the highest. Figure 5.9 is a sensorgram produced when all three mAbs were applied to the chip sequentially. The lack of a step-up in response units as each new mAb was added indicates that the mAbs all bind to the same or overlapping epitopes on the rituximab idiotype. The binding of one mAb blocks the binding of another idiotype specific mAb to rituximab.

Figure 5.7. BIAcore analysis of MB2-A4. Sensorgram illustrates rapid binding to rituximab on chip with very slow off rate from which the high affinity constant is calculated.
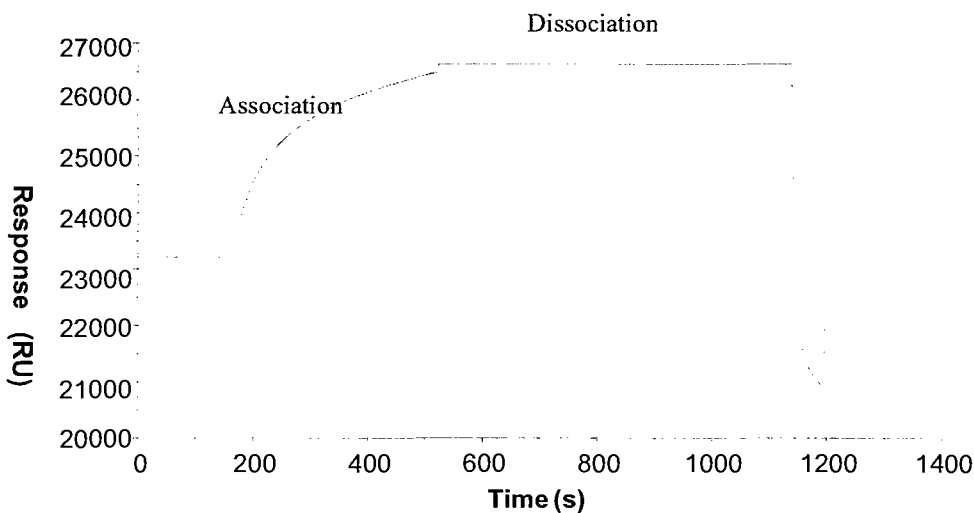
Dissociation rate constant	K_d	=	$2.3 \times 10^{-6} \, s^{-1}$
Association rate constant	K_a	=	$1.4 \times 10^{5} \, M^{-1} s^{-1}$
MB2 A4 Affinity constant	K_A	$= K_a / K_d$ =	$6.1 \times 10^{10} \, M^{-1}$

Figure 5.8. BIAcore analysis of three purified anti-iodiotype mAb indicating that MB2 A4 has highest affinity.
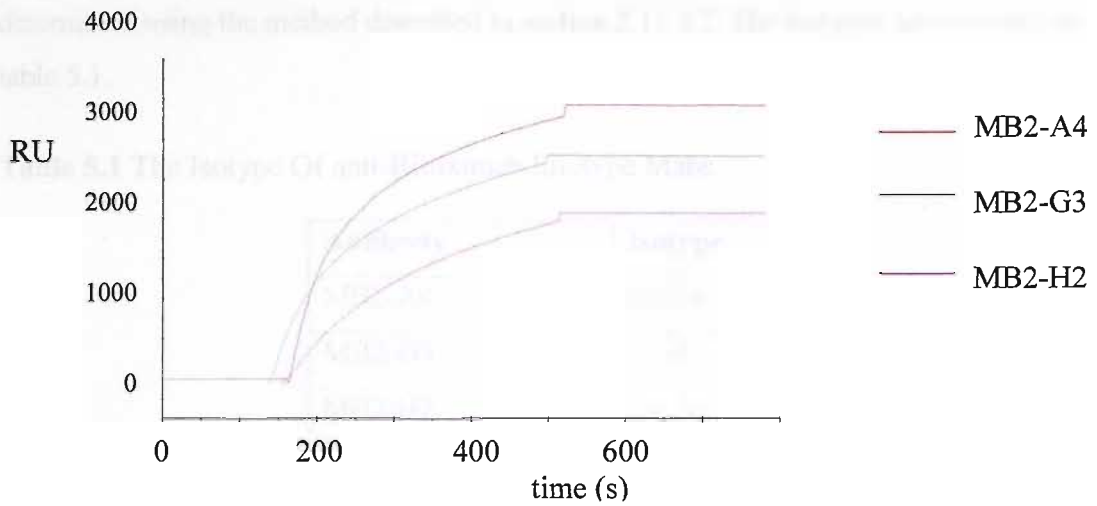
MB2 G3 Affinity constant KA   = Ka/ Kd   = $1.09 \times 10^5 / 1.01 \times 10^{-5} = 1.08 \times 10^{10} \text{M}^{-1}$

MB2 H2 Affinity constant KA   = Ka/ Kd   = $4.57 \times 10^4 / 3.3 \times 10^{-6} = 1.4 \times 10^{10} \text{ M}^{-1}$

Figure 5.9. BIAcore analysis of three anti-idiotype mAb applied sequentially to rituximab coated chip. Lack of step up in response units between mAb indicate that the binding of one mAb prevents the binding of the others indicating that all three mAb bind the same or overlapping epitopes.

166
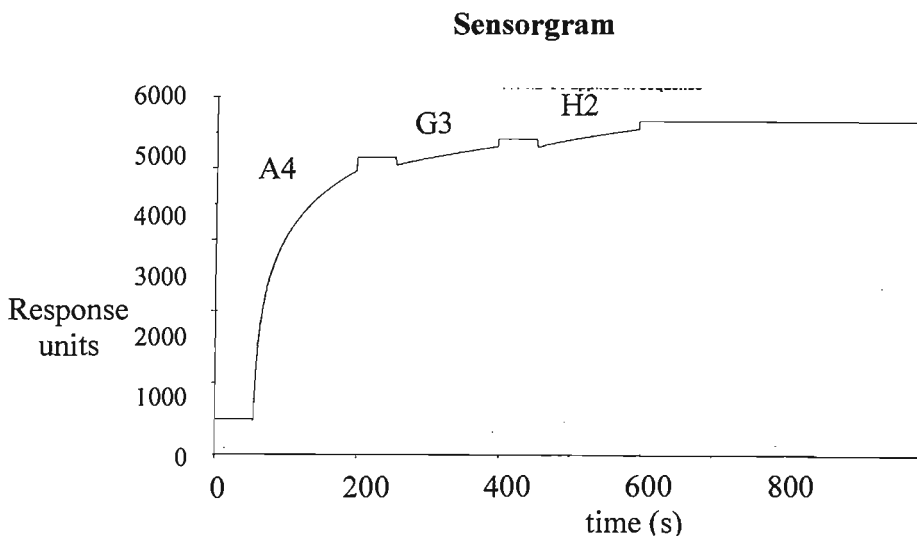
To complete the characterisation of these mAbs their immunoglobulin isotype was determined using the method described in section 2.11.3.2. The isotypes are recorded in table 5.1.

Table 5.1 The Isotype Of anti-Rituximab Idiotype Mabs.

Antibody	Isotype
MB2-A4	IgG2a
MB2-G3	IgG1
MB2-H2	IgG2a

Having determined that MB2-A4 was the mAb with the greatest affinity for rituximab, the hybridoma was further cultured with lower concentrations of FCS. This simplified the process of purification of the mAb. As can be seen in Figure 5.10 after this additional period of culture, analysis of the culture supernatant by SPE reveals a clear monoclonal band. After further culture and purification of the mAb, MB2-A4 was once again tested by ELISA to confirm specificity and sensitivity for binding rituximab. Figure 5.11 indicates that using this anti-idiotype mAb, rituximab can be detected by ELISA when diluted to a concentration of less than 10ng/ml and that there is no significant cross-reactivity with serum or the control mAbs.

Figure 5.10. After expansion of hybridoma MB2 A4 and culture in lower concentrations of FCS SPE gel demonstrates easily seen monoclonal band in unconcentrated supernatant with very little contaminating protein making purification easier.
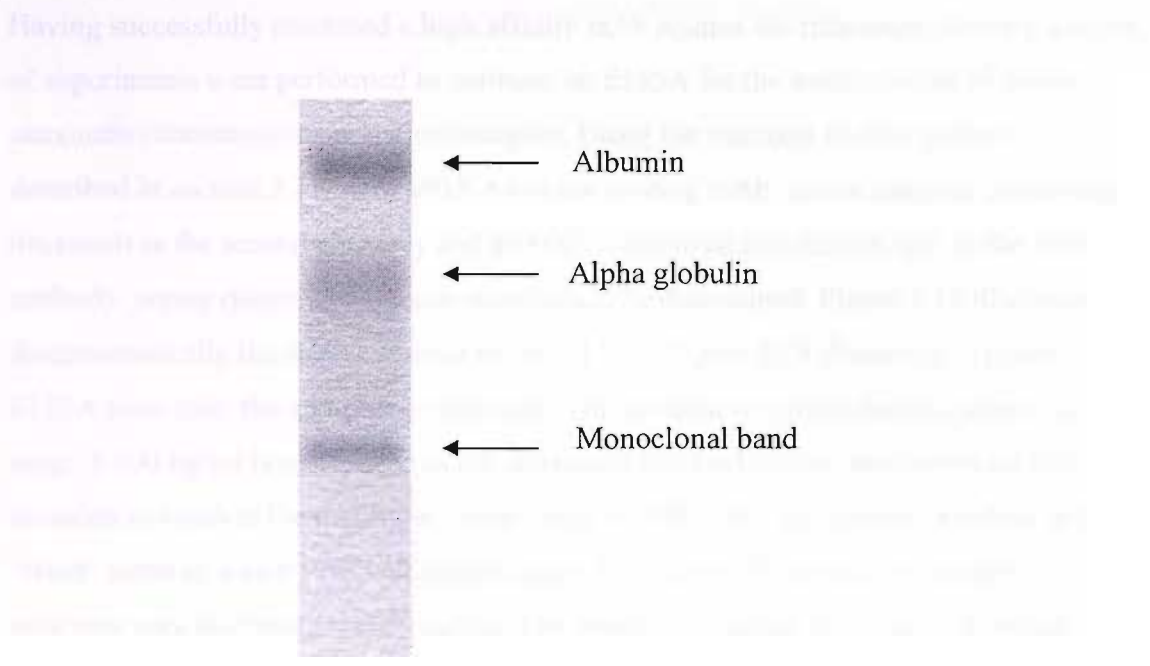
Figure 5.11 Assay indicating sensitivity and specificity of ELISA using MB2 A4 for detection of rituximab in human serum. ELISA plate coated with MB2-A4, blocked with PBS/1%BSA then incubated with serial dilutions of serum with or without added rituximab, chAT80, chAT13/5.
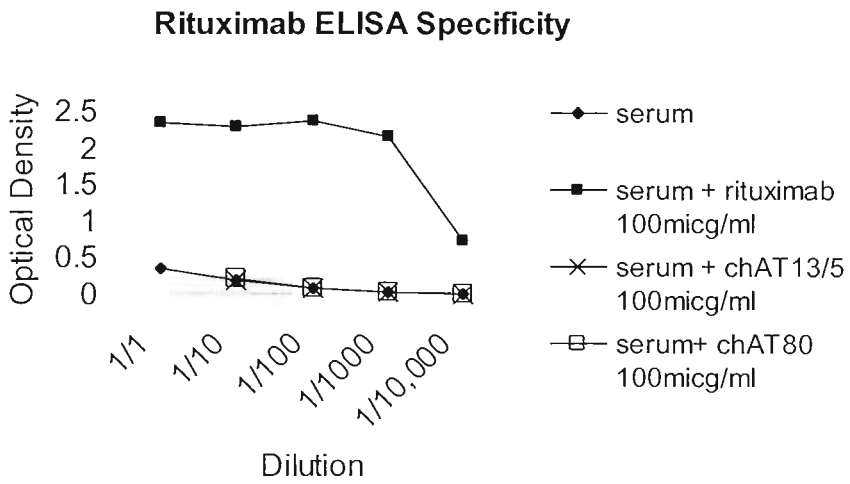
5.4 OPTIMISATION OF SERUM RITUXIMAB ASSAY

Having successfully produced a high affinity mAb against the rituximab idiotype a series
of experiments were performed to optimise an ELISA for the measurement of serum
rituximab concentrations in patient samples. Using the standard ELISA protocol
described in section 2.11, with MB2-A4 as the coating mAb, serum samples containing
rituximab as the second antibody and an HRP conjugated anti-human IgG as the final
antibody, serum rituximab concentrations could be determined. Figure 5.12 illustrates
diagrammatically the steps involved in this ELISA. Figure 5.13 illustrates a typical
ELISA plate after the addition of substrate. The gradient in optical density across the
range 3-100 ng/ml is easily seen in the rituximab standard curves, performed on this
occasion to confirm the quality of a new batch of MB2-A4. An absence of colour in the
'blank' wells to which PBS was added rather than rituximab containing samples
indicates very low background readout. The absence of colour in the wells to which
control mAbs have been added confirms the previously described specificity of the assay.
Patient serum samples required dilution up to 10,000 x in order to fall on the steepest
portion of the standard curve. Samples were therefore tested at multiple dilutions to
ensure a useful readout from the assay as shown with, in this case, three different
dilutions performed per sample (1/2000,1/4000, 1/8000).

For every occasion upon which the ELISA was performed a new rituximab standard
curve was generated. Figure 5.14 illustrates an ELISA performed to determine the
minimum concentration of MB2-A4 required to effectively coat the ELISA plate. As no
difference in readout was seen on reducing the coating concentration to 2 µg/ml this was
used for all subsequent experiments. In figure 5.15 the standard curve produced when
using a polyclonal HRP labelled anti-human IgG is compared to that derived when the
monoclonal anti-human IgG antibody (SB2-H2) was used. The greater slope of the
standard curve seen when using the monoclonal HRP labelled anti-Hu IgG increases the
sensitivity of the assay and was therefore considered superior and used with all
subsequent assays.

Figure 5.12 Diagrammatic illustration of steps in assay for serum rituximab concentration.

A.

Immunosorbent ELISA plate coated
with MB2-A4

B.

Serum sample containing rituximab
added to coated plate.

C.

HRP labelled anti-human Fc
antibody   added to ELISA plate
and incubated.
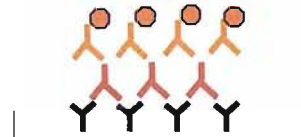
D.

Substrate   added to ELISA plate,
incubated for 30 minutes then reaction
stopped with H_2SO_4. Optical density of
each ELISA plate well measured and
used to calculated concentration of
rituximab in sample using standard curve.
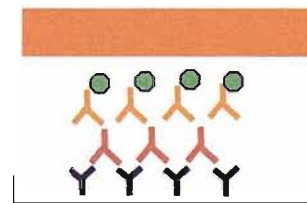
Figure 5.13. Example of ELISA plate illustrating low background, high specificity (low or zero detection of control mAb chAT80 and chAT13/5), high sensitivity (detecting rituximab at concentrations of < 3ng/ml) and patient samples requiring multiple dilutions to ensure sample concentration lies within linear detection range of assay.

Coating concentration

10μg/ml 2μg/ml 5μg/ml 10μg/ml
old   new   new   new

Concentration of rituximab

0ng/ml
10ng/ml
50ng/mll
25ng/ml
12.5ng/ml
6.25ng/ml
3.125ng/ml
1.5635ng/ml

ChAT80 duplicates at 3 dilutions 1000-10ng/ml

ChAT13/5 duplicates at 3 dilutions 1000-10ng/ml

Samples at 3 dilutions
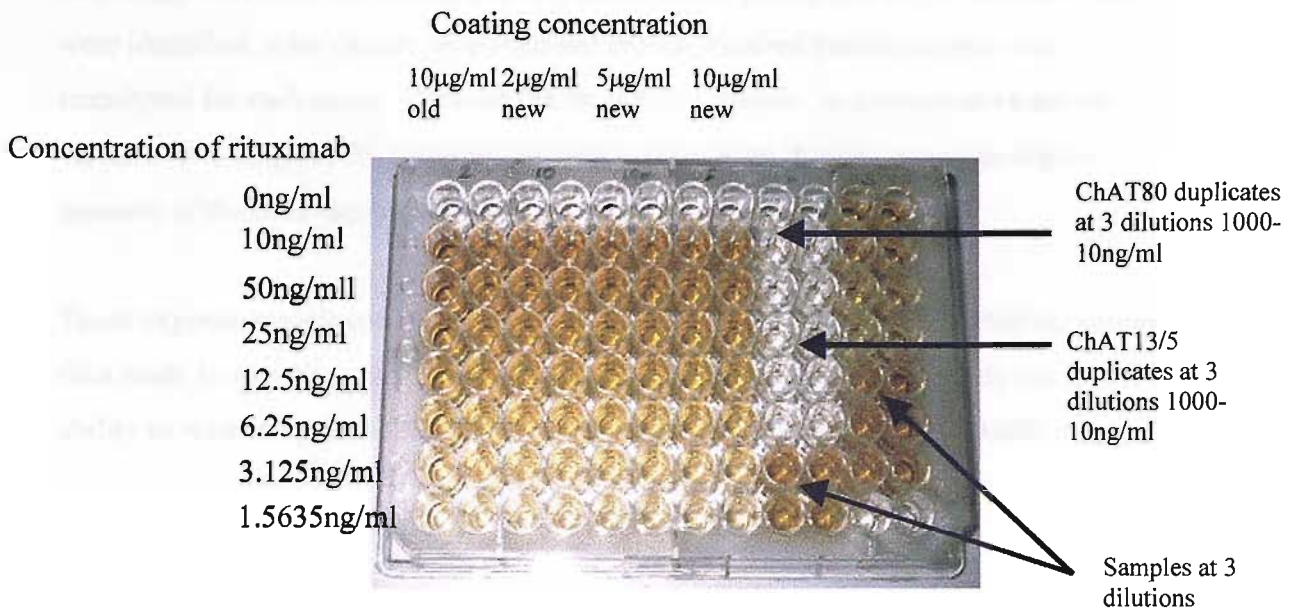
Figure 5.14. ELISA standard curves indicate that coating the ELISA plate at a concentration as low as 2 micg/ml enables detection of rituximab over the concentration range 5-100 ng/ml.

Standard curves
optimising coating concentration

optical density

concentration (ng/ml)

— 2micg/ml MB2 A4

— 5micg/ml MB2 A4

⋯ 10micg/ml MB2 A4
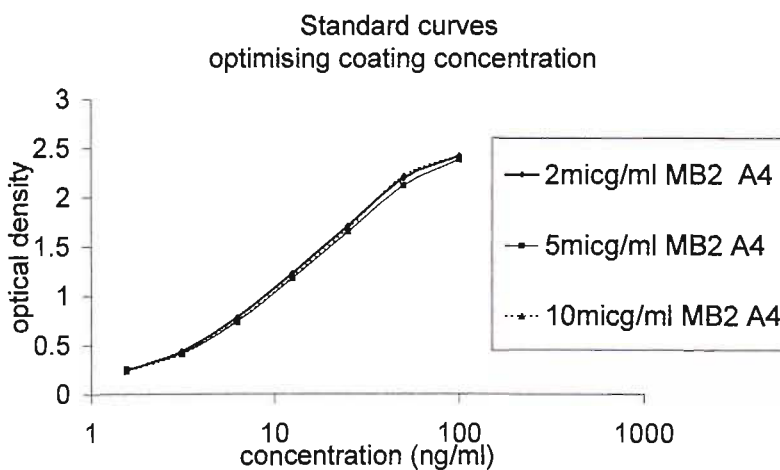
Using Exel software a straight line was fitted to the standard curve plotted on a logarithmic scale. Only points lying in the linear portion of the standard curve were used to fit this line and only samples diluted to a concentration that fell within this linear portion of the standard curve were accepted for analysis, as illustrated in figure 5.16. All samples were analysed at least twice. As a quality assurance measure in order to identify inter-assay variation and ensure that any errors in the production of the standard curve were identified, a previously aliquoted and frozen standard patient sample was reanalysed for each assay. The read out from these aliquots in 5 consecutive assays varied over a range of 35.2-45.6µg/ml with a mean of 41.8µg/ml giving an objective measure of the inter-assay variation.

These experiments clearly show that MB2A4 is extremely sensitive in detecting serum rituximab. In fact, the sensitivity of the assay is not limited by the antibody but by the ability to accurately dilute a standard curve and samples by a factor of 10,000.

Figure 5.15 ELISA to determine the optimum HRP conjugated antibody for use in serum rituximab assay. ELISA plate prepared in duplicate with serial dilutions of rituximab. The standard curve produced with a polyclonal HRP conjugated anti Human IgG is compared to that seen with the monoclonal HRPconjugated anti-Human IgG (SB2-H2).

Standard curves with polyclonal or monoclonal HRP
anti Hu IgG

◇ HRP anti Hu IgG polyclonal

■ HRP anti Hu IgG monoclonal

od

ng/ml
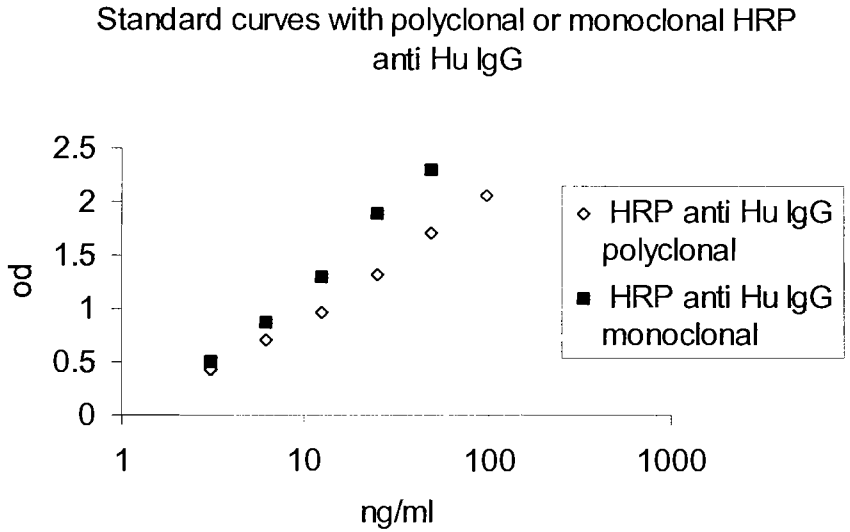
Figure 5.16. Example of ELISA standard curve used to determine concentration of rituximab in serum. Exel software is used to generate equation that enables calculation of concentration of rituximab in a samples analysed using this ELISA .

STD curve for determination of serum rituximab concentration

optical density

$y = 0.6421Ln(x) - 0.351$
$R^2 = 0.9961$

concentration (ng/ml)
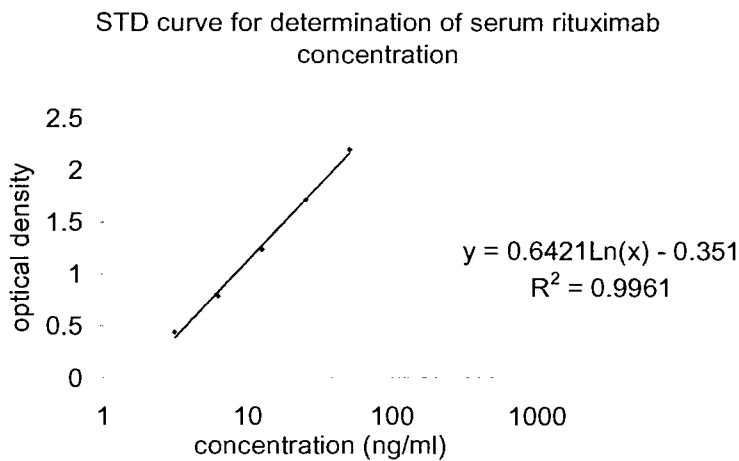
5.5 RITUXIMAB CONCENTRATION DURING FRACTIONATED RIT

5.5.1 Method

Serum samples were collected immediately prior to and following every administration of rituximab during the fractionated RIT trial protocol and then 3 monthly during the first year of follow-up. Where possible the samples were taken from the arm contra-lateral to rituximab administration. The serum samples were frozen and assays performed in batches utilising the ELISA described above (5.4).

5.5.2 Results

A full data set of serum rituximab concentrations has now been collected for all the patients in the first dose cohort and a partial data set for those in the second dose cohort. Figure 5.17 illustrates the variation in rituximab concentration with time for 4 representative patients correlating this with the timing of administration of rituximab. As can be seen the serum rituximab concentration rises with each of the 4 weekly doses of 375 mg/m^2 induction rituximab. Further peaks in the serum concentration are seen with each dose of RIT correlating with the 100 mg/m^2 pre-dose administered prior to ^{131}I rituximab. The serum rituximab concentration was then seen to fall gradually back to undetectable levels over the course of 6-12 months. In each patient the pattern of change in serum rituximab concentration was consistent however figure 5.17 illustrates the wide variation in both the peak rituximab concentration and the rate of rituximab clearance between patients. It is of interest to note from figure 5.17 that, in the majority of patients who have relatively slow clearance of rituximab, at the time of administration of the first dose of RIT there remains a significant concentration of circulating rituximab making the need for a pre-dose in these patients questionable. The inter-patient variation in serum rituximab concentration is more clearly illustrated in figure 5.18 where the serum levels for all patients at selected time points are plotted on the same graph. Rituximab serum levels were analysed at week 3 immediately prior to the final dose of induction rituximab, week 7 immediately prior to the pre-dose for the first dosimetric dose of RIT and week 15 immediately prior to the pre-dose for the second dosimetric dose of RIT and then at 25 weeks, 8 weeks after completion of the RIT protocol.

Figure 5.17. Serum rituximab concentrations in four patients over the course of the trial protocol illustrating a three fold difference in peak rituximab concentrations and a 20-fold difference in the level 3 weeks after completion of a standard 4 week course of rituximab. By the time the second dose of RIT is administered (week 17) the difference between serum rituximab levels in all the patients that responded is less marked.

Serum rituximab concentration

NM

+ rituximab administered

* ^{131}I rituximab administered

TP

micg/ml

JH

JB

weeks
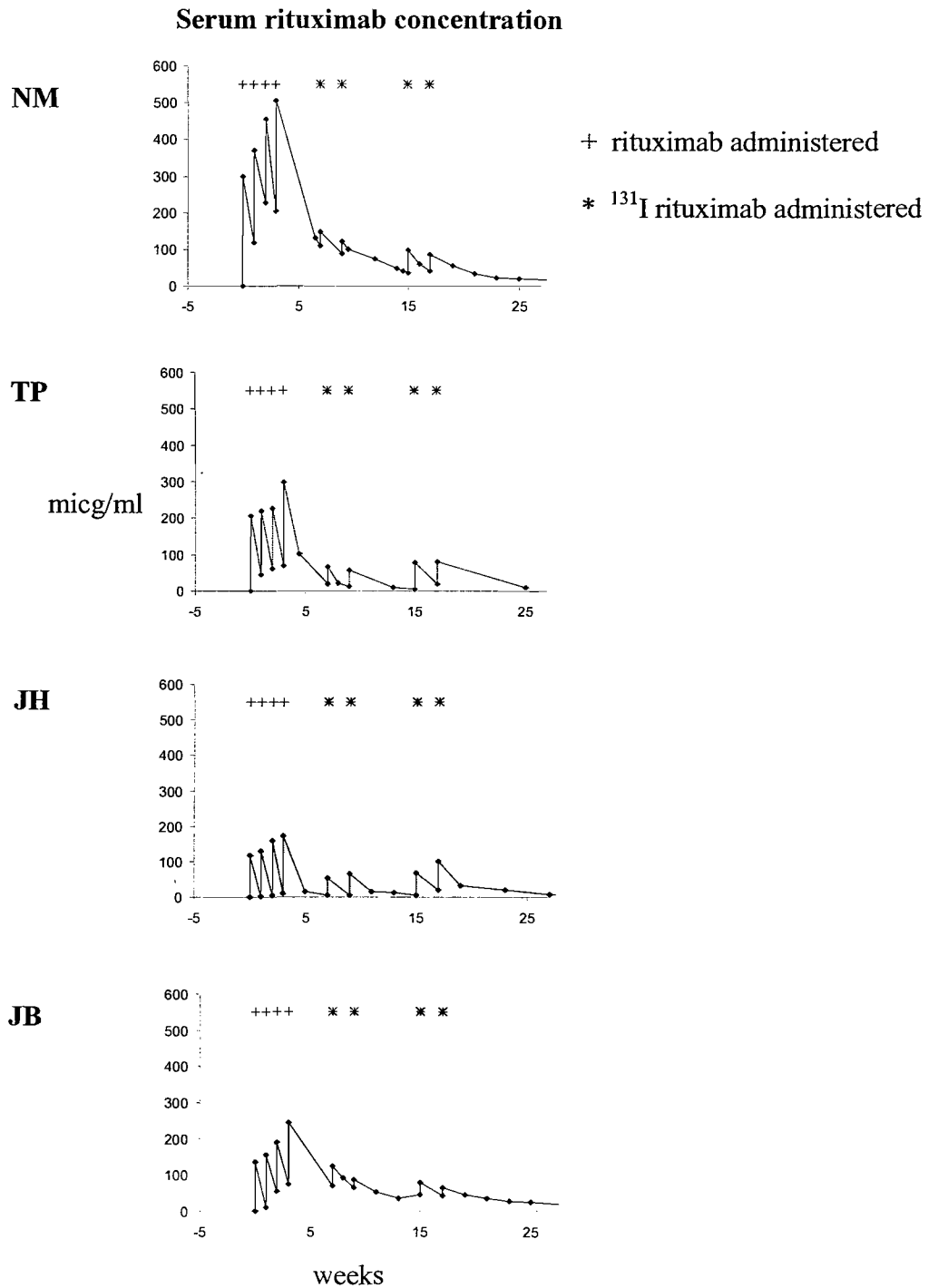
Figure 5.18. Serum rituximab concentrations at selected time points during the fractionated RIT trial protocol illustrating the range of serum rituximab concentrations in 9 consecutive patients. The error bars represent 2 SEM following repetition of the assay on the same sample on 3 separate occasions.

Serum Rituximab Concentration
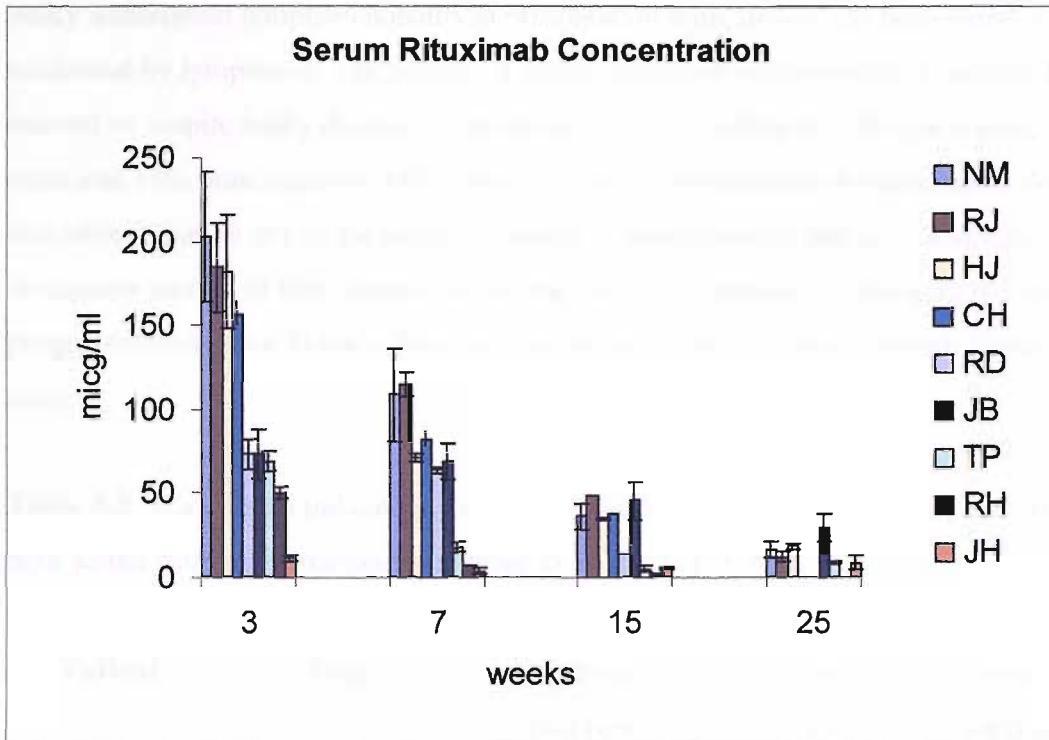
The error bars in figure 5.18 are derived from repeated assays on the same sample. The assays on some of the early samples were separated by several months and degradation of these samples may account for a component of the variation in these cases. The error bars are widest for the samples with the highest concentration. This is probably because at the highest concentrations dilution of serum by at least a factor of 10,000 is required. The number of serial dilution steps required will amplify any small errors in the early dilution steps. Automating the dilution process could in the future significantly reduce the error introduced by sample dilution. To date it has been performed by serially diluting the samples by a factor of 10 four times using a Gilson pipette.

Table 5.2 documents the parameters that indicate tumour load at trial entry alongside serum rituximab concentration at week 3. A remarkably consistent correlation between the tumour load and the week 3 serum rituximab concentration is shown. Patient NM with low volume mesenteric nodes at presentation and negative bone marrow had a week 3 serum rituximab concentration nearly 20 times the level found in patient JH who had bulky widespread lymphadenopathy at presentation with 50% of the bone marrow infiltrated by lymphoma. The pattern of serum rituximab concentration in patient JB is of interest as despite bulky disease at presentation with a confluent 15cm para-aortic nodal mass and 15% bone marrow infiltration the serum concentration declined more slowly in this patient than in any of the others. Possible explanations for this are considered in the discussion section of this chapter. In this patient post treatment CT imaging documents a progressive reduction in the volume of lymphoma between 6 and 12 months from trial entry.

Table 5.2. Parameters indicating tumour load in fractionated RIT trial patients correlated with serum rituximab concentration prior to 4th dose of rituximab.

Patient	Stage	% Bone marrow involved	Tumour mass > 5cm max dimension	Serum rituximab concentration week 3
NM	2A	0	-	203
RJ	3A	0	-	185
HJ	4A	<5	-	182
CH	4A	5	-	158
RD	2A	0	+	73
JB	4A	15	+	73
TP	3A	-	+	69
RH	4A	15	+	51
JH	4A	50	+	12

5.6 MB2-A4: A TOOL FOR ANALYSIS OF RITUXIMAB BINDING

Having successfully produced a rituximab idiotype specific mAb, the ability of MB2-A4 to detect rituximab when bound to the surface of tumour cells was investigated in collaboration with Dr Mark Cragg a post-doctoral research fellow in Professor Glennie's laboratory. For these experiments we used a range of CD20 positive B cell lines and MB2A4 labelled with FITC according to the method described in 2.5.2. A modification of the immunoflourescence antibody binding method described in 2.6.2 was used. Following binding of rituximab to EHRB or Raji B cells and washing to remove excess unbound rituximab, cells were incubated with 10 µg/ml FITC-labeled MB2A4 at 4°C for 20 minutes, before more washing and flow cytometry. Unexpectedly, these experiments indicated that MB2A4 was indeed able to bind to Rituximab coated cells. Therefore, a number of additional experiments to confirm the integrity and specificity of this interaction were performed. First, a series of experiments were performed where cells were coated with a range of different mAb including other anti-CD20 mAb, other chimeric mAb and 2B8 (the non-chimeric but idiotypic twin of rituximab). These experiments, detailed in Figure 5.19, show clearly that only cells coated in rituximab, or the murine parent 2B8 with identical idiotypic variable domains, were bound by MB2A4. No other anti-CD20 mAb or chimeric mAb was bound by MB2A4. The result was surprising, as it had been expected that once rituximab has bound to CD20 on a cell its idiotype would be obscured and unavailable for binding to an idiotype specific mAb such as MB2A4.

Figure 5.19. Plot of mean flourescence intensity (MFI) measured on FACS after incubating B-NHL cells that have been pre-incubated with a panel of CD20 and control antibodies with FITC labelled MB2 A4. This illustrates the specificity of MB2 A4 for the rituximab idiotype (shared with 2B8) and ability for MB2 A4 to detect rituximab when bound to the surface of CD20 expressing cells.

Rituximab anti-idiotype mAb (MB2A4) binds to rituximab bound to tumour cells
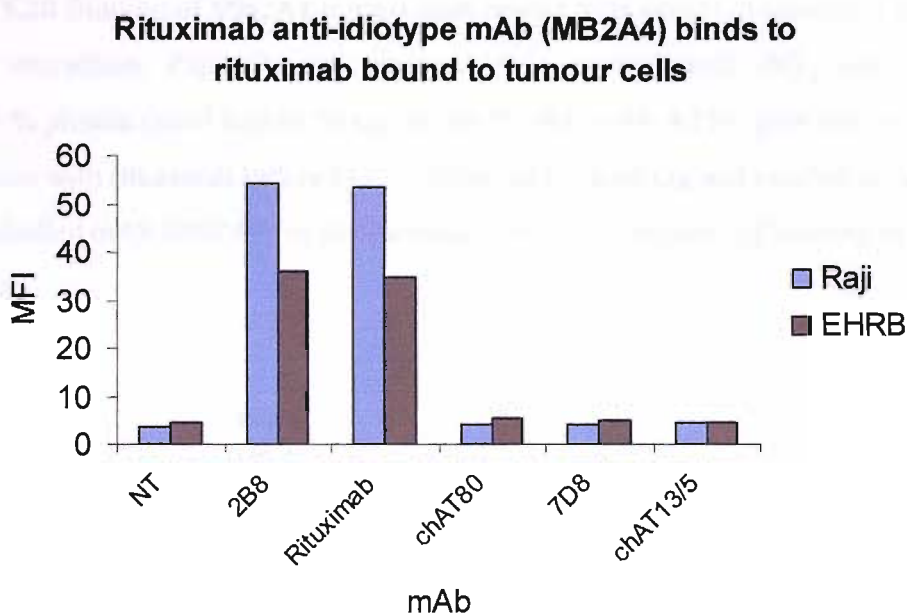
5.6.1 Mode of binding of MB2A4

In order to determine the mechanism through which MB2A4 was binding to rituximab when bound to cells a series of experiments were undertaken.

The first possibility addressed was whether rituximab was binding to the cells via FcγRIIb, thus allowing the idiotype regions to be free for the anti-Id to bind. To address this possibility a series of experiments were performed using high concentrations of normal human plasma which would be expected to out-compete rituximab binding to

FcγRIIb. The mAb AT10 was also used to directly block the FcγRIIb. In addition rituximab F(ab')2 fragments incapable of binding through FcγR were used to explore the role of the FcγR in binding MB2A4. These experiments (Figure 5.20) demonstrated that MB2A4 bound to rituximab on the surface of lymphoma cells whether or not the Fc:FcR interaction was blocked or absent.

Figure 5.20 Binding of MB2A4 to rituximab coated cells occurs independent of the Fc:FcR interaction. Raji cells were pre-incubated in normal media (NT, open bar), 33 % plasma (solid bar) or 50 µg/ml anti-FcγRII mAb AT10 (grey bar), prior to incubation with rituximab IgG or F(ab')2 followed by washing and incubation with FITC-labelled mAb MB2A4. In all situations MB4 A2 is capable of binding to rituximab.

120 100 80 60 40 20 0

MFI

IgG   F(ab')2
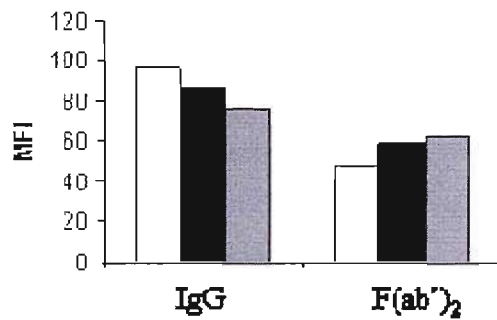
To probe the binding mechanism further we next sought to determine whether rituximab binding to CD20 could be blocked by the addition of MB2A4 prior to rituximab binding the cell surface. These experiments (Figure 5.21), show clearly that MB2A4 but not another anti-Id mAb (specific for another anti-CD20) was able to block rituximab binding to CD20 on cells in a dose-dependent manner. These data indicate that whilst rituximab cannot bind to CD20 in the presence of high levels of the anti-Id, once rituximab is bound to CD20, the anti-Id may bind to rituximab. From these experiments we conclude that the sites for anti-Id and CD20 binding are indeed the same, confirming our suggestion that binding of antigen via the mAb complementarity determining regions (CDRs) in the V-regions, blocks access of the anti-Id mAb. Following on from this we

continued to investigate an explanation for the simultaneous binding of antigen and anti-Id mAb at the cell surface. The simplest explanation is that one Fab arm of rituximab is bound to CD20, whilst the second Fab arm is bound by the anti-Id. This would require rituximab to exhibit a reasonably high off-rate, allowing one Fab arm to be released from CD20-binding. Recently, co-workers within our group assessed the off-rate of various anti-CD20 mAb fragments and showed that rituximab has a relatively fast off-rate in comparison to other anti-CD20 mAb [169]. Furthermore, off-rate, unlike on-rate is highly sensitive to differences in temperature [170 171], therefore, we addressed whether the binding of MB2A4 to rituximab-coated cells was temperature-sensitive. These experiments detailed in Figure 5.22, clearly show the temperature-dependence of MB2A4 binding, indicating that an increase in temperature (and hence off-rate) greatly facilitates the binding of the anti-Id. Presumably, within this model, MB2A4 carries out a bridging and stabilizing function, binding two separate Fab-bound rituximab molecules, thereby preventing rapid dissociation from the cell surface (Figure 5.23). Interestingly, and in support of this model Dr Mark Cragg was unable to detect binding of MB2A4 to the Fab' fragment of rituximab.

Figure 5.21. Pre- incubation with MB2 A4 blocks binding of rituximab to cells. FITC-labelled rituximab was added to Raji cells in the presence of varying concentrations of either MB2A4 (■) or SAB1.3 (♦). With MB2 A4 dose dependent blocking of the binding of rituximab is seen. With SAB1.3 another anti-idiotype to a different anti-CD20 mAb no block to the binding of rituximab is evident.
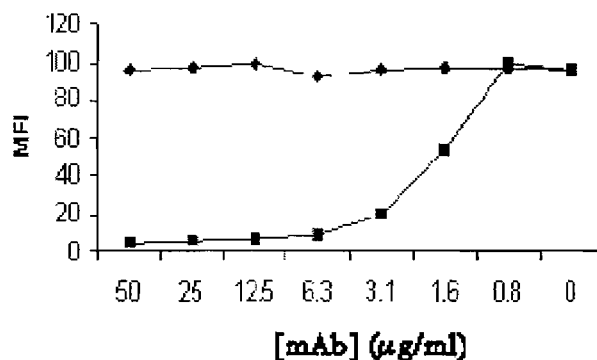
Figure 5.22 Binding of MB2A4 to rituximab is temperature dependent. MB2 A4-FITC (solid line) or SAB1.3-FITC (dashed line) was incubated with rituximab coated cells at 4 °C (♦), 20°C (■) or 37°C (▲) before washing and detection of FITC-mAb binding.
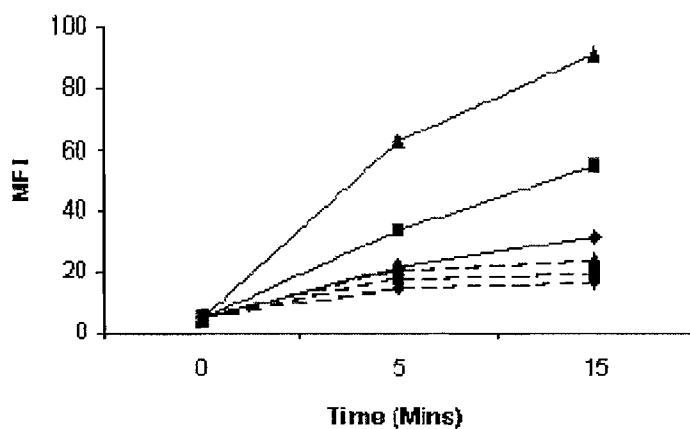
5.7 DISCUSSION

In this chapter the development of a reproducible sensitive and specific assay for the determination of serum rituximab concentrations has been described. This assay has been applied to patients within the study of fractionated RIT. Although the numbers are too small to draw firm conclusions, the results from the patients studied so far concur with the published literature in which an association between tumour load and serum rituximab concentration is reported[63]. Individual patients within the study highlight some interesting aspects of the pharmacokinetics of rituximab. In patient JH, a patient with extensive bone marrow involvement and bulky lymphadenopathy the rituximab concentration initially fell very rapidly to very low levels within 3 weeks of the induction course of rituximab. Following the final dose of RIT however, by which time there had

been a complete clinical response to the treatment, the rate of fall in serum rituximab concentration was significantly slower. This supports the hypothesis that the serum rituximab concentration is dependent at least partly upon tumour load. If, as has been suggested though not proven, higher serum concentrations are causally linked to response this finding will make attractive the use of maintenance rituximab schedules and fractionated RIT schedules. Such schedules will result in the administration of rituximab or ^{131}I rituximab after the tumour load has declined thereby exposing the remaining tumour cells to higher concentrations of rituximab.

Although tumour load appears to be an important determinant of serum rituximab concentration it is clearly not the only factor. Serum rituximab concentration is also likely to be influenced by the initial concentration of non-malignant CD20 expressing B-lymphocytes in the blood, bone marrow and spleen as well as by non-specific clearance through binding to Fc receptors. FcRn receptors found on endothelial cells have been shown to play an important part in the regulation of serum IgG levels [172]. It seems possible that the extent of non-specific binding of rituximab to Fc receptors may vary between patients and may be dependent on the presence of Fc receptor polymorphisms. Genomic polymorphisms, corresponding to phenotypes expressing valine or phenylalanine at amino acid 158 on the FcγIII receptor have been shown to influence the affinity of IgG1 for the Fc receptor. Patients that are homozygous for FcγIIIa 158 valine have been shown by Cartron et al to have a significantly higher clinical response rate to rituximab [29]. If rituximab levels are influenced by Fc receptor polymorphisms this may explain in part the association between serum rituximab concentrations and response. Investigation of such an association should now become relatively straightforward with the advent of an easily available sensitive and specific ELISA for serum rituximab concentrations.

The inter-patient variation in serum rituximab concentrations seen in the study is dramatic. Using the trial schedule it is quite clear that in some patients with a relatively low tumour load there are substantial amounts of rituximab still circulating at the time of administration of the pre-dose for the first fraction of RIT suggesting that the pre-dose

may be unnecessary in these patients. It is possible that administration of additional rituximab in these patients may have a detrimental effect on the biodistribution of ^{131}I rituximab by blocking binding not only to normal B cells but also to tumour cells. In other patients there is rapid clearance of rituximab from the serum following the induction course of rituximab and it may be that in these patients the pre-dose is still required to optimise the biodistribution of ^{131}I rituximab. In the future analysis of serum rituximab concentrations following induction rituximab may enable individualisation of the RIT pre-dose and help ensure optimisation of the biodistribution of RIT.

Rituximab is now widely used in combination with chemotherapy. The possibility that there is synergy between the cytotoxic effects of the mAb and chemotherapy has been proposed although an additive cytotoxic effect remains the most likley. There is as yet no consensus on the optimum schedule for integrating the two agents. Two influential studies using the combination of rituximab and CHOP chemotherapy for the treatment of DLBCL have recently been published. The two trials used different scheduling of the rituximab with CHOP. In the GELA study rituximab was given on day 1 of each of 8 CHOP cycles [37]. In the US intergroup conducted study rituximab was administered 7 days and 3 days prior to cycle one and 48 hours prior to cycles 3, 5 and 7 of CHOP chemotherapy [173]. Only the GELA study demonstrated a significant survival advantage with the addition of rituximab. One possible explanation for this is that the synergy between chemotherapy and antibody is critically dependent on the quantity of rituximab present at the time of administration of chemotherapy. Modelling of the serum rituximab pharmacokinetics for these two regimens suggests that not only was the total administered dose of rituximab lower in the Intergroup study but also the serum concentration at the time of administration of CHOP was substantially lower in the Intergroup (ECOG) study [174]. Whether or not this accounts for the difference in outcomes between the two studies or whether other differences in trial design, such as the second randomisation to maintenance rituximab in the Intergroup study, explain the differences in outcome remains to be determined. The availability of an anti-rituximab idiotype mAb may however facilitate the study of these questions

The data obtained in this study indicate that the pharmacokinetics of rituximab are complex and influenced by multiple factors. The observation that JB a patient with bulky disease continued to have relatively high levels of circulating rituximab over 6 months after the administration of rituximab remains unexplained (figure 5.18). Potential explanations for the unexpectedly slow clearance of rituximab in this patient include, residual tumour acting as a reservoir of rituximab that may then re-enter the circulation or some impact of Fc gamma receptor polymorphisms. Irrespective of the explanation it is clear that delivering a prescribed dose based on body surface area is inadequate and that following further research using the assay developed in this study individualisation of the dosing of rituximab may become possible. The assay may facilitate the tailoring of the scheduling to maximise the benefit seen when rituximab is delivered in combination with chemotherapy or RIT offering the potential for improved clinical outcomes.

The observation that the anti-rituximab mAb MB2A4 can bind rituximab while bound to tumour cells has opened new potential areas of tanslational research. It provides the clinical investigator with a tool to improve our understanding of the mechanism through which rituximab molecules bind to cells and interact with one another on the surface of tumour cells. It may also prove possible to using immunohistochemical techniques to identify rituximab on the surface of tumour cells exposed to rituximab in vivo. If so it may aid in our understanding of the microscopic biodistribution of rituximab within tumours and thereby improve our understanding of the mechanism through which the pre-dose for RIT works and how to optimise the timing and dose of pre-dose. MB2A4 is now being marketed commercially by Serotec Ltd Oxford UK. (Catalogue No. MCA2260).

Chapter 6

Summary and Conclusions

6 SUMMARY AND CONCLUSIONS

The efficacy of RIT in the treatment of relapsed indolent NHL is now well established. Following the US FDA approval of both ^{131}I tositumomab and ^{90}Y ibritumomab tiuxetan and the European Medicines Agency (EMEA) approval of the latter, RIT is likely to become increasingly accessible for patients with NHL. Despite these clinical advances and the prospect of more widespread use of RIT for indolent NHL many questions remain unanswered with regard optimising the therapeutic approach. Furthermore our knowledge of the biodistribution of radioimmunoconjugates and how the scheduling of RIT influences this remains limited. The developments in antibody engineering, new B cell targets as well as an increased availability and greater spectrum of radioisotopes have all contributed to the proliferation of potential combinations and permutations of antibody, isotope, dose and schedule over recent years.

The aims of this thesis have been to address some of these questions with a particular focus on the scheduling and fractionation of RIT. Given the large number of potential fractionation schedules, the initial work described in chapter 3, involved pre-clinical investigation of RIT fractionation to define the most promising fractionation strategies to be taken forward into the clinic. Preliminary experiments in two syngeneic murine models of NHL and two xenograft models of human B cell NHL in SCID mice were undertaken. In both the syngeneic and the xenograft models a dose response to RIT was demonstrated. This important observation offers support to the hypothesis that outcomes may be improved if the total dose of RIT can be escalated through fractionation. The RIT fractionation experiments were curtailed in the syngeneic model due to the unexpected rapid development of mouse anti-rat antibody responses (MARA).

The experiments performed in xenograft models were limited by the radiosensitivity of SCID mice and the inability to safely increase radiation doses. Despite this, these experiments clearly demonstrated a survival advantage for RIT when compared to unlabelled anti-CD20 mAb and confirmed the recent clinical findings in which the response rate to ^{90}Y ibritumomab tiuxetan was found to be superior to that with rituximab alone [46]. This preclinical work provided an understanding of the nature of experimental investigation and offered the opportunity to contribute to a significant publication in the RIT field[38].

The pre-clinical work-up provided the essential experience needed in the characterisation and ^{131}I labelling of mAbs for RIT. Following this work the protocol for the production of ^{131}I rituximab of clinical grade was developed. This protocol was subsequently used in the clinical study of fractionated ^{131}I rituximab described in chapter 4. The clinical trial is ongoing however data from the first three dose cohorts is reported here. The trial is designed to assess the safety and efficacy of 4 weekly infusions of rituximab followed by 2 fractions of ^{131}I labelled rituximab given 8 weeks apart in relapsed 'low grade' NHL. The use of the chimeric mAb rituximab has enabled fractionation without risk of a HAMA response. The use of an induction course of unlabelled rituximab is intended to clear the bone marrow of tumour prior to RIT thereby reducing haematological toxicity and enabling delivery of the treatment to patients where more than 25% of the bone marrow is replaced by lymphoma, a group previously excluded from treatment with RIT. Delivering the treatment in 2 fractions with an 8 week interval allowing some time for bone marrow recovery between doses has enabled escalation of the total dose of RIT delivered. This is intended to exploit the dose response for RIT suggested by the pre-clinical studies and supported by the impressive results achieved with myeloablative doses of RIT followed by ASCT. Using rituximab in RIT is attractive both because as a chimeric mAb repeated administration are less likely to result in HACA/HAMA but also importantly because of its well established anti-lymphoma effect in the naked state and ability to set up intracellular signals on binding and induce apoptosis.

The clinical study follows a conventional dose escalation design. The haematological data from the first 3 dose cohorts have suggested that it is possible to deliver whole body doses 30% greater than the recognised MTD for a single dose of ^{131}I labelled tositumomab without experiencing dose limiting myelotoxicity and that it may be possible to use this novel protocol to treat patients with bone marrow involvement by lymphoma in excess of 25%. All 12 patients in the first 3 dose cohorts have experienced responses with response durations equal to or in the majority of cases, superior to that seen with their previous chemotherapy regimen. There have been 3 CRs, 8 PRs and 1 mixed response. This high response rate, though it must be interpreted with caution in this non-randomised trial, is promising and indicates the potency of the combination of rituximab and ^{131}I and suggests potential for the fractionated approach.

Some of the most interesting data to emerge from the clinical study to date relate to the pharmacokinetics of ^{131}I rituximab and unlabelled rituximab. The first important observation is that the mean effective half-life of ^{131}I rituximab in this study is substantially longer than that reported for ^{131}I labelled murine anti-CD20 mAbs (102 vs. 59hrs). The mean effective half-life is also substantially longer in this study than in the one previous report on the pharmacokinetics of ^{131}I rituximab (102 v 88 hrs) [161]. From our work presented here, it would appear that these differences may be largely attributed to the differences in the scheduling between the studies.

Sequential pharmacokinetic analyses prior to the delivery of any rituximab and then prior to each fraction of RIT have enabled analysis of the impact of scheduling on the clearance of ^{131}I rituximab. Following the induction rituximab the mean effective half-life of ^{131}I rituximab doubled from 43 to 97 hours. There was a further increase in the effective half-life from 97 to 107 hours between the first and second doses of ^{131}I rituximab. The difference in effective half-life between first and second doses of RIT was most marked for those with a heavy tumour burden at the outset and correlated with a continued clinical response during the course of the treatment. These findings strongly support the hypothesis that availability of CD20 antigen for binding has a major impact on the clearance of the radioimmunoconjugate. The pre-dose and induction rituximab

clear B lymphocytes from the blood and bone marrow as well as starting the reduction in tumour burden that is continued with the sequential fractions of RIT.

The toxicity, response and pharmacokinetic data from the clinical study have formed the basis for oral presentations at both the British Cancer Research Meeting 2004 and the prestigious American Society of Hematolgy Meeting 2004[175]. A high quality publication is anticipated once data collection is complete on the 4th dose cohort.

The fifth chapter of this thesis focuses on the production of an anti-rituximab idiotype mAb and the development of an assay for the measurement of serum rituximab concentrations. This proved a highly successful strategy resulting in the production of a series of hybridomas that produce mAb specific for the rituximab idiotype. The most promising of these mAbs was used to develop an ELISA that can detect rituximab in the serum at nanomolar concentrations. There is interest in commercialising this assay from industry and the mAb is already being produced in milligram quantities and marketed for use in research by Serotec Ltd Oxford UK (Catalogue No. MCA2260). Serial serum samples from patients within the clinical study have been analysed using this assay revealing a striking correlation between tumour burden and serum rituximab concentration concurring with the finding that the clearance of ^{131}I rituximab is dependent on the availability of CD20 antigen and therefore tumour burden.

The serum rituximab assay may have wide application and may assist in individualising the scheduling of not only RIT but also rituximab for a wide variety of malignant and non-malignant indications. By identifying the patients with rapid clearance, it may facilitate the decision making process when identifying which patients are most likely to benefit from a higher dose or maintenance doses when rituximab is used as a single agent. Finally it may also have a role in optimising the scheduling of rituximab with chemotherapy. Since the publication of the GELA study, in which a survival benefit was demonstrated from the addition of rituximab to CHOP chemotherapy for DLBCL, the use of rituximab in combination with chemotherapy has become widespread [176]. There are many different schedules and there is no consensus as to the optimum timing of the

rituximab with the chemotherapy, however pre-clinical and clinical data is emerging to suggest that the timing of chemotherapy adminstration relative to mAb infusion is important [177] [174]. A tool that enables straightforward measurement of serum rituximab concentration may well assist in answering these important questions.

In addition to its use in a serum rituximab concentration assay, the anti-rituximab idiotype mAb has provided new insights into the binding of rituximab to CD20 at the cell surface level. We have been able to demonstrate that the anti-idiotype mAb actually binds rituximab while it is bound to CD20 on tumour cells. This unexpected finding relates to the rapid off rate of rituximab and the ability of MB2A4 to bind to one arm of the rituximab while the other remains bound to CD20 on cells. This collaborative work has resulted in two further high quality publications[178] [179].

In conclusion RIT is now fulfilling its long heralded promise in the field of lymphoma treatment. Fractionation of ^{131}I rituximab appears both feasible and effective. It is hoped that the work described in this thesis, through increasing our knowledge of the pharmacokinetics of naked and labelled rituximab and by increasing our understanding of the effects of scheduling in RIT, may ultimately lead to improved outcomes for the patients afflicted with these illnesses.

Appendix 1

Trial Protocol
Updated 15/7/03

Phase I/II Study of fractionated Radioimmunotherapy in Relapsed non-Hodgkin's Lymphoma using ^{131}I labelled Rituximab

1. Introduction

1.1 Non-Hodgkin's Lymphoma

Non-Hodgkin's lymphomas (NHL) comprise over a dozen different neoplasms of the lymphoid system that together are sixth in incidence and mortality amongst all neoplasms in the US [1]. In Europe the incidence of NHL is 15 per 100 000 inhabitants in females, 12.2 in males, and is rising faster than any other malignancy [2].

In terms of treatment decisions NHL can be divided into the "indolent" and the "aggressive" lymphomas. Despite the remarkable sensitivity of most lymphomas to initial chemotherapy and advances in drug development, the majority of patients with advanced disease subsequently relapse and die of their disease [3]. Furthermore patients with advanced "low grade" lymphomas remain incurable and survival has not altered for this group of patients since the 1960's [4]. There is therefore, an urgent need to identify alternative treatment strategies to improve these unsatisfactory results.

Increasing awareness of lymphocyte biology has identified a range of immunotherapeutic strategies for lymphoma. The most clinically significant of these new developments has been the use of antibody-based treatments, following the FDA approval of the monoclonal antibody (mAb), Rituximab in November 1997 [5,6].

1.2   Rituximab

Rituximab is a chimeric (mouse-human) anti-CD20 mAb directed against the CD20 antigen. CD20 is expressed on mature B cells, present on 95 % of B cell lymphomas and is thought to act as a calcium channel that regulates progression through the cell cycle [7]. Cross-linking of CD20 by anti-CD20 mAb results in apoptosis through a caspase dependent pathway and may trigger complement dependent cytotoxicty (CDC) or antibody directed cell cytotoxicity (ADCC) [8,9]. Despite the anticipated depletion of B-lymphocytes following treatment with Rituximab significant immunological compromise and susceptibility to infection has not been seen. Rituximab is licensed for use in relapsed or refractory "low grade" CD20 positive B cell lymphoma.

Initial phase I dose escalation trials performed by Maloney and colleagues demonstrated the safety of a dose of $375mg/m^2$ given weekly for 4 weeks [5]. This dose level was therefore used in the pivotal phase II trial, which led to the FDA approval [6]. In this trial of 166 previously treated patients, there was an overall response rate of 48% (6% complete response and 42% partial response). The median duration of response at the time of publication was 13.2 months. Subset analysis showed a greater (60%) response rate in those with follicular lymphoma but a much lower response rate 13% in those with small lymphocytic lymphoma. In this and subsequent studies serious adverse effects were minimal.

Subsequent studies have demonstrated clinically useful activity for Rituximab against a number of other CD20 positive histologies including diffuse large B cell (DLBC) lymphoma, mantle cell lymphoma, post-transplant lymphoproliferative disorder, Waldenstrom's macroglobulinaemia and hairy cell leukaemia [10]. The safety and efficacy of extended treatment and retreatment with Rituximab has also been demonstrated [11].

1.3 Radioimmunotherapy

The last few years have seen very significant progress with the development of radiolabelled antibodies or radioimmunotherapy (RIT) of B cell lymphomas (12,13). The sensitivity of lymphomas to external beam radiation has long been known and the development of mAb to deliver targeted radiotherapy or RIT has further theoretical advantages over unconjugated mAb. Enhanced anti-tumour activity might be anticipated from the delivery of a radioisotope to the tumour over that seen with mAb alone and has been demonstrated to occur in pre-clinical syngeneic lymphoma models [14]. In addition not all tumour cells have to be targeted directly by virtue of the 'crossfire' effect, which enables the killing by radiation of adjacent tumour cells that are either antigen negative or those cells to which the mAb has failed to penetrate. The range of this crossfire effect depends upon the radioisotope selected but is approximately 30 cell diameters for [131]I. Radiolabelled anti-CD20 monoclonal antibodies (mAb) have emerged as a highly promising approach in the treatment of advanced "low grade" NHL and two such reagents namely ^{131}I labelled tositumomab is currently under evaluation by the US FDA and ^{90}Y-labelled ibritumomab tiuxetan has recently been given a provisional licence (15-21). Both of these antibodies are murine in origin. The expectation is that RIT will soon become increasingly available for the treatment of "low grade" lymphomas.

1.4 Rationale for the Study

Despite highly promising clinical results with RIT in "low grade" NHL there remains uncertainty as to the optimal treatment approach. Currently a single administration of non-myeloablative radiolabelled murine anti-CD20 mAb (^{131}I labelled tositumomab [Bexxar™] and ^{90}Y-labelled ibritumomab tiuxetan [Zevalin™]) has become the "standard" practice. Although the CR rates are considerably greater with this type of RIT (40-70%) than with unlabeled Rituximab (5-10%), the durability of response appears to be similar at around 11 months [16]. Data from Press's group in Seattle using high doses of ^{131}I labelled anti-CD20 (B1) have yielded apparently higher responses rates and considerably increased duration of responses [22, 23]. These clinical studies suggest that there may be a radiation dose response for RIT.

Using a mouse mAb as part of one of the current RIT strategies has the major limitation that multiple treatments are not routinely possible due to the frequent development of human anti-mouse antibody responses (HAMA) [24]. Developing HAMA makes further RIT difficult or impossible. However, with the advent of chimeric humanised antibodies such as Rituximab, human anti-chimeric antibody responses (HACA) are rarely seen, occurring in as few as 1% of patients [5]. The lack of HAMA or HACA makes multiple or fractionated treatments possible, which in turn will enable higher cumulative doses of RIT to be delivered. Rituximab will be given initially as an unlabelled antibody in "standard" doses of $375mg/m^2$ weekly. Rituximab has proved to be extremely effective in clearing lymphoma cells from the bone marrow compartment and should enable larger doses of RIT to be delivered preferentially to nodal and visceral disease. Clearing of significant bone marrow disease should reduce subsequent myelosuppression using radiolabelled Rituximab. We therefore wish to test the feasibility of this approach and hypothesise that an increased dose of radiation to tumour delivered by fractionated chimeric anti-CD20 antibodies may increase both the response rate and duration of response.

2. Study Objectives

The primary objective of this project is to test the safety and efficacy of fractionated RIT in relapsed CD20 positive non-Hodgkin's Lymphoma in a Phase I/II dose escalation study using 2 fractionated doses of Iodine-^{131}I labelled Rituximab.

The primary efficacy endpoint will be Overall response rate (ORR); combined Complete Response (CR) and Partial Response (PR), with secondary end points time to disease progression and response duration for the responders.

3. Overall study design and plan

Eligible patients will be recruited who have relapsed or refractory CD20 +ve Non Hodgkins Lymphoma classified as follicular, small lymphocytic, mantle cell or transformed NHL. Patients will undergo an initial bone marrow assessment prior to

receiving 4 standard doses of 375mg/m^2 unlabelled Rituximab, which will be given initially weekly for 4 weeks (weeks 0-3) according to established standard protocols. Patients with greater than 25% bone marrow involvement at the initial bone marrow examination will have a further bone marrow examination performed following 4 weeks of unlabelled Rituximab. All patients with less than 25 % bone marrow involvement will then go onto have 2 courses of fractionated RIT with ^{131}I labelled Rituximab during weeks 9 and 17 using individualised patient dosimetry. This will consist of a predose of "cold" Rituximab 100mg/m^2 followed by a tracer dose of 5mCi (185 MBq) ^{131}Iodine labelled 5mg of Rituximab. The biodistribution of radiolabelled Rituximab will be measured by quantitative whole body gamma camera imaging undertaken immediately after and on day 2/3 and day 7 after tracer radiolabelled mAb administration. This data will be used to calculate the ^{131}I RIT therapy activity required to deliver a prescribed whole body dose. An additional tracer dose of ^{131}I Rituximab will be given prior to commencing the above described treatment protocol followed by three gamma camera images. This will enable us to determine the influence of the predose and induction Rituximab on the pharmacokinetics and biodistribution of the ^{131}I Rituximab.

Activity will be escalated to achieve a total predicted whole body dose of 30 cGy, 60cGy, 90 cGy, 120cGy, 150cGy delivered in 2 equal fractions 8 weeks apart. 3 patients will be treated at each dose cohort. Previous experience has shown that less than 10% of patients develop Grade IV haematological toxicity following a single dose of 75cGy delivered by murine ^{131}I labelled tositumomab with full recovery achieved in almost all patients by 8 weeks [17]. The 8-week RIT treatment interval chosen will allow marrow recovery at each dose level without compromising treatment efficacy. Full blood count and serum Rituximab antibody levels will be monitored weekly (weeks 1-25) using an anti-Rituximab idiotype specific antibody measured by ELISA assay. Additional blood samples will be taken prior to the first therapy and 6 weeks after each therapy for cytogenetic analysis to determine the increase in frequency of stable chromosomal translocations. This has been validated as an accurate measure of cumulative bone marrow radiation exposure(25).

Radiolabelled Rituximab will be administered in the dedicated Nuclear Medicine isolation suite and patients will be cared for in this facility until their whole body activity falls below the legal limit for discharge. Immunoreactivity and specific activity of radiolabelled Rituximab will be checked on an individual patient basis. The use of Rituximab does not appear to affect subsequent engraftment of stem cells if subsequent high dose therapy is indicated (26).

Sequential blood samples (10mls) will be stored for quantitative PCR analysis to detect t(14;18) translocation in follicular lymphoma at study entry and thereafter at 3, 6, 9 and 12 months. Quantitative PCR analysis to detect t(14;18) translocation and cytogenetic analysis will be performed on bone marrow samples taken at initial presentation and on selected samples performed 8 weeks after completeion of therapy. Immunophenotyping will also be performed at these time points. Patients will be offered entry into the ongoing study of immune responsiveness, which involves looking for antibody levels against tetanus toxoid and requires an additional 10 ml blood sample and will be supervised by Dr Ottensmeier (Ethics No 2242/99).

4. Selection of Study population

4.1 Patient Inclusion Criteria

- Patients must be aged 18 years or older.
- Patients must have a histologically confirmed CD20 +ve non-Hodgkin's lymphoma, classified as small lymphocytic, follicular, mantle cell lymphoma or transformed NHL.
- Patients must have been treated with at least one chemotherapy regimen and have lymphoma which has relapsed or progressed, or failed to achieve an objective response (CR or PR) on their last chemotherapy regimen.
- Patients must have a Karnofsky performance status of at least 60% and an anticipated survival of at least 6 months.
- Patients must have an absolute granulocyte count of above 1,500/mm^3, and a platelet count of above 100,000/mm^3 post 4 weeks of unlabelled Rituximab.

- Patients must have adequate renal function (defined as serum creatinine <1.5 times upper limit of normal), hepatic function (defined as total bilirubin <1.5 times upper limit of normal), and hepatic transaminases (defined as AST <5 times upper limit of normal)
- Patients must have given informed consent prior to study entry.

4.2 Patient Exclusion Criteria

- Patients with a mean of >25% of the intratrabecular marrow space involved with lymphoma on bone marrow biopsy following induction rituximab therapy.
- Patients who have received cytotoxic chemotherapy or radiation therapy within 4 weeks prior to study entry.
- Patients who have had prior haematopoietic stem cell transplant.
- Patients with active obstructive hydronephrosis.
- Patients with evidence of active infection requiring i.v. antibiotics at the time of study entry.
- Patients with advanced heart disease or other serious illness that would preclude evaluation.
- Patients with known HIV infection.
- Patients who are pregnant or breast-feeding. Male and female patients must agree to use effective contraception for 6 months following Iodine-131 Rituximab antibody therapy.
- Patients with prior malignancy other than lymphoma, except for adequately-treated skin cancer, cervical cancer in situ, or other cancer for which the patient has been disease-free for 5 years.
- Patients with progressive disease within 1 year of irradiation arising in a field that was previously irradiated with more than 35 Gy.
- Patients with previous allergic reactions to iodine.

5.   Treatment Overview

Thyroid blockade will be achieved by pretreatment with potassium iodide tablets starting at least 24 hours prior to the first infusion of the iodine-131 labelled rituximab and this will be continued for at least 14 days following the therapeutic doses.

5.1   Rituximab infusion

Thirty to 60 minutes before Rituximab patients will be premedicated with paracetamol 1g po and antihistamine (chlorpheniramine 8mg po) unless contraindicated for an individual patient. The i.v. infusion will be given over 1 hour or longer depending on infusion-related adverse experiences as outlined in the established unit protocol. Rituximab will also be given prior to the Radioimmunotherapy as described in the section below.

5.2   Supportive Therapy

Although the incidence of serious infusion reactions (i.e. anaphylactoid-like reactions with Rituximab) appears to be very low (less than 1%), emergency support for an anaphylactic reaction will be available. Infusion reactions with Rituximab or iodine-131 labelled Rituximab are typically mild to moderate in nature and consist of fever, nausea, vomiting, rigors, hypotension, pruritis, erythematous rash, urticaria, mucous membrane congestion, arthralgias and or myalgias [20]. If these symptoms occur paracetamol and/or chlorpheniramine may be given. The use of steroids is discouraged unless other measures are ineffective. Rigors generally abate within 30 minutes without pharmaceutical intervention. If any of these symptoms occur during antibody infusion the rate of antibody infusion should be decreased or stopped as shown overleaf:

Rituximab Infusion Rate Adjustments

Fever	Rigors	Mucosal Congestion/ Oedema	% Drop in Systolic BP	Infusion Rate Adjustment
38.5-38.9°C	Mild to Moderate	Mild to Moderate	30-49	Decrease by ½
>39.0°C	Severe	Severe	50	Stop Infusion*

*   Temporarily discontinue infusion until adverse experiences have reversed (generally 15-30 min) and then resume infusion at 25-50% of initial rate.

6.   Preparation of ^{131}I labelled Rituximab

[131]I will be obtained from Nordion and will be sterile and pyrogen free. Clinical grade Rituximab will be obtained from Roche pharmaceuticals and stored locally by Pharmacy. Rituximab will be labelled with Iodine-131 using the Iodogen method and the specific activity, labelling efficiency and immunoreactivity will be measured. A labelling efficiency of 90% will be expected to proceed to patient administration. The Limulus Amebocyte Lysate (LAL) assay will be used to detect endotoxins associated with Gram-negative bacteria prior to administration to patients.

7.   Administration of ^{131}I labelled Rituximab

[131]I labelled Rituximab will be diluted in 30 ml of 0.9% sodium chloride for injection and given as an intravenous infusion over 20 minutes using an infusion pump and a 0.22 micron iv filter in the set-up of the primary line. The method will be similar to that used and established in previous protocols within our institution using ^{131}I labelled anti-CD20 (B1) [17-20].

8. Patient Numbers

A minimum of three patients per dose level will be used according to previously published studies, requiring at least 15 patients. Response categories will consist of CR, PR, stable disease and progressive disease according to internationally recognised disease criteria. Standard National Cancer Institute Canada (NCIC) Common Toxicity Criteria (CTC) will be used and the dose level will be increased as long as Grade 2 toxicity is not seen in more than 2 patients 6 weeks after the second RIT infusion. In the event that 3 patients have not reached this point at the time of evaluation, a maximum of two further patients will be recruited at that dose level.

Dose limiting toxicity will be defined as any of the following adverse events occurring during the first cycle.

9. Toxicity Recording

Haematology and blood biochemistry will be performed weekly following the Iodine – 131 labelled Rituximab first therapeutic dose administration and for up to 13 weeks after the last therapeutic dose.

9.1 Haematological toxicity

Haematological toxicity will be recorded as outlined below

- **Nadir neutrophil**

Absolute neutrophil count (ANC) : < 0.5 x 10^9/L for > 7 days

or

< 0.1 x 10^9/L for > 3 days

- **Thrombocytopenia**

< 25 X 10^9/L or thrombocytopenia with bleeding, or requiring platelet transfusion

- **Febrile neutropenia** defined as:

- ANC < 0.5 x 10^9/L and
- fever either as three elevations of oral temperature above $> 38^{\circ}$C in a 24-hour period, measured every 8 hours,
- or a single oral temperature $> 38.5\,^{\circ}$C, provided that single episode of fever is not clearly related to other events (e.g. blood transfusion)

9.2 Non-Haematological toxicity

Is not expected, however any grade 3 or 4 major organ toxicity will be reported according to NCIC defined criteria.

10. Dosimetry Protocol

10.1 Gamma Camera Calibration

Whole body mode	Day 0	Day 2, 3 or 4	Day 6 or 7
Date			
DOSE CALIBRATOR ACTIVITY			
^{131}I Standard MBq			
Time Measured			
GAMMA CAMERA COUNTS - geometric mean			
A: ^{131}I Standard C_S			
Time started			
B: Background C_B			
Time started			
CALCULATION			
1. Time from initial count			
$T = T_S$ (2 or 3) $- T_{S1 \, (day \, 0)}$	$T_1 \quad = \quad 0$	$T_2 \quad =$	$T_3 \quad =$
2. Background corrected counts			
$C_S - C_B$	$C_{S1} \quad =$	$C_{S2} \quad =$	$C_{S3} \quad =$
3. Percent initial count [Table 1]			
%ISC $= 100$ x C_S / C_{S0}	$\%ICS_1 = 100$	$\%ICS_2 =$	$\%ICS_3 =$
4. Counts per MBq			
C_S / MBq			

10.2   GAMMA CAMERA IMAGING

Syringe activity MBq	
Post injection activity MBq	
Injected activity MBq	
Patient weight [kg]	
Patient height [m]	
^{131}I antibody infusion start time	
^{131}I antibody infusion completion time	

	Day 0	Day 2 or 3	Day 6 or 7
Gamma camera distance from table dual heads [cm]			
Background counts [GM]			
Patient total body counts [GM]			
Time from start of ^{131}I infusion to start of image acquisition	t_1 hr	t_2 hr	T_3 hr

10.3   CALCULATION OF ^{131}I ACTIVITY

The following equation is used to calculate the ^{131}I activity required to deliver the prescribed whole body dose in cGy:

$$^{131}\text{I activity [MBq]} = \frac{\underline{\text{Desired total body dose [cGy]}}}{1.433 \times T_{eff} \times S \text{ Value}}$$

Where:
S Value is calculated from Table 2 [attached] based upon body mass [kg]
T_{eff} is calculated graphically as follows:

Calculate background corrected geometric mean counts for 3 time points

Time point	
1	C1 = C_A-C_{BA} =
2	C2 = C_A-C_{BA} =
3	C3 = C_A-C_{BA} =

Calculate % injected activity [%IA]

Timepoint	
1	$\% IA_1 = 100\%$
2	$\% IA_2 = \dfrac{C2}{C1} \times 100 = \%$
3	$\% IA_3 = \dfrac{C3}{C1} \times 100 = \%$

T_{eff} is calculated graphically from the whole body time activity curve

The calculations are used to prescribe total body activity at each dose level. As whole body retention may change with successive treatments, it will be necessary to repeat the dosimetry study before each therapy administration.

Prescribed activities will be as follows:

15 cGy x 2	Cumulative whole body dose	30 cGy
30 cGy x 2	Cumulative whole body dose	60 cGy
45 cGy x 2	Cumulative whole body dose	90 cGy
60 cGy x 2	Cumulative whole body dose	120 cGy
75 cGy x 2	Cumulative whole body dose	150 cGy

It is anticipated that patients treated at the 15 cGy and 30cGy single fraction level will be managed as 24-hour admissions within a shielded unsealed source therapy room. Patients treated at higher activities will require 4 – 10 day in-patient admissions in a shielded unsealed source therapy room.

Whole body activity will be monitored daily using a ceiling mounted gamma probe with constant geometry. No immediate post therapy scintigraphy will be undertaken.

References

1. American Cancer Society. Cancer Facts and Figures - 2000.   Non Hodgkins Lymphoma. Available at: http:/www.cancer.org/statistics/cff2000/graphicaldata.

2. J.FERLAY, F. BRAY, R. SANKILA AND D.M. PARKIN. EUCAN: Cancer Incidence, Mortality and Prevalence in the European Union 1996, version 3.1. *IARC CancerBase* No. 4. Lyon, IARCPress, 1999.

3. ARMITAGE JO: Treatment of non-Hodgkins lymphoma. *N. Engl. J. Med.* (1993) 328:1023-1030.

4. HORNING SJ: Natural history of and therapy for the Indolent non Hodgkin's lymphomas. *Semin Oncol.*(1993)20:75-88.

5. MALONEY DG, GRILLO-LOPEZ AJ, WHITE CA, et al. : IDEC-C2B8 anti-CD20 monoclonal antibody therapy in patients with relapsed low-grade non-Hodgkin's lymphoma. *Blood.* (1997) 90:2188-2195

6. MCLAUGHLIN P, GRILLO-LOPEZ AJ, LINK BK, et al.: Rituximab chimeric anti-CD20 monoclonal antibody therapy for relapsed indolent lymphomas: half of patients respond to a four-dose treatment program. *J Clin Oncol.* (1998)16:2825-2833

7. TEDDER TF, ENGEL P: A regulator of cell cycle progression of B lymphocytes. *Immunol Today* (1994) 15:450-454.

8. VAN DER KOLK LE, EVERS LM, VAN LIER RA, et al. : Intracellular pathways of CD20-induced apoptosis. *Blood* (1999) 630-631a (suppl 1,)

9. SCHWANER l, VON ENGELHARDT V, JORDANOVA M, et al. : Rituximab induced complement cascade activation is related to adverse events and bone marrow involvement. *Blood.* 2000;96(suppl 1):507a #2181

10. ILLIDGE TM, BAYNE MC : Antibody Therapy in Lymphoma; *Expert Opinion in Pharmacotherapy* (2001) 2(6) 953 – 961

11. DAVIS TA, GRILLO-LOPEZ AJ, WHITE CA et al: Rituximab anti-CD20 monoclonal antibody therapy in non-Hodgkin's lymphoma: safety and efficacy of re-treatment. *J Clin Oncol* (2000) 18(17):3135-43

12. ILLIDGE TM, JOHNSON PWJ. : Emerging Role of RIT in the Management of Haematological Malignancies. *Brit J Haem* (2000) 108(4):679-688

13. ILLIDGE TM, BROCK S. Radioimmunotherapy of Cancer : Using Monoclonal Antibodies to Target Radiotherapy *Current Pharmaceutical Design*, 2000, 6, 1399-1418

14. ILLIDGE TM, CRAGG MS, McBRIDE H, et al. : The Importance of Antibody-Specificity in Determining Successful Treatment of Radioimmunotherapy of B-cell Lymphoma ; *Blood* (1999) 94 (1) 233-243

15. WITZIG TE, WHITE CA, WISEMAN GA, et al.: Phase I/II trial of IDEC-Y2B8 radioimmunotherapy for treatment of relapsed or refractory CD20+ B-cell non-Hodgkin's lymphoma. *J Clin Oncol.* (1999)17:3793-3803

16. WITZIG, TE, WHITE CA, GORDON LI, et al.: Final results of a randomized controlled study of Zevalin^{TM} radioimmunotherapy regimen versus a standard course of rituximab immunotherapy for B-cell NHL *Blood.* (2000) 96 (11) : 831a

17. KAMINSKI MS, ZASADNY KR, FRANCIS IR, et al.: Radioimmunotherapy of B-cell lymphoma with [Iodine 131] anti-B1 (anti CD20) antibody. *N. Eng. J. Med.*(1993) 329:459-465.

18. KAMINSKI MS, ZASADNY KR, FRANCIS IR, et al.: I-131 anti-B1 radioimmunotherapy for B cell lymphoma. *J Clin Oncol.*(1996)14:1974-1981.

19. KAMINSKI MS, ESTS J, KENNETH R, et al.: Radioimmunotherapy with iodine 131 tositumomab for relapsed or refractory B-cell non-Hodgkin's lymphoma: updated results and long term follow-up of the University of Michigan experience. *Blood* (2000) 98 (4):1259-1265

20. KAMINSKI MS, ZELENETZ AD, PRESS O, et al.: Multi-centre, phase III study of iodine-131 tositumomab (anti-B1 antibody) for chemotherapy refractory low grade or transformed low grade non-Hodgkin's lymphoma (abstract) *Blood.*(1998) 92 ; 316a.

21. VOSE J, SALEH M, LISTER A, et al.: Iodine-131 anti-B1 antibody for non-Hodgkin's lymphoma (NHL): overall clinical trial experience. *Proc. Am. Soc. Clin. Oncol.* (1998). 38 ; 10a

22. PRESS OW, EARY JF, APPELBAUM FR, et al.: Radiolabelled antibody therapy of B cell lymphoma with autologous bone marrow support. *N Engl. J. Med.* (1993) 329:1219-1224.

23. LIU SY, EARY JF, PETERSDORF SH, et al. Follow-up of relapsed B cell lymphoma patients treated with iodine-131-labeled anti-CD20 antibody and autologous stem cell rescue. *J Clin Oncol.* (1998)16:3270-3278

24. SCHROFF RW, FOON KA, BEATTY SM, et al: Human anti-murine immunoglobulin responses in patients receiving monoclonal antibody therapy. *Cancer Res.* (1985) 45:879-885.

25. WONG J, Wang J, LUI A, et al.: Evaluating changes in stable chromosomal translocation frequency in patients receiving radioimmunotherapy. *Int J Radiation Oncol Biol Phys.* (2000)46(3):599-607.

26. BUCKSTEIN R, IMRIE K, SPANER D, et al.: Stem cell function and engraftment is not affected by 'in vivo purging' with rituximab for autologous stem cell treatment for patients with low-grade non-Hodgkin's lymphoma. *Semin Oncol* (1999) 26:115-122 (suppl 14).

BIBLIOGRAPHY

1. Kohler G, Milstein C. Continuous cultures of fused cells secreting antibody of predefined specificity. *Nature* 1975;256(5517):495-7.

2. Glennie MJ, van de Winkel JG. Renaissance of cancer therapeutic antibodies. *Drug Discov Today* 2003;8(11):503-10.

3. Shipp M MP, Harris NL. Non-Hodgkin's Lymphomas. In: V. T. DeVita SH, and S. A Rosenberg, editor. *In: Cancer principles and practice of oncology.* Philadelphia/New York: Lippincott-Raven, 1997:2165.

4. SEER. SEER cancer statistics review, 1973-1997. Bethesda, Md.: national Cancer Institute, 1997.

5. Ries LG KC, Hankey BF, Miller BA, Clegg L, Edwards BK (eds). SEER Cancer Statistics Review, 1973-1996,. Bethesda, MD,: National Cancer Institute., 1999.

6. Harris NL, Jaffe ES, Stein H, Banks PM, Chan JK, Cleary ML, et al. A revised European-American classification of lymphoid neoplasms: a proposal from the International Lymphoma Study Group. *Blood* 1994;84(5):1361-92.

7. WHO. Pathology and Genetics of Tumours of Haemopoetic and Lymphoid tissues. *World health Organisation classification of tumours.* Lyon: IARC Press, 2001.

8. Armitage JO, Weisenburger DD. New approach to classifying non-Hodgkin's lymphomas: clinical features of the major histologic subtypes. Non-Hodgkin's Lymphoma Classification Project. *J Clin Oncol* 1998;16(8):2780-95.

9. Gallagher CJ, Gregory WM, Jones AE, Stansfeld AG, Richards MA, Dhaliwal HS, et al. Follicular lymphoma: prognostic factors for response and survival. *J Clin Oncol* 1986;4(10):1470-80.

10. Hiddemann W, Longo DL, Coiffier B, Fisher RI, Cabanillas F, Cavalli F, et al. Lymphoma classification--the gap between biology and clinical management is closing. *Blood* 1996;88(11):4085-9.

11. Mac Manus MP, Hoppe RT. Is radiotherapy curative for stage I and II low-grade follicular lymphoma? Results of a long-term follow-up study of patients treated at Stanford University. *J Clin Oncol* 1996;14(4):1282-90.

12. Wilder RB, Jones D, Tucker SL, Fuller LM, Ha CS, McLaughlin P, et al. Long-term results with radiotherapy for Stage I-II follicular lymphomas. *Int J Radiat Oncol Biol Phys* 2001;51(5):1219-27.

13. Horning SJ, Rosenberg SA. The natural history of initially untreated low-grade non-Hodgkin's lymphomas. *N Engl J Med* 1984;311(23):1471-5.

14. Czuczman MS, Grillo-Lopez AJ, White CA, Saleh M, Gordon L, LoBuglio AF, et al. Treatment of patients with low-grade B-cell lymphoma with the combination of chimeric anti-CD20 monoclonal antibody and CHOP chemotherapy. *J Clin Oncol* 1999;17(1):268-76.

15. Marcus R, Imrie K, Belch A, Cunningham D, Flores E, Catalano J, et al. CVP chemotherapy plus rituximab compared with CVP as first-line treatment for advanced follicular lymphoma. *Blood* 2005;105(4):1417-23.

16. Forstpointner R, Dreyling M, Repp R, Hermann S, Hanel A, Metzner B, et al. The addition of rituximab to a combination of fludarabine, cyclophosphamide, mitoxantrone (FCM) significantly increases the response rate and prolongs survival as compared with FCM alone in patients with relapsed and refractory follicular and mantle cell lymphomas: results of a prospective randomized study of the German Low-Grade Lymphoma Study Group. *Blood* 2004;104(10):3064-71.

17. van Besien K, Sobocinski KA, Rowlings PA, Murphy SC, Armitage JO, Bishop MR, et al. Allogeneic bone marrow transplantation for low-grade lymphoma. *Blood* 1998;92(5):1832-6.

18. Haas RL, Poortmans P, de Jong D, Aleman BM, Dewit LG, Verheij M, et al. High response rates and lasting remissions after low-dose involved field radiotherapy in indolent lymphomas. *J Clin Oncol* 2003;21(13):2474-80.

19. Meerwaldt JH, Carde P, Burgers JM, Monconduit M, Thomas J, Somers R, et al. Low-dose total body irradiation versus combination chemotherapy for lymphomas with follicular growth pattern. *Int J Radiat Oncol Biol Phys* 1991;21(5):1167-72.

20. Richaud PM, Soubeyran P, Eghbali H, Chacon B, Marit G, Broustet A, et al. Place of low-dose total body irradiation in the treatment of localized follicular non-Hodgkin's lymphoma: results of a pilot study. *Int J Radiat Oncol Biol Phys* 1998;40(2):387-90.

21. Horning SJ. Natural history of and therapy for the indolent non-Hodgkin's lymphomas. *Semin Oncol* 1993;20(5 Suppl 5):75-88.

22. Grillo-Lopez AJ. Rituximab: an insider's historical perspective. *Semin Oncol* 2000;27(6 Suppl 12):9-16.

23. Miller RA, Maloney DG, Warnke R, Levy R. Treatment of B-cell lymphoma with monoclonal anti-idiotype antibody. *N Engl J Med* 1982;306(9):517-22.

24. Meeker TC, Lowder J, Maloney DG, Miller RA, Thielemans K, Warnke R, et al. A clinical trial of anti-idiotype therapy for B cell malignancy. *Blood* 1985;65(6):1349-63.

25. Grossbard ML, Press OW, Appelbaum FR, Bernstein ID, Nadler LM. Monoclonal antibody-based therapies of leukemia and lymphoma. *Blood* 1992;80(4):863-78.

26. Hale G, Clark M, Waldmann H. Therapeutic potential of rat monoclonal antibodies: isotype specificity of antibody-dependent cell-mediated cytotoxicity with human lymphocytes. *J Immunol* 1985;134(5):3056-61.

27. Dyer MJ, Hale G, Hayhoe FG, Waldmann H. Effects of CAMPATH-1 antibodies in vivo in patients with lymphoid malignancies: influence of antibody isotype. *Blood* 1989;73(6):1431-9.

28. Clynes R, Takechi Y, Moroi Y, Houghton A, Ravetch JV. Fc receptors are required in passive and active immunity to melanoma. *Proc Natl Acad Sci U S A* 1998;95(2):652-6.

29. Cartron G, Dacheux L, Salles G, Solal-Celigny P, Bardos P, Colombat P, et al. Therapeutic activity of humanized anti-CD20 monoclonal antibody and polymorphism in IgG Fc receptor FcgammaRIIIa gene. *Blood* 2002;99(3):754-8.

30. van der Kolk LE, Grillo-Lopez AJ, Baars JW, Hack CE, van Oers MH. Complement activation plays a key role in the side-effects of rituximab treatment. *Br J Haematol* 2001;115(4):807-11.

31. Cragg MS, Glennie MJ. Antibody specificity controls in vivo effector mechanisms of anti-CD20 reagents. *Blood* 2004;103(7):2738-43.

32. Weng WK, Levy R. Expression of complement inhibitors CD46, CD55, and CD59 on tumor cells does not predict clinical outcome after rituximab treatment in follicular non-Hodgkin lymphoma. *Blood* 2001;98(5):1352-7.

33. Cragg MS, French RR, Glennie MJ. Signaling antibodies in cancer therapy. *Curr Opin Immunol* 1999;11(5):541-7.

34. Tutt AL, French RR, Illidge TM, Honeychurch J, McBride HM, Penfold CA, et al. Monoclonal antibody therapy of B cell lymphoma: signaling activity on tumor cells appears more important than recruitment of effectors. *J Immunol* 1998;161(6):3176-85.

35. Illidge TM, Cragg MS, McBride HM, French RR, Glennie MJ. The importance of antibody-specificity in determining successful radioimmunotherapy of B-cell lymphoma. *Blood* 1999;94(1):233-43.

36. Demidem A, Lam T, Alas S, Hariharan K, Hanna N, Bonavida B. Chimeric anti-CD20 (IDEC-C2B8) monoclonal antibody sensitizes a B cell lymphoma cell line to cell killing by cytotoxic drugs. *Cancer Biother Radiopharm* 1997;12(3):177-86.

37. Coiffier B, Lepage E, Briere J, Herbrecht R, Tilly H, Bouabdallah R, et al. CHOP chemotherapy plus rituximab compared with CHOP alone in elderly patients with diffuse large-B-cell lymphoma. *N Engl J Med* 2002;346(4):235-42.

38. Du Y, Honeychurch J, Cragg MS, Bayne M, Glennie MJ, Johnson PW, et al. Antibody-induced intracellular signaling works in combination with radiation to eradicate lymphoma in radioimmunotherapy. *Blood* 2004;103(4):1485-94.

39. Selenko N, Maidic O, Draxier S, Berer A, Jager U, Knapp W, et al. CD20 antibody (C2B8)-induced apoptosis of lymphoma cells promotes phagocytosis by dendritic cells and cross-priming of CD8+ cytotoxic T cells. *Leukemia* 2001;15(10):1619-26.

40. Honeychurch J, Glennie MJ, Johnson PW, Illidge TM. Anti-CD40 monoclonal antibody therapy in combination with irradiation results in a CD8 T-cell-dependent immunity to B-cell lymphoma. *Blood* 2003;102(4):1449-57.

41. Jerne NK. Towards a network theory of the immune system. *Ann Immunol (Paris)* 1974;125C(1-2):373-89.

42. Bradt BM, DeNardo SJ, Mirick GR, DeNardo GL. Documentation of idiotypic cascade after Lym-1 radioimmunotherapy in a patient with non-Hodgkin's lymphoma: basis for extended survival? *Clin Cancer Res* 2003;9(10 Pt 2):4007S-12S.

43. McLaughlin P, Grillo-Lopez AJ, Link BK, Levy R, Czuczman MS, Williams ME, et al. Rituximab chimeric anti-CD20 monoclonal antibody therapy for relapsed indolent lymphoma: half of patients respond to a four-dose treatment program. *J Clin Oncol* 1998;16(8):2825-33.

44. Yokota T, Milenic DE, Whitlow M, Schlom J. Rapid tumor penetration of a single-chain Fv and comparison with other immunoglobulin forms. *Cancer Res* 1992;52(12):3402-8.

45. Farah RA, Clinchy B, Herrera L, Vitetta ES. The development of monoclonal antibodies for the therapy of cancer. *Crit Rev Eukaryot Gene Expr* 1998;8(3-4):321-56.

211

46. Witzig TE, Gordon LI, Cabanillas F, Czuczman MS, Emmanouilides C, Joyce R, et al. Randomized controlled trial of yttrium-90-labeled ibritumomab tiuxetan radioimmunotherapy versus rituximab immunotherapy for patients with relapsed or refractory low-grade, follicular, or transformed B-cell non-Hodgkin's lymphoma. *J Clin Oncol* 2002;20(10):2453-63.

47. Becker W, Behr T. High dose radioimmunotherapy in relapsed B-cell lymphoma with I-131 rituximab. *Ann Hematol* 2001;80 Suppl 3:B130-1.

48. Kaminski MS, Zasadny KR, Francis IR, Milik AW, Ross CW, Moon SD, et al. Radioimmunotherapy of B-cell lymphoma with [131I]anti-B1 (anti-CD20) antibody. *N Engl J Med* 1993;329(7):459-65.

49. Vose JM, Colcher D, Gobar L, Bierman PJ, Augustine S, Tempero M, et al. Phase I/II trial of multiple dose 131Iodine-MAb LL2 (CD22) in patients with recurrent non-Hodgkin's lymphoma. *Leuk Lymphoma* 2000;38(1-2):91-101.

50. Juweid ME, Stadtmauer E, Hajjar G, Sharkey RM, Suleiman S, Luger S, et al. Pharmacokinetics, dosimetry, and initial therapeutic results with 131I- and (111)In-/90Y-labeled humanized LL2 anti-CD22 monoclonal antibody in patients with relapsed, refractory non-Hodgkin's lymphoma. *Clin Cancer Res* 1999;5(10 Suppl):3292s-3303s.

51. Kaminski MS, Fig LM, Zasadny KR, Koral KF, DelRosario RB, Francis IR, et al. Imaging, dosimetry, and radioimmunotherapy with iodine 131-labeled anti-CD37 antibody in B-cell lymphoma. *J Clin Oncol* 1992;10(11):1696-711.

52. Dechant M, Bruenke J, Valerius T. HLA class II antibodies in the treatment of hematologic malignancies. *Semin Oncol* 2003;30(4):465-75.

53. DeNardo GL, Kukis DL, Shen S, DeNardo DA, Meares CF, DeNardo SJ. 67Cu- versus 131I-labeled Lym-1 antibody: comparative pharmacokinetics and dosimetry in patients with non-Hodgkin's lymphoma. *Clin Cancer Res* 1999;5(3):533-41.

54. Einfeld DA, Brown JP, Valentine MA, Clark EA, Ledbetter JA. Molecular cloning of the human B cell CD20 receptor predicts a hydrophobic protein with multiple transmembrane domains. *Embo J* 1988;7(3):711-7.

55. Press OW, Farr AG, Borroz KI, Anderson SK, Martin PJ. Endocytosis and degradation of monoclonal antibodies targeting human B-cell malignancies. *Cancer Res* 1989;49(17):4906-12.

56. Tedder TF, Engel P. CD20: a regulator of cell-cycle progression of B lymphocytes. *Immunol Today* 1994;15(9):450-4.

57. Mathas S, Rickers A, Bommert K, Dorken B, Mapara MY. Anti-CD20- and B-cell receptor-mediated apoptosis: evidence for shared intracellular signaling pathways. *Cancer Res* 2000;60(24):7170-6.

58. Maloney DG, Grillo-Lopez AJ, Bodkin DJ, White CA, Liles TM, Royston I, et al. IDEC-C2B8: results of a phase I multiple-dose trial in patients with relapsed non-Hodgkin's lymphoma. *J Clin Oncol* 1997;15(10):3266-74.

59. McLaughlin P, Grillo-Lopez A, Link B, Levy R, Czuczman M, Williams M, et al. Rituximab chimeric anti-CD20 monoclonal antibody therapy for relapsed indolent lymphoma: half of patients respond to a four-dose treatment program. *J Clin Oncol* 1998;16(8):2825-2833.

60. Davis TA, White CA, Grillo-Lopez AJ, Velasquez WS, Link B, Maloney DG, et al. Single-Agent Monoclonal Antibody Efficacy in Bulky Non-Hodgkin's Lymphoma: Results of a Phase II Trial of Rituximab. *J Clin Oncol* 1999;17(6):1851-.

61. Hainsworth JD, Litchy S, Burris HA, 3rd, Scullin DC, Jr., Corso SW, Yardley DA, et al. Rituximab as first-line and maintenance therapy for patients with indolent non-hodgkin's lymphoma. *J Clin Oncol* 2002;20(20):4261-7.

62. Maloney DG, Liles TM, Czerwinski DK, Waldichuk C, Rosenberg J, Grillo-Lopez A, et al. Phase I clinical trial using escalating single-dose infusion of chimeric anti-CD20 monoclonal antibody (IDEC-C2B8) in patients with recurrent B-cell lymphoma. *Blood* 1994;84(8):2457-66.

63. Berinstein NL, Grillo-Lopez AJ, White CA, Bence-Bruckler I, Maloney D, Czuczman M, et al. Association of serum Rituximab (IDEC-C2B8) concentration and anti-tumor response in the treatment of recurrent low-grade or follicular non-Hodgkin's lymphoma. *Ann Oncol* 1998;9(9):995-1001.

64. Piro LD, White CA, Grillo-Lopez AJ, Janakiraman N, Saven A, Beck TM, et al. Extended Rituximab (anti-CD20 monoclonal antibody) therapy for relapsed or refractory low-grade or follicular non-Hodgkin's lymphoma. *Ann Oncol* 1999;10(6):655-61.

65. Ghielmini M, Schmitz SF, Cogliatti SB, Pichert G, Hummerjohann J, Waltzer U, et al. Prolonged treatment with rituximab in patients with follicular lymphoma significantly increases event-free survival and response duration compared with the standard weekly x 4 schedule. *Blood* 2004;103(12):4416-23.

66. Gordan LN, Grow WB, Pusateri A, Douglas V, Mendenhall NP, Lynch JW. Phase II trial of individualized rituximab dosing for patients with CD20-positive lymphoproliferative disorders. *J Clin Oncol* 2005;23(6):1096-102.

67. Bertrand Coiffier FB, Catherinne Thieblemont, Olivier Hequet, Philippe Arnaud, Charles Dumontet, Daniel Espinouse, Gilles Salles. Rituximab Re-Treatment in B-Cell Lymphoma Patients: Efficacy and Toxicity in 59 Patients Treated in One Center. *Proceedings of the American Society of Haematology* 2002:abstract1390.

68. Davis TA, Grillo-Lopez AJ, White CA, McLaughlin P, Czuczman MS, Link BK, et al. Rituximab Anti-CD20 Monoclonal Antibody Therapy in Non-Hodgkin's Lymphoma: Safety and Efficacy of Re-Treatment. *J Clin Oncol* 2000;18(17):3135-3143.

69. Denham JW, Denham E, Dear KB, Hudson GV. The follicular non-Hodgkin's lymphomas--I. The possibility of cure. *Eur J Cancer* 1996;32A(3):470-9.

70. Press OW, Rasey J. Principles of radioimmunotherapy for hematologists and oncologists. *Semin Oncol* 2000;27(6 Suppl 12):62-73.

71. Vriesendorp HM, Quadri SM, Stinson RL, Onyekwere OC, Shao Y, Klein JL, et al. Selection of reagents for human radioimmunotherapy. *Int J Radiat Oncol Biol Phys* 1992;22(1):37-45.

72. Batra SK, Jain M, Wittel UA, Chauhan SC, Colcher D. Pharmacokinetics and biodistribution of genetically engineered antibodies. *Curr Opin Biotechnol* 2002;13(6):603-8.

73. Lane DM, Eagle KF, Begent RH, Hope-Stone LD, Green AJ, Casey JL, et al. Radioimmunotherapy of metastatic colorectal tumours with iodine-131-labelled antibody to carcinoembryonic antigen: phase I/II study with comparative biodistribution of intact and F(ab')2 antibodies. *Br J Cancer* 1994;70(3):521-5.

74. Milenic DE, Yokota T, Filpula DR, Finkelman MA, Dodd SW, Wood JF, et al. Construction, binding properties, metabolism, and tumor targeting of a single-chain Fv derived from the pancarcinoma monoclonal antibody CC49. *Cancer Res* 1991;51(23 Pt 1):6363-71.

75. Ober RJ, Radu CG, Ghetie V, Ward ES. Differences in promiscuity for antibody-FcRn interactions across species: implications for therapeutic antibodies. *Int. Immunol.* 2001;13(12):1551-1559.

76. Press OW, Howell-Clark J, Anderson S, Bernstein I. Retention of B-cell-specific monoclonal antibodies by human lymphoma cells. *Blood* 1994;83(5):1390-7.

77. Turner JH, Martindale AA, Boucek J, Claringbold PG, Leahy MF. 131I-Anti CD20 radioimmunotherapy of relapsed or refractory non-Hodgkins lymphoma: a phase II clinical trial of a nonmyeloablative dose regimen of chimeric rituximab radiolabeled in a hospital. *Cancer Biother Radiopharm* 2003;18(4):513-24.

78. Postema EJ, Raemaekers JM, Oyen WJ, Boerman OC, Mandigers CM, Goldenberg DM, et al. Final results of a phase I radioimmunotherapy trial using (186)Re-epratuzumab for the treatment of patients with non-Hodgkin's lymphoma. *Clin Cancer Res* 2003;9(10 Pt 2):3995S-4002S.

79. van Osdol W, Fujimori K, Weinstein JN. An analysis of monoclonal antibody distribution in microscopic tumor nodules: consequences of a "binding site barrier". *Cancer Res* 1991;51(18):4776-84.

80. Buchsbaum DJ, Wahl RL, Glenn SD, Normolle DP, Kaminski MS. Improved delivery of radiolabeled anti-B1 monoclonal antibody to Raji lymphoma xenografts by predosing with unlabeled anti-B1 monoclonal antibody. *Cancer Res* 1992;52(3):637-42.

81. Garkavij M, Tennvall J, Strand SE, Norrgren K, Nilsson R, Sjogren HO. Improving radioimmunotargeting of tumors: the impact of preloading unlabeled L6 monoclonal antibody on the biodistribution of 125I-L6 in rats. *J Nucl Biol Med* 1994;38(4):594-600.

82. Badger CC, Krohn KA, Peterson AV, Shulman H, Bernstein ID. Experimental radiotherapy of murine lymphoma with 131I-labeled anti-Thy 1.1 monoclonal antibody. *Cancer Res* 1985;45(4):1536-44.

83. Sharkey RM, Natale A, Goldenberg DM, Mattes MJ. Rapid blood clearance of immunoglobulin G2a and immunoglobulin G2b in nude mice. *Cancer Res* 1991;51(12):3102-7.

84. Kaminski MS, Zasadny KR, Francis IR, Fenner MC, Ross CW, Milik AW, et al. Iodine-131-anti-B1 radioimmunotherapy for B-cell lymphoma. *J Clin Oncol* 1996;14(7):1974-81.

85. Witzig TE, White CA, Wiseman GA, Gordon LI, Emmanouilides C, Raubitschek A, et al. Phase I/II trial of IDEC-Y2B8 radioimmunotherapy for treatment of relapsed or refractory CD20(+) B-cell non-Hodgkin's lymphoma. *J Clin Oncol* 1999;17(12):3793-803.

86. Siegel E. The beginnings of radioiodine therapy of metastatic thyroid carcinoma: a memoir of Samuel M. Seidlin, M. D. (1895-1955) and his celebrated patient. *Cancer Biother Radiopharm* 1999;14(2):71-9.

87. DeNardo GL, O'Donnell RT, Shen S, Kroger LA, Yuan A, Meares CF, et al. Radiation dosimetry for 90Y-2IT-BAD-Lym-1 extrapolated from pharmacokinetics using 111In-2IT-BAD-Lym-1 in patients with non-Hodgkin's lymphoma. *J Nucl Med* 2000;41(5):952-8.

88. Jurcic JG, Larson SM, Sgouros G, McDevitt MR, Finn RD, Divgi CR, et al. Targeted alpha particle immunotherapy for myeloid leukemia. *Blood* 2002;100(4):1233-9.

89. McDevitt MR, Sgouros G, Finn RD, Humm JL, Jurcic JG, Larson SM, et al. Radioimmunotherapy with alpha-emitting nuclides. *Eur J Nucl Med* 1998;25(9):1341-51.

90. O'Donoghue JA. Optimal therapeutic strategies for radioimmunotherapy. *Recent Results Cancer Res* 1996;141:77-99.

91. Knox SJ, Goris ML, Wessels BW. Overview of animal studies comparing radioimmunotherapy with dose equivalent external beam irradiation. *Radiother Oncol* 1992;23(2):111-7.

92. Steel GG, Deacon JM, Duchesne GM, Horwich A, Kelland LR, Peacock JH. The dose-rate effect in human tumour cells. *Radiother Oncol* 1987;9(4):299-310.

93. Till JE, Mc CE. A direct measurement of the radiation sensitivity of normal mouse bone marrow cells. *Radiat Res* 1961;14:213-22.

94. Sgouros G. Bone marrow dosimetry for radioimmunotherapy: theoretical considerations. *J Nucl Med* 1993;34(4):689-94.

95. Juweid MES, R.M. Siegel, J.A. Estimates of red marrow dose by sacral scintigraphy in radioimmunotherapy patients having non-Hodgkins lymphoma and diffuse bone marrow uptake. *Cancer Research* 1995;55(suppl):5827-31.

96. Wiseman GA, White CA, Stabin M, Dunn WL, Erwin W, Dahlbom M, et al. Phase I/II 90Y-Zevalin (yttrium-90 ibritumomab tiuxetan, IDEC-Y2B8) radioimmunotherapy dosimetry results in relapsed or refractory non-Hodgkin's lymphoma. *Eur J Nucl Med* 2000;27(7):766-77.

97. Wong JY, Wang J, Liu A, Odom-Maryon T, Shively JE, Raubitschek AA, et al. Evaluating changes in stable chromosomal translocation frequency in patients receiving radioimmunotherapy. *Int J Radiat Oncol Biol Phys* 2000;46(3):599-607.

98. Wahl RLK, S. Zasadny, K.R. Patient-specific whole-body dosimetry: principles and a simplified method for clinical implementation. *J.Nucl.Med.* 1998;39:14S-20S.

99. Wahl RLZ, K.R. MacFarlane, D. Iodine-131 antibody for B-cell lymphoma: an update on the Michigan Phase I experience. *J.Nucl.Med.* 1998;39(suppl):21s-27s.

100. Wiseman GA, Kornmehl E, Leigh B, Erwin WD, Podoloff DA, Spies S, et al. Radiation Dosimetry Results and Safety Correlations from 90Y-Ibritumomab Tiuxetan Radioimmunotherapy for Relapsed or Refractory Non-Hodgkin's Lymphoma: Combined Data from 4 Clinical Trials. *J Nucl Med* 2003;44(3):465-474.

101. DeNardo SJ, Williams LE, Leigh BR, Wahl RL. Choosing an optimal radioimmunotherapy dose for clinical response. *Cancer* 2002;94(4 Suppl):1275-86.

102. Koral KF, Dewaraja Y, Clarke LA, Li J, Zasadny KR, Rommelfanger SG, et al. Tumor-absorbed-dose estimates versus response in tositumomab therapy of previously untreated patients with follicular non-Hodgkin's lymphoma: preliminary report. *Cancer Biother Radiopharm* 2000;15(4):347-55.

103. Sgouros G, Squeri S, Ballangrud AM, Kolbert KS, Teitcher JB, Panageas KS, et al. Patient-Specific, 3-Dimensional Dosimetry in Non-Hodgkin's Lymphoma Patients Treated with 131I-anti-B1 Antibody: Assessment of Tumor Dose-Response. *J Nucl Med* 2003;44(2):260-268.

104. Hartmann Siantar CL, DeNardo GL, DeNardo SJ. Impact of nodal regression on radiation dose for lymphoma patients after radioimmunotherapy. *J Nucl Med* 2003;44(8):1322-9.

105. Kaminski M, Zelenetz, A., Leonard, J., Saleh, M., Jain, V.,. Bexxar® Radioimmunotherapy Produces a Substantial Number of Durable Complete Responses in Patients with Multiply Relapsed or Refractory Low Grade or Transformed Low Grade Non-Hodgkin's Lymphoma. *Blood* 2002;100(11 part1):Abstract1382.

106. Gregory S, Kaminski, M., Zelenetz, A., Jain, V.,. Characteristics of Patients with Relapsed and Refractory Low Grade Non-Hodgkin's Lymphoma Who Sustained Durable Responses Following Treatment with Tositumomab and Iodine I 131 Tositumomab (Bexxar®). *Blood* 2002;100(11 part2):Abstract 4791.

107. Horning S, Younes, A., Lucas, J., Podoloff, D., Jain, V.,. Rituximab Treatment Failures: Tositumomab and Iodine I 131 Tositumomab [Bexxar®] Can Produce Meaningful Durable Responses. *Blood* 2002;100(11 part1):Abstract 1385.

108. Coleman M MSK, Susan J. Knox, Andrew D. Zelenetz, Julie M. Vose. [89] The BEXXAR Therapeutic Regimen (Tositumomab and Iodine I 131 Tositumomab) Produced Durable Complete Remissions in Heavily Pretreated Patients with Non-Hodgkins Lymphoma (NHL), Rituximab-Relapsed/Refractory Disease, and Rituximab-Naive Disease. Session Type: Oral Session. *American Society of Haematology 45th Annual Meeting* 2003:Abst 89.

109. Davis TA, Kaminski MS, Leonard JP, Hsu FJ, Wilkinson M, Zelenetz A, et al. The radioisotope contributes significantly to the activity of radioimmunotherapy. *Clin Cancer Res* 2004;10(23):7792-8.

110. Kaminski MS, Tuck M, Estes J, Kolstad A, Ross CW, Zasadny K, et al. 131I-tositumomab therapy as initial treatment for follicular lymphoma. *N Engl J Med* 2005;352(5):441-9.

111. Bennett JM, Kaminski MS, Leonard JP, Vose JM, Zelenetz AD, Knox SJ, et al. Assessment of treatment-related myelodysplastic syndromes and acute myeloid leukemia in patients with non-Hodgkin lymphoma treated with tositumomab and iodine I131 tositumomab. *Blood* 2005;105(12):4576-82.

112. Gordon L.I TEW, J. L. Murray,. Yttrium-90 ibritumomab tiuxetan radioimmunotherapy produces high response rates and durable remissions in patients with relapsed or refractory low grade, follicular or transformed B-cell NHL: Final results of a randomized controlled trial. *Proc of the Am Soc Clin Onc* 2003:2315a.

113. Gordon LI, Witzig TE, Wiseman GA, Flinn IW, Spies SS, Silverman DH, et al. Yttrium 90 ibritumomab tiuxetan radioimmunotherapy for relapsed or refractory low-grade non-Hodgkin's lymphoma. *Semin Oncol* 2002;29(1 Suppl 2):87-92.

114. Gordon LIW, T.E. Emmanouilides, C,et al:. 90Y ibritumomab tiuxetan in aggressive NHL: Analysis of response and toxicity. *Proc Am Soc Clin Oncol* 2002;21:266a.

115. DeNardo SJ, DeNardo GL, O'Grady LF, Hu E, Sytsma VM, Mills SL, et al. Treatment of B cell malignancies with 131I Lym-1 monoclonal antibodies. *Int J Cancer Suppl* 1988;3:96-101.

116. DeNardo GL, DeNardo SJ, O'Donnell RT, Kroger LA, Kukis DL, Meares CF, et al. Are radiometal-labeled antibodies better than iodine-131-labeled antibodies: comparative pharmacokinetics and dosimetry of copper-67-, iodine-131-, and yttrium-90-labeled Lym-1 antibody in patients with non-Hodgkin's lymphoma. *Clin Lymphoma* 2000;1(2):118-26.

117. DeNardo GL, DeNardo SJ, Shen S, DeNardo DA, Mirick GR, Macey DJ, et al. Factors affecting 131I-Lym-1 pharmacokinetics and radiation dosimetry in patients with non-Hodgkin's lymphoma and chronic lymphocytic leukemia. *J Nucl Med* 1999;40(8):1317-26.

118. Hajjar G, M. SR, J. B. Interim results of a phase I/II radioimmunotherapy trial in relapsed/ refractory non-Hodgkin's lymphoma (NHL) patients given Y-90 labeled anti-CD22 humanised monoclonal antibodies. *Blood* 2001(ASH abst. 2560):611a.

119. Press OW, Unger JM, Braziel RM, Maloney DG, Miller TP, LeBlanc M, et al. A Phase II Trial of CHOP chemotherapy followed by tositumomab/iodine I 131 tositumomab for previously untreated follicular non-Hodgkin's

lymphoma: Southwest Oncology Group protocol S9911. *Blood* 2003:2003-01-0287.

120. Press OW, Eary JF, Appelbaum FR, Martin PJ, Badger CC, Nelp WB, et al. Radiolabeled-antibody therapy of B-cell lymphoma with autologous bone marrow support. *N Engl J Med* 1993;329(17):1219-24.

121. Liu SY, Eary JF, Petersdorf SH, Martin PJ, Maloney DG, Appelbaum FR, et al. Follow-up of relapsed B-cell lymphoma patients treated with iodine-131-labeled anti-CD20 antibody and autologous stem-cell rescue. *J Clin Oncol* 1998;16(10):3270-8.

122. Gopal AK, Gooley TA, Maloney DG, Petersdorf SH, Eary JF, Rajendran JG, et al. High-dose radioimmunotherapy versus conventional high-dose therapy and autologous hematopoietic stem cell transplantation for relapsed follicular non-Hodgkin lymphoma: a multivariable cohort analysis. *Blood* 2003;102(7):2351-7.

123. Gopal AK, Rajendran JG, Petersdorf SH, Maloney DG, Eary JF, Wood BL, et al. High-dose chemo-radioimmunotherapy with autologous stem cell support for relapsed mantle cell lymphoma. *Blood* 2002;99(9):3158-62.

124. Bush RS, Gospodarowicz M, Sturgeon J, Alison R. Radiation therapy of localized non-Hodgkin's lymphoma. *Cancer Treat Rep* 1977;61(6):1129-36.

125. Tubiana M, Carde P, Burgers JM, Cosset JM, Van Glabbeke M, Somers R. Prognostic factors in non-Hodgkin's lymphoma. *Int J Radiat Oncol Biol Phys* 1986;12(4):503-14.

126. Kamath SS, Marcus RB, Jr., Lynch JW, Mendenhall NP. The impact of radiotherapy dose and other treatment-related and clinical factors on in-field control in stage I and II non-Hodgkin's lymphoma. *Int J Radiat Oncol Biol Phys* 1999;44(3):563-8.

127. Beaumier PL, Venkatesan P, Vanderheyden JL, Burgua WD, Kunz LL, Fritzberg AR, et al. 186Re radioimmunotherapy of small cell lung carcinoma xenografts in nude mice. *Cancer Res* 1991;51(2):676-81.

128. DeNardo SJ, Kukis DL, Miers LA, Winthrop MD, Kroger LA, Salako Q, et al. Yttrium-90-DOTA-peptide-chimeric L6 radioimmunoconjugate: efficacy and toxicity in mice bearing p53 mutant human breast cancer xenografts. *J Nucl Med* 1998;39(5):842-9.

129. Press OW, Eary JF, Appelbaum FR, Martin PJ, Nelp WB, Glenn S, et al. Phase II trial of 131I-B1 (anti-CD20) antibody therapy with autologous stem cell transplantation for relapsed B cell lymphomas. *Lancet* 1995;346(8971):336-40.

130. Kaminski MS, Estes J, Zasadny KR, Francis IR, Ross CW, Tuck M, et al. Radioimmunotherapy with iodine (131)I tositumomab for relapsed or refractory B-cell non-Hodgkin lymphoma: updated results and long-term follow-up of the University of Michigan experience. *Blood* 2000;96(4):1259-66.

131. Hall EJ. Radiation biology. *Cancer* 1985;55(9 Suppl):2051-7.

132. Kroger LA, DeNardo GL, Gumerlock PH, Xiong CY, Winthrop MD, Shi XB, et al. Apoptosis-related gene and protein expression in human lymphoma xenografts (Raji) after low dose rate radiation using 67Cu-2IT-BAT-Lym-1 radioimmunotherapy. *Cancer Biother Radiopharm* 2001;16(3):213-25.

133. Griffith MH, Yorke ED, Wessels BW, DeNardo GL, Neacy WP. Direct dose confirmation of quantitative autoradiography with micro-TLD measurements for radioimmunotherapy. *J Nucl Med* 1988;29(11):1795-809.

134. Roberson PL BD. Reconciliation of tumour dose response to external beam radiotherapy versus radioimmunotherapy with 131I labelled antibody for colon cancer model. *Cancer Res* 1995;55(suppl):5811s-6s.

135. Coggle JE. Absence of late radiation effects on bone marrow stem cells. *Int J Radiat Biol Relat Stud Phys Chem Med* 1980;38(5):589-95.

136. Meyn RE. Apoptosis and response to radiation: implications for radiation therapy. *Oncology (Huntingt)* 1997;11(3):349-56; discussion 356, 361, 365.

137. Schlom J, Molinolo A, Simpson JF, Siler K, Roselli M, Hinkle G, et al. Advantage of dose fractionation in monoclonal antibody-targeted radioimmunotherapy. *J Natl Cancer Inst* 1990;82(9):763-71.

138. Buchsbaum DJ, Wahl RL, Normolle DP, Kaminski MS. Therapy with unlabeled and 131I-labeled pan-B-cell monoclonal antibodies in nude mice bearing Raji Burkitt's lymphoma xenografts. *Cancer Res* 1992;52(23):6476-81.

139. Buchsbaum DJ, Khazaeli MB, Mayo MS, Roberson PL. Comparison of multiple bolus and continuous injections of 131I-labeled CC49 for therapy in a colon cancer xenograft model. *Clin Cancer Res* 1999;5(10 Suppl):3153s-3159s.

140. Roberson PL, Dudek S, Buchsbaum DJ. Dosimetric comparison of bolus and continuous injections of CC49 monoclonal antibody in a colon cancer xenograft model. *Cancer* 1997;80(12 Suppl):2567-75.

141. DeNardo GL, DeNardo SJ, Lamborn KR, Goldstein DS, Levy NB, Lewis JP, et al. Low-dose, fractionated radioimmunotherapy for B-cell malignancies using 131I-Lym-1 antibody. *Cancer Biother Radiopharm* 1998;13(4):239-54.

142. DeNardo GL, DeNardo SJ, Goldstein DS, Kroger LA, Lamborn KR, Levy NB, et al. Maximum-tolerated dose, toxicity, and efficacy of (131)I-Lym-1 antibody for fractionated radioimmunotherapy of non-Hodgkin's lymphoma. *J Clin Oncol* 1998;16(10):3246-56.

143. Meredith RF, Khazaeli MB, Liu T, Plott G, Wheeler RH, Russell C, et al. Dose fractionation of radiolabeled antibodies in patients with metastatic colon cancer. *J Nucl Med* 1992;33(9):1648-53.

144. Wiseman GC, P. Micallef, I. et al. interim safety results of a phase I trial of two sequential doses of yttrium-90 ibritumomab tiuxetan for previously treated patients with low-grade non-Hodgkin's lymphoma. *ASCO* 2003:abstract 2312.

145. Shen S, Duan J, Meredith RF, Buchsbaum DJ, Brezovich IA, Pareek PN, et al. Model prediction of treatment planning for dose-fractionated radioimmunotherapy. *Cancer* 2002;94(4 Suppl):1264-9.

146. Slavin S, Strober S. Spontaneous murine B-cell leukaemia. *Nature* 1978;272(5654):624-6.

147. Cobb LM, Glennie MJ, McBride HM, Breckon G, Richardson TC. Characterisation of a new murine B cell lymphoma. *Br J Cancer* 1986;54(5):807-18.

148. Johnson GD, Beutner EH, Holborow EJ. Developments in immunofluorescence: the need for standardization. *J Clin Pathol* 1967;20(5):720-3.

149. Elliott TJ, Glennie MJ, McBride HM, Stevenson GT. Analysis of the interaction of antibodies with immunoglobulin idiotypes on neoplastic B lymphocytes: implications for immunotherapy. *J Immunol* 1987;138(3):981-8.

150. Loevinger. *MIRD Primer for Absorbed Dose Calculations.* New York: The Society of Nuclear Medicine Inc, 1988.

151. Wahl RL. The clinical importance of dosimetry in radioimmunotherapy with tositumomab and iodine I 131 tositumomab. *Semin Oncol* 2003;30(2 Suppl 4):31-8.

152. Du Y, Honeychurch J, Cragg MS, Bayne MC, Glennie MJ, Johnson PW, et al. Antibody induced intracellular signaling works in combination with radiation to eradicate lymphoma in radioimmunotherapy. *Blood* 2003.

153. Uchida J, Lee Y, Hasegawa M, Liang Y, Bradney A, Oliver JA, et al. Mouse CD20 expression and function. *Int Immunol* 2004;16(1):119-29.

154. Biedermann KA, Sun JR, Giaccia AJ, Tosto LM, Brown JM. scid mutation in mice confers hypersensitivity to ionizing radiation and a deficiency in DNA double-strand break repair. *Proc Natl Acad Sci U S A* 1991;88(4):1394-7.

155. Wei BR, Ghetie MA, Vitetta ES. The combined use of an immunotoxin and a radioimmunoconjugate to treat disseminated human B-cell lymphoma in immunodeficient mice. *Clin Cancer Res* 2000;6(2):631-42.

156. Ochakovskaya R, Osorio L, Goldenberg DM, Mattes MJ. Therapy of disseminated B-cell lymphoma xenografts in severe combined immunodeficient mice with an anti-CD74 antibody conjugated with (111)indium, (67)gallium, or (90)yttrium. *Clin Cancer Res* 2001;7(6):1505-10.

157. Scatchard. The attraction of proteins for small molecules and ions. *Ann. N. Y. Acad. Sci.* 1949;51:660-672.

158. McBride HM. PhD Thesis: University of Southampton, 1993:Appendix 1.

159. Cragg MS, Morgan SM, Chan HT, Morgan BP, Filatov AV, Johnson PW, et al. Complement-mediated lysis by anti-CD20 mAb correlates with segregation into lipid rafts. *Blood* 2003;101(3):1045-52.

160. Press OW, Corcoran M, Subbiah K, Hamlin DK, Wilbur DS, Johnson T, et al. A comparative evaluation of conventional and pretargeted radioimmunotherapy of CD20-expressing lymphoma xenografts. *Blood* 2001;98(8):2535-43.

161. Scheidhauer K, Wolf I, Baumgartl HJ, Von Schilling C, Schmidt B, Reidel G, et al. Biodistribution and kinetics of (131)I-labelled anti-CD20 MAB IDEC-C2B8 (rituximab) in relapsed non-Hodgkin's lymphoma. *Eur J Nucl Med Mol Imaging* 2002;29(10):1276-82.

162. Cheson BD, Horning SJ, Coiffier B, Shipp MA, Fisher RI, Connors JM, et al. Report of an international workshop to standardize response criteria for non-Hodgkin's lymphomas. NCI Sponsored International Working Group. *J Clin Oncol* 1999;17(4):1244.

163. Chaiwatanatorn K, Lee N, Grigg A, Filshie R, Firkin F. Delayed-onset neutropenia associated with rituximab therapy. *Br J Haematol* 2003;121(6):913-8.

164. Maloney DG, Grillo-Lopez AJ, White CA, Bodkin D, Schilder RJ, Neidhart JA, et al. IDEC-C2B8 (Rituximab) anti-CD20 monoclonal antibody therapy in patients with relapsed low-grade non-Hodgkin's lymphoma. *Blood* 1997;90(6):2188-95.

165. Ghielmini M, Schmitz SF, Burki K, Pichert G, Betticher DC, Stupp R, et al. The effect of Rituximab on patients with follicular and mantle-cell

lymphoma. Swiss Group for Clinical Cancer Research (SAKK). *Ann Oncol* 2000;11 Suppl 1:123-6.

166. Papadaki T, Stamatopoulos K, Stavroyianni N, Paterakis G, Phisphis M, Stefanoudaki-Sofianatou K. Evidence for T-large granular lymphocyte-mediated neutropenia in Rituximab-treated lymphoma patients: report of two cases. *Leukemia Research* 2002;26(6):597-600.

167. Mattes MJ, Griffiths GL, Diril H, Goldenberg DM, Ong GL, Shih LB. Processing of antibody-radioisotope conjugates after binding to the surface of tumor cells. *Cancer* 1994;73(3 Suppl):787-93.

168. Iacona I, Lazzarino M, Avanzini MA, Rupolo M, Arcaini L, Astori C, et al. Rituximab (IDEC-C2B8): validation of a sensitive enzyme-linked immunoassay applied to a clinical pharmacokinetic study. *Ther Drug Monit* 2000;22(3):295-301.

169. Teeling JL, French RR, Cragg MS, van den Brakel J, Pluyter M, Huang H, et al. Characterization of new human CD20 monoclonal antibodies with potent cytolytic activity against non-Hodgkin lymphomas. *Blood* 2004;104(6):1793-800.

170. Johnstone RW, Andrew SM, Hogarth MP, Pietersz GA, McKenzie IF. The effect of temperature on the binding kinetics and equilibrium constants of monoclonal antibodies to cell surface antigens. *Mol Immunol* 1990;27(4):327-33.

171. Mason D W, A. Kinetics of antibody reactions and the analysis of cell surface antigens. In: D W, editor. *Handbook of experimental Immunology*: Blackwells Scientific Publications, 1986:Chapter 38.

172. Ghetie V, Ward ES. Multiple roles for the major histocompatibility complex class I- related receptor FcRn. *Annu Rev Immunol* 2000;18:739-66.

173. Habermann T. WE, Morrison V. et al. Phase 3 trial of rituximab CHOP (R-CHOP) v CHOP with a second randomisation to maintenance rituximab or observation in patients 60 years of age and oler with diffuse large B cell lymphoma (DLBCL). *Blood* 2003;102(11):abstract 8.

174. Valente N. CD, Ng C. et al. Pharmacokinetic comparoson of two different dosing regmens of rituxan plus CHOP (CHOP-R) in ECOG/CALGB/SWOG (E4494) and GELA LNH-98 trials of older patients with diffuse large B-cell Lymphoma (DLBCL). *Blood* 2003;102(11):Abstract 1498.

175. Illidge T. BM, Zivanovic M., Du Y., Lewington V., Johnson P. Phase I/II Study of Fractionated Radioimmunotherapy (RIT) in Relapsed Low Grade Non-Hodgkin's Lymphoma (NHL). *Blood* 2004;104(11):Absract 131.

176. Coiffier B. Rituximab in combination with CHOP improves survival in elderly patients with aggressive non-Hodgkin's lymphoma. *Semin Oncol* 2002;29(2 Suppl 6):18-22.

177. Honeychurch J. GM, Johnson P., Illidge T. Cyclophosphamide Induced CD11b+ Cells Can Inhibit Anti-CD40 Monoclonal Antibody (mAb) Therapy of B-Cell Lymphoma. *Blood* 2004;104(11):Abtract 3280.

178. Cragg MS, Bayne MB, Tutt AL, French RR, Beers S, Glennie MJ, et al. A new anti-idiotype antibody capable of binding rituximab on the surface of lymphoma cells. *Blood* 2004;104(8):2540-2.

179. Cragg MS, Bayne MC, Illidge TM, Valerius T, Johnson PW, Glennie MJ. Apparent modulation of CD20 by rituximab: an alternative explanation. *Blood* 2004;103(10):3989-90.